SURFACE PROPERTIES OF AQUEOUS POLYMER SOLUTIONS

by

John Clifford Scott, M.Sc., D.I.C., Grad.Inst.P.

A Thesis submitted for the degree of Ph.D. of the University of London, 1971.

ABSTRACT

The reduction of turbulent flow energy dissipation is of considerable importance in many high speed liquid flow situations. Oscillating flow techniques represent a fairly reproducible means of examining the flow properties of the materials which promote the phenomenon of "drag reduction", and the present work concerns the application of one type of acoustic excitation to the investigation of polymer materials which are very effective in the reduction of turbulent drag in water.

Systems of transverse surface waves, or ripples, were examined, and it was found that the properties of ripples on the surface of drag-reducing polymer solutions were much less dependent on the flow properties of the bulk liquid than on the presence of surface activity in the solutions. In one of the polymer series examined, that of poly(ethylene oxide), the surface activity completely dominated the ripple propagation.

Reviews are given of the surface properties of liquids in general, polymer solutions in particular, and of the factors determining the propagation of liquid surface waves. A completely new technique of ripple measurement developed for this investigation, using moiré fringes, is described, and results are presented of measurements on poly(ethylene oxide)/water systems using this technique.

Although certain experimental imperfections concerned

with surface contamination are indicated by the results, the distinctive ripple damping behaviour of poly(ethylene oxide) has been shown to support the conclusions of modern hydrodynamic ripple theory. Evidence is also presented which suggests that this particular polymer exhibits adsorption characteristics not previously reported: A certain "irreversibility" in the adsorption appears to exist at the air/water surface which results in the production of strong surface activity effects at very low polymer concentrations.

CONTENTS

CHAPTER 1 INTRODUCTION

A Turbulent Flow Drag Reduction 1.

B The Flow of Polymer Solutions 4.

C The Application of Acoustic Techniques to the Study of Polymer Solutions 9.

D The Possibility of an Adsorption Effect in Drag Reduction 13.

CHAPTER 2 THE SURFACE PROPERTIES OF LIQUIDS

(i) Surface Tension Theory 16.

(ii) The Measurement of Surface Tension 24.

a) Capillary Rise 27.

b) The Wilhelmy Plate 29.

c) Ring and Plate Detachment 31.

d) The Langmuir Film Balance 31.

e) Bubble Pressure and Drop Weight 32.

f) Drop Shape 33.

g) Ripples 34.

h) Oscillating Jets 36.

(iii) Surface Rheology 38.

(iv) Dilational Surface Properties 42.

CHAPTER 3 LIQUID SURFACE WAVES

(i) Early Investigations 53.

(ii) The Development of Modern Hydrodynamic Ripple Theory 54.

(iii) The Predictions of Ripple Theory 59.

(iv) The Physical Interpretation of Ripple Theory 63.

(v) Agreement of Theory with Experiment 68.

(vi) The Possible Failure of Ripple Theory 72.

(vii) Techniques of Surface Wave Measurement

a) Early Work 76.

b) The Telescope Focussing Technique 79.

c) The Beam Deflection Technique 81.

d) The Wave Crest Focussing Technique 84.

e) The Acousto-Mechanical Technique 84.

f) The Optical Interference Technique 89.

g) Summary of Techniques 90.

CHAPTER 4 THE APPLICATION OF MOIRÉ FRINGE TECHNIQUES TO SURFACE WAVE MEASUREMENT

A Review of Moiré Methods

(i) Introduction 93.

(ii) Moiré-Optical Analogies 96.

(iii) Strain Measurement 101.

(iv) Topography Measurement 102.

(v) Refractive Index Measurement 109.

B Moiré Fringes Applied to Surface Wave Measurement

(i) The Optical System 112.

(ii) The Construction of the Apparatus 114.

(iii) The Theory of the Measurement Technique 122.

(iv) Measurement Sensitivity 130.

(v) Choice of Fringe System 138.

(vi) Optical Alignment 141.

(vii) The Operating Technique 143.

(viii) The Processing of Results 145.

(ix) Advantages of the Moiré Technique 154.

CHAPTER 5 THE ADSORPTION OF POLYMERS AT THE WATER/AIR SURFACE

(i) General 156

(ii) Poly(ethylene glycol) 158

(iii) Polyvinyl Alcohol 162

(iv) Poly(ethylene oxide) 168

(v) Polymethacrylic Acid 185

(vi) Summary of Experimental Work 187

(vii) The Theoretical Treatment of Polymer Adsorption 190

CHAPTER 6 EXPERIMENTAL PROCEDURES

(i) Materials

a) Water Preparation 192

b) The Ripple Tank 196

c) Solution Preparation 198

d) Spreading Technique 201

(ii) Surface Tension Measurement 205

(iii) The Measurement of Ripple Properties. 208

CHAPTER 7 · RESULTS AND DISCUSSION

A Preliminary Investigation

(i) General Approach 212

(ii) The Ripple Damping Properties of Pure Clean Water 214

B POLY(ETHYLENE OXIDE)

(i) Introduction 221

(ii) The first Solution Experiments 225

(iii) Spread Monolayers

a) Results 228

b) The lack of reproducibility 231

c) Comparison with published work 237

d) Deductions from Hydrodynamic Ripple Theory 240

(iv) Solution Properties

a) Results 249

b) Equilibrium 253

c) Irreversibility 258

(v) Comparison with Poly(ethylene glycol) 266

a) Spreading 267

b) Solutions 268

(vi) Discussion. 268

Appendix 1 Image distortion produced by an irregular refractive index discontinuity in a single lens, variable magnification imaging system. 272

Appendix 2 Use of the Lucassen and Hansen wave damping theory for the measurement of surface dilational elasticity 275

Guide to symbols used in the text 281

Bibliography 281

Acknowledgements 291

Glossary 292

CHAPTER 1

INTRODUCTION

A. TURBULENT FLOW DRAG REDUCTION.

When the shear velocity gradients present in the laminar flow of a liquid exceed a certain critical value dependent on the density and viscosity of the liquid, the flow ceases to be wholly in the flow direction. In fully developed turbulent flow, the liquid distant from solid boundaries executes rapid vortex motions, superimposed on the average flow. Energy is dissipated by this irregular motion, and in a practical flow situation such as the pumping of liquid through a pipe, more work has to be done on a given volume of liquid than if laminar flow conditions were maintained. A typical result of this behaviour is shown in figure 1.1a, which is a graph of the rate of flow of a liquid through a pipe as a function of the pressure difference between the ends of the pipe. A simple liquid such as water exhibits this type of curve, in which the initial straight section through the origin represents laminar flow. Turbulent flow will occur at a certain increased flow rate, and after an indefinite transition region, the curve follows another straight line. It can be seen from the lesser slope of this line that the work done on a given volume of liquid will be greater under these conditions than in the laminar region.

The addition of small quantities of certain materials to water and other liquids has been found to change this normal behaviour significantly in the turbulent region. Concentrations of the order of between 10^{-6} and 10^{-4} by weight of some high molecular weight soluble polymers reduce

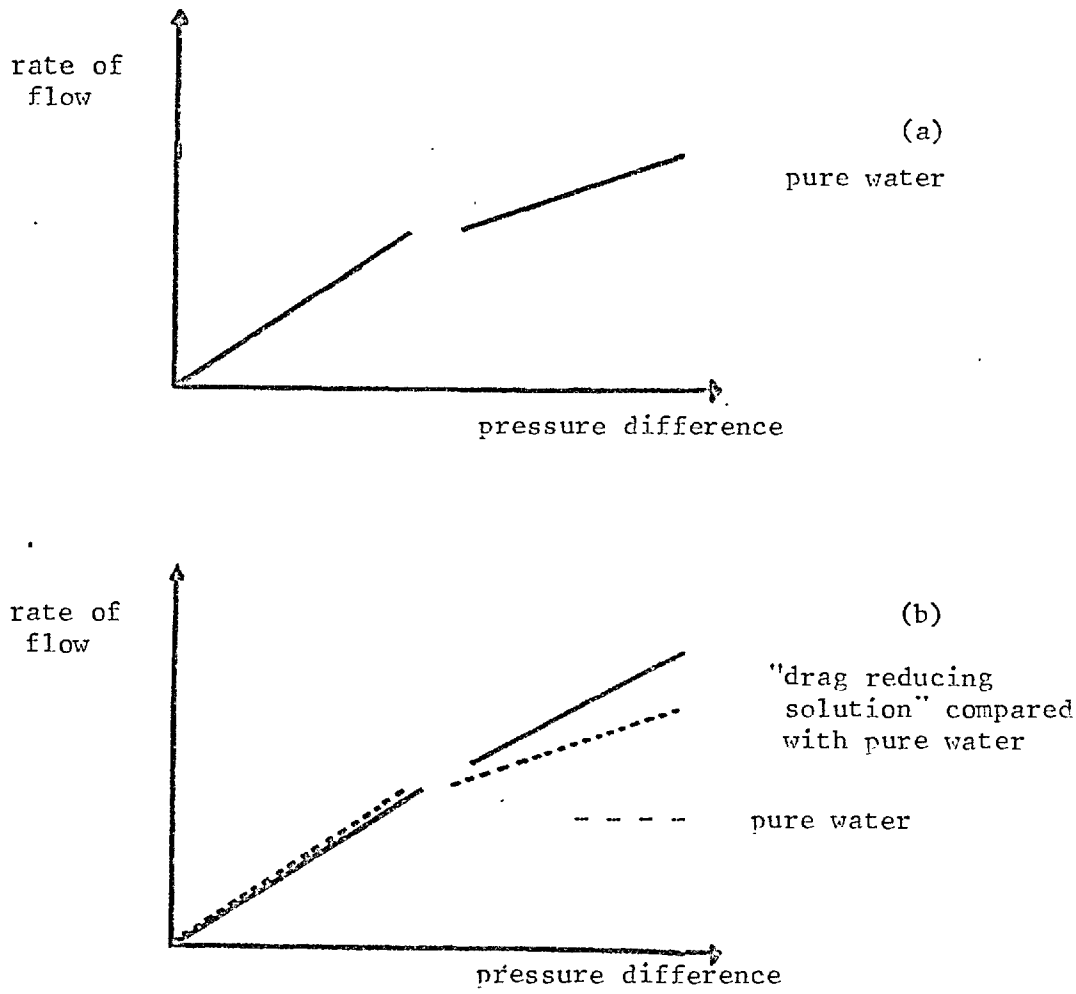


Figure 1.1 Illustration of the drag reducing effect : although the laminar flow viscosity of the drag reducing solution is greater than that of water, resulting in a decreased flow rate, the flow rate shows a considerable improvement in the fully developed turbulence region.

the pressure needed to force a quantity of liquid through the pipe by a factor as high as 80%. This "drag reduction" is often called the Toms Effect, since Toms (1948) was the first to recognise it, in the flow of chlorobenzene containing polymethylmethacrylate. Figure 1.1b shows the type of curve found for this phenomenon. Whereas the slope of the laminar region is slightly reduced, as would be expected from the increase in liquid viscosity due to the polymer molecules, the slope of the fully turbulent region is drastically increased.

Although interest in the phenomenon has been intense following the work of Fabula (1963) on solutions of poly(ethylene oxide) in water, a complete explanation of the effect has still not been found. The mechanism of turbulence itself is not fully understood, and the descriptive laws applicable to most liquids, such as water, are incapable of predicting such large effects as are found in certain polymer solutions. The difficulties are increased by the extremely low concentrations of polymer which will produce a large effect.

The polymers which are found to be most effective are generally those which are linear and have a high average molecular weight, the drag reduction for a given concentration increasing as the chain length increases within the same homologous series. Thus, Hoyt and Fabula (1964), in an extensive review of a wide range of possible materials, found that the most effective polymers were those with straight chains and molecular weights greater than 2×10^5. The four outstanding materials found were poly(ethylene oxide), polyacrylamide, sodium carboxymethylcellulose, and

guar gum. Poly(ethylene oxide) appears to be the most efficient, and has been extensively used in investigations p ly for this high efficiency, and partly because of the wide range of molecular weight fractions commercially available.

B. THE FLOW OF POLYMER SOLUTIONS.

Polymer solutions in general exhibit complex flow properties, and are usually non-Newtonian in laminar flow. The presence of dissolved polymer molecules produces shear rate dependence and often elastic effects. A 1% solution of poly(ethylene oxide), molecular weight 4×10^6, has a viscosity which decreases rapidly with increasing shear rate (Harding and Rose, 1969). This is termed pseudo-plasticity. 1% solutions of some commercially available polyacrylamides not only show pseudo-plasticity, but after stirring, the liquid is observed to come to rest and then move in reverse for a short distance. This recoil, or "recoverable shear" is evidence of shear elasticity, caused by the interaction of the polymer chains with the solute and with each other.

Having given these examples in order to demonstrate that polymers in solution are expected to show rather irregular flow effects, it should be stressed that for the concentrations found to show drag reduction, these effects are very small, and rarely detectable. The laminar flow viscosity measured in some of the solutions is so close to that of pure solvent that pseudo-plasticity could never have more than a negligible effect (Gadd, 1965).

Another manifestation of polymer viscoelasticity is in the occurrence of "normal stress effects". When the solution is subjected to simple shear, the polymer chains expand slightly, and although normally isotropic, the solution acquires an axis of principal strain, inclined at 45° to the shear direction (Treloar, 1968). In addition to the stress tangential to the flow direction therefore, there is a normal stress component, related to the storage of elastic energy in the solution. The presence of normal stress was detected by Gadd (1965) in the deflection of fine jets of poly(ethylene oxide) solution, concentration 3×10^{-5}, from a submerged flat plate. This effect eventually disappears with ageing of the solution, indicating a lessened significance in relation to drag reduction, which still persists (Brennen and Gadd, 1967).

Theoretical models proposed to explain the effect have considered a form of "slip" of the liquid near the solid boundary (eg. Gadd, 1966), as well as the effects of elasticity, but none yet seems to give a perfectly satisfactory explanation. The difficulties are increased by the variety of materials which have been observed to produce drag reduction. Savins (1969) reports up to 83% reduction in micellar soap systems, and asbestos fibre is apparently also effective. A possible link between these dissimilar materials concerns their anisotropy, but it is by no means clear whether this would be related directly to the elongated nature of the particles, or to the associated elastic effects, or even to a mixture of both.

Experimental investigation of drag reducing liquids has proved very difficult. Apart from measurements of the effect itself in a variety of different flow systems, there appear to be few measurements which give information about either the materials themselves or the structure of the turbulence they produce. Standard techniques of investigation of turbulent flow observing the pressure fluctuations in pitot tubes and the variation of heat transfer from a hot wire seem to be invalid because polymer is likely to become adsorbed on to the solid surfaces introduced into the liquid, changing their response to the turbulent fluctuations. Recent investigations using forms of laser velocity meter (eg. Rudd, 1969) show considerable promise, the technique measuring Doppler shifts in light scattered from particles in the flowing liquid.

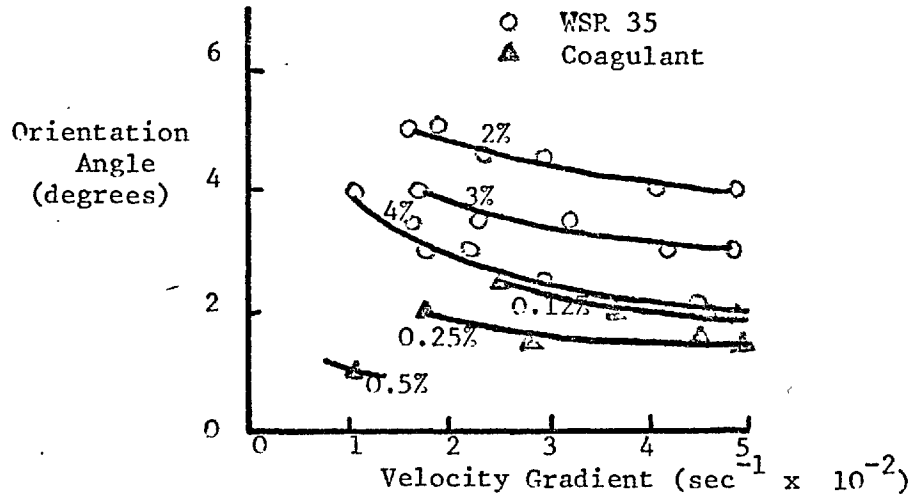
Investigation of the laminar flow properties of the polymers has also proved rather unproductive. Viscosity has been measured (eg.Little,1967) but, at the drag-reducing concentrations, deviation from pure solvent viscosity is small. Accurate capillary viscometry is complicated by the effects of adsorption of polymer on the inner walls of the tube, effectively reducing the diameter (Öhrn, 1955). Another property of the polymer in solution which should indicate how it is reacting to the liquid flow is the flow birefringence. At rest, the segments of the molecule are orientated randomly at each "joint", and for a very large number of segments, the chain tends to coil into an almost spherical volume, giving the liquid isotropic optical properties. According to the analysis of Peterlin (1967a) extending the statistical approach of Rouse (1953)

and Zimm (1956), when the solvent flows through the random coil, the hydrodynamic interaction between molecule and solvent tends to stretch the coil by a small amount and induce axes of anisotropy in the liquid.

This anisotropy is related to the normal stress effects described above, and may be detected by its effect on polarized light. The presence of any small particles in a liquid, whether dissolved or suspended, changes the refractive index of the liquid, and if non-spherical particles are given a preferred orientation, then the refractive index seen by plane polarized light will depend on the angle between the plane of polarization and the particle orientation.

As a dilute polymer solution is subjected to steady shear, an initially spherical random coil will be distorted by the shear gradient across it. The distorted molecule is then acted on by the flow in the same way as on an elongated rigid molecule, becoming oriented initially at 45° to the flow direction, and as the velocity gradient increases, this angle is reduced, often to less than 5°.

The result of this combined distortion and rotation is the establishment of optical axes in the liquid. The two measurable quantities in a birefringent system are the change in refractive index, or birefringence, and the extinction angle, which is equivalent to the orientation of the principal axis of the strain ellipsoid in the flow field. The magnitude of the birefringence is related to the molecular strain, and gives an indication of the way the polymer chain is reacting to the shear flow.



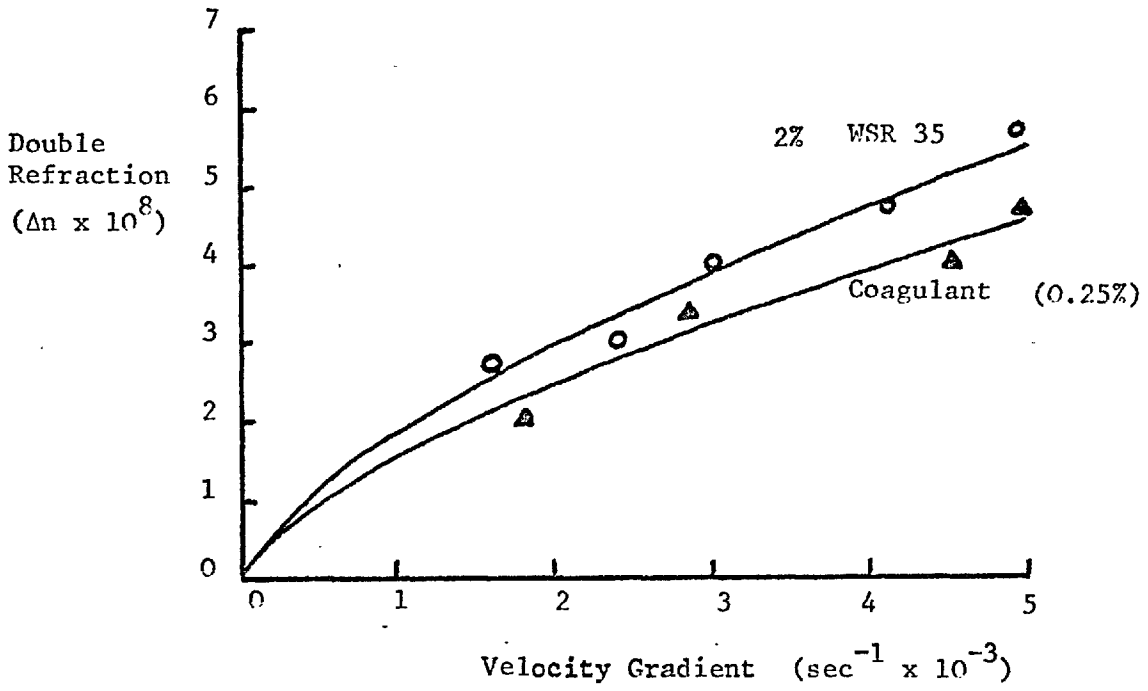


figure 1.2 Flow birefringence in two of the "Polyox" series of poly(ethylene oxide) samples (Little, 1967, 1969a).

Little (1967, 1969a) has reported flow birefringence measurements on the Union Carbide "Polyox" range of poly(ethylene oxide) fractions often used in drag investigations. His results for two molecular weight fractions are given in figure 2. The two samples shown are WSR 35 and Polyox Coagulant of average molecular weights $^{2} \times 10^{5}$ and 6×10^{6} respectively. The orientation of the molecules is seen to be rapidly approaching close alignment with the flow, the effect being greater for the higher molecular weight fraction, and the birefringence is produced at much smaller concentrations for the longer molecules. This agrees with the expected dependence of flow orientation and deformation on chain length for a fairly concentrated solution (Peterlin, 1954), but these high concentrations invalidate the interpretation of the results using the available dilute solution theory, and are of limited use in predicting the behaviour of drag reducing concentrations. The apparatus used for this work produced shear in the annulus between concentric cylinders, the outer one being rotated. Little encountered experimental difficulties in the extension of the working range to more significant polymer concentrations, and the achieved range of investigation is rather limited, both in concentration and in shear rate variation.

C. THE APPLICATION OF ACOUSTIC TECHNIQUES TO THE STUDY OF POLYMER SOLUTIONS.

The advantage of acoustic methods of investigation is that they produce accurately reproducible changing flow conditions. Steady flow investigations cannot indicate the time taken by the system to reach the measured steady state, and since the microscopic flow changes present in

turbulent flow are characteristically of a short time scale, steady flow measurements may not be very relevant. Thus, although the results of Little described above would allow prediction of the inclination and extension of polymer molecules in a given steady shear flow system, no indication can be given of whether these conditions are likely to occur in a practical flow system disturbed by rapid fluctuations.

The introduction of a variable time scale into the flow makes available information about the response time of the system, and therefore represents a useful dynamic extension to the steady flow measurements.

The propagation of longitudinal acoustic waves in polymer solutions produces rapid liquid particle oscillations in the propagation direction, and the polymer molecules are hydrodynamically distorted in the way described above for steady shear flow. The molecular rotation produced in shear flow does not occur in longitudinal waves, since the only velocity gradients are in the direction of particle motion. Apart from this factor, it seems valid to assume (Peterlin, 1967b) that the mechanism of polymer molecule distortion is identical in the two cases. Polymer distortion in the form of birefringence has been detected in solutions of polystyrene in toluene (Hilyard and Jerrard, 1962), although its magnitude is so small that it may not always be possible to produce consistent results (Darlington, 1967). The acoustic intensities used have to be close to the onset of streaming and cavitation in order to produce measurable birefringence even with fairly concentrated solutions.

The propagation of transverse waves (shear waves) in polymer solutions will not be limited by cavitation, as no acoustic pressure is directly communicated to the liquid. Since particle motions are at right angles to the propagation direction, momentum will not be communicated to the liquid in this direction, even though the wave motion is highly damped, and streaming will not therefore occur. A purely viscous simple liquid will only support shear waves because of the viscous interaction between adjacent liquid layers when one layer is made to execute a sinusoidal in-plane oscillation. Transverse momentum is propagated in the direction perpendicular to the oscillating plane. Because of the non-conservative nature of the propagation mechanism, the energy loss is extremely high. It is evident that the liquid motion in this form of wave system is more relevant to the flow system being investigated than is the longitudinal wave system, and it is worthy of consideration as a possible investigation.

Thurston and Schrag (1964) have measured the shear wave birefringence of a 2% solution of polystyrene in Aroclor 1248 (a chlorinated di-phenyl) by analysing a narrow circularly polarized beam of light travelling through the liquid parallel to an oscillating plate and perpendicular to its vibration direction. There is a limitation present with this technique, in that the light beam cannot approach the plate closely without anomalous effects, and it is possible that reflection of the beam from the plate at a glancing angle, following Pen'kov (1961), may give an increase in sensitivity. Thurston and Schrag detected enough birefringence to measure with simple techniques,

and therefore it should also be possible to improve the sensitivity considerably by the employment of electronic signal averaging techniques. Improvements of this nature may permit the measurement of the birefringence of aqueous polymer solutions at low concentrations, although it should be mentioned that an attempt to execute these improvements as part of the present investigation was not successful. The difficulties were of a practical nature, concerned with the production of large amplitude in-plane oscillations of a flat wave-generating plate, and reduction of electronic noise, and time did not allow their solution.

A third form of acoustic investigation initially considered to be of use in the investigation of the flow properties of aqueous polymer solutions is that using transverse surface waves or ripples. The particle motion associated with ripples is basically circular, particles at the surface describing circles about a horizontal axis perpendicular to the propagation direction. The behaviour of a homogeneous liquid in a ripple system includes steady velocity gradients in a rotating flow pattern as well as a rapid transition between the oscillating surface particles and the less mobile particles at greater depth. Since this flow is in some respects similar to the particle motions in turbulent flow near a solid surface, it was considered that the effect of drag reducing concentrations of polymers on the damping of waves should be investigated.

As will be shown in Chapter 7, the expectation of homogeneity in the solutions was in error. It was found that the surface wave properties,

particularly the damping, were principally controlled by surface elasticity rather than by the bulk liquid properties. The exceptional surface activity of poly(ethylene oxide), to be described fully later, produces such a great surface concentration that bulk liquid effects would be heavily masked.

D. THE POSSIBILITY OF AN ADSORPTION EFFECT IN DRAG REDUCTION.

The possibility that the strong adsorbing effect of polymers may be connected with the drag reduction phenomenon has been suggested by Davies and Ponter (1966). It has been observed by workers measuring drag reduction that low drag can persist in the system for long periods after the replacement of drag reducing liquid with pure solvent. El'perin and Smolski (1965) report this in the investigation of aqueous carboxymethylcellulose solution flowing through a glass pipe. Upon replacing the solution with distilled water, drag reduction was found to persist, even sometimes to improve. Their explanation of this was that drag reduction must be related to the formation on the pipe walls of an adsorbed polymer layer, which is not immediately removed by washing, and this conclusion is supported by the soapy feel of solid surfaces after their prolonged immersion in the polymer solutions.

An attempt to repeat the above observations was made by Little (1969b) using a closely similar system, and he found reduction persistence of 4 or 5 minutes. However the addition of tracer dye to the drag reducing fluid showed that after displacement by the undyed clean water of the polymer from the main part of the tube, enough dyed fluid was

still coming from pressure tap connections to maintain a reducing effect, and that the earlier results may have been in error because of this.

The two most effective drag reducing polymers are found to be extremely surface active. Poly(ethylene oxide) was shown by Little (1967) to adsorb on to glass spheres; its adsorption behaviour at the liquid/air surface was investigated in the present work, and will be described in Chapter 7. The other efficient class of drag reducing polymer, the polyacrylamides, was found to be much less active at the liquid/air surface, although adsorption on to solid surfaces is marked. The ability of polyacrylamides to form polymer "bridges" between colloidal particles explains their widespread use in flocculation (the rapid removal of colloidal material from a liquid by particle aggregation).

The significance of adsorption effects is not yet known, and it is possible that the adsorption behaviour of the polymers is purely coincidental to their drag reducing properties. From a turbulent flow point of view, a polymer layer would need to be 10^{-2}cm thick for its concentrating effect to affect the boundary layer. Equilibrium adsorption on a solid surface in a layer corresponding to "monolayer coverage", is predicted to produce layers only about 10^{-6}cm thick (Silberberg, 1962), although Öhrn (1958) has reported layers of 1.5×10^{-5} cm thickness in a polystyrene/toluene system using precision viscometry in narrow capillaries. This suggests multilayer adsorption, which is difficult to explain with polymer molecules. Little (1967) attempted a correlation of turbulent flow properties with the existing

theory of multilayer adsorption due to Brunauer, Emmett, and Teller (1938) but the implications of this are not clear.

The phenomenon of turbulent flow drag reduction has been shown to be an extremely strange effect without precedent in either of the two inadequately understood areas of science involved: turbulent flow and polymer physics. Acoustic methods of investigation have been little employed, and the present work is an attempt to investigate the polymers using surface waves, one of the forms of acoustic excitation outlined above. Although the study of surface waves on polymer solutions has been found not to indicate the properties of the solutions in flow situations relevant to drag reduction, the technique has been established as a useful means of investigation of the behaviour of the molecules in solution, in particular close to the liquid/air interface.

CHAPTER 2

SURFACE PROPERTIES OF LIQUIDS

(i) Surface Tension Theory.

The boundary between a liquid phase and a gaseous phase appears to be sharp when observed visually, but on the scale of molecular dimensions, the transition between the phases is more gradual. Violent disturbances resulting from the similarity between the magnitudes of molecular kinetic energy and binding energy promote a continually changing interface. The binding forces in a pure liquid have more effect on molecules within the bulk of the liquid than on those situated at a surface, and they tend on average to make the surface slightly depleted in order to minimise the total energy of the system. The slightly greater mean intermolecular distance at the surface produces a net attraction in the surface layers, observed as a force acting in the surface which tends to reduce the total surface area (Walton, 1969).

It is this force which is known as surface tension or capillarity. Although the intermolecular attraction tends to minimise the area of the liquid/gas interface, in equilibrium the force is independent of total area, because except for extremely small volumes of liquid, the molecules will always settle into the same statistical distribution. The time needed for the attainment of equilibrium surface tension in a pure, homogeneous liquid composed of simple small molecules appears to be very small.

Surface tension may be defined in a way more adapted to practical use as the force per unit length exerted in the tangent plane to the surface in a direction normal to an element of a line drawn in that surface through any point (Champion and Davy, 1959). In c.g.s. units, which will be used throughout this work to conform with the usual practice in liquid surface physics, it is measured in dyn.cm^{-1}. The Helmholtz free energy per unit area of surface, usually termed surface energy, has units erg.cm^{-2}, and is identical to the surface tension in the pure liquid case. It follows from rigorous thermodynamics that this identity is not applicable to multicomponent systems such as occur when dissolved material is present in the surface.

The surface tension of a pure liquid is usually modified by the addition of other materials. Aqueous solutions of inorganic salts have surface tensions higher than that of pure water, and on the other hand dissolved organic material usually decreases the surface tension. The reduction of surface tension by the presence of dissolved organic material is most often due to the presence in the molecular composition of hydrophilic parts (such as hydroxyl groups, -OH), which are readily acceptable to the water structure, and hydrophobic parts such as hydrocarbon chains, which are not energetically acceptable to the arrangement of the water molecules. On diffusing to the water surface, this type of molecule is able to orientate itself so that the hydrophobic portion stands out of the surface while the hydrophilic part occupies a position in the surface. The short range nature of intermolecular forces

means that the water structure is no longer dislocated by the "foreign" hydrophobic chain, and the energetically welcome hydrophilic group is allowed to interact with the water molecules. The whole organic molecule is in a more stable state at the surface than in the bulk, and a disproportionate number will accumulate there. The violent thermal motion of the liquid is expected to maintain dynamic equilibrium between molecules entering and leaving the surface, and the excess of solute molecules in the surface will be constant for a given bulk concentration.

This process of becoming attached to, or positioned in the surface is called adsorption, and the reverse mechanism, in which a molecule returns to the bulk liquid is known as desorption. Materials whose molecules find themselves energetically suited to positioning at an interface are surface active, and are also called surfactants.

Since a free surface is required for the above type of process, the resulting adsorbed layer of molecules is essentially one molecule thick. This monomolecular layer, or monolayer is therefore in some respects two-dimensional, which fact often considerably simplifies the analysis of mechanical interaction between surface molecules. Whereas the adsorption of gases on to solid surfaces can result in layers deeper than monolayers, i.e., multilayers (Brunauer, Emmett and Teller, 1938), this behaviour is not observed at a liquid/air surface.

It was mentioned earlier that the attainment of equilibrium surface tension in a pure liquid was a rapid process. The time taken is so short that experimental techniques of tension measurement such as the oscillating jet method (see Section (ii)h) fail to detect any difference from equilibrium at surface lifetimes as short as 10^{-3} sec. Measurements of the shape of rapidly moving bell-shaped sheets of liquid indicate qualitatively that surface tension may be higher at shorter lifetimes, but the interpretation of these results is not easy.

When a surface is freshly created in an aqueous solution of a surface active agent, equilibrium is observed to be considerably more delayed than in the pure liquid. This is due to the disproportionately high surface concentration of active molecules necessary for equilibrium, and the time required for their relatively slow diffusion from the bulk to the surface. At about 1 msec, therefore, the surface tension is nearly the same as that for pure water, equilibrium gradually taking place in a time which can vary between several milliseconds and several days, depending on the properties of the active molecules and their concentration.

The mechanisms so far described have been of the effects on surface tension of dissolved surface active material. Monolayers may also be formed of insoluble compounds, by the techniques of "spreading". The spreading of oil on water was described by Franklin (1774) and it may be deduced from his account that the resulting layer was about 25 Å thick. This is of the order of molecular dimensions, and denotes the presence of an oil monolayer. Spread and adsorbed monolayers have the

same sort of effect on the surface tension. A given insoluble layer contains a fixed quantity of active material, and its concentration in the surface is therefore dependent on the extent of the area covered, in contrast to a layer adsorbed from solution, which is in equilibrium with the bulk and will always show a constant surface concentration for a given bulk concentration, independent of surface area. (It is usually assumed in solutions of surface active agents that the total adsorbed amount is small compared to the total dissolved amount). It is in this differing reaction to area changes that the principal distinction between the two types of monolayer lies.

The thermodynamics of solution surfaces has been analysed by Gibbs (1928). It is convenient to describe the surface composition in terms of surface excesses Γ_i (moles. $cm.^{-2}$, positive or negative) of the i components present in the surface. The surface excess represents the difference in surface concentration between the real system and an imaginary system in which the liquid is homogeneous up to a perfect geometrical boundary. It approaches the absolute surface concentration when the solution is very dilute, but is only identical when all the active material is adsorbed at the surface, as with a spread monolayer. The relevant equation describing the behaviour of a plane surface of a liquid (component 1) at constant temperature containing a single dissolved component (2) can be written (eg. Gaines, 1966) as

$$d\sigma + \Gamma_1 d\mu_1 + \Gamma_2 d\mu_2 = 0 \qquad 2.1$$

where σ is the surface tension, and μ_i is the chemical potential of component i. The mathematical surface represented by this equation may be arbitrarily defined, and is conventionally taken to be where the solvent surface excess vanishes.

Thus

$$d\sigma = -\Gamma_2 d\mu_2 \qquad 2.2$$

Writing the chemical potential μ_2 of the solute as

$$\mu_2 = \mu_2^0 + RT \ln f_2 N_2 \qquad 2.3$$

where R is the gas constant, T the absolute temperature, μ_2^0 is a constant, and f_2, N_2, the activity coefficient and the mole fraction of the solute, eqn. 2.2 becomes

$$\Gamma_2 = \frac{-f_2 N_2}{RT} \frac{\partial \sigma}{\partial (f_2 N_2)} \qquad 2.4$$

This is Gibbs' adsorption isotherm, which allows the solute surface excess to be found from the variation of surface tension with solute concentration. The behaviour of the solution is termed "ideal" if $f_2 = 1$, making eqn. 2.4.

$$\Gamma_2 = \frac{-N_2}{RT} \cdot \frac{\partial \sigma}{\partial (N_2)} \qquad 2.5$$

For a very dilute solution, the mole fraction N_2 is proportional to the concentration c, giving

$$\Gamma_2 = \frac{-N_2}{RT} \cdot \frac{\partial \sigma}{\partial c} \qquad 2.6$$

Lucassen-Reynders and van den Tempel (1964) generalize the above Gibbs treatment, removing the arbitrary step of choosing the surface excess (or adsorption) of solvent to be zero and considering the effect of the surface conditions on the activity coefficients f_i. Their general "equation of state", relating surface tension to excess of solute molecules present in the surface, will reduce to the ideal case on making the activity coefficient unity, but remains valid for more complex cases.

Three previously determined empirical relations between σ, c, and Γ_2 follow in the ideal case:-

a) the Szyszkowski (1908) equation,

$$\sigma_o - \sigma = RT\Gamma_\infty \ln(c/a + 1) \qquad 2.7$$

b) the Langmuir (1917) equation,

$$\Gamma_2 = \Gamma_\infty \frac{c}{c + a} \qquad 2.8$$

and c) the Frumkin (1925) equation,

$$\sigma_o - \sigma = - RT\Gamma_\infty \ln(1 - \Gamma/\Gamma_{2\infty}) \qquad 2.9$$

σ_o is the pure liquid surface tension, Γ_∞ the saturation value of the adsorption, and a is a constant which represents the solute concentration for which adsorption is half the saturation value. a is thus a measure of the surface activity of the solute.

As indicated, the Gibbs equation provides a means of determination of the relation between the solute surface excess and the solution concentration. This important relation is known as the adsorption isotherm, and it may also be obtained by comparison of the σ/c curve with a σ/Γ curve obtained by spreading the material as an insoluble monolayer, and measuring the surface tension before appreciable desorption can take place. The three equations given above are also very useful in characterisation of the surface properties. The Langmuir isotherm (eqn. 2.8) was shown by Lucassen-Reynders and van den Tempel to be applicable to a wide range of systems, many of which appeared to have ideal surfaces in spite of the non-ideal nature of their bulk solutions. The Szyszkowski equation (2.7) follows from a combination of the Langmuir isotherm with the Gibbs relation (eqn. 2.6). The Frumkin equation (2.9) also follows from this relationship, and is the surface equation of state for ideal behaviour.

Lucassen-Reynders (1966) showed that ideal surface behaviour occurs when hydrophobic chain interaction is unimportant, as with substances having short hydrocarbon chains. One of the more common forms of non-ideal behaviour was described by Frumkin (1925) in the adsorption of long chain fatty acids, and is called "regular" behaviour. In this

case, the logarithm of the activity coefficient of each component varies linearly with the squared concentration of the other component (Lucassen-Reynders and van den Tempel, 1964). Equations representing the equation of state and the adsorption isotherm are given by Lucassen and Lucassen-Reynders (1967) as:-

$$\frac{\sigma_o - \sigma}{-RT\ \Gamma_\infty} = \ln(1 - \Gamma/\Gamma_\infty) + \frac{H^s}{RT}(\Gamma/\Gamma_\infty)^2 \qquad 2.10$$

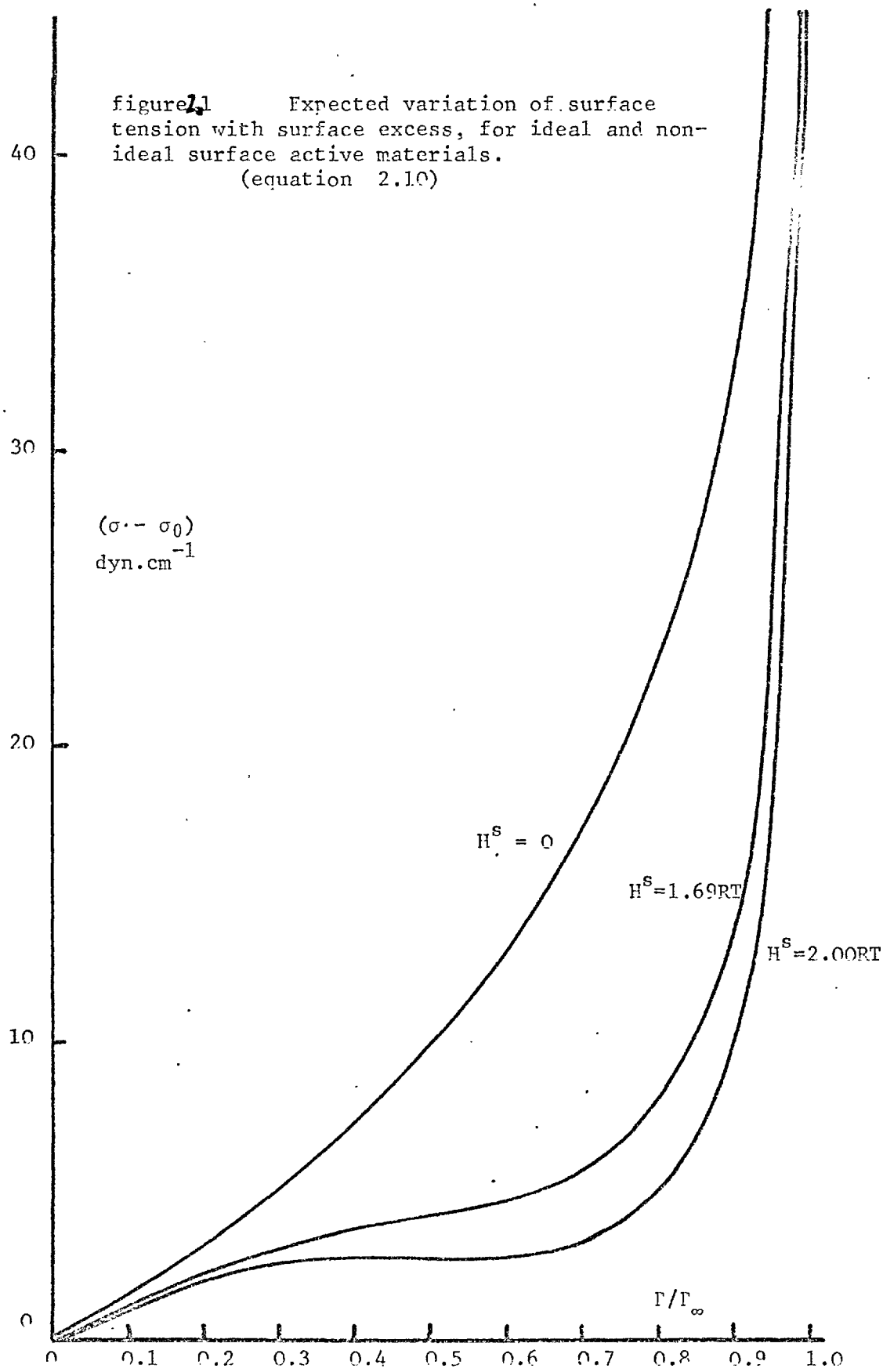
$$c/a = \frac{\Gamma/\Gamma_\infty}{1 - \Gamma/\Gamma_\infty} \exp\left\{\frac{-2H^s}{RT} \cdot \Gamma/\Gamma_\infty\right\} \qquad 2.11$$

When the non-ideality parameter H^s reduces to zero, equations 2.10 and 2.11 become identical to equations 2.9 and 2.8 above, which represent the ideal surface. Figure 1.1 shows the variation of $(\sigma_o - \sigma)$ expected as the non-ideality parameter increases from zero. The adsorption Γ is seen to increase much more rapidly at low surface pressures than in the ideal case.

(ii) The Measurement of Surface Tension.

It was mentioned in the previous section that the time taken for a solution of surface active material to reach surface equilibrium could vary over a very wide range of time scales. In most practical applications of surface active agents, it is necessary to know how quickly equilibrium will be established and how the surface tension

figure 1.1 Expected variation of surface tension with surface excess, for ideal and non-ideal surface active materials. (equation 2.10)



will change with time, these considerations often being as important as the final surface properties. The following description of the measurement techniques used in surface tension investigations will stress their usefulness in this respect. Another consideration of importance in the discussion of a technique is its applicability to the study of spread surface layers. The comparison of solution properties with spread monolayer properties is often found helpful, and is preferably carried out using the same measurement technique.

Liquid surface tension is observed as a scalar quantity indicative of the energy of the liquid surface. This energy is proportional to the surface area, and the tension always acts towards a reduction of this area. Measurement of surface tension is usually by means of measuring the force needed to maintain a surface in a state of deformation. Techniques to be considered here are

(a) capillary rise

(b) the Wilhelmy plate

(c) ring and plate detachment

(d) the Langmuir film balance

(e) bubble pressure and drop weight

(f) bubble and drop shape

(g) ripples

(h) oscillating jets

Although not strictly an absolute surface tension measurement, the Langmuir film balance method, which measures differential surface tension, or surface pressure, is included because of its application to systems of spread monolayers.

(a) Capillary rise.

When a liquid wets a solid surface, it spreads until it reaches a specific angle of contact at the junction of the three phases, solid, liquid, and gas (or vapour). When a capillary tube is placed in the liquid, the surface tension acts upwards round the periphery of the cylindrical liquid column and produces an upward movement which ceases when the tension is balanced by th· weight of liquid. Similar effects occur between parallel plates and between a pair of vertical plates touching with a small included angle (Champion and Davy, 1959). Some difficulties of interpretation arise in this type of measurement, mainly concerned with the presence of a solid surface at the critical part of the liquid/air interface (Walton, 1969). The method is most useful in cases where the angle of contact between liquid and solid is nearly zero (ie. complete wetting and spreading), because in this instance, capillary rise should be independent of the properties of the solid. This independence is not always found. For a glass tube, the column height may depend on the ionic content of the glass, on the production process, and the method of ageing (Holland, 1964).

Ignoring these finer points, capillary methods are often found to be very accurate, although requiring empirical calibration. This calibration obviates the need to know accurately the dimensions of the capillary bore, the effects of bore unevenness being minimised by the adjustment of the tube position so that the meniscus is always measured in the same section. The use of capillary techniques for the investigation of surface active solutions is hampered by the length of time needed for equilibrium to take place by diffusion of solute along the narrow liquid column. This time may be prohibitively long for practical use (Padday, 1960). Another form of capillary method involves the measurement of the hydrostatic pressure needed to make a concave meniscus a perfect plane (Ferguson and Kennedy, 1932). A small volume of liquid is placed at the end of a horizontal capillary, and the gas pressure in the tube is slowly increased, forcing the liquid to the end of the bore, where its reflection properties are examined with a microscope. When this meniscus reflects as a plane, the surface tension associated with it, which before tended to keep the liquid in the tube, can no longer do this, and the gas pressure is balanced only by the meniscus force at the other end of the liquid cylinder. The principal advantage of the method lies in the small volume of liquid needed. As with all capillary techniques, the interaction of the solid surfaces with the liquid is a disadvantage, and the preparation of the open end of the tube imposes an extra experimental difficulty in this particular case.

(b) The Wilhelmy plate.

In this technique, a thin flat plate is suspended vertically in the surface, and in the case of an acute contact angle, the meniscus curvature produced by the spreading of the liquid on it will exert a downward pull proportional to the plate perimeter touching the surface and the surface tension. Knowledge of the contact angle is required, but this is an easier condition in this case than it was with capillary rise methods. For liquids such as water and aqueous solutions, where the contact angle is near zero, the glass surface can be made experimentally predictable by fine grinding. Wetting can be observed to take place by the changed translucency of the wet surface of the glass.

There are two principal ways of using the Wilhelmy plate for measurement of surface tension changes, measuring either the force exerted by the surface for a fixed plate immersion, or the plate immersion for a fixed force. In the first case,

$$\Delta\sigma = \Delta F/2p \qquad 2.12$$

where $\Delta\sigma$ is the change in surface tension, ΔF the measured force change, and p the perimeter of the solid/liquid boundary. For a fixed force, a reduction of surface tension is balanced by the increased gravitational force due to partial withdrawal of the plate from the surface. The relevant expression is

$$\Delta\sigma = \tfrac{1}{2}\rho_1 g t \Delta h \qquad 2.13$$

where ρ_1 is the liquid density, g the gravitational acceleration, t the plate thickness, and Δh the distance withdrawn. Between these two extremes, there are a variety of simple variations. The plate may be hung from a horizontal beam fixed to a torsion wire, the tension-opposing force being provided partly by balancing weights and partly by wire torsion. This type of apparatus has been described by Nakamura and Sasaki (1967), who amplify the rotation of the beam under the surface pull by an optical lever. The wire and lever are calibrated together by suspending weights from the plate position.

It is one of the advantages of the system that the actual method of measurement may be adapted to suit the accuracy required, the basic surface interaction remaining simple. The liquid bulk is minimally affected by the intrusion of the plate and time variation should be an accurate indication of the true surface behaviour. Blank et al. (1970) use a constant immersion arrangement, making the force measurement automatic with an electric balance, for the investigation of long period cyclic variation (0.4 to 4.0 cycles per minute). Time varying behaviour is thus conveniently measurable, and both spread and solution monolayers may be investigated. In his comparison of the available techniques of static surface tension measurement, Padday (1960) found the Wilhelmy plate the most satisfactory.

The principal disadvantage of the method is that it still relies to a certain extent on the properties of the liquid close to the solid surface. Although roughening the plate improves the wetting, effects of evaporation from the thin layer of surface active solution are rather

uncertain, and the movement of the plate in and out of the surface may encourage deposition of material on it, affecting its wetting properties. These effects may be reduced by total enclosure of the surface.

(c) Ring and plate detachment.

If the Wilhelmy plate is withdrawn slowly from the surface, and the maximum pull measured immediately before detachment, then wetting difficulties should be minimised. The detachment of both plates and horizontal platinum rings was compared to the Wilhelmy plate measurements by Padday (1960), who found that they tended to produce relatively high results for the surface tension of solutions. The lack of reproducibility of this method was mentioned by Boucher et al. (1967). These effects were ascribed to the stretching of the surface as maximum pull is reached, which reduces the effective adsorption and increases the measured surface tension. The method is therefore not suitable for solutions whose equilibrium is not rapid so that time variation cannot be studied.

(d) The Langmuir film balance.

This is not strictly a method of surface tension measurement, as it measures differences of tension, often called surface pressures following the analogy which compares the reduction of surface tension by added surface active molecules with the increase of pressure in a two-dimensional "gas". A floating barrier divides a rectangular trough into two surfaces, one of which is kept clean, and the other of which is used for the spreading of monolayers. Differences of surface tension between the two

surfaces produce a horizontal force on the barrier, which may be counterbalanced by levers and weights of known magnitude. The original balance (Langmuir, 1917) used air jets to prevent surface leakage round the ends of the barrier, but this is now usually accomplished by the use of thin flexible foils joined to barrier and trough. Torsion wire restoring devices are often used in place of the lever and weight method. Because the same bulk liquid is used for both surfaces, the technique is not suitable for solution measurements.

(e) Bubble pressure and drop-weight.

The excess pressure inside a gas bubble formed in a liquid is related to the surface tension. A steady flow of gas from a capillary orifice submerged in the liquid will produce a bubble of steadily increasing pressure, the maximum being reached just before bubble detachment (Champion and Davy, 1959). The surface tension may be found be measuring the peak pressure and the capillary radius at the open end. The method is often called Jaeger's method, and it has been found useful for measurement of surface tension over a temperature range, although it cannot be used when the equilibrium is not rapid, due to changing surface area at the moment of measurement. Sugden (1922) gives tables of corrections to be made for the influence of capillary radius on the bubble size.

The drop weight method is a sort of inverse of the bubble method. The mass or volume of a drop falling from a vertical capillary tube is determined by the outside diameter of the end of the tube, the liquid density, and the surface tension at the moment of falling (Harkins and Brown, 1919). The rate of flow must be small if "overloading" of a drop is to be prevented, and the continuously expanding surface makes interpretation difficult unless equilibrium times are known to be very short. Boucher et al. (1967) have used this method with surface active solutions, obtaining results in agreement with Wilhelmy plate determinations. In attempting to investigate the time variation of polymer solution surface activity, Glass (1968a, b) measured the weights of drops at different lifetimes. Evidence will be presented in Chapter 7 which suggests that some of these measurements are in error, due to the assumptions made in prediction of the equilibrium behaviour of the solutions. The technique appears to be useful only for solutions which achieve equilibrium during the period of drop formation. Care must be taken with volatile liquids to prevent evaporation from the drops.

(f) Bubble and drop shape.

The measurement of the shapes of bubbles and drops has been shown by Ferguson (1913) to allow the deduction of surface tension. A drop is formed on the lower end of a capillary tube, and is photographed in well-collimated light. Measurement of only three dimensions from a single photograph using a travelling microscope allows the surface tension

to be calculated if the liquid density is known. This technique is ideal for the investigation of time varying behaviour in solutions, since the drop may be left undisturbed for long periods. The surface area is small, which reduces contimination problems, and perturbations due to the presence of a solid surface are minimised by making the measurements well away from the boundary. Although care must be taken to avoid heating of the drop by the light beam, and the vibration of the system during the exposure, it is not clear why the method has not been used more often in investigations of surface active solutions. Frisch and Al-Madfai (1958) used the drop shape method to investigate the time-varying behaviour of polymer solutions over periods of up to 3 hours.

(e) Ripples.

This technique will only be outlined here, since a more detailed treatment is given in Chapter 3. The wave velocity of ripples whose wavelength is smaller than 1.7 cm. is principally determined by the surface tension, although gravity plays a lesser part which decreases with decreasing wavelength. Kelvin (1871) derived a relation between surface tension, gravitational acceleration, density and wavelength, neglecting the effects of damping, and although theoretically restricted to an ideal, non-viscous liquid, this relation (equation 3.5) is still quite accurate in the presence of viscosity and surface elasticity. More rigorous theory should be employed to deduce the

true surface tension in the presence of appreciable surface elasticity (Lucassen and Hansen, 1966). For this theory, both the wavelength and damping should be known.

The technique is one of the more satisfactory so far described in that the measurements are independent of contact with solid surfaces. The investigation of time variations in solutions between surface ages of 1 minute and 1 day are possible, and the technique is equally applicable to the study of spread monolayers. Although rapid expansions and contractions are taking place during the passage of the waves, the surface tension measured is that corresponding to the mean adsorption at the time of measurement. Brown (1936) showed that the particle motions at the surface were such that the mean adsorption would be the same as on a still liquid. In the study of adsorbed surface layers, the ripple technique is most valuable for its ability to measure surface tension and surface elasticity simultaneously (section (iv)). Independent measurements of σ are often needed in order to interpret the results obtained from solutions of the hydrodynamic theory, so ripples are not primarily useful as a surface tension measurement. In the absence of exact solutions of the hydrodynamic equations, the accuracy of the method is probably not as high as that of a supplementary determination, e.g. by Wilhelmy plate.

(h) Oscillating jets.

If a jet of liquid issues horizontally from an elliptical orifice at high speed, the surface tension will attempt to reduce the perimeter of the elliptical jet cross-section to its minimum value, which is when the section is circular. On reaching this circular section, the shape will still be changing, and will eventually become elliptical with the original principal axes transposed. There is thus an oscillation of the sectional shape, and because of the forward velocity of the jet, the oscillation is observed as a wave-like disturbance stationary with respect to the orifice. The theory of these oscillations, due to Bohr (1909, 1910) and Stocker (1920) relates the wavelength of the oscillation to the jet velocity, density, surface tension, and the ratio of the major and minor axes of the cross-section at its peak amplitude. This latter quantity is measured by the focussing effect of the liquid cylinder on collimated monochromatic light.

Observations are made on the jet over a series of wavelengths, and because the surface was freshly formed at the orifice, it is possible to estimate its lifetime at different positions along the jet travel. The measurements are therefore dynamic, and it is possible to study the surface tension variation within the first 20 msec of the life of the surface. Sutherland (1950) used the technique to investigate the time-varying behaviour of surface active solutions, although it was later found (Rideal and Sutherland, 1952; Defay and Hommelen, 1958) that the results were more sensitive to the shape of the orifice than

had been expected, making some of them rather doubtful. Bohr's analysis was for an accurately elliptical orifice, and the only way of achieving this appears to be by making large numbers of approximately correct jets, and rejecting any which do not give predicted results.

One of the difficulties in producing an adequate theory for the oscillating jet phenomenon is that in the tube leading up to the orifice the liquid is not travelling at a uniform speed, but has a velocity profile imposed by the walls of the tube (Hansen et al. 1958). When the tube constraint ceases as the liquid leaves the tube, the profile gradually disappears, but close to the tube, in the "low surface age" region, results cannot obey the free jet theory.

Of the measurement techniques described above, the only ones which can be conveniently used with accuracy on solutions are the Wilhelmy plate, the drop weight, drop shape, ripple, and jet techniques. The only real advantage of the jet method lies in its ability to measure within 20 msec of surface formation, surface tensions far outside this region being inaccessible. Drop weight methods can be used for equilibrium measurements in solutions showing no further variation after about 30 seconds. The remaining techniques, Wilhelmy plate, drop shape, and ripple methods are all excellently suited to solution measurements for systems expected to show time varying behaviour in surfaces more than a few seconds old. The drop shape method is not

quite as versatile as the other two, as spread monolayers cannot be studied.

It will be seen in Chapter 3 that not all of the ripple measurement techniques are ideally suited to the study of time-varying surfaces. The moiré fringe method described in Chapter 4 has been used to determine simultaneously both the surface tension and the surface dilational elasticity of time varying systems. This versatility is tempered by the relatively low accuracy of ripple methods in the surface tension measurement compared with the other two methods.

(iii) Surface Rheology.

When a surface containing adsorbed organic surface active material is stretched, the concentration of material in a given area immediately decreases, and the surface tension increases. A force thus arises which opposes the expansion. This effect, or its inverse, in which naturally occurring surface tension differences cause surface motions tending to reduce the differences, has been observed many times, the earliest apparently being by James Thomson in 1855 (Scriven and Sternling, 1960). It is usually known as the Marangoni effect, since it was discussed by Marangoni (1871), one of the first to appreciate the phenomenon, although it is sometimes called the Plateau-Marangoni-Gibbs effect, in recognition of the explanation given by Marangoni and Gibbs of Plateau's observations on the damping of the oscillations of a needle

held in the surface.

It is apparent that the surface has elastic properties in dilation, which combined with certain shear viscous effects suggest that it should be treated according to a unified rheological treatment such as is found valuable for bulk material description (Tschoegl, 1958). This approach would treat the surface as a two-dimensional viscoelastic fluid, with four elastic constants: dilational elasticity, ε_d , dilational viscosity, η_d , shear elasticity, ε_s , and shear viscosity, η_s.

There are basic physical difficulties in the thorough application of this type of analogy between the elastic properties of a surface and those of a two-dimensional fluid. The principal difficulty concerns the shear properties of the surface. Whereas the analogy with bulk rheology would treat the surface as a thin sheet of fluid, in practice, its interaction with the adhering bulk liquid phase must be taken into account, and experiments intending to measure the shear forces in the interfacial layer should ideally be done in conditions where the bulk flow is completely specified and understood.

It is found experimentally that the motion of an adsorbed layer in shear, without changing the surface area, is accompanied by a viscous energy loss. There are expected to be viscous forces associated with the planar relative motion of the adsorbed molecules in the surface, and it is presumably these forces which would be described by the shear terms in the rheological specification of the monolayer. In addition

to these purely surface forces, the adsorbed layer will also be subjected to forces from the flow of the substrate which must therefore be analysed in order to separate the effects.

The two principal techniques in which shear viscosity effects have been measured, and from which "surface viscosity" has been inferred are the torsional pendulum method and the canal viscometer. The torsional pendulum consists of a horizontal disk or ring suspended by a wire and touching the liquid surface. The damping of the oscillations of the disk is taken to be a measure of the total viscous interaction of the pendulum with liquid and surface. Effects due to the presence of the liquid are assumed to be accounted for by the measurement of damping in a pure liquid surface, and surface viscosity is calculated using formulae adapted to two-dimensional measurement from analogous liquid viscosity theory (eg. Bulas and Kumins, 1958, Boyd and Vaslow, 1958). The method is sometimes modified for continuous rotation of the disk relative to the surface, either by rotation of the disk or by rotation of the liquid. For example, using the rotating liquid variation, Davies and Mayers (1960) measured the induced speed of flow of the surface trapped between two concentric stationary rings. Appreciating the complexity of the hydrodynamics in this system, the authors calibrated the apparatus using films whose "viscosities" had been previously determined using a quite different technique. Recent work by Mannheimer and Schechter (1970) has removed some of the interpretative difficulties of this circular channel "viscous traction" principle,

and their results await independent confirmation. Goodrich (1969) drew attention to the inadequately understood and therefore ignored hydrodynamics of the techniques commonly used for surface viscosity investigations, and presented a rigorous theory to describe the extremely complicated liquid flow associated with the rotation of a disk in the interface.

The second principal technique, the canal viscometer, is often used for insoluble monolayers, and represents the two-dimensional analogue of the capillary flow viscometer for bulk liquid flow. A surface tension gradient is set up which forces the surface material between a pair of parallel vertical planes in the surface, and the area flow is related to the gradient and "surface viscosity" by two-dimensional capillary theory. A correction is usually made for "subphase drag" (eg. Joly, 1938, 1964). A thorough hydrodynamical analysis does not seem to have been carried out on this system, and its results must be treated with caution. Gaines (1966) observed that the "correction" terms introduced in estimation of subphase drag are often as large as half of the uncorrected results. The technique is useful only for insoluble layers, and cannot be used in many systems because of the variation of concentration along the canal caused by the surface pressure difference.

In comparison of the published results of three independent investigations on the same system, Gaines (1966, p.104) showed that "discrepancies of an order of magnitude or more are the rule". The principal difficulties and inadequacies of the application of surface shear concepts to real liquid surfaces appear to be not so much in

experimental design as in interpretation. The surface shear constants ε_s and η_s are likely to have a solid physical basis in terms of molecular motion in the interface, and the experimental techniques developed for examination of the effects of shearing motions involving the surface are possibly the only ways of determining these constants. However, the interpretations applied to many of the experimental results so far produced have involved making simplifying assumptions about the flow conditions present in the systems, and rigorous hydrodynamic investigation of certain of these systems has indicated that these assumptions may not be justified. The value of the resulting "surface viscosity" deductions in the absolute physical description of monolayers is therefore questioned. A series of "surface viscosity" measurements with a single apparatus is likely to have value as a means of comparing different surfactants, but comparisons between different techniques is liable to error.

The value of a unified surface rheology is seen to be greatly diminished at present by the lack of adequate information about the true shear properties of monolayers. The dilational properties are founded on better understood concepts, such as surface tension, adsorption and diffusion, and are therefore of more use in the description of the surface.

(iv) Dilational Surface Properties.

The surface dilational elastic modulus, or surface compressional modulus, ε , caused by the change of monolayer concentration with surface area may be defined by

$$\varepsilon = \frac{d\sigma}{d(\ln A_e)}$$

$$= \frac{d\sigma}{d(\ln\Gamma)} \cdot \frac{d(\ln\Gamma)}{d(\ln A_e)} \qquad 2.14$$

where A_e is the area of a surface element. The units of ε are the same as for surface tension, dyn. cm^{-1}. For an insoluble monolayer, the complex modulus is completely real, and is equal to the dilational elasticity, ε_d. Since the change of adsorption is completely specified by the change of area covered,

$$\frac{d(\ln\Gamma)}{d(\ln A_e)} = -1 \qquad 2.15$$

In this case, ε_d follows directly from the surface equation of state, the σ/Γ curve. For ideal, Szyszkowski - Langmuir adsorption, described by the equation

$$\sigma_o - \sigma = -RT\Gamma_\infty \ln(1 - \Gamma/\Gamma_\infty) \qquad 2.9$$

where Γ is the adsorption of the active agent, the elasticity is given by

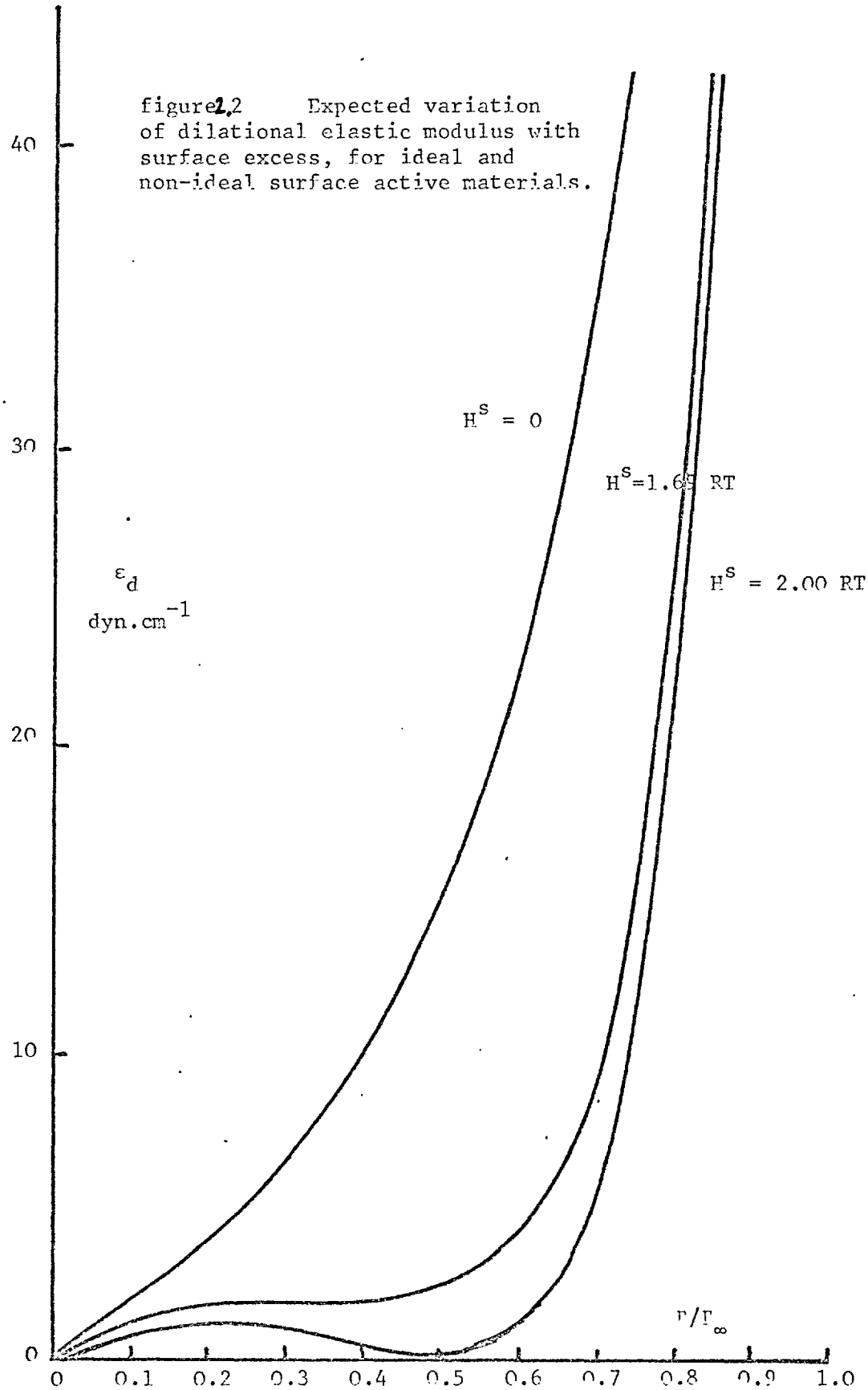
$$\frac{\varepsilon_d}{RT\Gamma_\infty} = \frac{\Gamma/\Gamma_\infty}{1 - \Gamma/\Gamma_\infty} \qquad 2.16$$

For non-ideal, regular behaviour, Lucassen and Lucassen-Reynders (1967) give the elasticity as

$$\frac{\varepsilon_d}{RT\Gamma_\infty} = \frac{\Gamma/\Gamma_\infty}{1 - \Gamma/\Gamma_\infty} - \frac{2H^s}{RT}(\Gamma/\Gamma_\infty)^2 \qquad 2.17$$

(from Equation 2.10)

figure 2.2 Expected variation of dilational elastic modulus with surface excess, for ideal and non-ideal surface active materials.



It can be seen that this equation reduces to equation 2.16 if the non-ideality parameter H^s is zero. Figure 2.2 shows the variation of ε_d with Γ/Γ_∞ for different values of H^s. It may be seen that, at least for high surface pressures, the elasticity is predicted always to increase with adsorption. It is characteristic of the theoretical surface activity treatments produced to date that elasticity should always increase. The only mechanism so far developed which modifies this is the time-dependent diffusional interchange between surface and bulk in solutions of certain surface active materials. It was shown in section (i) that the equilibrium surface tension of a solution was independent of surface area, and that elasticity is only evident when the surface extension is fast compared with the diffusion process. In this case, there is delay between a change of area and the resulting change of surface tension, which can be expressed in the complex dilational modulus. The dilational viscosity η_d, the imaginary component of the modulus, is no longer zero, and the purely elastic component of the modulus ε_d is lower than would be expected from the equation of state. In cases where there is instantaneous equilibrium between local values of σ, Γ and the solution concentration immediately below the surface, the variation of surface tension during a change of area is governed by the diffusion of active material from bulk to surface. $-d(\ln\Gamma)/d(\ln A_e)$ is no longer equal to unity, but depends on the rate of surface expansion relative to the time scale of the diffusion process. In the special case of a sinusoidal expansion of angular frequency ω, the effect of the

diffusion may be expressed by the dimensionless parameter τ (Lucassen-Reynders and Lucassen, 1969) which is defined by

$$\tau = \frac{dc}{d\Gamma} \cdot \sqrt{\left(\frac{D}{2\omega}\right)} \qquad 2.18$$

where D is the diffusion coefficient of the solute. In this case, the dilational viscosity η_d is given by

$$\eta_d = \frac{-d\sigma}{d\Gamma} \cdot \frac{\tau}{\omega(1 + 2\tau + 2\tau^2)} \qquad 2.19$$

(dimensions: dyn. cm^{-1} sec) and the diffusional elasticity ε_d is given by

$$\varepsilon_d = \frac{-d\sigma}{d\Gamma} \cdot \frac{1 + \tau}{(1 + 2\tau + 2\tau^2)} \qquad 2.20$$

(dimensions: dyn. cm^{-1}). τ is a quantity defining the relative magnitudes of the diffusion process and the surface expansion. For the special case of an insoluble monolayer, D is effectively zero, and τ is therefore zero for any frequency. ε_d is predicted by the equation of state, and η_d is always zero. A soluble layer will approach this behaviour as τ tends to zero at high frequency, but as the frequency decreases, τ increases, and the surface becomes viscoelastic. ε_d is then reduced from its "insoluble layer" value, eventually becoming zero for very high τ, and η_d simultaneously increases from zero to a maximum before reducing to zero again at high τ. Since ε_d

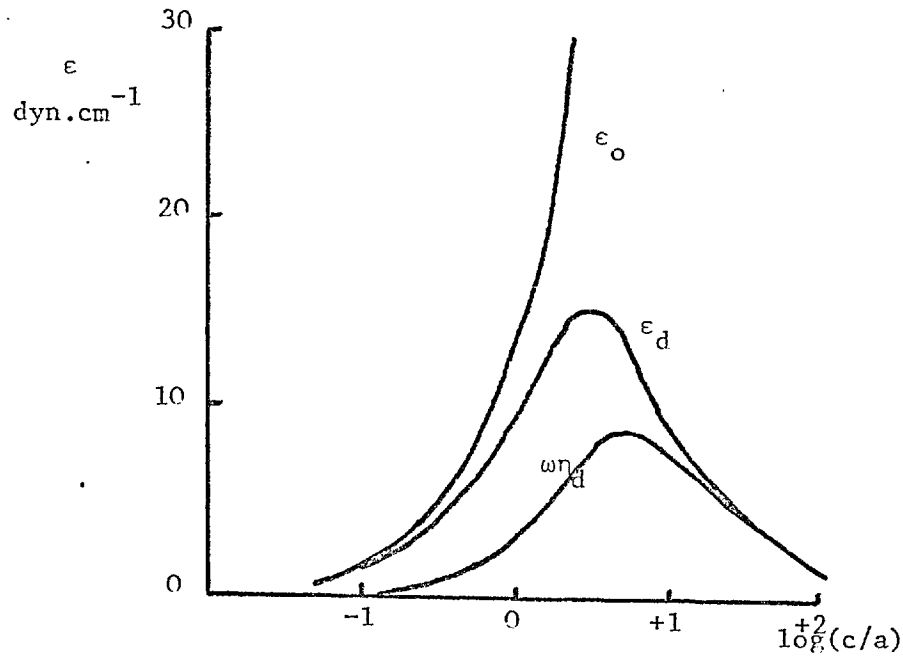


Figure 2.3 Predicted dilational elastic constants at 200 Hz for an ideal solution, compared with the curve which would be obtained in the absence of diffusion (Lucassen-Reynders and Lucassen, 1969). In this example, a = 10^{-6} moles.cm^{-1}, RT Γ_∞ = 15.0 .

and η_d cannot be evaluated without the σ/Γ curve, the equation of state, it is useful to examine the ideal surface as an illustration of the effects of diffusion. Figure 3 shows the predicted values of the dilational elastic constants for a solution which is ideal, $a = 10^{-6}$ moles. cm.$^{-3}$, $RT\Gamma_\infty = 15.0$, and the frequency of sinusoidal expansion ($= \omega/2\pi$) is 200 Hz. For comparison, a curve is also shown which represents the elasticity which would have been found for the same equation of state in the absence of diffusion. This is the same curve as appeared in figure 1. At high bulk concentration c, $\tau \to \infty$, the surface loses its viscoelasticity and acts as a "pure" liquid. This also occurs at low ω. When τ is small, however, and diffusion is negligible, the surface behaves purely elastically, according to the "no diffusion" curve shown in figure 3.

This special case of surface expansion, in which the area is changed cyclically, is useful in the consideration of surface wave properties. For a general, non-sinusoidal expansion, the complex modulus can be defined as

$$\varepsilon = \frac{d\sigma}{d(\log_e A_e)} = \varepsilon_d + \eta_d \, d/dt \qquad 2.21$$

If the rate of expansion is constant, then when the system has reached dynamic equilibrium, ε_d is zero, and the change in surface tension $d\sigma$ is given by

$$\eta_d = \frac{d\sigma}{d(\log_e A_e)/dt} \qquad 2.22$$

The contribution of diffusive processes to the dilational viscosity is the principal viscoelastic mechanism so far encountered experimentally. Molecular considerations are also likely to have a time varying effect on the elasticity, analogous to the concept of bulk viscosity in liquids. Some protein monolayers are observed to undergo changes with time, probably due to molecular adjustment and interaction, and Fukawa et al. (1961) observed similar time effects in polyvinyl alcohol solutions. This type of mechanism is expected to influence the viscosity term. A further contribution would occur if there were an appreciable time required for the molecules to have an effect on the surface tension after reaching the surface.

The effects of surface elasticity are observed in many different systems. It is believed to be one of the principal factors in the stability of foams and thin films (Kitchener, 1964), and Levich (1962) uses the concept to explain why the speed of gas bubbles rising through surface active solutions sometimes indicates that the bubble surface is immobile, instead of a continuously changing fluid surface. Elasticity has also been shown to be the controlling factor in the damping of transverse surface waves or ripples (Levich, 1941; Dorrestein, 1951; Hansen and Mann, 1964). The periodic expansions and contractions associated with the wave are opposed by the elastic forces, causing damping much higher than that found in a pure liquid. In addition, Lucassen (1968) has shown that the presence of elasticity permits the surface to support a longitudinal wave. These important effects of

elasticity will be discussed in greater detail in Chapter 3.

(v) The Measurement of the Surface Dilational Modulus.

For ideal and regular adsorption, the elasticity component of the modulus in the absence of diffusion is predicted by equations 2.16 and 2.17 above. In the general case, it may be found by measurement of the slope of an experimentally determined σ/Γ curve. Blank, Lucassen and van den Tempel (1970) automate this method in the study of protein monolayers. The area of the spread layer is changed cyclically by the movement of one barrier of a Langmuir trough, and surface tension is monitored continuously by a Wilhelmy plate attached to an electric balance.

The dilational viscosity has been measured by van Voorst Vader et al. (1964). A Langmuir trough was provided with a pair of symmetrical moving barriers designed to move apart continuously at an increasing rate, thereby producing a constant rate of expansion. A Wilhelmy plate was used to measure the surface tension during the expansion, being placed midway between the barriers to avoid disturbance by the surface flow. The equilibrium surface tension of a steadily expanding solution surface depends on the rate of expansion, but equilibrium is not instantaneous. The initial variation of tension with time is linear, since the purely elastic nature of the modulus is initially dominant. As the surface becomes appreciably depleted, the surface tension begins to approach a steady value representing a dynamic equilibrium between the active material diffusing to the surface and the dispersion of this material by the steady surface expansion. The materials chosen for the investigation all fitted

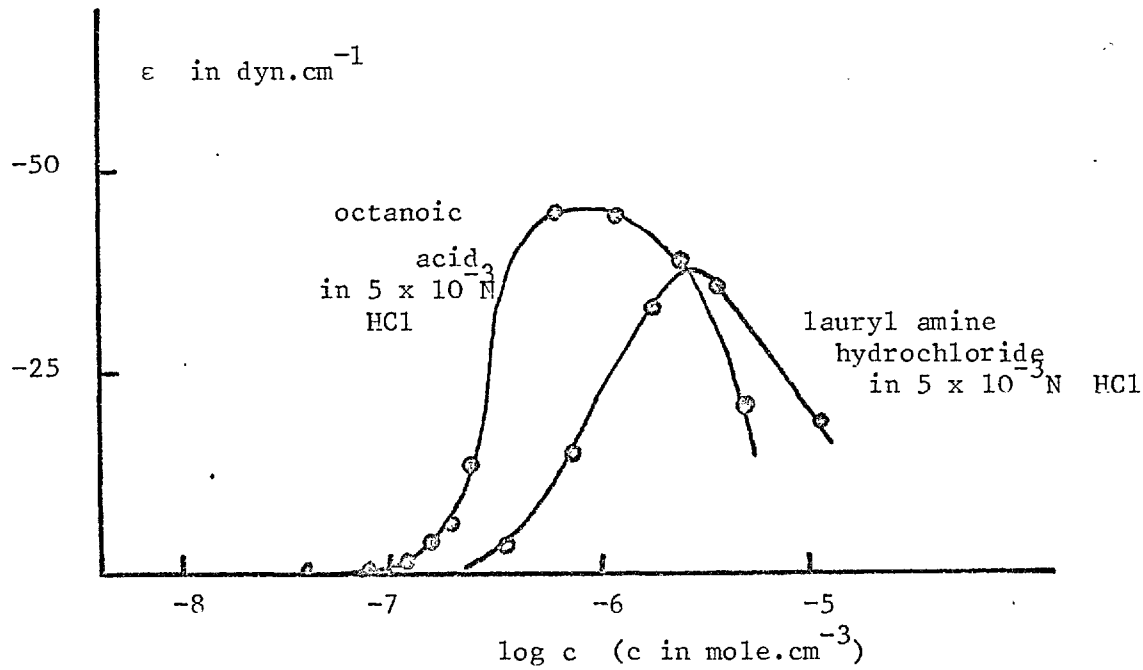


figure 14. Values of dilational elastic modulus deduced from measurement of 200 Hz ripples on two solution systems (Lucassen and Hansen, 1966).

Szyszkowski ideal adsorption curves, and the results were analysed on this basis, which allowed diffusion constants to be calculated.

The dependence of the propagation characteristics of ripple systems on the elastic properties of the surface allow estimates of the dilational elasticity to be made from wave measurements. The present state of the theory will only allows quantitative examination of systems where dilational viscosity effects do not exist. Lucassen and Hansen (1966) give first order solutions of the hydrodynamic equations which allow both the surface tension and dilational elasticity to be calculated from the wavelength and damping of ripples generated on the surface (Appendix 2). Results derived from these measurements on both spread and solution-adsorbed monolayers were shown to be in good agreement with results obtained from the σ/Γ curve, except at high concentration, where diffusional interchange was likely to occur. Figure 4 shows Lucassen and Hansen's wave damping elasticity measurements for two different solutions. Each curve exhibits a maximum and a decrease of measured elasticity at high concentration. This behaviour agrees qualitatively with the predicted effect of dilational viscosity.

CHAPTER 3

LIQUID SURFACE WAVES

(i)Early Investigations.

The calming effect of certain oils when spread on rough seas has been recognised for centuries and according to Lucassen-Reynders and Lucassen (1969), the effect was reported by Pliny the Elder in his "Historia Naturalis". Benjamin Franklin (1774) concluded that the oil mainly affected the small wave-length ripples whose roughness allows the wind to catch hold of the waves. Aiken (1883), discussing the same phenomenon, mentions a maximum in the damping effect as the density of the oil layer increases. He showed that the calming effect was due to variations in the surface tension of the distorted surface.

Kelvin, (1871) in an analysis of the behaviour of pure liquids, showed that whereas long waves (for water, $\lambda \gg 1.7$cm) were principally gravity controlled, short waves, or ripples, ($\lambda \ll 1.7$cm) were mainly surface tension controlled. His analysis resulted in the development by Rayleigh (1890) and others of the ripple method of surface tension measurement (see section (vii)a). Although Stokes (1845) produced an expression for the damping of waves on pure liquids, the complete quantitative hydrodynamic analysis of ripples, incorporating the type of behaviour found in systems with adsorbed layers and monolayers has only been accomplished recently.

(ii)The Development of Modern Hydrodynamic Ripple Theory.

The difference between the properties of liquid surface waves on solutions and on pure liquids arises from the surface activity of the dissolved material. The slightly different form of surface activity which occurs when a layer of foreign material is spread on to the surface has a similar effect, producing surface tension changes. As was described in chapter 2, the presence of an adsorbed or spread monolayer at the liquid surface gives the surface elastic properties, which arise from the change of surface pressure or surface tension with monolayer concentration. The periodic crest expansions and trough contractions associated with the passage of a surface wave will be opposed by this elasticity and an abnormal particle motion will be impressed on the underlying liquid, causing much higher viscous energy dissipation in the bulk than would occur with a pure liquid. Levich (1941, 1962) incorporated this concept into his wave damping theory. He analysed the effect of the surface active film for two limiting cases, the first representing a pure liquid, with no surface activity, and the second representing a surface film with infinite elasticity. In this latter case, the surface merely bends as the wave passes, without contracting at the troughs or expanding at the crests, and causes high damping.

Levich erroneously assumed that at values of elasticity between the two limiting cases, the damping would simply increase monotonically. However, analysis of the intermediate range by Dorrestein (1951), Hansen and Mann (1964), and van den Tempel and van de Riet (1965) showed that the damping rises to a maximum at low elasticities, decreasing again as the upper limit of elasticity is approached. Levich did however introduce the useful concept of dilational viscosity, a time variable component of the dilational elasticity. He pointed out that for a monolayer reversibly adsorbed from solution, an expansion of the surface and the consequent depletion of the monolayer would be followed by a diffusion of dissolved molecules to the surface, where they would be adsorbed, tending to re-establish the equilibrium. Similarly, molecules in the compressed areas would tend to leave the surface for the bulk solution. This effect would produce a decrease in the effective value of the elasticity seen by the wave, and would be most effective at low frequencies where the greatest time is allowed for the diffusional interchange to take place.

The above-mentioned analyses of the hydrodynamic theory, and a further one due to Goodrich (1961), begin from the same fundamental precepts, but tend to differ in the formulation of the boundary conditions existing at the surface. The most exact formulation of the boundary conditions imposed by the presence of a surface active layer would be in terms of the four formal rheological constants which describe the surface. These are the surface dilational elasticity, ε_d , the surface dilational

viscosity, η_d , both described by Levich (1962), the surface shear elasticity, ϵ_s , and the surface shear viscosity, η_s . By analogy with their counterparts in the rheology of isotropic viscoelastic liquids and solids, the first two occur during the change of surface area without shear, and the second pair in the production of plane shear without area changes.

It was shown in Chapter 2 that the shear constants are not as meaningfully defined as the dilational constants, but it is usual to assume that the dilational coefficients are much greater than the shear coefficients. This has the advantage of making the surface stress tensor isotropic, and appears to be well justified in the present case, with the predominantly dilational surface motion associated with the plane surface waves.

Another simplification of the basic surface rheology in the surface wave application is to assume that ϵ_d and η_d are constant and independent of the magnitude of surface area changes. While this is never absolutely true, the extremely small extensions and constractions about the equilibrium value due to the surface wave allow linearity to be assumed over the range of application of the sinusoidal ripple theory.

Considering an element of surface of area A_e the surface dilational modulus is defined (Lucassen-Reynders and Lucassen, 1969) by

$$\epsilon = \epsilon_d + \eta_d \frac{\partial}{\partial t} = d\sigma/d(\log_e A_e) \qquad 3.1$$

If it is independent of the time taken for an area change then $\eta_d = 0$ and the surface is purely elastic. In general, however, time dependence is likely to appear, for example through the mechanism mentioned by Levich, in which the elasticity is reduced by the diffusion of active molecules to the surface from the bulk. Another time-dependent effect which would appear in the viscosity term, can occur if a finite time is required between the adsorption of a molecule and its subsequent influence on the surface pressure (Lucassen and Hansen, 1966).

The Hansen and Mann (1964) treatment of the boundary conditions to the hydrodynamic equations expresses the surface properties in terms of a "film elasticity", k_e , and a "film relaxation parameter" k_r . These are not identical with the two principal rheological constants described above. k_e , while basically similar to the dilational elasticity when there is no bulk-to-surface diffusion, is actually complex, and incorporates this diffusional interchange. k_r represents a dilational viscosity due to molecular rearrangements in the surface. This mode of approach would be more useful if it were found that a significant proportion of the damped energy went into the surface layer itself as a result of the mechanisms of rearrangement, as the situation would then be similar to the three-dimensional analogue of viscosity. It appears however that the great majority of the dissipation occurs in the bulk substrate, and the more important viscous effects are those appearing as a time-dependence of the dilational elasticity rather than as an energy loss produced by in-surface interaction. The solutions in terms of the more

useful ε_d and η_d , are given in detail by Lucassen-Reynders and Lucassen (1969), and are quoted in Section (iii).

Van den Tempel and van de Riet (1965) evaluated the damping using concepts similar to those described above, except that instead of working with ε_d and η_d , they extended the theory to the more practical system of a solution of a surface-active agent whose adsorption follows the Szyszkowski-Langmuir isotherm (see Chapter 2), and the damping is calculated directly in terms of solution concentration.

(iii) The Predictions of Ripple Theory.

Only the results of the hydrodynamic theory will be described here, since the detailed analysis is given adequately in the treatments mentioned above. One of the more satisfactory in this respect is the exposition of the theory given by Lucassen-Reynders and Lucassen (1969), which emphasises the importance of the results concerning longitudinal waves, and their relation to the better known transverse waves, or ripples. Since wave motion is propagated continuously, the damping may be considered either with respect to time or with respect to space. Dorrestein (1951) chose to evaluate the time decay behaviour, but it is more usual to express the results of theory in the spatial variation, as this is much easier to observe and measure. For low bulk liquid viscosity, the relation between the time damping coefficient α and the distance damping coefficient β is given by

$$\alpha = -\beta\frac{\partial\omega}{\partial\chi} \qquad 3.2$$

where ω is the radial frequency of the wave, and $\chi = 2\pi$ / wavelength.

$$\frac{\partial \omega}{\partial \chi} = V_g \qquad 3.3$$

is the group velocity of the wave.

The basic hydrodynamic equations contain terms which represent non-linear behaviour of the surface at high wave amplitudes, which leads to distortion of the waveform and eventually to surface rupture. The practical use of wave systems at these high amplitudes is very limited, and so it is acceptable to restrict the solutions to wave amplitudes very much smaller than their wavelength, enabling the non-linear terms to be neglected.

In the form described by Lucassen-Reynders and Lucassen (1969), the hydrodynamic theory for small amplitude ripples is completely general and is valid for the interface between any two fluid media. For the liquid/air surface, the effect of air motion may be neglected because of the low density and viscosity of air. Solution of the basic hydrodynamic equations using the boundary conditions based on the surface rheological concepts described above, produces a dispersion equation, a relation between the wave frequency and the complex wave number which represents the measurable properties of the wave motion. The complex wave number is completely specified by the wavelength λ and the distance damping coefficient β, and is given in terms of the surface tension σ the surface elasticity ε, the densities and viscosities of the bulk phases composing the surface, and the gravitational acceleration g. The most general form of the dispersion equation is given by Lucassen-Reynders and Lucassen (1969), but is extremely complicated, and not easy

to manipulate into the various practical situations of surface waves. The computer analyses by Hansen and Mann (1964) and van den Tempel and van de Riet (1965) are attempts to produce physically significant data from the equation. The main difficulties encountered in the exact treatment of the dispersion equation arise from the presence of higher order terms in λ and β.

The computer solutions of Hansen amd Mann expressed the damping in terms of a viscoelastic dilational modulus, using dimensionless variables involving the surface tension, and so they are only useful in cases where the surface tension can be assumed constant over the range considered. They are equally valid for insoluble monolayers and solutions, since only the elastic properties of the surface need be specified. The solutions of van den Tempel and van de Riet differ in this respect because the theory is applied specifically to solutions whose adsorption follows the Szyszkowski-Langmuir equation of state. The damping is calculated as a function of solution concentration, a practical variable, instead of the general rheological constants.

Approximate solutions of the equation may be produced by introducing restrictions on its validity. In the case of a liquid/air surface, with zero surface dilational modulus (implying a pure liquid), without surface active material and low viscosity, obeying the inequality

$$\eta \ll \frac{\rho\omega}{\chi^2} \qquad 3.4$$

the energy dissipation is not great, and the dispersion equation reduces

to that of Kelvin (1871) for an ideal non-viscous liquid:-

$$\sigma\chi^3 + \rho g\chi = \omega^2\rho \qquad 3.5$$

The inequality 3.4 holds for a pure water surface at low frequencies. For surfaces which exhibit a finite surface dilational modulus, Lucassen-Reynders and Lucassen (1969) demonstrate that the Kelvin equation is still remarkably accurate. At low elasticities, the wavelengths predicted by the equation are slightly less than those found, and at high elasticities, the predictions are in excess of experimental results. Both types of deviation are explained by the effects of energy dissipation.

The Stokes (1845) equation for the damping on liquids with zero elasticity,

$$\beta_o = \frac{4\chi^3\eta}{3\rho\omega} \qquad 3.6$$

can also be derived from the general dispersion relation, while the other limiting case chosen by Levich (1941) and Goodrich (1961), that of infinite elasticity, is given by:-

$$\beta_\infty = \frac{1}{6}\chi^2\sqrt{\frac{2\eta}{\omega\rho}} = \frac{1}{4}\beta_o\sqrt{\frac{\omega\rho}{2\eta\chi^2}} >> \beta_o \qquad 3.7$$

(Reynolds, 1880, Lamb, 1895). Investigations of the region of elasticity between these two extremes by Dorrestein (1951), Hansen and Mann (1964), and van den Tempel and van de Riet (1965) has shown the existence of a maximum at low elasticity. For a purely elastic surface, having no dilational viscosity effects such as those described

in section (ii), the damping should rise to

$$\beta_{max} = \frac{1}{3}\chi^2\sqrt{\frac{2\eta}{\omega\rho}} \qquad 3.8$$

when the value of the surface dilational elasticity reaches

$$\varepsilon_{max} = \frac{\sqrt{(2\omega^3\rho\eta)}}{\chi^2} \qquad 3.9$$

(Lucassen and Hansen, 1966).

An approximate equation can be produced which relates the wave damping β to the surface tension and surface elasticity by neglecting powers higher than 1 in the general equation. This is given by Lucassen-Reynders and Lucassen (1969) as:-

$$\beta = \frac{2\eta\chi^2}{\rho V_g} \cdot \frac{\frac{1}{8}\sqrt{2}.\chi^3.\eta^{-3/2}.\omega^{-5/2}.\rho^{-1/2}.\varepsilon^2 - \frac{1}{2}\sqrt{2}.\chi^2.\eta^{-1/2}.\omega^{-3/2}.\rho^{-1/2}.\varepsilon + 1}{\chi^2.\eta^{-1}.\omega^{-1}.\rho^{-1}.\varepsilon^2 - \sqrt{2}.\chi^2.\eta^{-1/2}.\omega^{-3/2}.\rho^{-1/2}.\varepsilon + 1} \qquad 3.10$$

where the group velocity,

$$V_g = \frac{3\sigma\chi^3 + g\rho}{2\omega\rho}$$

$$= \frac{3}{2}\frac{\omega}{\chi}\left\{1 - \frac{2}{3}\frac{g\chi}{\omega^2}\right\} \qquad 3.11$$

The accuracy of this approximation improves as the wavelength increases. Lucassen and Hansen (1966) also derive from the theory an expression which allows the surface properties σ and ε_d to be calculated from measured values of wavelength and damping. This equation is valid only

in cases of negligible dilational viscosity, η_d , and is quoted in Appendix 2, together with a computer program written as part of the present investigation in order to derive elasticity values from ripple characteristics.

(iv) The Physical Interpretation of Ripple Theory.

In order to appreciate the significance of theresults produced by the ripple theory, especially in the important intermediate elasticity range, it is useful to understand the nature of ripple motion in general. For an ideal non-viscous pure liquid, the particle motion accompanying a ripple or transverse wave is the sum of equal amplitude horizontal and vertical oscillations, with a phase difference of 90° (figure3.1a). Each liquid particle therefore describes a circle in a vertical plane about an axis parallel to the wave front. The amplitude of this motion decreases exponentially with distance of the mean particle position below the surface and at a depth equal to the wavelength, the particle amplitude is reduced to 0.2% of its value at the surface. In a pure real liquid, the effect of finite liquid viscosity is to distort the circular paths, but for viscosities and frequencies low enough to satisfy inequality 3.4 , this distortion is small.

If the surface dilational properties are modified by the presence of a surface active layer, then the surface will support a tangential stress, and although for low elasticities the relative amplitudes at the surface of the horizontal and vertical components of the particle motion remain almost constant, the phase angle between the components increases from 90°

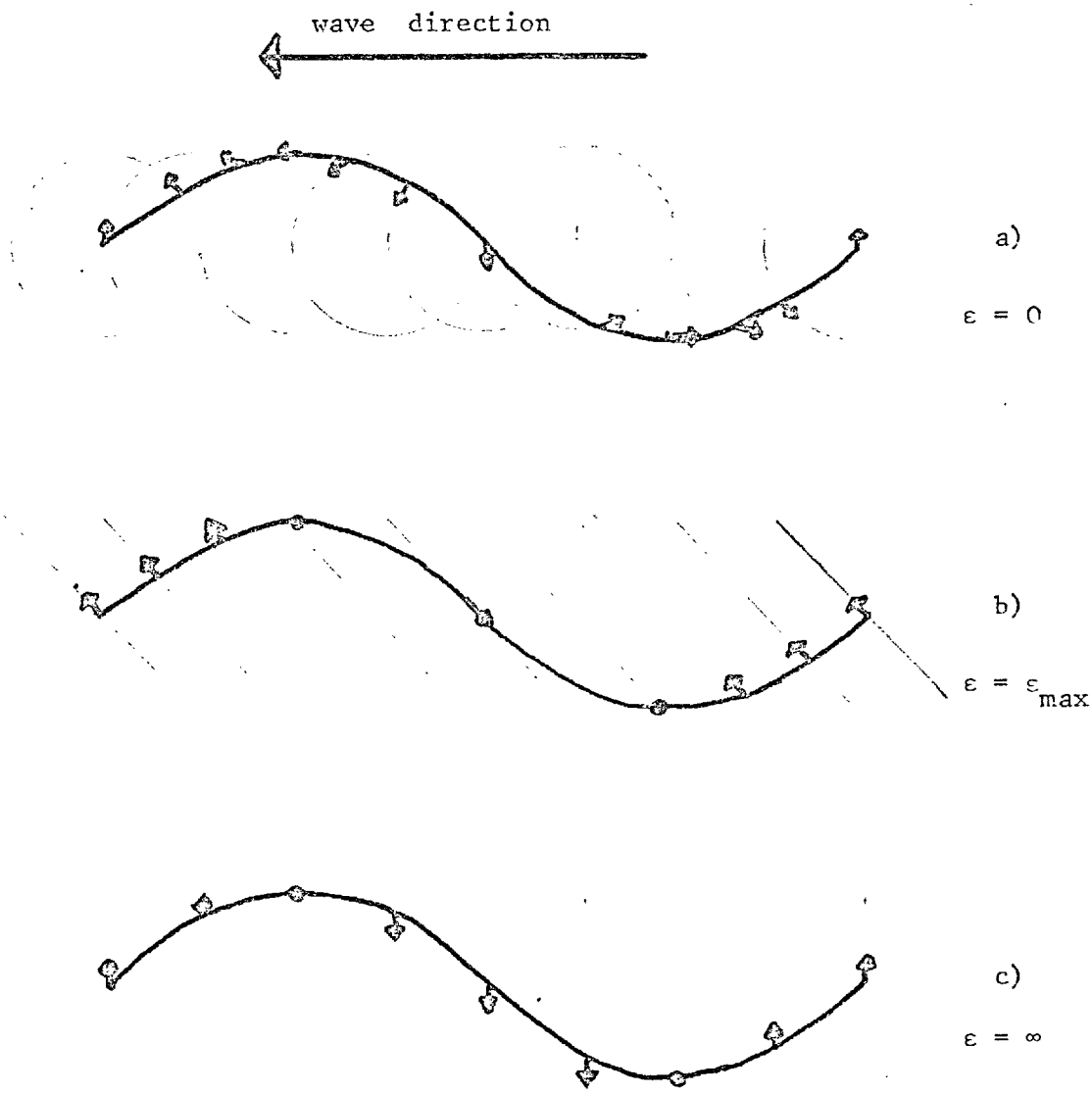


figure 3.1 Particle motions associated with different stages in the variation of dilational elasticity : a) $\varepsilon = 0$, pure clean liquid surface; b) $\varepsilon = \varepsilon_{max}$, ripple damping reaches maximum value; c) $\varepsilon = \infty$, surface completely rigid.

eventually reaching 180° when the damping reaches its maximum. At this stage, the particle motion in the surface layer is no longer circular, and the particles oscillate in a straight line inclined at 45° to the horizontal (figure3.1b). Below the surface the liquid is essentially the same as in the pure liquid case, and the particles will tend to persist in their naturally circular motion; high energy dissipation will therefore occur as a result of the large velocity changes between surface and bulk. This argument continues to hold for the region of elasticity above that where the phase angle has reached 180°, except that as infinite elasticity is approached, horizontal motion is completely prevented, and the particles are forced into vertical oscillation (figure3.1c).

It is obvious that this simple picture, although explaining why damping on an elastic surface should be higher than that on a pure liquid, fails to indicate why the greatest damping should occur at particle inclination 45° instead of at the greatest elasticity, where horizontal motion is not allowed. Comparison of equations 3.7 and 3.8 shows that the damping peak, at comparatively low values of elasticity, is approximately twice that at infinite elasticity. Work by Lucassen(1968) indicates that the high damping is associated with the existence of longitudinal surface waves. Although van den Tempel and ven de Riet (1965) reported the existence of a second type of solution to the wave equation which had a greater wavelength and much higher damping, it was left to Lucassen formally to identify this solution as representing longitudinal waves, a previously undetected type of liquid surface wave in which

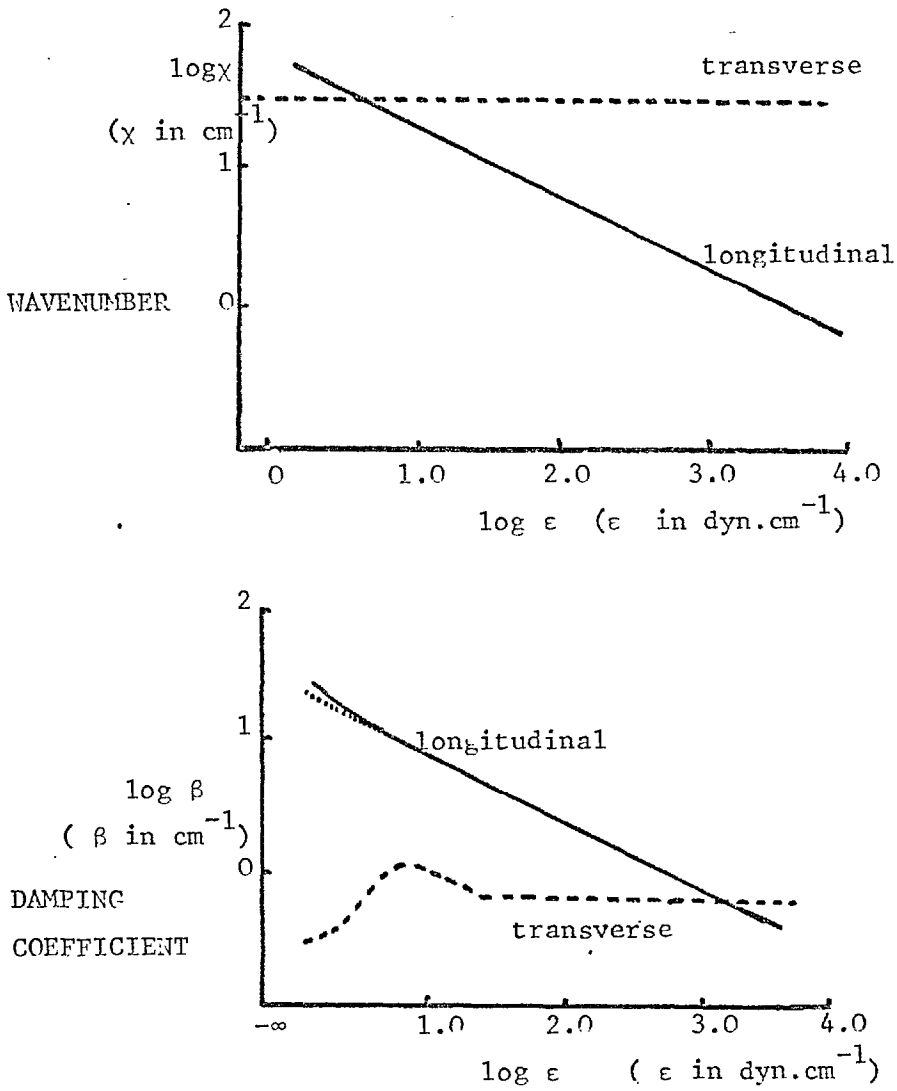


figure 3.2 Predicted propagation characteristics of longitudinal and transverse waves at 200 Hz (ρ = 1.0 g.cm^{-3}; η = 0.01 poise; σ = 70 dyn.cm^{-1}) (Lucassen, 1968).

particle motion at the surface is entirely horizontal. An analogy with the properties of an elastic sheet is useful in understanding this type of wave, since the elasticity of the sheet will allow propagation of a compression/dilation disturbance as well as a transverse wave.

Lucassen's calculations and experimental verification of the properties of longitudinal waves show (figure 3.2) that for elasticities below ε_{max}, the wave speed is lower than for transverse waves, and the damping is very much higher than for ripples. Above the critical elasticity, the longitudinal wave speed becomes much higher than the transverse wave speed, and the damping remains very high. It is this constantly high attenuation of the longitudinal waves which makes their detection difficult. At the critical elasticity itself, it appears that the two wave speeds are identical, with longitudinal damping still greatly in excess of transverse damping.

As the transverse ripples propagate across a liquid surface of low dilational modulus, the compression and dilation of the surface is effectively imposing a longitudinal wave motion on it, whose wavelength is the same as that of the transverse wave. This imposed wavelength at the ripple frequency is usually considerably different from the wavelength which a longitudinal wave would naturally assume, but at the critical elasticity, when the wave speeds coincide, the wavelengths will be identical, and a form of "resonance" occurs between the two modes of wave propagation. Since the longitudinal wave motion is so heavily damped at these low elasticities, it is natural that the energy

dissipation should be higher than usual.

(v) Agreement of Theory with Experiment.

The first complete curves relating wave damping and wavelength to the surface properties were given by Hansen and Mann (1964). A damping peak at intermediate elasticities was found, and it was also predicted that the effect of appreciable diffusional interchange between surface and bulk (see Section (ii)) would be to reduce the value of the damping maximum. The use of the curves to test the hydrodynamic theory in practical cases is greatly restricted since the variables were chosen in terms of a fixed surface tension. In practical systems, a surface tension change usually accompanies changing surface elasticity, and the Hansen and Mann curves are not simply adaptable.

Van den Tempel and van de Riet (1965) evaluated the wave characteristics of a more practical system, that of a solution which obeyed the simplest surface equation of state, that of Szyszkowski-Langmuir adsorption (see Chapter 2). The results are in terms of solution concentration, expressed in units of a, the concentration at which the adsorption reaches half of its saturation value. Some of the results are shown in figures 3.3 and 3.4. The more soluble the active agent, the greater a becomes; diffusion is correspondingly more important, and peak damping is decreased. The peak is found to occur always at a concentration close to a. Lucassen and Lucassen-Reynders (1967) extend this type of approach from the ideal Szyszkowski-Langmuir behaviour to the more general "regular" surface behaviour (see Chapter 2)

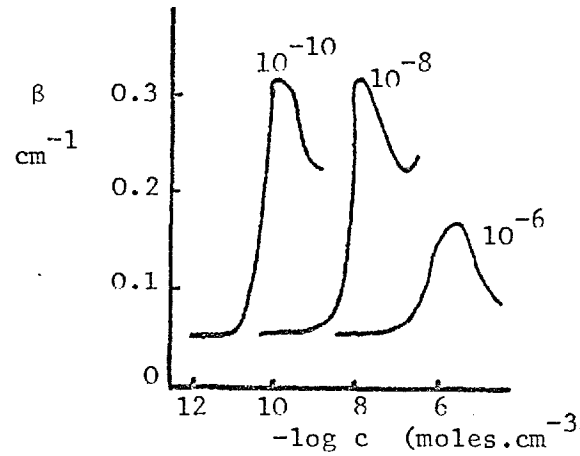


figure3.3. Predicted wave damping at 50 Hz for soluble surfactant, $\Gamma_\infty = 2 \times 10^{-10}$ mole.cm^{-2}; for a = 10^{-10}, 10^{-8}, 10^{-6} mole.cm^{-3}. (van den Tempel and van de Riet, 1965)

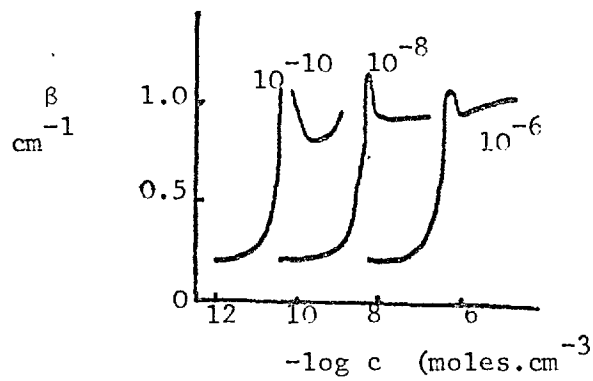
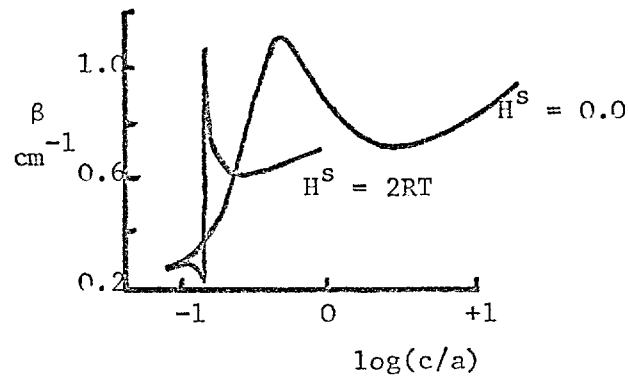


figure3.4. Predicted wave damping at 200 Hz for soluble surfactant, $\Gamma_\infty = 6 \times 10^{-10}$ mole.cm^{-2}, for a = 10^{-10}, 10^{-8}, 10^{-6} mole.cm^{-3}. (van den Tempel and van de Riet, 1965)

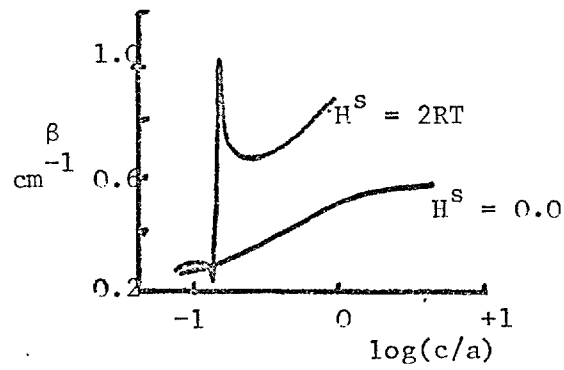
which incorporates ideal behaviour as a limiting case (Lucassen-Reynders and van den Tempel, 1964). As shown in figure 3.5, increasing the non-ideality parameter H^s sharpens the damping peak. In addition, the peak-diminishing effect of the bulk-to-surface diffusional interchange is reduced in non-ideal cases.

The agreement of the theory is excellent in the zero elasticity limit, which describes pure liquid properties. The results of Goodrich (1961) and Davies and Vose (1965) follow the predictions of the theory very closely over the range 20Hz to 900 Hz. The Kelvin (1871) equation relating wavelength to surface tension (equation 3.5) is shown to be useful even in the presence of appreciable surface elasticity (Lucassen-Reynders and Lucassen, 1969). In the intermediate elasticity region, the damping peak predicted by the theory is found experimentally in many systems (Lucassen and Hansen, 1966, 1967; Davies and Vose, 1965). Lucassen and Hansen demonstrate that in the absence of diffusional interchange, when the surface should be purely elastic, the value of the damping at the peak is given quite accurately by equation 3.8. Values of surface tension and surface compressional modulus calculated from λ and σ measurements on solutions of octanoic acid and lauryl amine hydrochloride agree closely with those determined statically, except at high concentration, when interchange becomes appreciable and the surface is expected to become viscoelastic. Perhaps even more important than the prediction of the observed peak is the discovery of longitudinal surface waves by Lucassen (1968) and their explanation by the hydrodynamic



a)

$a << 10^{-6}$



b)

$a = 15 \times 10^{-6}$

figure 5. The effect of non-linearity on the damping peak: the damping of 200 Hz ripples on a) an insoluble monolayer, $a << 10^{-6}$ gm.cm.$^{-3}$ b) a very soluble monolayer, $a = 15 \times 10^{-6}$ gm.cm^{-3}. (Lucassen and Lucassen-Reynders, 1967)

theory. It was shown that the damping peak for transverse waves or ripples is connected with the existence of these waves.

Although the volume of experimental evidence in support of the hydrodynamic theory so far developed is still very small, this is principally because of the wide range of surface types available, and their inadequate physical description. The recent concept of longitudinal waves is as yet little developed, but it would appear to provide an extremely useful addition to the dynamic techniques of liquid surface observation.

(vi) The Possible Failure of the Ripple Theory.

The interpretation of wave damping described in sections (ii), (iii), and (iv) has not yet reached universal acceptance. Garrett and Zisman (1970), and Shuler and Zisman (1970) prefer to infer direct information about the molecular structure of monomolecular films from measurements of damping without recourse to consideration of the concepts mentioned in section (ii). The mechanism described by Garrett and Zisman is basically of a surface film causing energy dissipation as it is forced into oscillation by the undulating surface, partly by intermolecular and intramolecular rearrangement within the film, and partly by "drag" between film and substrate. This picture of the hydrodynamic effect of a monolayer need not necessarily be in complete opposition to the concepts described by Lucassen-Reynders and Lucassen (1969), since the dissipation of energy in the liquid substrate associated with the rapid change between the deep liquid, circular motion and the more linear surface

motion could be described as a sort of "drag" of the monolayer on the substrate. Energy will also be dissipated by the in-layer rearrangements of the molecules, as realised by Hansen and Mann (1964).

Spread monolayers of various linear poly(organosiloxanes), were the systems investigated by Garrett and Zisman and the damping measurements plotted against area per unit mass of spread material show up to four independent peaks, sometimes separated by extremely low minima. Dorrestein's (1951) theory, deriving wave damping in terms of surface dilational properties is criticised for its inability to "explain or identify the molecular mechanisms responsible for the striking capillary wave damping caused by monomolecular films". In view of the restriction by Dorrestein of his analysis to the general concept of surface elasticity, it seems rather unfair to expect the reasons for the elasticity to be elucidated in addition.

The hydrodynamic picture as described above has explained damping in terms of the tangential forces produced when a monolayer covered surface is expanded and compressed, whatever the mechanisms responsible for these forces. The forces themselves are related to the surface tension variation with surface area per molecule, the σ/A curve, and only if this curve can be accurately specified for a given monolayer can the elasticity be deduced, and the damping predicted from hydrodynamic theory. Garrett and Zisman did not produce sufficient evidence that the previous conclusions of hydrodynamic theory were in any way in error. The predictions of the theory, as described above, show that in a system

such as described by ideal or regular equations (Chapter 2) whose surface elasticity, or surface dilational modulus increases monotonically from zero to infinity, the damping rises sharply to a maximum at low elasticities, to fall again as infinite elasticity is reached. This behaviour is predicted in all complete attempts at solution of the hydrodynamic equations so far produced, namely those of Dorrestein (1951), Hansen and Mann (1964), van den Tempel and van de Riet (1965), Lucassen (1968), and Lucassen-Reynders and Lucassen (1969). A graph of damping against monolayer concentration, solution concentration, or area per unit mass is expected to have a single peak for a given frequency only if at that frequency, the surface elasticity reaches a critical value with respect to the surface tension which is related to the existence of longitudinal surface waves. If the σ/A curve did not show simple variation, the resulting ε/A curve (which is the first derivative of the σ/A curve) would also fail to be a simple curve. The concurrent variation of elasticity and surface tension could be such that there were several different A where elasticity and surface tension produced critical elasticity conditions, and the hydrodynamic theory would then predict the existence of the same number of damping peaks.

The possibility of this extension to the theory seems to have been overlooked by Garrett and Zisman, although the σ/A curves published in the 1970 paper. as well as in an earlier report (Fox, Taylor, and Zisman, 1947) show a rather complicated behaviour. The published curves are not detailed enough for meaningful elasticity values to be inferred,

although the authors do mention that previous damping measurements (Garrett and Bultman, 1963) indicated that damping tended to be high when the elasticity was within a particular range. This would tend to support Dorrestein's theory.

Garrett and Zisman deduce from the "failure" of the Dorrestein theory to explain the complicated poly(organosiloxane) behaviour, that energy is dissipated by rearrangement of molecules as well as by the "drag" on the liquid substrate, and that it is this rearrangement which produces damping peaks at certain molecular areas. The detailed mechanism of the mode of damping is not specified, although it is stated several times that at a damping peak energy is removed from the wave motion in order to execute a specified configurational rearrangement. This concept is repeated in an almost simultaneous report by Shuler and Zisman (1970), on the surface properties of poly(ethylene oxide) monolayers. One damping maximum of the two which exist in this system is linked with the apparent collapse of the film at high surface pressures, although it is not made clear how wave energy is fed into what should be an irreversible configurational change without the rate of energy dissipation eventually decreasing as the change is completed.

The unexplained discrepancies described here, allied with their authors' inadequate appreciation of the consequences of rigorous hydrodynamic theory on the lines of Hansen and Mann (1964) and the others mentioned above, cast some doubt on the detailed explanations given of the dynamic effects of monolayers. Although much work remains to be done in the extension of ripple theory to more complicated systems,

it has not yet been shown that it is unsuitable in principle for application to such systems. It would be a very good test of the theory if the relevant surface parameters of systems such as those described by Garrett and Zisman, Shuler and Zisman, could be accurately determined independently of ripple measurements, but this is extremely difficult. As the authors themselves point out, the ripple damping behaviour seems to be the most sensitive test of surface properties at present available.

(vii) Techniques of Surface Wave Measurement.

(a) Early Work.

It was shown in section (iii) that the two principal quantities required to describe the properties of a given liquid surface were wavelength and damping. Since Faraday (1831) made his descriptive observations on the properties of vibrating liquid surfaces, considerable progress has been made in the measurement of these two quantities, although the accurate measurement of both as complementary observations has only been the aim of the most recent experiments. Following Stokes' (1845) expression for the wave damping on a homogeneous viscous liquid without surface elasticity:

$$\beta_o = \frac{4 \chi^3 \eta}{3 \rho \omega} \qquad 3.6$$

where β_o is the damping coefficient, $\chi = 2\pi /$ wavelength, η and ρ the liquid viscosity and density, $\omega = \pi$ xfrequency, and Kelvin's (1871) relation between wavelength and pure ideal liquid parameters, which may be written

$$\sigma \chi^3 + \rho g \chi = \omega^2 \rho \qquad 3.5$$

(where σ is the surface tension), there have been many experimental observations on pure liquids, principally of wavelength alone, by way of determining surface tension. Kelvin's relation was for an ideal non-viscous liquid, but it was found to be valid for many real liquids, at low frequencies where viscous damping is small.

The need to "freeze" the travelling wave motion stroboscopically so that the wavelength could be accurately measured was often ingeniously fulfilled by the early investigators, who were without the relatively modern convenience of the electronic stroboscope. Rayleigh (1890) observed the system through a pair of slits attached to the two tines of a tuning fork vibrating at the wave frequency. Dorsey (1897), Barnett(1898), Subramanyam (1926), and Ghosh, Banerji and Datta (1926) used modifications of the Rayleigh technique. Grünmach (1902), Kalähne (1902), and Bouasse(1937) overcame the wave motion by observing stationary wave systems, and Schultze (1907) employed a rotating strobe disc. Spark sources are described by Palmer (1911), who generated synchronous sparks with an induction coil, and Vincent (1898), who used a single spark from a Leyden jar in order to produce photographs of many wave motion demonstrations. The low wave velocity and ease of production of ripple systems makes them ideal for demonstrations of basic wave properties. Davis (1926, 1928) developed the method to a high degree of achievement in the acoustic design of auditoria, and the monograph by Llowarch (1961) describes ripple techniques in detail.

The modification by Ghosh, Banerji, and Datta of the Rayleigh method for stationary waves incorporated a novel visualisation device (figure 3.6).

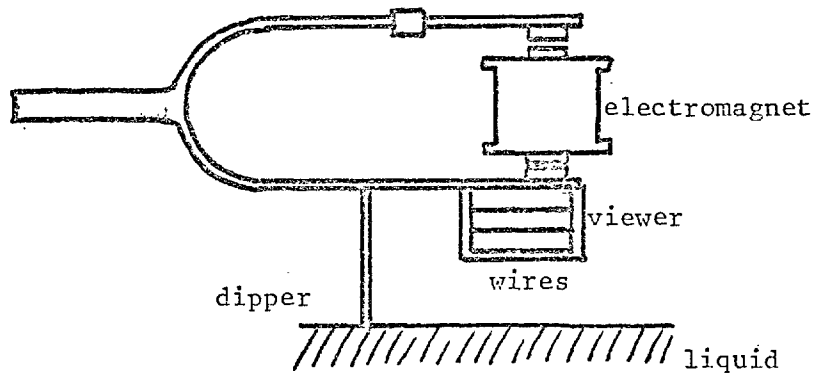


figure 36. Device for viewing systems of tuning-fork generated stationary waves. (Ghosh, Banerji, and Datta, 1926)

A pair of straight parallel wires held parallel to the liquid surface and vibrated in a vertical plane by the same maintained tuning fork which generates the waves were viewed in parallel light reflected from the distorted surface, and appeared to be deformed with the ripple waveform. The synchronous motion of the wires produced a stroboscopic effect, and photographs of the wires allowed wavelength measurement. This production of a line image carrying the wave shape was first achieved by Smith (1889), who photographed a horizontal bar by reflection from a mercury surface, and measured the wavelength of the ripple-produced serrations. The great advantage of line-image distortions is that they provide an instantaneous, continuous record of the wave travel over a considerable distance, although the two techniques described here are obviously limited in sensitivity and

precision for measurements other than of wavelength. Tyler (1941) projected the stroboscopic image of the wave-carrying surface on to a screen to increase the measurement accuracy.

(b) The Telescopic Focussing Technique.

The work of Watson (1901, 1902) is remarkable in that he was able to measure both wavelength and damping with the same apparatus. Wave height was measured by the focussing effect of crests and troughs on light reflected from the surface. The essence of the method is that if a point or line source of light is viewed by reflection in the liquid surface, using a telescope, then the departure from flatness of the surface produces a focussing effect on the light proportional to the surface curvature (figure 37). At the troughs and crests the optical axis of the

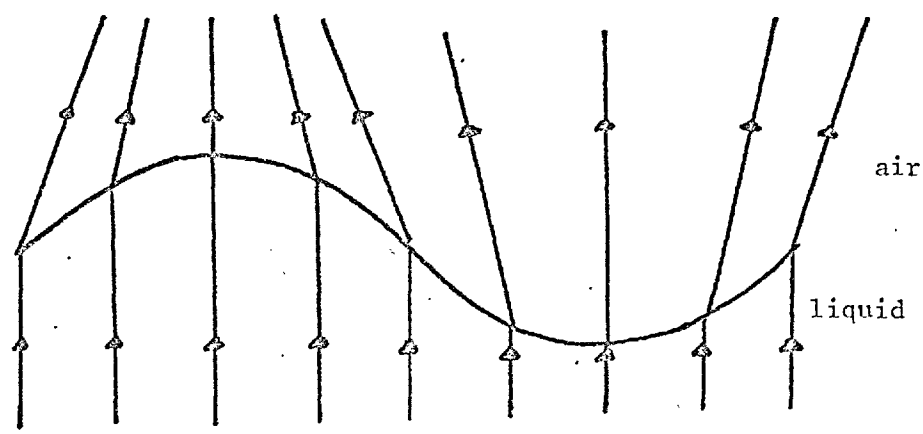


figure 37. The focussing of parallel light by a sinusoidal ripple.

source/surface/telescope system is left undeviated, but the focussing effect is a maximum, and the telescope objective to eyepiece distance must be adjusted to re-focus the image of the source. This adjustment is proportional to the wave curvature, and can be calibrated for a given arrangement of components. Watson used his measurements of pure liquid damping to calculate liquid viscosities. Brown (1936), Vines (1960), and Goodrich (1961) used versions of the same apparatus in the investigation of ripple damping on water. Goodrich found good agreement of his results with a simplified formula applicable for pure liquids at high frequency. Combination of equations 3.5 and 3.6 neglecting the gravitational term gives

$$\beta_0 = \frac{8 \pi \eta f}{3 \sigma} \qquad 3.12$$

The excellent agreement of Goodrich's results in water with this simplified formula contrasts with the considerably higher damping found by Brown with essentially the same arrangement. Goodrich's conclusion that the water surface measured by Brown must have been slightly contaminated seems reasonable in view of the extreme difficulties invariably found in the preparation and maintenance of water surfaces at high purity (see Chapter 6 and Gaines, 1966). Contamination by certain materials can produce damping measurements considerably in excess of pure water values at trace concentrations so low that measured surface tension is not detectably changed.

Davies and Vose (1965) extensively improved the Watson method, and by using the high intensity stroboscopic point source produced by a scanning cathode-ray projection tube, they extended the possible

frequency range from the limit to 920 Hz (on a pure water surface). In the earlier work of 250 Hz, this represents a decrease in the smallest wavelength measurable approximately by a factor 2.7, which is extremely valuable. A criticism which could be made of techniques relying on the focussing effect of wave troughs and crests is that they are highly sensitive to waveform distortion, while lacking adequate means of detecting its presence. Although the waveform generated by a sinusoidal disturbance is sinusoidal at small amplitudes, quadratic terms in the hydrodynamic equation introduce non-linearity as the wave height increases with respect to the wavelength. Wilton (1915) and Crapper (1957) indicate that the shape of the waves proceeds as in figure 3.8 as the amplitude increases. Since the focussing effect is measured only at crests and troughs, distortion may be well advanced before it is recognised.

Neither Goodrich nor Davies and Vose describe the measurement of wavelength in their investigations, although Davies and Vose indicate that it was always measured. It would be expected that the accuracy of a direct measurement would not be high in heavily damped systems, because few waves would be visible.

(c) The Beam Deflection Technique.

A further optical method, described by Thiessen and Scheludko(1967) and Thiessen and Schwartz (1967) uses a standing wave system generated in a cylindrical cell by oscillations of the cell in the vertical direction (figure 3.9). A light beam reflected from the surface produces a line on a ground glass screen, the line length being proportional to the wave

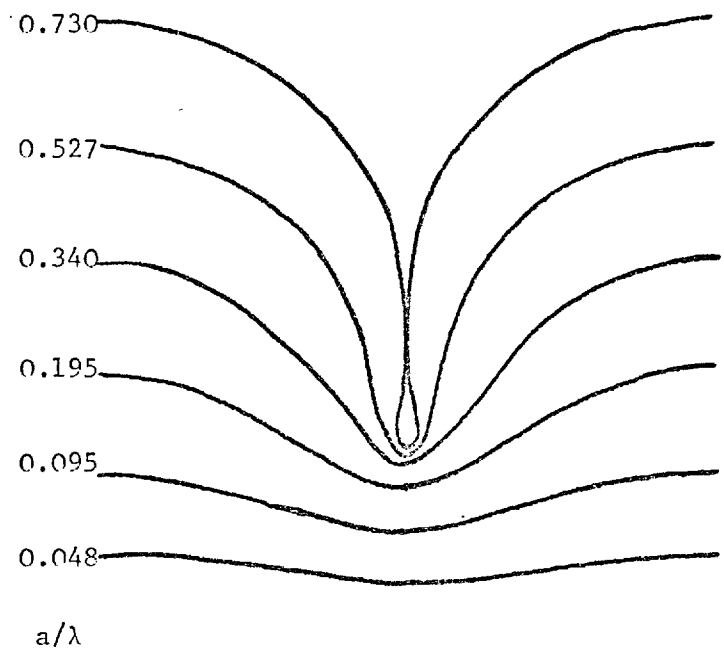


figure 38. Predicted surface shapes for large amplitude capillary waves, with several ratios of amplitude to wavelength.(Crapper, 1957)

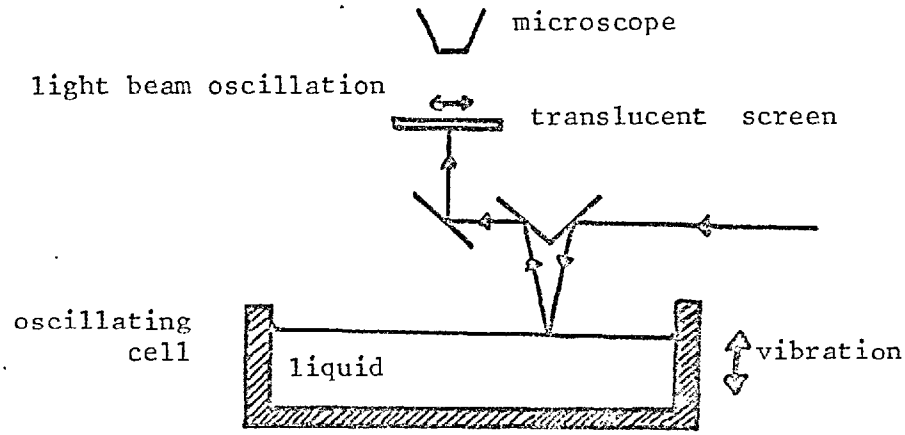


figure 3.9. The principle of the standing wave "beam deflection" technique employed by Thiessen and Scheludko (1967).

amplitude, or, more correctly, to peak wave slope. Since the system is of standing waves, instead of measuring the change of amplitude with distance, the line length is measured for a given cell amplitude, a calibration being necessary using pure water in place of the solution being investigated. This technique has the disadvantage that it must be assumed that the efficiency of transfer of energy from the vibrating cell into the liquid surface is independent of surface properties. Since resonant wave systems are observed, the frequency of excitation must be changed as surface tension changes modify the wave speed. This could have confusing results with surfaces whose properties showed time-dependence or relaxation effects.

(d) The Wave Crest Focussing Technique.

A third optical technique has recently been described by Garrett and Zisman (1970). This is a travelling wave method, and although it uses the focussing effect of the wave crests, differs from the telescope method in that the light focussed by the liquid lenses comprising the wave train is allowed to reach a real line focus on a translucent screen held a known distance above the surface (figure 3.10). The variation of the position of sharp focus with distance travelled by the waves allows the damping to be calculated, and the wavelength can be found by placing the screen close to the surface and measuring the distance occupied by a number of complete wavelengths. A synchronous electronic stroboscope was used for illumination. Although wavelengths were apparently measured, this information is not presented in the paper.

Work by Walbridge (1968) on the same type of system, originally based on the work of Schooley (1949), indicated that line images produced by light deviated by points of maximum wave slope are more accurately measured than images coming from the crests. However, this technique may be less convenient that the Garrett and Zisman method, and it has not, to date, been incorporated into a damping measurement technique.

(e) The Acousto-Mechanical Technique.

The technique of wave measurement which has been used most extensively in liquid surface investigations is the only non-optical method so far found capable of providing reliable information. This is the acousto-mechanical method, based on the work of Mann and Hansen

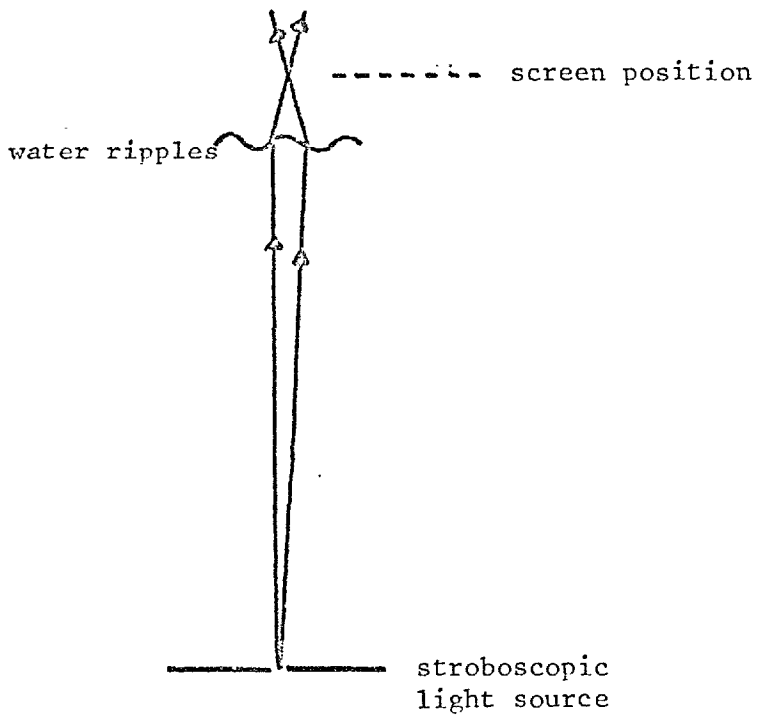


figure 3.10. The Wave Crest Focussing technique of Garrett and Zisman (1970), in which the ripples act as cylindrical lenses.

(1963 a and b), in which waves are sensed by their reaction on a wire probe placed in the surface and connected to a record-player cartridge (figure 3.11). If the generating probe and detecting probes are straight and parallel to each other, both in the surface, then the received signal is a maximum, and the standing wave pattern between the two probes can be investigated by varying their separation (Mann and Ahmad, 1969). The wavelength is measured either as the distance between adjacent points at which the input and output signals are in phase, using Lissajous' figures, or as twice the distance between successive maxima or minima as the separation changes. Damping can be calculated from the variation of output signal with probe separation, using the data reduction method described by Mann and Ahmad. The accuracy achieved by this method appears to be very high, because of the large number of sampling points as the separation increases, and the use of computer curve fitting.

Bendure and Hansen (1967) use essentially the same apparatus with a "constant wavelength" technique. The probe separation is kept fixed, and the excitation frequency is varied to produce a resonant standing wave system. If the damping coefficient for pure water is known in advance, then the damping for adsorbed or monolayer surfaces may be inferred from the reduced amplitude of the detector signal. The method is therefore relative, and suffers from the same uncertainties about the validity of a pure water calibration as the Thiessen and Scheludko (1967) technique (section (vii) (c)). Again the imposed frequency variation invalidates the method for measurement of surfaces exhibiting relaxation effects near the frequency used.

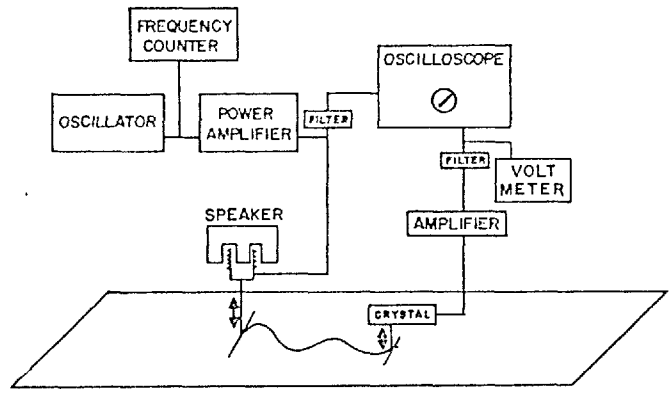


figure3.11 Block diagram of the acousto-mechanical ripple measurement technique of Mann and Hansen (1963a).

The acousto-mechanical method has to date produced the fullest information on surface ripple characteristics. Lucassen and Hansen (1966, 1967) have reported wavelength and damping information for a variety of monolayer and solution systems. The method is the only one of those described here which is also capable of the detection of longitudinal surface waves (Lucassen, 1968). Since there is little vertical particle motion expected with longitudinal waves, none of the optical methods described here would detect them. The acousto-mechanical technique of Mann and Hansen was simply modified by Lucassen to generate longitudinal waves instead of the original ripples (figure 3.12). The signals applied to

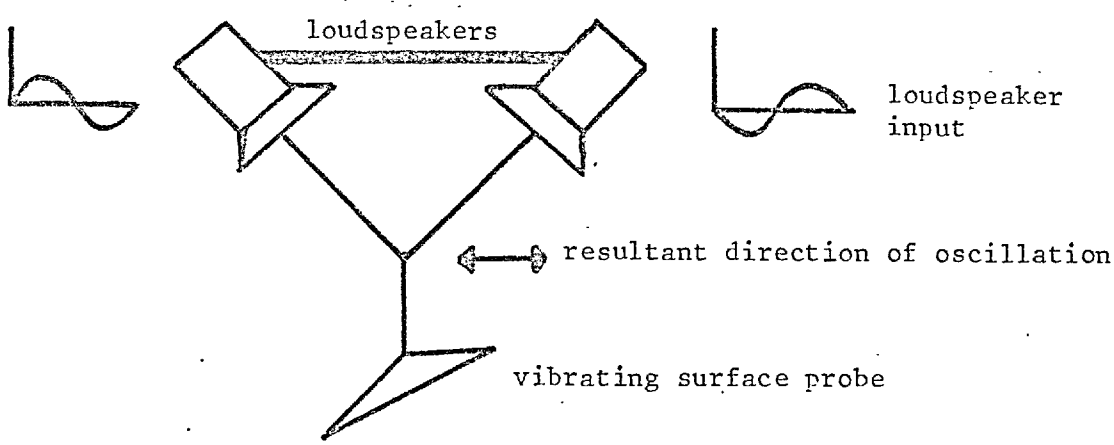


figure 3.12. Lucassen's (1968) modification of the acousto-mechanical ripple generator for the production of longitudinal surface waves.

the two loudspeaker coils are suitably phased to produce a resultant motion which is purely horizontal. The Hansen and Mann apparatus was also successfully modified by Hansen, Lucassen, Bendure, and Bierwagen (1968) for measurement of interfacial ripples on a water/mercury boundary, with and without surface active agents.

(f) The Optical Interference Technique.

An entirely new approach to the measurement of surface waves has recently been reported by Battezzati (1970). It is another optical technique, but differing from the others in that whereas they measured either the effect of the surface on the direction of reflected light or on the focussing properties of the surface, this one examines the optical interference produced at infinity by monochromatic light reflected by all parts of the wave surface (figure 3.13). For large wavelengths, amplitudes

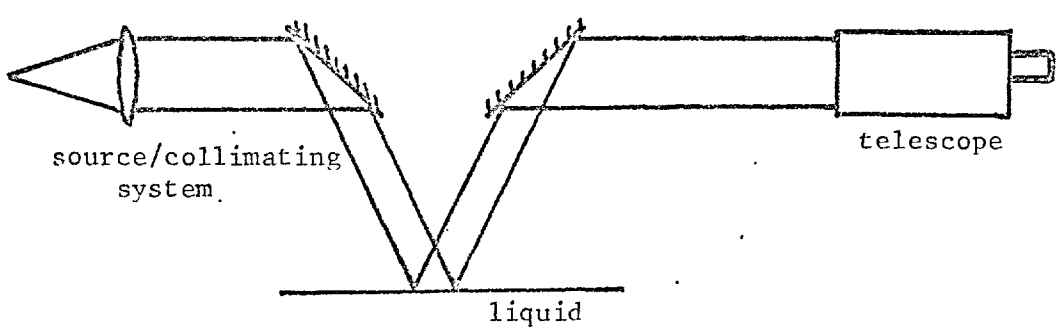


figure 3.13. The optical interference method of ripple measurement (Battezzati, 1970).

may be measured by measuring the difference in angle between the two images of the slit coming from the two points of maximum slope of the wave, but as the wavelength decreases, diffraction becomes more important, and the amplitude is given by the interference order of the central fringe of the pattern.

Wavelength is measured by the use of the regularly deformed surface as a reflection diffraction grating, using different angles of incidence as the wavelength changes. The effect of damping is to broaden or split some of the diffraction orders, but this is apparently not serious with the higher orders, 1% precision being claimed for wavelength measurement. The principal advantage of this technique appears to lie in the possibility of high frequency work, results at 1KHz being reported. Although the sensitivity is not explicitly given in the paper, the author mentions that it is low compared with other techniques.

(g) Summary of Techniques.

Each one of the above-described techniques measures damping by the consecutive determination of a wave property at different positions relative to the source. None is capable of the simultaneous measurement of two wave heights, except perhaps by duplication of apparatus, and damping can consequently only be measured on surfaces whose properties do not vary within the time taken to make separate determinations. If it is assumed that the initial wave height remains constant for a given mechanical input, independent of surface properties, then the variation of the amplitude at a single point implies the required damping variation. This is the procedure followed by Thiessen and Scheludko (1967) (section (vii) (c)) and

Bendure and Hansen (1967) (section (vii) (e)), both varying monolayer concentration, and Mann and Hansen (1963), who considered time variation, although the assumption of constant wave generating efficiency had not been thoroughly vindicated either experimentally or theoretically. A further difficulty follows because none of the methods so far used has a means of detecting wave profile distortion until the distortion is so serious that the damping measurements are affected. Although in a pure liquid calibration of a "constant initial amplitude" method the damping may be predictable on linear theory, the presence of a monolayer may produce anomalous damping due to breakdown of the layer by the high amplitude dilations. A decrease in damping near the generator was reported by Avetisyan and Trapeznikov(1964) to occur at "substantial amplitudes", and although these amplitudes were not more precisely specified, it is probable that layer breakdown was responsible. The effect must be recognised as a hazard in any measurement technique which cannot detect non-linear wave behaviour in the observed region.

Even if the constant wave generation efficiency assumption were shown to be justified, the measurement of damping variation by monitoring at a single point is of limited value, since wavelength information cannot be accurately measured in a changing system. This failure is especially marked in the acousto-mechanical technique, where wavelength information comes from the change of probe separation. The corresponding problem in the resonant standing wave systems of Thiessen and Scheludko (1967) and Bendure and Hansen (1967) is the maintenance of resonant conditions at a fixed wavelength. This could be accomplished with a servo frequency

control system. Although all of the wave measurement methods described above are capable of accurate results for equilibrium damping, and the acousto-mechanical technique incorporates a high precision wavelength measurement in addition, none of them is useful for investigation of time-varying systems by both wavelength and damping.

The new moiré fringe method to be described in Chapter 4 can be used on time varying systems as well as static surfaces, since a permanent record is produced of the wave profile over a large area of surface at a single instant of time. These wave record pictures can be analysed when convenient, and provide simultaneous measurements of wavelength and damping.

Of all the available techniques, the acousto-mechanical technique appears to be the most generally useful. It can be used on opaque surfaces, and is simply modified for interfacial investigations and even longitudinal wave detection. The principal difficulty in its use is in the problem of data reduction, as stationary waves are used, and computer curve fitting on the lines of Mann and Ahmad (1969) appears to be necessary. Wavelength and damping are measured with extremely high accuracy.

The beam deflection technique of Thiessen and Scheludko (1967) has the advantage of simplicity, at the expense of assuming constant wave generating efficiency. The constant wavelength, variable frequency aspect of the technique complicates the consideration of viscoelastic surfaces. The rest of the methods are basically restricted by their coarse wavelength measuring facilities, but the damping measurements produced in the Wave Crest Focussing Technique of Garrett and Zisman (section (vii) (d), appear to be of high quality, and the experimental technique is simple.

CHAPTER 4

THE APPLICATION OF MOIRÉ FRINGE TECHNIQUES TO SURFACE WAVE MEASUREMENT.

A. REVIEW OF MOIRÉ METHODS

(i) Introduction.

Moiré fringes may be defined as observed modulations of light present in a pattern caused by the interaction of two or more independent sets of regular lines. They are observed commonly between the folds of net curtains, between two sets of railings, and in moiré, or "watered" silk (figure 4.1). This material is produced from glossy corded silk cloth by pressing two similar pieces together, the image of one being embossed on the other. The visible surface finish of the silk varies from position to position, depending on the relative alignment of the cords producing each area.

Although the formation of moiré fringes is usually explained simply by geometrical considerations (Oster, Wassermann, and Zwerling, 1964), the visual effect of the fringes is complicated by the effects of optical illusion, and there are conditions imposed by the psycho-physical response of the eye, on the angle between the component line sets, and their pitch difference, which must be satisfied before the fringes are observed. When the distance between the lines becomes very small with respect to the spacing of the gratings, diffraction effects become significant (Guild, 1956), putting further restrictions on the fringe observation, and modifying the intensity profile of the fringes.

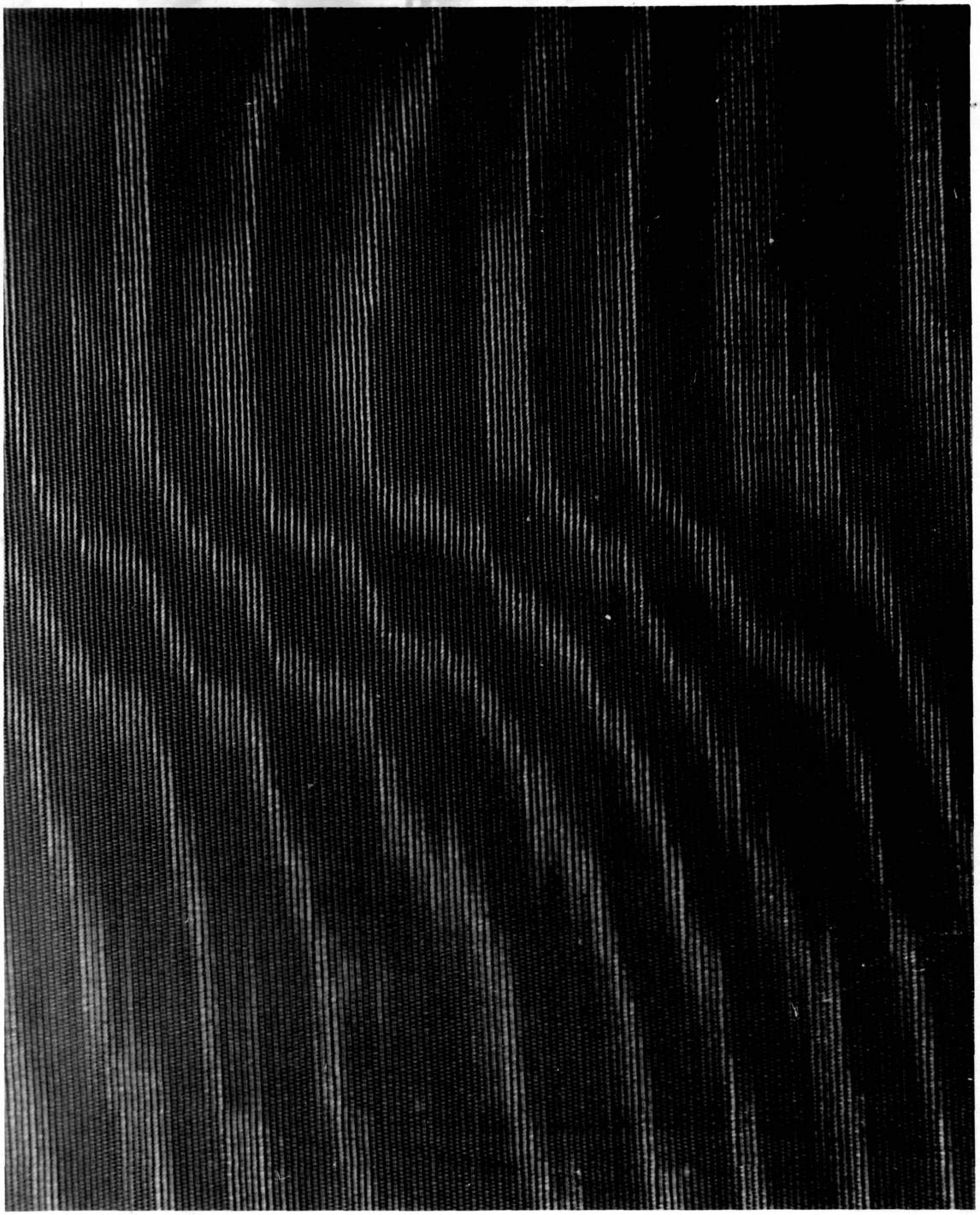


Figure 41 Moiré Silk.

The first scientific work on moiré fringes was published in 1874 by Lord Rayleigh who reported their use in testing optical diffraction gratings. The quality of the fringes produced when two replica gratings are superposed at a small angle gives a measure of the accuracy of the original grating and of the replication. Righi (1887, 1888) produced an extensive paper in 1887, dealing with many theoretical aspects of fringe production, including the profile of fringes when the light and dark parts of the gratings are not equal, and the formation of fringes with concentric circle gratings and radial line gratings. In dealing with the construction of gratings for displacement measurement, he observed that finer gratings give a higher sensitivity, but that diffraction effects occur. Ronchi (1925) advanced the theory to the interaction of straight lines with concentric circles, which produces parabolas, hyperbolas, or ellipses, depending on the relative pitch of the two grids.

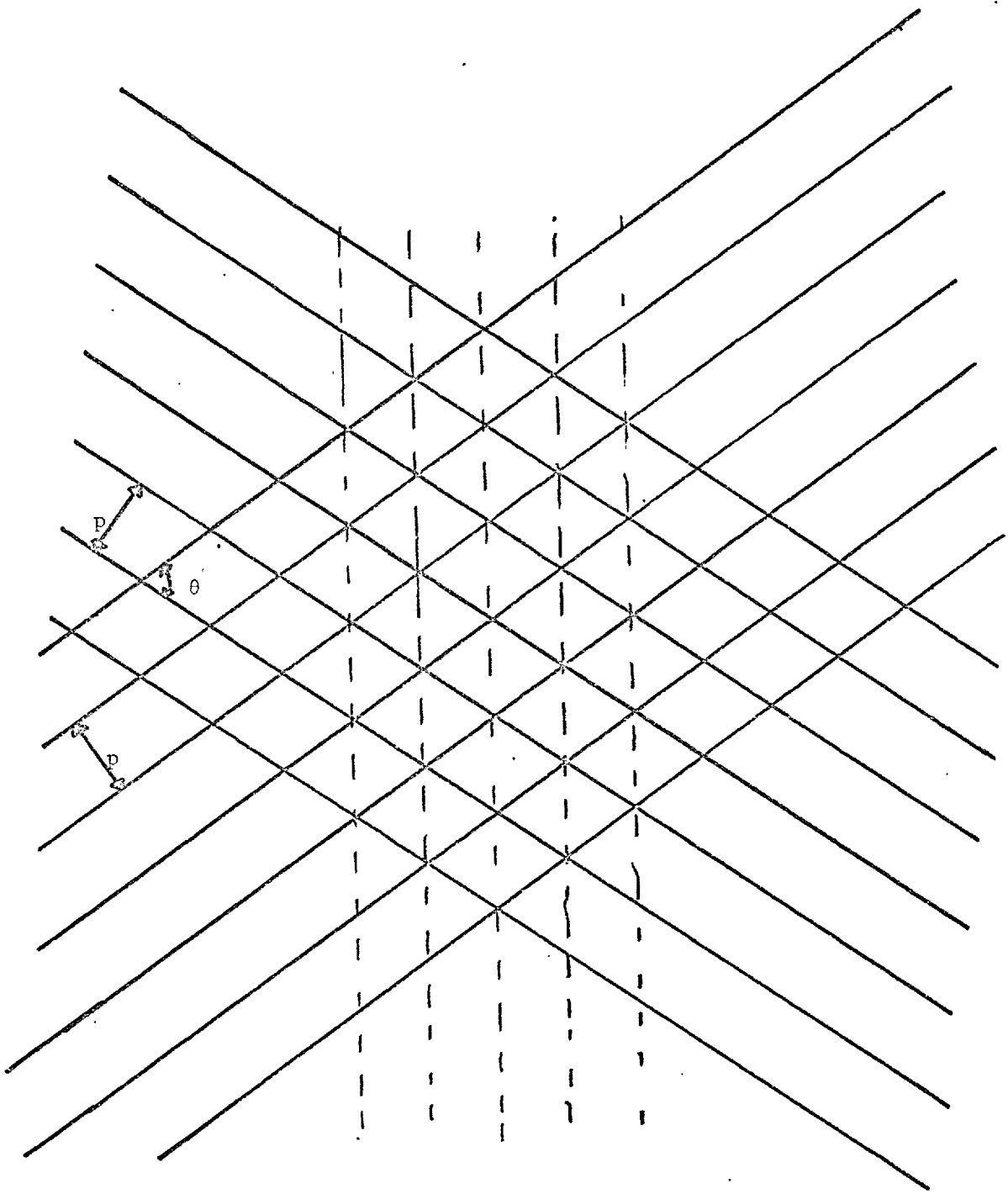
Guild (1956, 1960) was concerned with the application of moiré fringes to high precision metrology. The output of a photocell receiving light through two fine gratings will pass through a complete cycle every time one grating is moved relative to the other by a distance equal to the pitch of the moving grating. The number of cycles may be counted electronically, producing a digital measurement of position suitable for modern information processing techniques.

Other common practical applications of moiré fringes which will be described in detail later are strain analysis, topography measurement, and refractive index measurement.

(ii) Moiré - optical analogies.

It is possible to draw an analogy between moiré fringes and optical interference fringes. If each grating is thought of as a set of wave fronts, the equal spacing representing monochromaticity, then the superposition of two such gratings will show how travelling waves would interact if they converged in a plane perpendicular to their wavefronts (figure 42). Reinforcement is shown by the crossing of lines, and destructive interference by the out-of-phase condition of the lines. Although effectively frozen at an instant of time, the pattern shows the positions of the interference maxima and minima, which remain fixed in space if both sets of lines progress at the same "wave" velocity.

If two identical, equi-spaced parallel line gratings are superposed, with a small angle between the rulings of the pair, then the observed fringe pattern is a set of straight lines, each line bisecting an obtuse angle made by a pair of crossing lines. If one of these gratings is distorted, then the fringes will change, the distortion being magnified. This can be seen from the displacement of a single line by one complete line spacing. The crossing point, and hence the fringe associated with that point, will be moved perpendicular to the fringe a distance equal to a complete fringe spacing. For small included angles, this is much larger than the grating pitch, and the displacement is thus magnified. It is this property of moiré fringes which produces the high sensitivity of moiré fringe measurement techniques, and it is in exactly this simple context that the method was first used by Rayleigh in 1874. A slightly displaced line from the ruling engine would result in a localised fringe



p = grating pitch

figure 42. Illustration of the Moiré-Coherent Optics analogy. The dotted lines represent the constructive interference contours of the two travelling wave systems, or the light areas of the moiré fringe pattern. The pitch p of the gratings corresponds to the wavelength of the coherent radiation.

displacement of much greater magnitude. Figure 3 shows the fringes from two identical copies of a coarse hand-ruled grating, illustrating the effect of ruling errors. It will be noticed that one fringe only is perfect in linearity, although not completely homogeneous. This is the fringe formed by the crossing of each line with the corresponding line on the other identical grating, and a distortion is completely cancelled by the opposite sense distortion from the other grating.

This illustrates a second useful property of moiré fringes, namely that of distortion cancellation. If it is required to measure displacements or distortions of one grating by comparing it with a second, then the moiré fringe system must be designed so that the required displacement is most visible. If the pattern in the absence of the displacement is complicated and irregular, small differences are more difficult to observe than with a pattern of simplicity and regularity. In applications where it is possible to use two identical gratings in contact, then the fringe system has the required simplicity, but in many applications, before comparison of the two gratings, one of them becomes slightly distorted - for example by imaging with a conventional lens system. This will produce fringe distortions, destroying the simple regular nature of the theoretical basic pattern. The distortion cancelling property of moiré fringe systems indicates that, for small distortions, if both gratings are equally distorted, the fringe pattern should again reduce to the simple regular one of the two gratings in contact. As seen in figure 3, although the undistorted central fringe is acceptably straight, its homogeneity has been affected by irregular positioning of the line

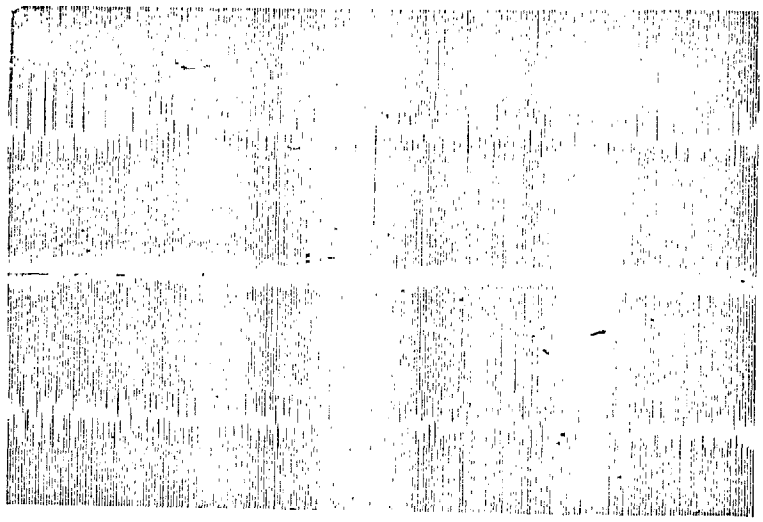
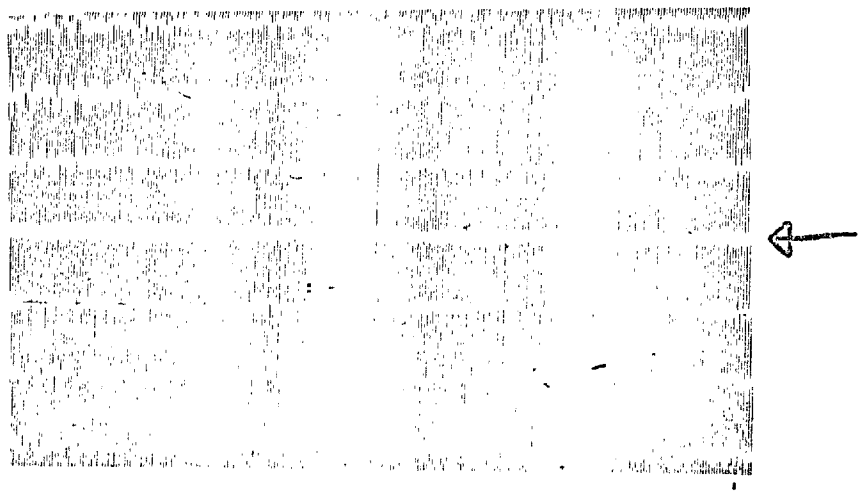


figure 43 Illustration of distortion cancellation in imperfect gratings where the distortion is common to both. Two different angle θ are shown.



crossing points, and this effect will undoubtedly limit the amount of initial distortion which can be tolerated.

This extremely useful effect of distortion cancellation can be shown to follow from the analogy with coherent light optics described earlier. Two-beam interferometry, represented by two gratings of equispaced straight parallel lines, requires the two beams to be of plane waves, so that the fringes produced in the basic pattern are also straight (cf. moiré fringe analogue). It is possible, however, to perform interferometry with non-plane wave conditions, and in fact with highly irregular, random wavefront geometry. This is what occurs in holographic interferometry. A hologram can be produced of any still object (with some restrictions on size), which, on reconstruction in coherent light, will produce a virtual image of the object in an extremely simple manner (Powell and Stetson, 1965; Fryer, 1970). The light coming from the hologram which produces this virtual image in the eye is a reconstructed wavefront of the light which would have reached the eye from the object itself. By accurate location of the optical components, this wavefront can be made exactly the same as the original wavefront, however complicated the original object. Thus, we have two identical wavefronts available, and distortion of one of them will produce measurable pattern differences in the same way as simple two-beam interferometry. This is closely analogous to the production of regular moiré fringe patterns with irregular identical gratings.

(iii) Strain measurement.

The measurement of mechanical strain involves the determination of the change in position of parts of an object with respect to the object itself. To understand the orders of magnitude involved, it is useful to choose an example such as steel. A typical yield strain for steel is 10^{-3}, so to measure this with 1% accuracy, a resolution of 10^{-5} is required. One way of achieving this is the use of large specimens, but this is usually inconvenient. The moiré technique provides a way of amplifying these small surface displacements into large fringe displacements, and is a more direct method of measurement than techniques such as bonded strain gauges and the use of photoelastic models.

The basic principle of the moiré method for strain measurement is that a regular line or dot grid is deposited on to the surface of the object. When the object is subjected to stress, this grid is compared optically with an undeformed reference grid, the moiré fringes formed between the two containing information about the strain in the object. The object grid can be etched on to the object using a photo-resist technique, or cemented on as "stripping film" (a thin photographic film on which the grating is produced before it is transferred to the object). Another technique is described by Zandman (1967), which deposits etched metal grids on to the object without distortion. Moiré techniques do have this disadvantage that the object must be specially treated, but they are still often preferable to the alternative methods. Moiré has been found to be especially useful in conditions of high temperature, where models are

invalid and strain gauges impossible. The usual method is to hold the reference grid very close to the object and its grid, but at high temperatures, it is difficult to avoid thermal dilation of the reference grid. Sciammarella and Ross (1964) worked on objects at temperatures up to 200°C with a reference grid of fused silica, but for higher temperatures, the object grating must be compared with the reference using a non-contact optical technique, such as that described by Dechaene, DeCock, and DeCaluwe (1968).

The principal disadvantage of this type of optical system for separating the gratings is that it has to be of such a high standard. The use of fine gratings and large observed areas restrict the choice to expensive telecentric systems. Luxmoore and House (1970) have devised a technique using holography combined with lenses which overcomes many of the problems. Instead of projecting the distorted object grid on to a reference grid, a hologram is made of the object grid in its rest position, which is then back-projected to interfere with the object grid itself. Spatial filtering is used to sharpen the fringes, thus increasing the sensitivity and accuracy.

(iv) Topography measurement.

Surface shapes can be determined by the fact that if a regular grid is laid in contact with a curved surface, and viewed at a distance, the observed spacing of the lines depends on the slope at each point on the surface. Comparison of this image with an undistorted reference grid

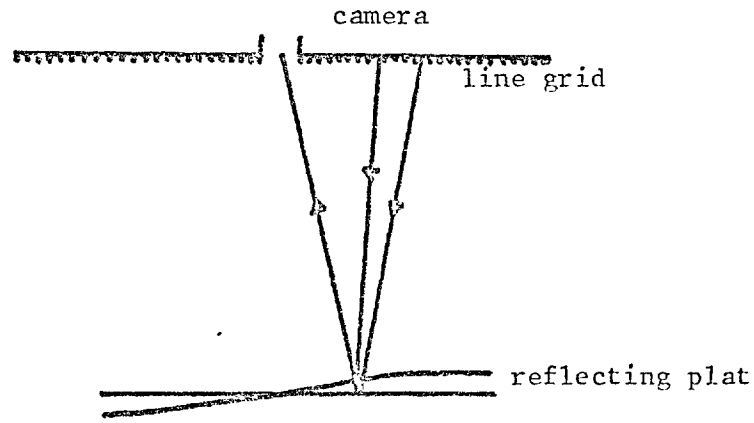


figure 4.4. The reflection moiré method of Ligtenberg (1955) for measurements on distorted flat plates.

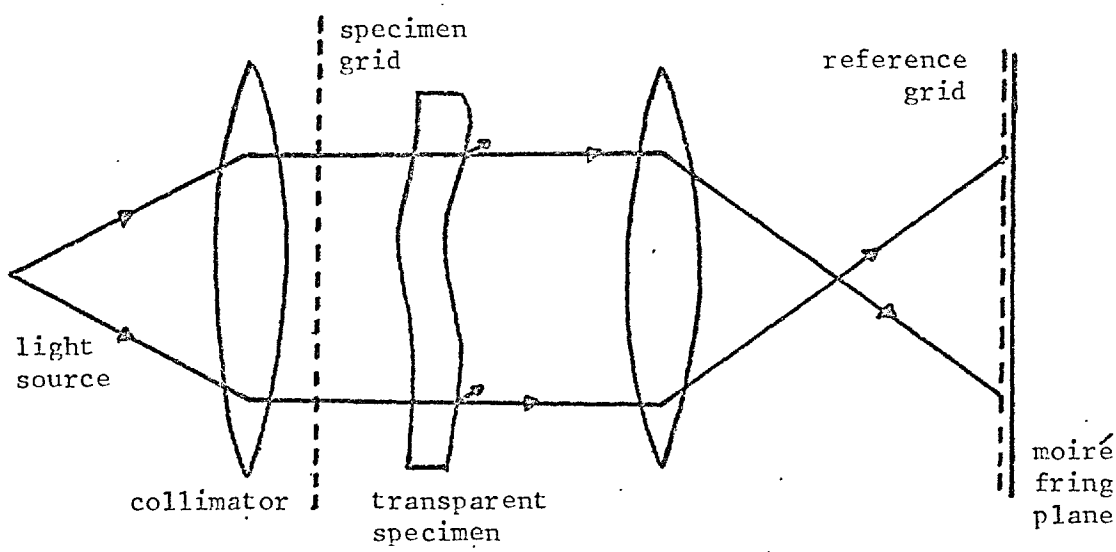


figure 4.5. Measurement of surface distortions in transparent solid models (Theocaris and Koutsabessis, 1965).

highlights the spacing changes with moiré fringes. The method of Ligtenberg (1955) was the first used for topography measurement, and measured the distortion of a reflecting flat plate by photographing a grid by reflection (figure 4.4). Photographs of distorted grids were compared by superposition with a photograph of the undistorted grid. Only small deviations from flatness are possible with this method, since sharp focussing is required.

Theocaris (1964) avoided the use of a reflecting object by holding the reference grating close to the object, moiré fringes being produced between the reference grating and its shadow on the object. Reflecting surfaces may also be examined using this system. Much of the moiré topography measurement work, exemplified by Theocaris (1964) has been aimed at measurement of principal stresses in transparent models, in conjunction with photoelasticity measurements. For these transparent models, the refraction produced by the distorted faces of the model may be used to measure the slope. Theocaris and Koutsabessis (1965) describe a general system which images one grating on to the reference grating, the light passing through the distorted specimen (figure 4.5). The reported accuracy of partial slope measurement using 500 lines per inch gratings was 3%, with a sensitivity of 2×10^{-4} radians.

Theocaris (1967) describes a reflection/shadow technique suitable for cylindrical shells which overcomes the difficulty of measuring highly curved surfaces . By rotating the cylinder and recording fringes from a narrow section as a "streak" on a moving film this has the effect of "uncurling" the cylinder, giving a single record of the whole circumference.

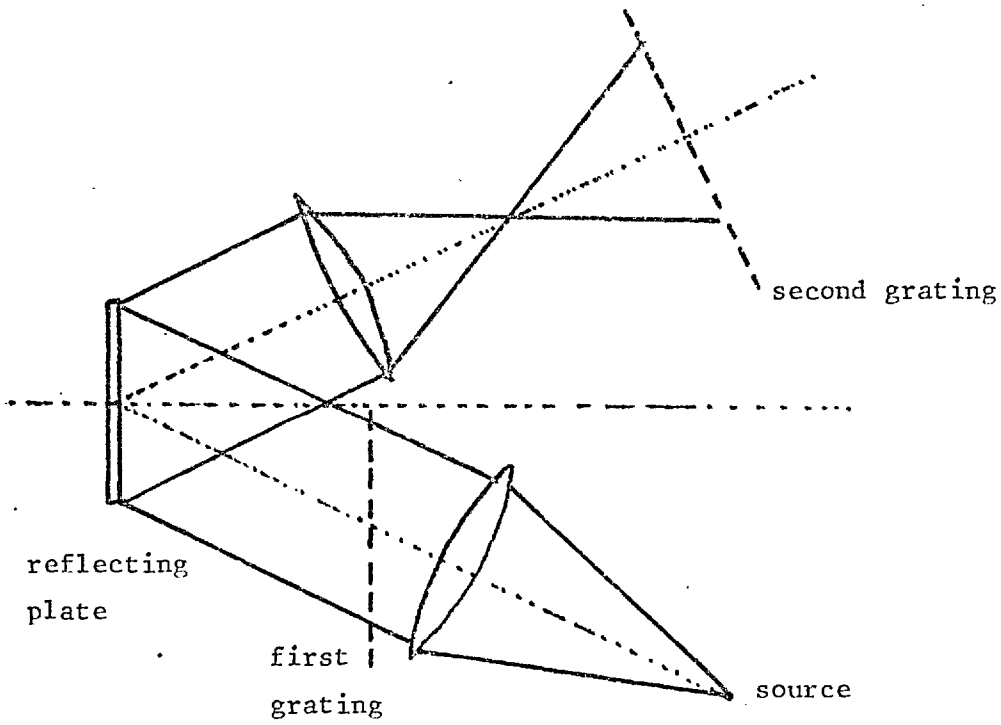


figure46 Moiré method for vibrating plates (Theocaris and Koutsabessis, 1967).

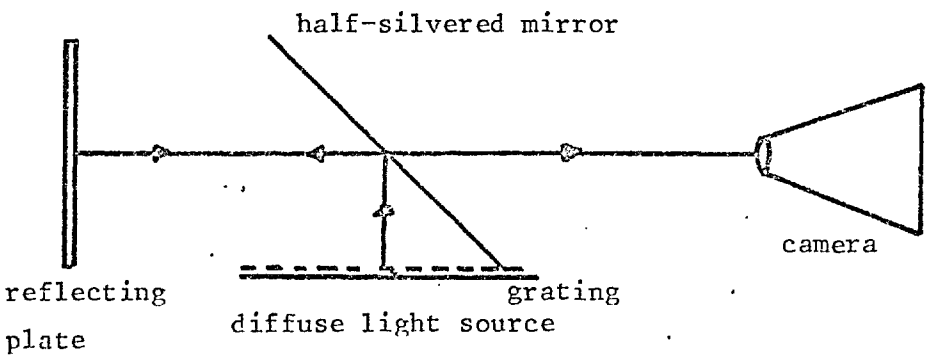


figure47. The method of Heise (1967) for measuring plate distortions.

The moiré method is extended to the vibrations of plates by Theocaris and Koutsabessis (1967) using an optical system shown in figure46. This is optically identical to that in figure45 except that the light deflections are produced by distortions in a vibrating reflecting plate instead of by a refractive index discontinuity. In continuous light observation shows the nodes of vibration while stroboscopic light yields the partial slopes.

Heise (1967) describes a method in which a plate is viewed through a half-silvered mirror held at 45° to the optical axis. The plane of the only grid is maintained parallel to the axis, and is projected on to the plate object (figure47). The curvature of this is measured by making two exposures on a single photograph at different camera positions off axis, fringes being obtained of constant plate curvature.

A technique using "multisource moiré patterns" is described by Theocaris and Koutsabessis (1968). Real fringes produced by two separated parallel line gratings, one of which is diffusely illuminated in monochromatic light, occur in a plane parallel to the gratings at a distance dependent on the relative line pitches of the gratings and their separation. The "multi-source" aspect of these fringes is that since the first grating is diffusely illuminated, real fringes are produced outside the two gratings as the diffraction modified shadow of the second grating in the light from the set of line sources comprising the first grating (figure48).

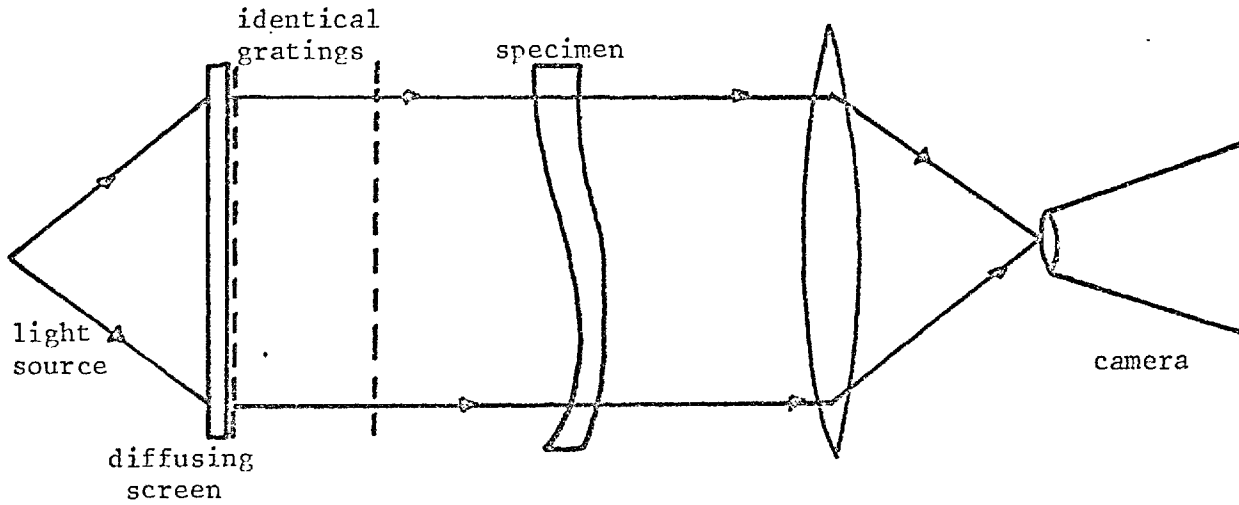


figure 48. The "multisource moiré" method of Theocaris and Koutsabessis (1968). The fringes produced by the two identical gratings are in a plane different from that of the specimen, and the camera position must be such that both fringes and specimen are in focus.

The fringes become distorted when refraction discontinuities occur in the object plane, which is outside the pair of gratings. This is essentially because the effect of the object on the light from each grating depends on the grating to object distance, and the resultant fringes distort by an amount proportional to the grating separation. The lens shown in figure 48 is employed to reduce the length of the optical path required, but the aberrations of this component are much less significant than in the systems previously described because the distortion information is already in the form of low spatial frequency moiré fringes when the light strikes the lens. In the other systems shown in figures 45 and 46, the distortion information is in the form of a small low spatial frequency modulation of the high G_1 "carrier" spatial frequency, and i- affected more by the lens distortion.

Takasaki, (1970), in applying coarse grid shadow moiré technique to the topography of large scale objects such as the human form, encountered the difficulty that with large angles of inclination of the object to the grating, it is possible to produce moiré patterns due to higher harmonics. For example, if the inclination is such that the observed shadow has a line frequency twice or three times that of the basic grating when observed at the viewing position, then spurious moiré patterns of lower contrast occur which can confuse the analysis of the moiré pictures. Takasaki makes use of the fact that only the fundamental pattern is independent of the positional "phase" of the grating (its position in its own plane), this pattern remaining stationary even when the grating is moved in its own plane, perpendicular to the rulings. A movement of the grating during the exposure serves to diffuse the unwanted images. The

work also displays the effect of using two spatially separate light sources with a single object/grating system. Simultaneous exposure produces two independent sets of fringe contours, and in places where the fringe density of both sets is high, "secondary moiré" is produced, being moiré fringes formed where the two component grids are themselves moiré produced. Since the two original moirés give contours of equal depth, the secondary moiré delineates contours of equal depth difference.

(v) Refractive index gradient measurement.

Refractive index gradients in a transparent medium produce light deflections which will have the same effect on a moiré pattern as a transparent solid with non-parallel sides (figure 45). The difference between the two systems is that a refractive index variation has a continuous effect on traversing light, whereas surface contours only affect the light path discontinuously.

When looking for surface distortions (or shapes) it is useful to produce contours of equal strain (or equal partial slope), which give accurate information at the points joined by the discrete fringes. This may also be performed for refractive index variation, but fringes would follow points where the distorting effect is constant, and in a refractive index variation, there would be points where the refractive index gradient in the direction normal to the grating lines is constant. Adequate information about the change of refractive index would only follow in cases where there were many contours. By simplifying the two-dimensional fields so far examined to essentially a one-dimensional system,

it is possible to display a continuous variation of the optical distortion along the chosen dimension.

If the object grating is distorted by the system so that the gradient changes only the line spacing along the full line length, then the lines remain parallel and fringe distortions will remain constant along the line direction. The variation is reduced to one dimension, that direction normal to the lines. With a system exhibiting this form of distortion, it is possible to produce fringes normal to the lines of the object grating, i.e., in the direction of refractive index variation whose distortion is parallel to the lines of the object grating, and proportional to the gradient (Nishijima and Oster, 1964; van Oss, 1964). This device has been employed in the present work, and will be described in detail later (Section B (iii)). Figure 9 shows the essence of the procedure, the pitch of the reference grating p_2 being related to that of the object grating p_1 by

$$p_2 = p_1 \cos \theta$$

where θ is the angle between the rulings.

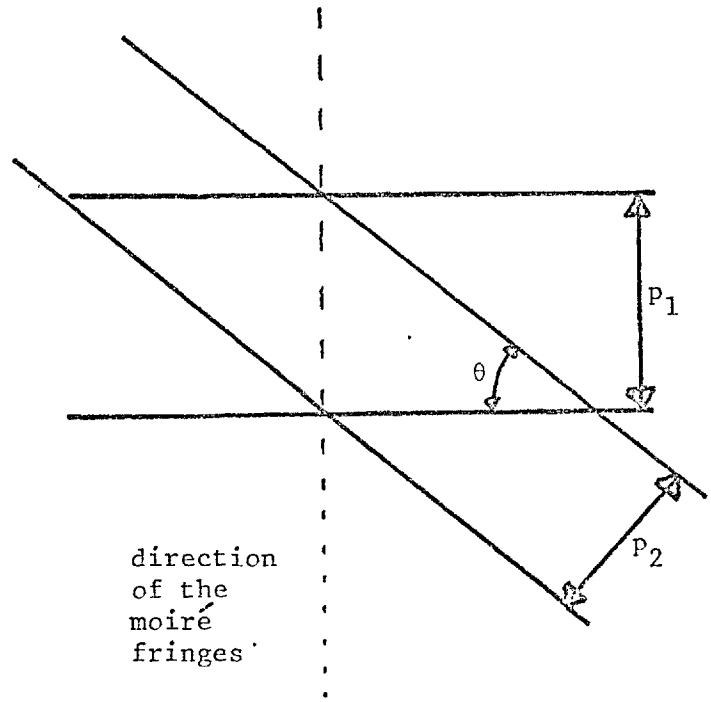


figure 49. The Nishijima/Oster grating arrangement, in which the grating pitches and the enclosed angle are such that fringes are produced perpendicular to the lines composing the larger pitch grid. For this to occur :-

$$p_2 = p_1 \cos\theta$$

B. MOIRÉ FRINGES APPLIED TO SURFACE WAVE MEASUREMENT.

(i) The optical system.

The principal information required to describe the surface wave properties of a given liquid surface was shown in Chapter 3 to consist of wavelengths and damping constants for a range of frequencies. The measurement of wavelength requires the observation of a property of the wave which changes along the wave in a cyclic manner. Quantitative information is unnecessary as long as the property is simply detectable. For example, Mann and Ahmad (1969) measured the distance between two positions of equal signal phase in a standing wave system where the separation of electrodynamic generating and receiving probes is adjustable. The measurement of damping requires knowledge of the relative magnitudes of a wave property at two positions along the path of a travelling plane wave. The absolute determination of wave height is not necessary, although it is useful to know that the amplitudes being observed are small enough for the use of the simplified wave equation to be justified.

The wave property measured should be simply related to variables in the hydrodynamic theory of wave propagation in order to simplify the interpretation, suitable quantities being the wave height and its derivatives, wave slope and wave curvature.

It was seen in A (iv) that the equal slope contours of a transparent solid can be found with moiré fringes, indicating that a distorted liquid surface could be measured in a similar way. A (v) described the simplification of measurements possible in one-dimensional systems, and it

has been found that a practical wave slope measurement system is possible using these effects. In any travelling wave technique, wave damping is most conveniently measured in a plane wave system because, for wave fronts of any other shape, the wave property would change with distance in the absence of energy dissipation, complicating the interpretation.

The moiré fringe system chosen for the examination of ripples was based on the work of Theocaris and Koutsabessis (1965) (figure45) incorporating the geometrical device first reported by Nishijima and Oster (1964) which produces fringes along the direction of light deflection (figure49). This was chosen because it could be arranged for the set of fringes to delineate wave normals, the fringe distortions being parallel to the wavefront, and proportional to the wave slope at each point on the wave train.

One major difference between the present work and that described by Theocaris and Koutsabessis (1965) is that in order to observe as large an area of surface waves as possible using an inexpensive medium aperture lens, the light from the collimator is not parallel, but focussed into the entrance pupil of the imaging lens. This minimises the lens distortion, but produces some magnification of the surface, which will be described in section B (v). A second difference, resulting from the necessarily horizontal plane of the liquid surface, is that for convenience of design and operation, the initially vertical optical axis has to be turned through 90° into the horizontal plane. The Theocaris system used identical gratings, the final lens producing a grating image of unity magnification. This could be done in the present system with a pair of gratings corrected for

the Nishijima/Oster geometrical device, but a greater degree of flexibility was achieved by varying the magnification slightly, using identical gratings corrected by this magnification.

The apparatus is shown diagrammatically in figure 10. Light from either the stroboscope or the electronic flash, passes through the pinhole and is focussed by the collimator through grating G_1 and the liquid tank, and into the imaging lens after suffering reflection at the front aluminised mirror. The final lens produces an image of G_1 in the plane of the second, reference grating, G_2, the light from the G_1 image which is allowed to pass producing moiré fringes on the ground glass screen adjacent to G_2. The laser is directed exactly along the optical axis back to the pinhole, and is used for alignment of the important surfaces. The previously mentioned magnification of the observed liquid surface can be seen to arise because the light from G_1 is converging into the final lens.

(ii) The construction of the apparatus.

The apparatus is split into two parts in order to avoid vibration of the liquid while the "camera" part of the apparatus is being operated. The liquid tank is mounted in a simple frame, containing the optical axis from sources to mirror. Vibration isolation between the frame and a rigid table is provided by a rubber mounting. The lens, grating G_2 and fringe recording system are located with the alignment laser on a 1 metre optical bench fixed to a rigid iron table. Connections between the two parts are restricted to necessary flexible wires. The stability of the optical axis

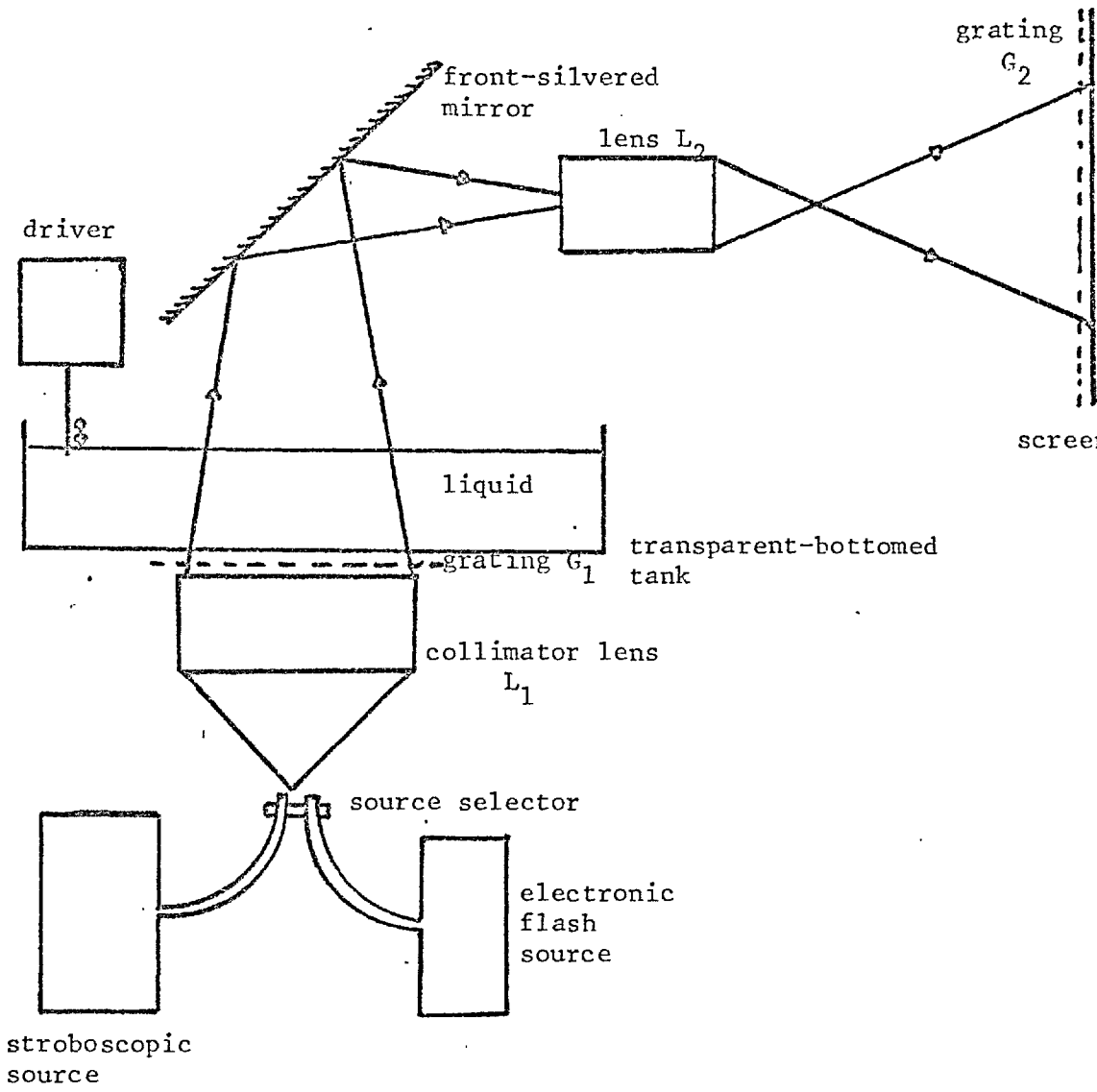


figure 10 Schematic diagram of the ripple observation apparatus.

passing between the two parts is ensured by the location of the two tables on the ground, and their considerable weight. There is a large amount of latitude possible in the choice of optical axis within the frame, so the initial relative placing of the two parts does not need to be accurate.

The light sources used to produce fringes consist of a stroboscope (Dawe 1203B) for visual observation of the fringes, and a photographic electronic flash unit (Dorma H-3) for producing permanent records of the patterns. This double source arrangement is employed because the exposure times necessary to produce a photographic contact print of the moiré fringes with the small pinholes required for precise collimation are long enough with the light available from the strobe unit for unwanted vibrations to produce blurred pictures. In spite of elaborate precautions to isolate the apparatus from ground-borne vibration, it was found that sufficient disturbance occurred in the region below 5Hz (where adequate isolation can only be produced by servo-controlled air cushions), notably from building foundation preparation in the area, to produce intolerable blurring. It was found, however, that a single flash from a small electronic flash unit was sufficient to make a photograph, and although the vibration is still present, its effects are now only in random distortions of the recorded fringes, whose effect will usually be minimised in the processing of the pattern measurements.

A 1mm diameter pinhole was employed with the flash source, in order to produce adequate collimation of the light. The effect of a larger pinhole is to spread the image of grating G_1 in the plane of G_2, thus

degrading the sharp edges of the fringes and the accuracy of their location. This precision is not needed with the stroboscopic source, as it is used only for visual observation and adjustment, and a 3mm diameter pinhole has been found adequate. The problem of placing a choice of source/pinhole combinations into the correct position on the optical axis has been solved using fibre optics. A 5mm diameter 12 inch incoherent light guide (Rank Fibrox Ltd.) links the brightest area of each source to a simple slide which moves between rigid end stops, each stop placing one of the alternative pinholes on the optical axis. The slide is moved by hand, and is retained in its correct position with adequate stability simply by friction and the bending resistance of the light guides. A more satisfactory means of providing a double light source would be to combine the two guides in a Y-junction so that the flash source optic fibres are symmetrically surrounded by those from the strobe source (figure 4.11). The cost of Y-junctions of this type is high, since they are made only to order, and the minor inconvenience of the slide arrangement does not justify the expense.

The light from the source/pinhole is collimated by a cheap 6 inch enlarger collimator held at fixed distance by a "Perspex" collar, and passes through the grating G_1. This grating is on a glass photographic plate, supported by three brass bolts with hemispherical tips, each carrying a fine thread adjustment, allowing movement of the grating both in position and inclination with respect to the optical axis. These constraints are maintained by gravity, although the position and orientation of the lines of the grating with respect to the direction of wave propagation is maintained by pieces of adhesive tape which allow small vertical motions only.

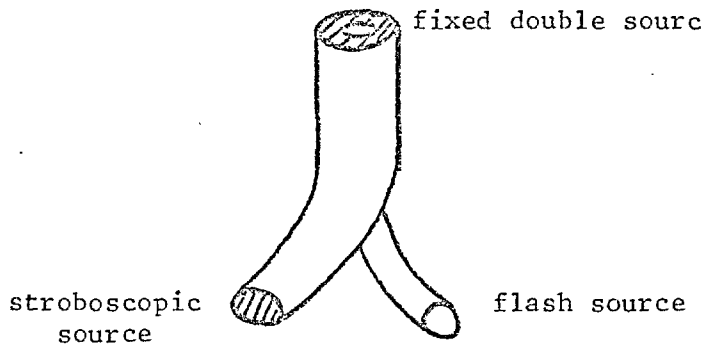


figure 4.11 Possible combination of two separate light sources using a fibre optics junction.

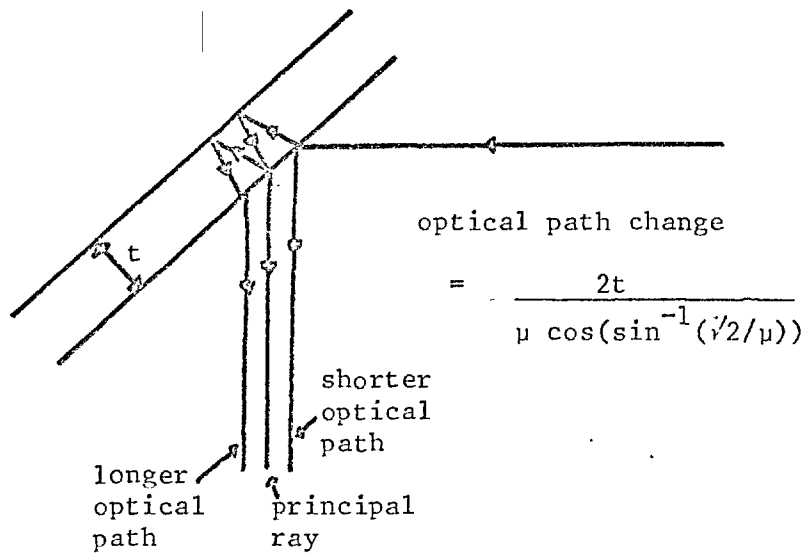


figure 4.12 The production of three images by the use of a rear-silvered mirror.

The gratings available for G_1 have line frequencies of 50, 65, 75,150, and 250 lines per inch. The 50 line grating is a master grating ruled by a printed circuit drawing machine, and the others are photographic copies of gratings owned by the National Physical Laboratory, kindly loaned for copying. It was found that gratings of line frequencies up to 250 lines per inch could be accurately copied by placing the emulsion of the master grating in contact with the emulsion of a high-contrast glass photographic plate such as "Kodalith" (Kodak Ltd.) or "Formolith" (Ilford Ltd.) and exposing under a focussed enlarger to minimise the effects of diffraction. Both of the above-mentioned types of plate were found to give gratings of extremely high quality and stability.

Light from grating G_1 enters the tank containing the liquid under investigation, made of $\frac{1}{2}$ inch thick "perspex" sheet, which is of excellent optical quality, and has sufficient strength and rigidity not to distort when full of liquid. A three-point adjustable support is used so that the tank base may be made perpendicular to the optical axis.

The mirror used to reflect the optical axis from the vertical to the horizontal is continuously adjustable in its inclination to the vertical between 40° and 50°, to allow for small variations in the placing of the mirror support on its vibration isolator. The glass blank used in the mirror is a piece of 3/8th inch float glass, chosen because the float glass process produces areas of glass of the necessary dimensions whose thickness changes by less than a small fraction of a light wavelength over the area. The fringe pattern is more sensitive to a light deflection

originating on the mirror than it is from any other component in the optical path. Front aluminising was used because the two principal reflections from the glass front of a rear reflecting mirror were observed to change the optical path (figure 4.12). The reflection from the front shortens the path by $2t / \mu \cos(\sin^{-1} \frac{\sqrt{2}}{\mu})$ whereas light suffering internal reflection after the orthodox reflection at the rear surface reappears with a path increase of the same amount. These small path differences produce a pair of images of G_1 to either side of the orthodox image along the axis, with magnifications correspondingly different. Observation of the fringe pattern shows the presence of two "ghost" G_1 images of greater and lesser pitch than the true image, which cause two sets of "ghost" fringes symmetrically inclined to the true horizontal fringes by a small angle. Although diminished in intensity with respect to the desired pattern, these fringes were found sufficiently confusing to necessitate their removal by front aluminising.

The lens used to project an image of G_1 into the plane of G_2 is a Kodak "Aero-Ektar", f2.5, 178mm, mounted rigidly on two optical bench fittings, each of which allows fine adjustment both vertically and horizontally perpendicular to the axis. Combined adjustment of these four linear dimensions allows accurate lens movement in four of the five degrees of freedom it possesses, the four being vertical and horizontal perpendicular linear motion, and the two rotations about horizontal and vertical perpendicular axes. The other degree of freedom, that of motion

along the optical axis, is adjustable by sliding the two bench fittings and clamping.

The support for gratings G_2 and the ground glass screen has been designed as a simplified camera structure. The vertical plane is maintained by the rigid wooden structure held in contact with the iron table by two strong horseshoe magnets. This structure straddles the optical bench, permitting $\pm$ 3 cm adjustment perpendicular to the axis in the horizontal direction. Adjustment of the camera unit is made by sliding it over the table before locking with the magnets. Grating G_2 is fixed rigidly to the camera by means of adhesive tape so that the grating rulings are held at the correct angle θ with respect to the vertical in order to produce horizontal fringes.

There is a light-proof box connected to the camera, which is designed to contain a roll of the photographic paper used to produce permanent records of the fringe patterns. The box lid blocks incident light with interlocking screens, although it is a simple push fit. Paper is drawn from a long felt-lined slit down one corner of the box, and is cut off from the roll as required.

The laser is used solely for alignment of the apparatus, the direction of the beam defining the optical axis. Each component in turn is adjusted as described in B (iv) so that the light reflected from its surface retraces its axial path back to the laser.

(iii) The theory of the measurement technique.

The optical system is shown schematically in figure 13, and comprises two identical gratings, a liquid surface and a lens. As described in sections A (v) and B (i), a fringe pattern is desired which consists of an equispaced set of straight parallel lines, running perpendicular to the rulings of grating G_1. This is possible using two gratings whose rulings are inclined at angle θ, and whose pitches P_1 and P_2 are related in the following way:-

$$P_1 = P_2 / \cos\theta \qquad 4.1$$

(after Nishijima and Oster, 1964)

G_1 being the larger grating (figure 9). The spacing of the resultant fringes, ΔY_o is given by

$$\Delta Y_o = P_1 \cot\theta \qquad 4.2$$

and since the fringe spacing is always chosen to be much greater than P_1, it follows that θ is small. The resulting difference in pitch between the two component gratings is small, which allows it to be produced as a small magnification in the same imaging process as that used for wave observation. This permits two identical gratings to be used, the magnification of G_1 being produced by adjustment of the position of the imaging lens between the two grating planes. Since the initial pitch of both gratings is P_1, the equation 4.1 becomes :-

$$m = P_1/P_2 = 1 / \cos\theta \qquad 4.3$$

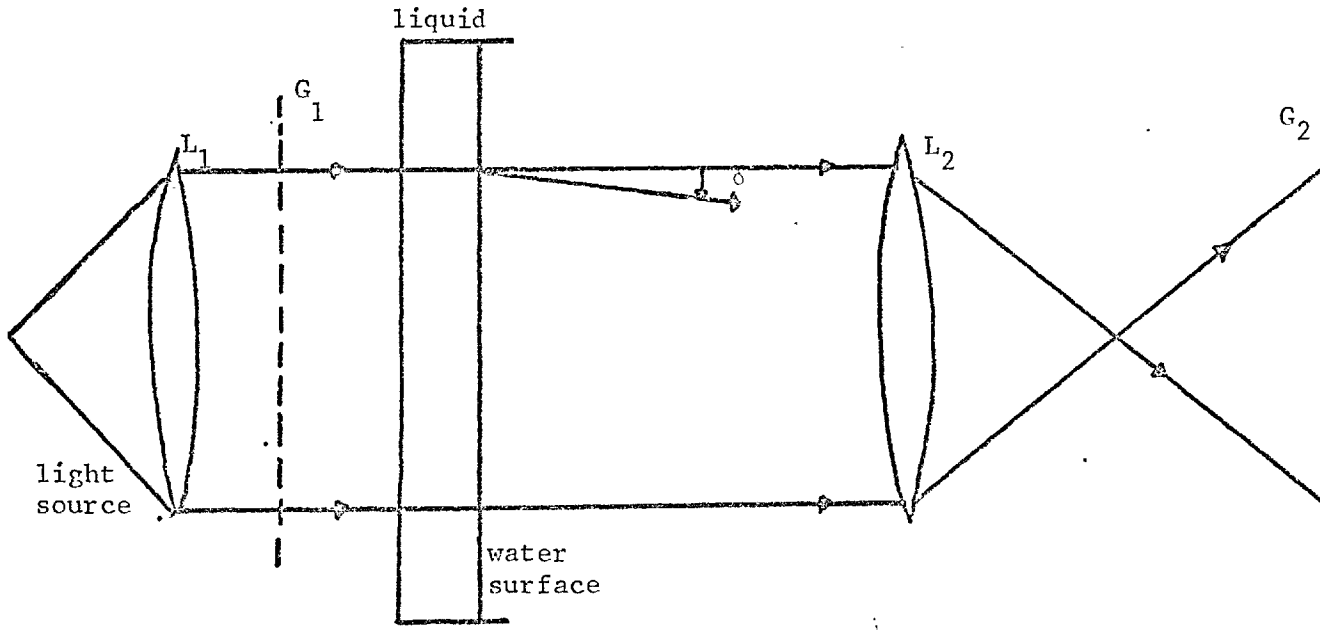


figure 4.13. The basic optical system used in the measurement of ripples.

Figure 4.14 shows fringes produced perpendicular to the rulings of the object grid in a drawn pair of coarse grids related as above.

When the liquid surface becomes distorted by the passage of waves, light travelling from G_1 to the lens becomes refracted towards the axis x_s (figure 4.15) through an angle δ given by

$$\delta = (\mu - 1) \cdot dh/dx_s \qquad 4.4$$

where μ is the refractive index and h is the liquid depth at any point. The axis x_s is parallel to the undisturbed surface. It is shown in Appendix 1 that the displacement produced in the real image by a light deflection δ, between G_1 and the lens is given by

$$\Delta x_i = -mh_1\delta \qquad 4.5$$

where Δx_i represents the displacement in the image plane, along the same axis as x_s, m is the image magnification, and h_1 is the optical distance between G_1 and the surface. The negative sign is a result of the image inversion produced by the lens.

Thus, for a ripple disturbance travelling in the x_s direction represented by

$$h = h_o \sin 2\pi(ft - x_s/\lambda) \qquad 4.6$$

where h_o is the wave amplitude, f the frequency, and λ the wavelength, the wave slope is

$$dh/dx_s = -2\pi h_o/\lambda \cdot \cos 2\pi(ft - x_s/\lambda) \qquad 4.7$$

and the image displacement associated with each part of the wave is given by:-

$$\Delta x_i = \frac{2\pi m h_o h_1(\mu-1)}{\lambda} \cdot \cos 2\pi(ft - x_s/\lambda) \qquad 4.8$$

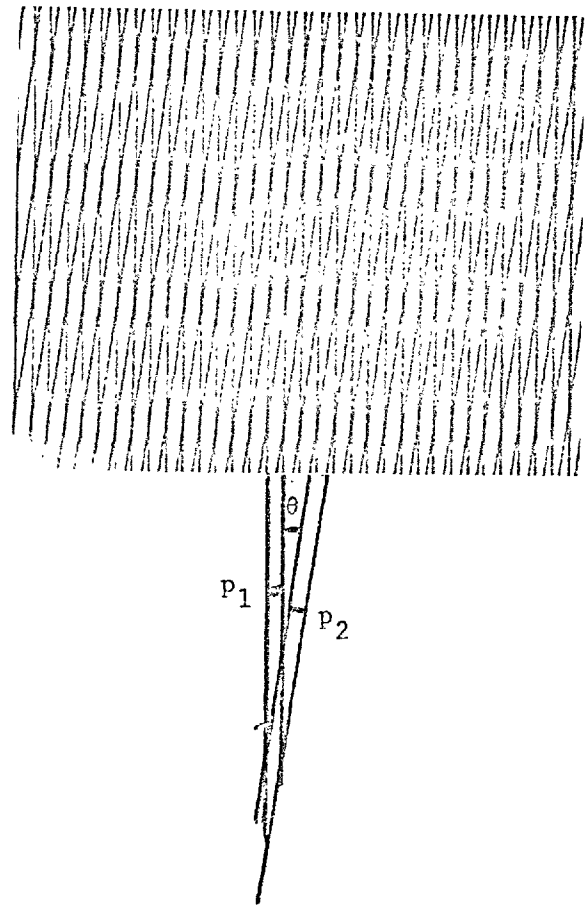


figure 4.14 Fringes being produced perpendicular to the rulings of the larger grid, following Nishijima and Oster (1964).

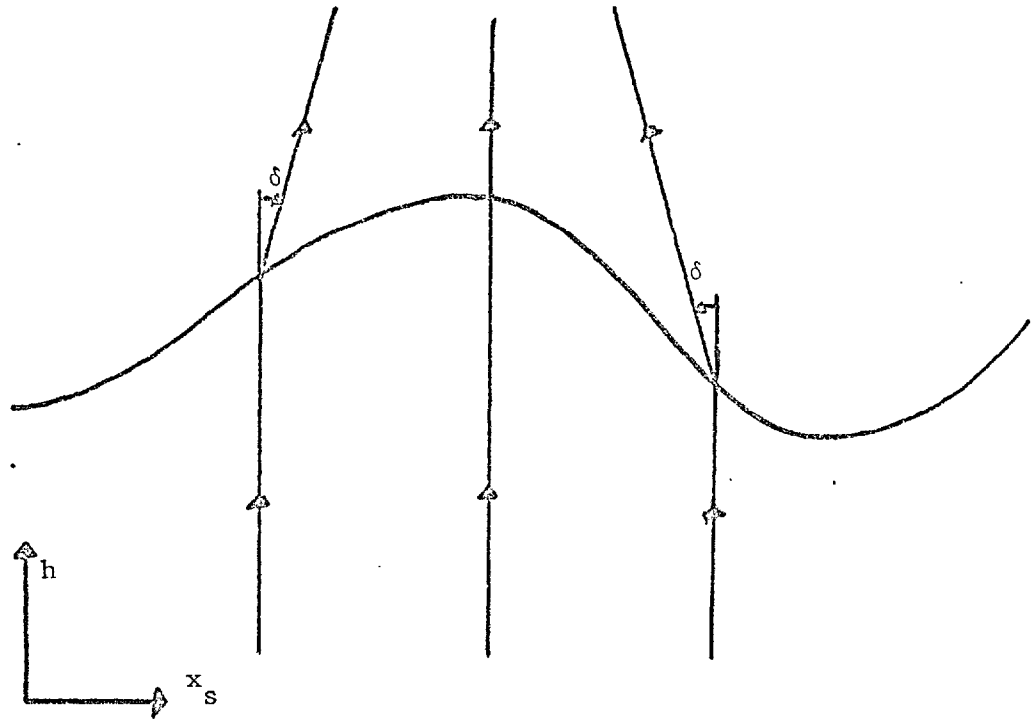


figure 4.15. The direction of light deflection by the ripple-bearing liquid surface.

If, as in the case being considered, the object is a grating whose rulings are perpendicular to the x_s, x_i direction, then this sinusoidal image distortion will produce an image similar to that shown in figure 4.16. This is a drawn grid whose mean pitch is the same as that of the object grid shown in figure 4.14.

In a moiré fringe pattern, if one line is displaced a small distance Δx then the resulting displacement of the fringe at that point will be $(\Delta x/p).\Delta Y_o$,

where p is the normal pitch of the grating, and Δy_o the normal fringe spacing. Thus, in the present system, the fringe displacement produced by a line displacement dx_i in a grating of pitch p_1 is

$$\Delta Y = (\Delta x_i / p_i) . \Delta Y_o \qquad 4.9$$

Combining equations 4.2 and 4.9,

$$\Delta Y = \Delta x_i \cot \theta \qquad 4.10$$

the resulting fringe displacement due to the sinusoidal wavetrain described above being given by equations 4.8 and 4.10 as:-

$$\Delta Y = \frac{2\pi m h_o h_1 (\mu - 1) \cot \theta}{\lambda} . \cos 2\pi(ft - x_s/\lambda) \qquad 4.11$$

Figure 4.17 shows the substitution of the figure 4.16 grid into the figure 4.14 configuration. The initially straight parallel horizontal fringes have become distorted normal to the rest direction of the fringes, and the distortion is related to the initial line position variations by eqn.4.10 The sinusoidal variation in line displacement, of amplitude equal to a complete grating spacing, is translated in the fringe process into a sideways fringe motion of amplitude equal to a whole fringe spacing.

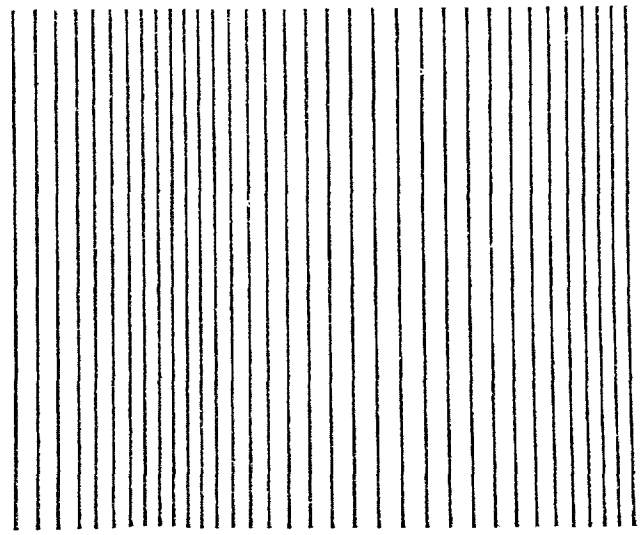


figure 4.16 The p_1 grid used in figure 4.14, distorted by a sinusoid.

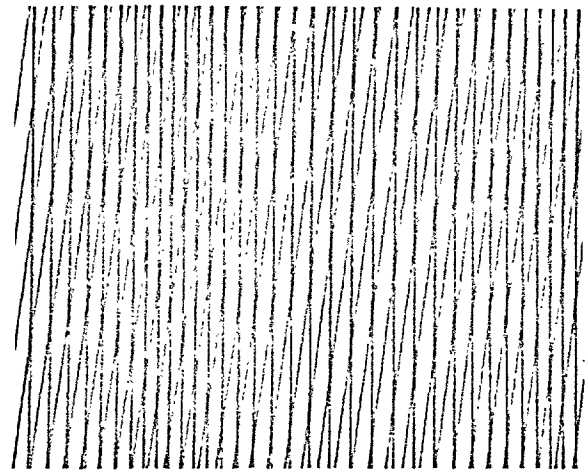


figure 4.17 The fringes obtained by using figure 4.16 in the figure 4.14 configuration.

The magnification of the motion is $\cot\Theta$, increasing as Θ decreases.

This pictorial example displays the source of the moiré sensitivity, and shows how a continuous record of the wave slope is produced, at a sampling rate equal to the grating line frequency.

It is often useful in comparisons of sensitivity with this type of one-dimensional fringe system to express the fringe motion as a function of the fringe separation. Although the fringe displacement ΔY , given by equation 4.11 is dependent on $\cot\Theta$, and will tend to infinity as Θ tends to zero, the sensitivity of the system to a given disturbance does not increase in the same way. The accuracy with which a fringe distortion may be detected or measured depends on how well the fringe is defined. Examination of figures 4.14 and 4.17 indicates that for a fringe pattern produced with low pitch grids, the light intensity across the pattern will be a smooth function, there being no sharp edges or visually well-defined fringe centre lines. The accuracy with which the fringe position is defined depends on what appears with visual observation to be the width of the fringe, which is directly linked with the repeat spacing of the fringe pattern,

It is therefore more useful when comparing the properties of different grating combinations to measure a distortion in terms of this spacing parameter. Such a sensitivity parameter as defined by $\Delta Y/\Delta Y_o$ is given by equations 4.4, 4.5, and 4.9 :-

$$\Delta Y/\Delta Y_o = (-m\, h_1(\mu - 1)/p_1) \,.\, dh/dx_s \qquad 4.12$$

For the sinusoidal wave disturbance described above, the maximum fringe displacement due to a liquid ripple of amplitude h_o and wavelength is given by (equations 4.7 and 4.12)

$$\left|\Delta Y/\Delta Y_o\right|_{max} = \frac{2\pi m\, h_o h_1 (\mu - 1)}{p_1 \lambda} \qquad 4.13$$

(iv) Measurement sensitivity.

In equation 4.13 the factors determining the response of the fringe system to a given wave disturbance are the optical distance h_1 between the grating G_1 and the liquid surface, the refractive index μ, and p_1, the pitch of G_1. The magnification m of G_1 in the image plane is almost unity, and should be considered in conjunction with p_1.

The choice of h_1 is guided by two considerations, (a) hydromechanical and (b) optical. In the solutions of the hydromechanical equations of the liquid surface, it is found that wave properties can be assumed to be independent of liquid depth when this is greater than half of the wavelength (Stephens and Bate, 1966). Compliance with this condition simplifies the analysis of results, and provides a lower limit to h_1. At the other extreme, as the surface moves closer to the lens, its image suffers distortion (in addition to the distortion in the grating image) and reduction of viewed area resulting from the geometry of the light path. With the present lens, of 178mm focal length, it is possible to use values of h_1 up to 100mm before the surface field distortion becomes intolerable. The only way of producing a real increase in sensitivity without incurring accentuated surface image distortion is to use a lens of greater focal

length. In this way, h_1 may be increased in the proportion of the focal length increase without affecting the distortion.

The spherical aberration of the lens produces grating image distortion in the G_2 plane, affecting the quality of the fringe pattern and producing measurement errors. The difficulty with the treatment of lens distortion is that for a fixed surface/lens/gratings geometry, any improvement in sensitivity produced by reducing p_1 affects the wave-produced distortion in the same way. Thus, although there will be a greater movement of the fringes for a given wave disturbance, there may be no overall improvement in measurement precision since the departures from linearity of the straight line basic fringe pattern increase in the same proportion.

In the present work, a means was devised of minimising the effects of lens distortion, using an analogy with holographic interferometry techniques which was described in section A(ii). It was observed that the theoretical straight line pattern which was achieved with perfect straight line gratings, but degraded when one of the gratings became distorted, can be regained almost completely if both of the gratings are arranged to have the same initial distortion. This notion was derived from the production, using holography, of what are essentially two-beam interferograms using two identical copies of the same complex optical wavefront (see Fryer, 1970). The distortion cancellation will never be complete in this technique, because the method of fringe production used at present requires a small rotation of one grating with respect to the

other, which inevitably separates the areas which are identical. The consequent reintroduction of distortion is however much smaller than the initial distortion, since the aberrations are continuous, and only the change over the distance of separation is significant.

The method by which the distortion cancellation is produced involves the initial alignment of the optical system in the manner described in section B(v), using the same depth of liquid in the tank as will be used in practice. The best pattern possible is found using a pair of identical gratings, correctly aligned with respect to the axis, and then the lens is moved towards G_1 in order to reduce the G_1 magnification to unity. A rotation of G_2 so that its rulings are parallel to the G_1 rulings then produces a "zero fringe" condition, i.e., the light passed by G_1 is almost completely blocked by G_2. In this condition, the lens distortions are most clearly visible, and the image of G_1 is known to be exactly the right size, so the reference grating is removed, to be replaced in dull red illumination by a "Formolith" Orthochromatic glass plate cut the required size, taped firmly to the camera with the emulsion facing the lens. With the whole system as still as possible, the plate is exposed, according to the results of a test exposure, and then developed and fixed using the recommended chemicals. This plate being then a distortion-corrected negative copy of G_1, a positive must be produced by contact printing on to a further plate as described in section B (ii).

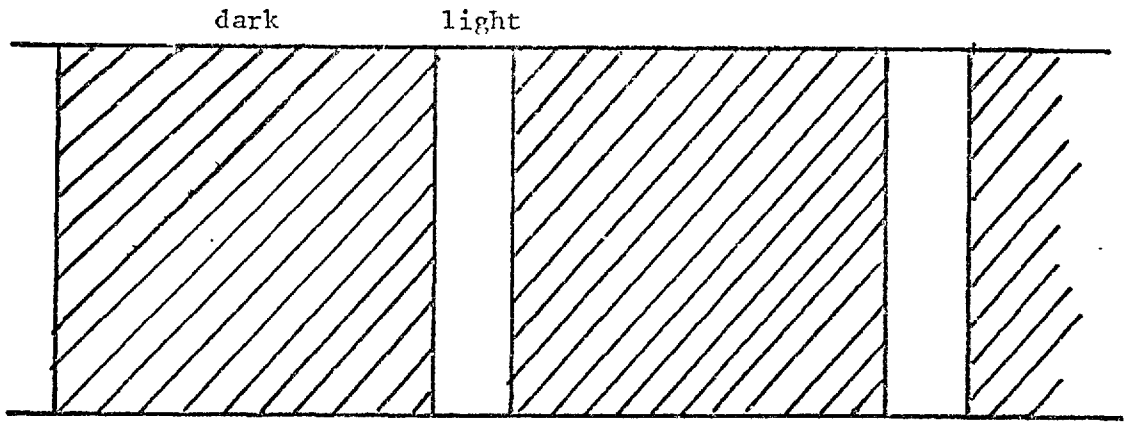
In replacing this positive grating, with the system exactly as it was during the exposure, it should be possible to prevent all light from reaching the ground glass screen - the "zero fringe" condition of setting up. This test gives a good indication of the quality of the copy. The lens and camera are adjusted to provide the necessary G_1 magnification, and G_2 is given its slight rotation to produce the desired fringe pattern.

The choice of gratings for fringe production is complicated by the assessment of the true measurement sensitivity for a given grating pair. It has been indicated above that a real sensitivity increase does not always follow from a decrease in grating pitch, although $\Delta Y/\Delta Y_o$ increases linearly. If we take as an example a pair of gratings whose line/space ratio is unity, it is seen that as the pitch decreases $\Delta Y/\Delta Y_o$ increases, but the lens distortion increases proportionately. This effect has been largely removed by the distortion cancellation methods described above, so for the purposes of further analysis, we can assume that $\Delta Y/\Delta Y_o$ does increase with decreasing grating pitch, although slightly less than predicted by equation 4.13. As the line frequency continues to increase, a second effect becomes important in determining the fringe quality and measurability, namely the diffraction of light by the gratings.

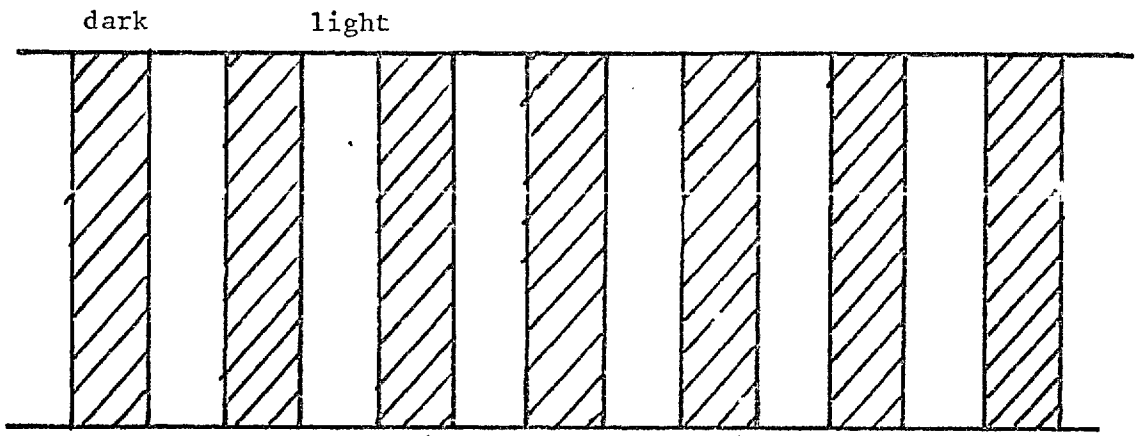
The lens can only handle light from the grating which is contained in a finite solid angle, so there is a limit to the spatial frequencies contained in an object which can be reproduced from a given object position. Spatial frequencies near the resolution limit of the lens will be filtered out of the image, blunting the sharp edges of the grid rulings. As the line frequency increases, the square profile of the grid rulings

is degraded eventually to a sinusoid, with reduced contrast. The fringes become much less optically dense, and the fringe intensity profile, which from simple geometrical considerations is composed of constant intensity and linearly varying intensity areas, becomes rounded and less predictable. The reduction in fringe contrast is the more important effect, as the precision with which fringes are located depends on their visibility.

While this effect cannot be removed completely in a system which relies on conventional lens optics, a way was found of making it less important. Although the image of a space on the object grating will always be degraded according to its width, the contrast between the centre of this image and the rest of the pattern depends on the distance between the object grid space and its nearest neighbour. Thus, although a 50 line grating with a light to dark ratio of 0.2 has the same space width as a 150 line grating whose light to dark ratio is 1.0, (figure 4.18), and the image degradation is the same, the "coarser" grid will have over 80% more dark space between the light areas, which improves the contrast. If both pairs of gratings are used at the same angle Θ, then the light part of the fringes should be the same in both cases, and it will be just as accurately measured in one pair as the other. The actual sensitivity to measurement has remained the same, although ΔY_o is greater in the "coarser" grid.



50 line grating (light/dark) = 0.2



150 line grating, (light/dark)= 1.0

figure 18. The production of finer fringes by using gratings of unequal dark and light areas.

This simplified analysis shows that the important factor in the measurement sensitivity for this system is not just the grating pitch or line frequency, but the resulting thickness of the light part of the fringe. The obvious step in producing a theoretical description of measurability and sensitivity which includes effects due to line/space ratios not equal to unity would be to replace the reference fringe spacing ΔY_o by a quantity representing the thickness of the measured part of the fringe. In the system just described, this would be the apparent width of the light area of the fringe set in each of the two cases. Whereas $\Delta Y/\Delta Y_o$ is useful in comparing the sensitivity changes which can be produced without changing the grating pair, the new parameter would enable comparison to be made between different pairs of gratings. Although a rough guide to the change produced in the fringes can be obtained by assuming that the light/dark ratio of a fringe corresponds to the light/dark ratio of the component grids, it has been found impossible to estimate the exact effect on the fringes from a grid change because the visually apparent thickness of the part of the fringe between maximum transmission and minimum transmission areas depends on a mixture of diffraction effects and human factors. Experimental investigation of the factors involved requires a large number of gratings covering wide ranges of grating pitch and line width.

The gratings employed for the majority of the present investigation were a distortion-corrected pair of 65 lines per inch grids whose light to dark ratio was 0.3 . It was found by experience that this pair gave patterns of fringes enabling as sensitive a wave measurement as 200 lines per inch gratings of unity ratio. The fringes are obviously coarser in structure, having fewer line crossings per unit distance, but their profile is distinct, with excellent light extinction between undistorted fringes, in contrast to the rounded appearance of the "finer" fringes, and their close spacing.

To summarise, it has been found that for applications of moiré fringes in which a one dimensional variation is being observed, sensitivity will increase as the pitch of the gratings decreases, but the accuracy and ease of measurement will only increase in proportion if the effects of lens distortion and resolution are simultaneously reduced. By following these principles, a system has been produced which is capable of accurate measurements of the wave slope of liquid surface ripples.

From equation 4.13, the wave height h_o which would produce unity fringe displacement ($\Delta Y = \Delta Y_o$) is given by:-

$$h_o = \frac{p_1 \lambda}{2\pi m \, h_1 (\mu - 1)} \qquad 4.13$$

For a practical system, putting in typical values,

$p_1 = 3.91 \times 10^{-2}$ cm.

$h_1 = 10.0$ cm.

$\lambda = 0.50$ cm.

$\mu = 1.333$

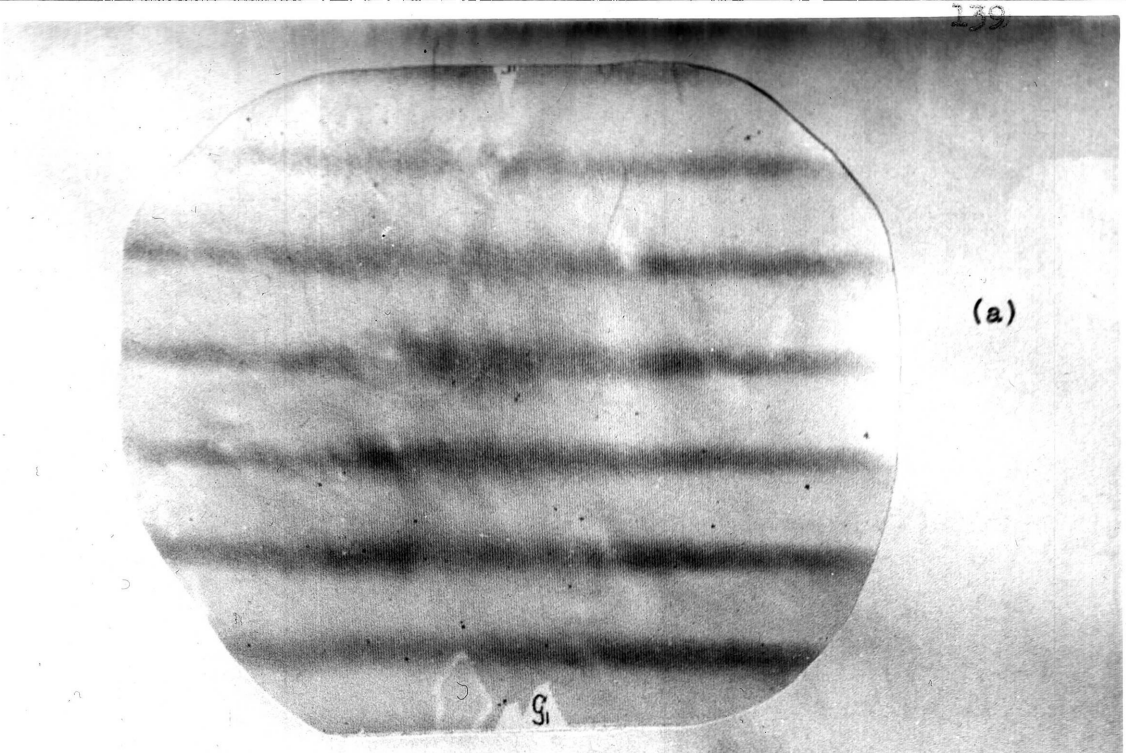
$m = 1.17$

$$h_o = \frac{3.91 \times 0.5 \times 10^{-2}}{2\pi \times 1.17 \times 10.0 \times 0.333}$$

$$= \underline{8.0 \times 10^{-4} \text{ cm.}}$$

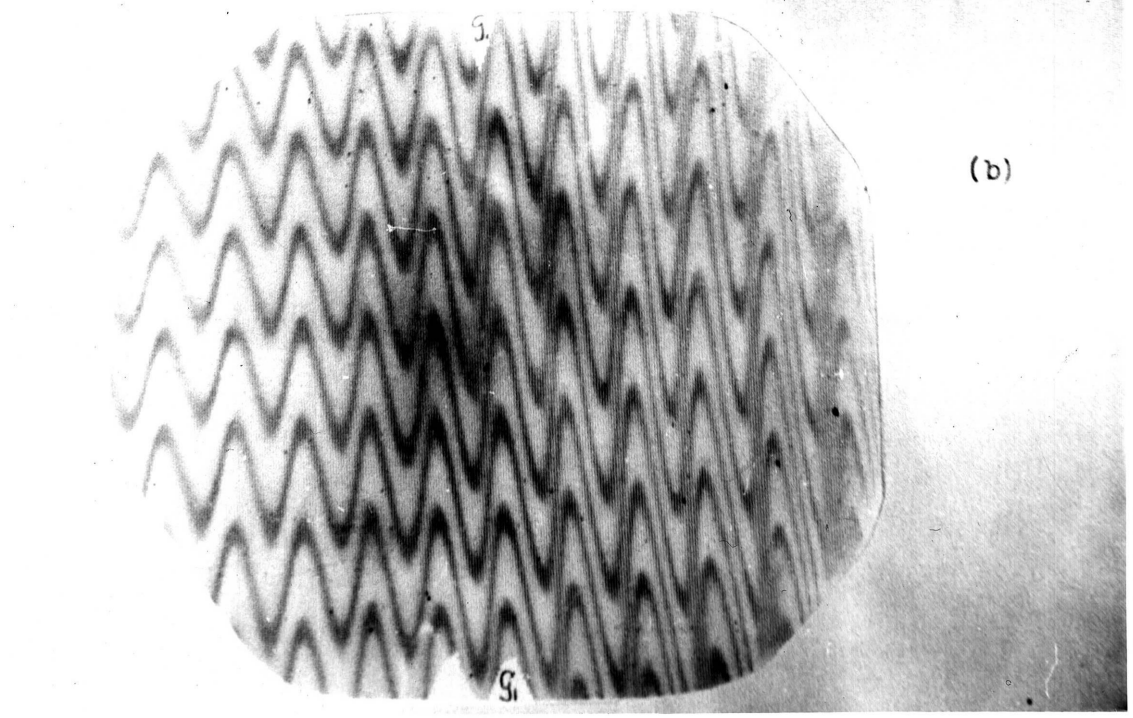
(v) Choice of fringe system.

As explained in section B(i), the fringe system produced by gratings corrected as described above is a set of parallel straight fringes, running perpendicular to the rulings of G_1, and along the expected propagation direction of the ripples. Each fringe is originally a wave normal, and when the waves travel down the tank, it displaces proportional to the wave slope, the displacement being along the wavefront (figure 19). The observed area of the surface wave system is therefore sampled by the set of fringes. In a truly plane wave system, the wave slope should be the same at all points of equal phase, so each fringe should have the same displacement in the perpendicular direction.



(a)

Figure 4.19. Patterns produced in the moiré fringe apparatus. (a) Basic, undistorted pattern, no waves present. (b) Damped system of 30 Hz ripples crossing the observed field from right to left.



(b)

If this were known to be the case, then the ideal system would be a single fringe running down the central wave normal, which would yield the variation of wave slope by simple measurement. However, it has been found difficult in practice to be certain that the wavefront is homogeneous, and although only a small variation is likely to occur across the full field width, if the wave generating system is properly adjusted, it is nevertheless useful to have a set of fringes showing how the wave slope varies at different wave normals, so that departures from ideal conditions may be recognised immediately.

It was found by trial and error that the division of the 10 cm wide observed area into five or six fringe spacings gave sufficient sampling points without reducing ΔY_o to a point where it was difficult to measure the resulting small fringe displacements. This arrangement also provides a pattern which can be quickly assessed by eye for optical system misalignments, wave front homogeneity, and the presence of waveform distortion. Figure 4.19 (b) shows a typical pattern of the type used for damping measurements. The provision of six symmetrically placed fringes allows observation of a maximum wave modulation which corresponds to $\Delta Y/\Delta Y_o = 1$, and this has been found to be adequately measurable using the digital measurement device described in section B (viii).

The pattern shown in figure 4.19 displays the increased measurability which results from the reduction in thickness of the part of the fringe to be measured. Fringes due to gratings of light/dark ratio of unity with the same ΔY_o would have a fringe width approximately equal to

half the fringe spacing, and would considerably complicate the picture. It should be remembered that the records produced by the camera, exemplified by figure 4.19, are negatives of the actual light distribution passed by the grating pair.

(vi) Optical alignment.

The sensitivity of moiré fringe patterns to small distortions of one of the component grids is very large, the sideways movement of one line resulting in a fringe displacement ($\cot \theta$) times the original movement, where θ is the angle between the rulings. It is imperative, therefore, that the optical components be accurately adjusted in order to ensure optimum fringe quality. The optical axis, about which all components are aligned, is the most important part of the system, and it must be easily referred to. In the wave visualisation method the axis is displaced through 90° to accommodate the horizontal liquid surface while allowing the majority of components to be maintained on a convenient horizontal axis.

Once the laser is mounted on the optical bench, directed into the empty frame of the liquid tank support, the "horizontal" axis is defined, and can be adjusted by a spirit level. The mirror is then adjusted relative to the beam so that the light reflected downwards can be returned by a quiescent mercury surface along its original path. The pinhole system with the light guides attached is arranged on its three-point fixing to be on the axis for both pinhole positions. The collimating lens and its spacing collar are now placed over the pinholes, resting on the same

supports, and adjusted so that transmitted light is focussed into the centre of the pinhole, while reflected light from the top surface of the lens retraces its path to the laser. After adjustment, these components are firmly taped into position. Grating G_1 is then placed on its three-point adjustment, which is arranged so that G_1 does not touch either the collimator or the tank, and returns the laser beam. The same procedure is used with the tank and its glass cover, before the tank is filled with a volume of liquid identical to that which will be used for measurement, the vertical being checked by the liquid surface reflecting the light back to the laser.

The final lens is then placed on the optical bench, and using the camera mount and the stroboscopic light source, the fringe pattern is adjusted to produce as good a set of straight fringes as possible, by moving only the lens and camera. The camera is then removed so that the lens can be adjusted relative to the laser. The many air/glass surfaces in the multi-component lens each produce a separate beam reflection, the locus upon which all of the reflected light spots fall in the plane of the laser stop being a straight line passing through the centre of the aperture. When correctly aligned, this line reduces to a point coincident with the aperture centre, and it is then known that the beam is passing through the centre of each component, perpendicular to its faces. On replacing the camera so that the reflection from G_2 also coincides with the aperture centre, the resultant pattern should show a significant improvement over the unaligned pattern. It is usual to repeat the lens/camera alignment procedure a further once or twice so that it is

certain that the optimum pattern has been produced. Lens and camera are then fixed firmly to the optical bench, and the system is ready for observations.

(vii) The operating technique.

Once aligned as described in the previous section, the apparatus is ready for use, and the tank after thorough cleaning is filled with the liquid for observation. Details of cleaning and solution preparation are given in Chapter 6 . If the alignment was carried out with the exact depth of liquid to be used, then no further adjustment is necessary.

The best way of generating ripples was found to be by using the vertical oscillations of a 1/16 inch thick "Perspex" plate, almost as long as the tank width. This plate which is suspended with its lower edge just touching the liquid surface, is excited into vibration by a pair of Goodmans vibrators, one at each end, operated in parallel at the same phase from a single audio power amplifier (Leak 20 Watt). The position of the plate with respect to the field and the rulings of G_1 can be adjusted by moving either or both of the vibrators, which stand on brackets at either side of the tank. The sine wave source is an Advance L.F. Signal Generator Type 81A, the frequency being monitored with a Gresham Lion Timer Counter Type GFT 15.

For the investigation of the wave properties at several different frequencies over a range of increasing solution or monolayer concentration, pure water is always examined initially, each frequency being selected in turn, and the amplitude being adjusted during continuous observation

using the strobe source so that the resulting picture is capable of adequate measurement (see section B(viii)). Taking care not to shake the frame containing the tank, the pinhole slide is moved to place the flash source on the axis, the stroboscope is switched off, and enough photo-sensitive paper is pulled out from the light-proof cassette to cover the observed field, the paper being held in contact with G_2 by the hinged ground glass screen. After a few seconds to allow any unwanted vibrations caused by adjustment to die away, the flash is triggered by push-button to expose the paper. The photographic paper used is Kodak Linagraph 553, which was designed as the recording medium for chart recorders with moving white light recording heads, and in consequence it produces high contrast at low light levels. After the exposure by single flash, the exposed section of the roll is cut off using a razor blade, and stored in a light-proof box until a batch is processed.

Processing takes place in the same darkroom as the initial exposure, illuminated by indirect dull yellow light, using Kodak DX80 developer diluted 1 + 4 with water, and "Kodafix" fixing solution diluted 1 + 8. 45 - 60 seconds is usually sufficient development time, and fixing is allowed at least 5 minutes. The prints are washed in running water for more than 15 minutes and dried lying face downwards. Relevant information about the exposure conditions is recorded immediately after exposure on the reverse of the print, in water-proof ball-point.

(viii) The processing of results.

The information needed to measure the wave damping was shown in B(i) to consist of the relative values of peak wave slope at two points down the wave normal, and the separation of the two points. Since the pictures produced by the moiré method show the variation of wave slope at a single instant in time, the wavelength is found by measuring the distance covered by a known number of whole waves. Wave slope is most simply measured at its peak values, from the distortion maxima of the fringes, and the two points of measurement are chosen to be a finite number of wavelengths apart, their actual separation following from the wavelength measurement.

Figure 4.20 represents the shape of the exponentially decaying sinusoid function portrayed by the fringe distortion. Measurement of y_1 and y_3, deflections on the same side of zero separated by q wavelengths would give the damping coefficient β as:-

$$\beta = \frac{\log_e y_1/y_3}{q\lambda}$$

and similarly, β is given by deflections to the opposite side of zero:-

$$\beta = \frac{\log_e y_2/y_4}{q\lambda}$$

It is found most convenient with the form of distortion in the present system to measure the sum of deflections in opposite directions, i.e., $y_1 + y_2$ and $y_3 + y_4$, for it is known that

$$\beta = \frac{\log_e (y_1+y_2)/(y_3+y_4)}{q\lambda} \qquad 4.14$$

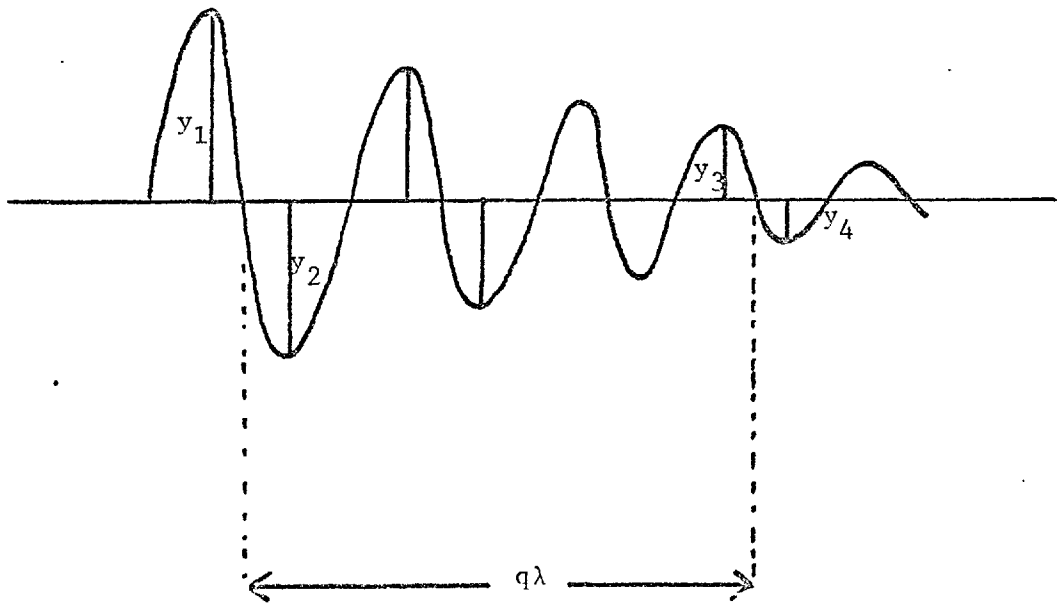


figure 20. Measurements on a decaying sinusoid to evaluate the damping coefficient.

Assuming that the magnification of the observed field is uniform, the quantities $y_1 + y_2 = Y_n$ for each of n wavelength increments can be found on a relative scale by simple measurement of the difference in position of the fringe between the two points of successive peak fringe distortion, positive and negative. It is not necessary to make the measurement accurately along perpendiculars from the undistorted fringe, as implied by figure 4.20, since as long as the same measurement direction is used for all Y_n, their relative magnitudes remain unaltered. It is usually most convenient to measure perpendicular to the fringe as this allows absolute wave slope magnitudes to be subsequently deduced as well as the damping.

The magnification of the observed field, shown in B (i) to arise from the geometry of focussing light from the collimator into the entrance pupil of the imaging lens, must be measured in order to know the true wavelength, and hence the distance between positions of relative wave slope measurement. There will be a further small addition to the surface magnification due to the term m in equation 4.13 resulting from the Nishijima/Oster grating correction procedure (section B (iii)). The total magnification is best determined experimentally, by measuring the size of the image of a calibrated object placed in the plane of the surface. The object used for this purpose is a 1/8th inch "Perspex" plate, as long as the tank width, wide enough to cover the largest possible observed field, and covered with painted parallel lines, running perpendicular to the fringes. When the plate floats on the surface with the lines uppermost,

the lines are almost in the plane of the surface, and produce regular interruptions in the undistorted fringe pattern, whose separation provide the measurement of field magnification, the real line separation being measured directly. These measurements and all other pattern measurements are made on the digital measurement device to be described.

Figure 4.21 shows a pattern of the type given by waves travelling on the surface. The position of each of the marked fringe positions is measured with respect to an arbitrary origin the position being expressed as a number between 1 and 1000. Addition of position numbers $a_1 - -a_6$ is done during measurement on a calculating machine, and then $b_1 - -b_6$ are subtracted from the total. The resulting quantity gives a total digital fringe distortion proportional to the mean wave slope as sampled by the fringes. A similar procedure is followed with $c_1 - -c_6$ and $d_1 - -d_6$, the resulting number referring to the mean wave slope at the second position. The ratio of the two resulting numbers,

$$\frac{\sum_6 a_i - \sum_6 b_i}{\sum_6 c_i - \sum_6 d_i} \qquad \text{is equivalent to} \qquad \frac{y_1 + y_2}{y_3 + y_4} \qquad \text{(see 4.14)}$$

The second quantity required, the separation of the two points, is found using the same digital apparatus, measuring the distance occupied by the largest number of complete wavelengths shown in the observed field. This procedure gives the minimum of error due to inaccurate end location and lens distortion of the surface area. The separation follows from the

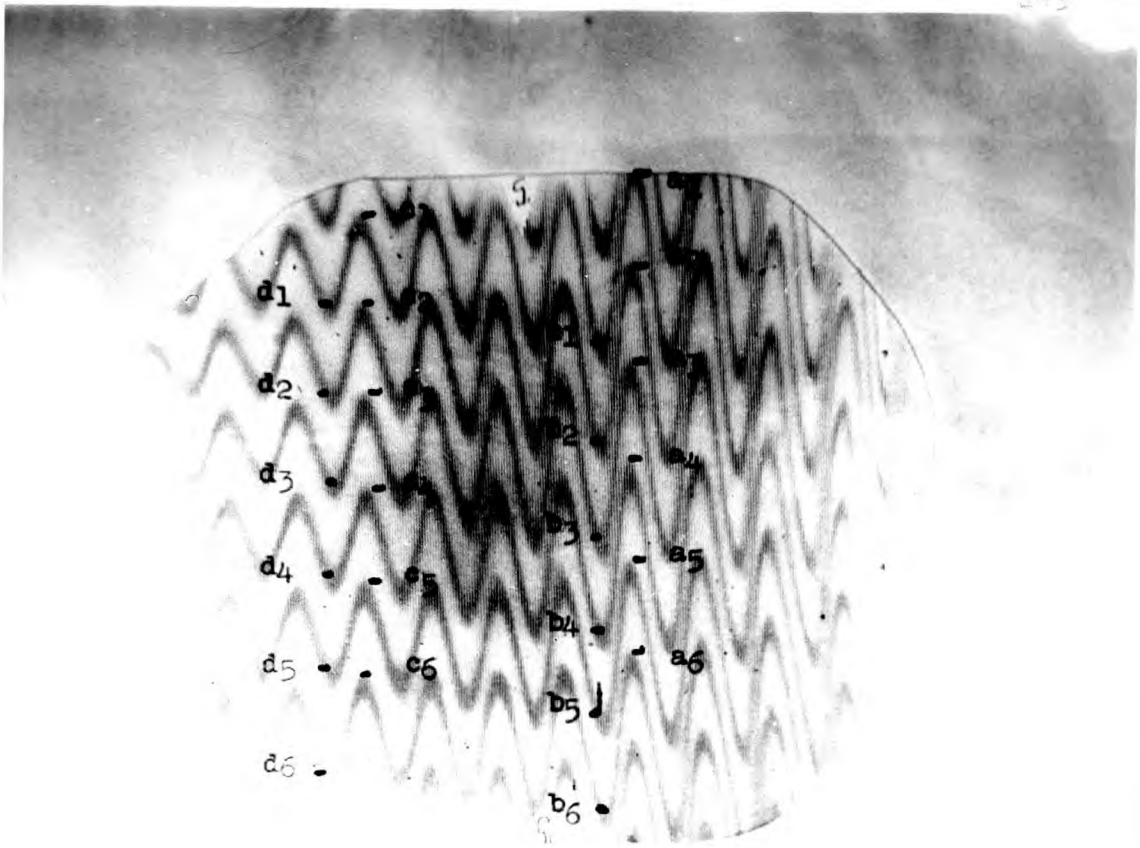


Figure 4.21. A typical pattern of the type used for measurement of wavelength and damping coefficient. The waves in the picture are travelling from right to left, and have frequency 30 Hz.

wavelength and the number of whole waves between the sampling points.

The choice of the two measurement points is governed by the need to have both wave distortions large enough for accurate measurement, as well as having their ratio sufficiently large to minimise the error introduced by the conversion into natural logarithms of numbers close to unity. The first peak is chosen to be the largest in the pattern, and the second is usually found to be adequately measurable if it is between 0.5 and 0.3 of this. The resulting ratios between 2.0 and 3.0 can be converted into natural logarithms without error magnification.

The instrument designed to enable rapid measurement of the moiré fringe patterns is based on the combination of a linear potentiometer, whose resistance is proportional to the extension of the slider, with a digital resistance meter. Figure 4.22 shows the principle of the instrument, in which the potentiometer slider is attached to a frame which slides on $\frac{1}{2}$ inch copper tubing. The three locating points of the frame on to the two parallel copper pipes are provided by copper pipe unions originally designed to give soldered joints between sections of the same $\frac{1}{2}$ inch pipe when used in plumbing. The solder was removed from the inside of the unions before assembly. The frame consists of a shaped piece of 16 swg aluminium, fixed to the three sliding unions by "Plastic Padding", a rigid cement which is stiff enough before setting to allow accurate adjustment of the parts. The fourth sliding tube, trapped firmly between the two fixed sliding tubes is allowed to rotate about the fixed tube and carries a "Perspex" strip engraved with a fine

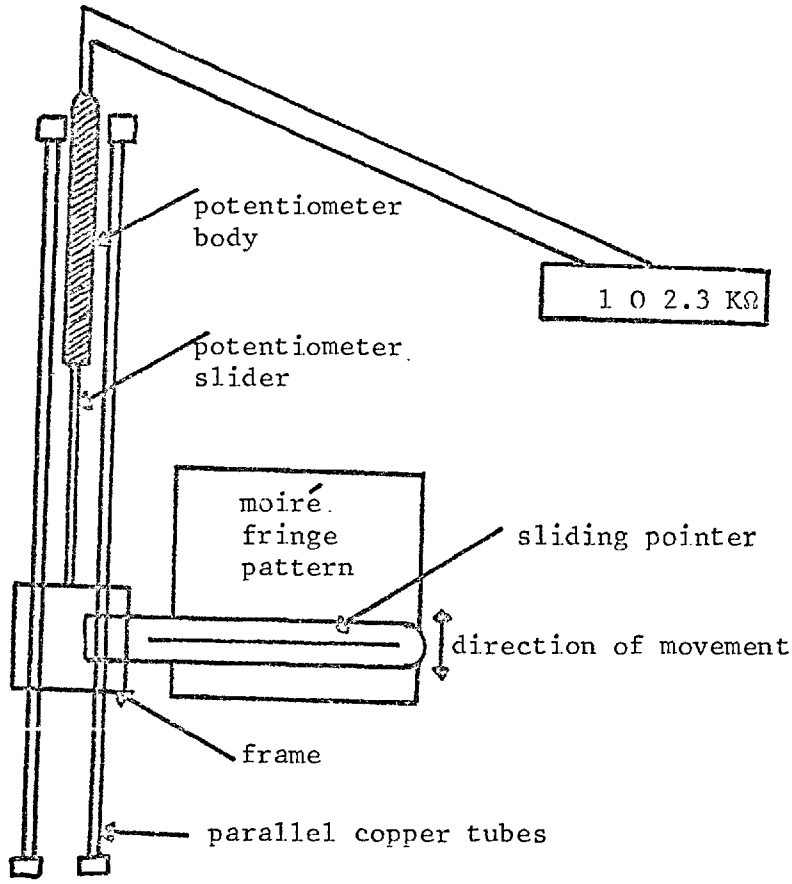


figure 22. The principle of the digital moiré fringe pattern measuring device.

line, perpendicular to the tube axis. This pointer can be scanned over a pattern which is taped on to the "Formica" base, the resistance of the connected potentiometer being proportional to the pointer position. The potentiometer (Ether Ltd.) has a total resistance of 102.4 Kilohms, and a travel of 6 inches. The nominal resolution of the potentiometer (limited by the space between the coil windings) is 0.0043 cm (0.0017 inch) which represents a resistance change of 29 ohm, and indicates the greatest accuracy to which the slide position can be measured. The precision is limited however, by the use of a three digit resistance meter (Honeywell VT100) on its 150 Kilohms range. The provision of the "0" or "1" overrange in this basically three digit instrument allows the full potentiometer resistance to be adequately covered, the last of the three digits representing a resistance change of 100 ohm. In the present application, the last digit represents approximately 0.015 cm which is therefore the overall resolution of the complete measurement system.

It is found in practice that this rather coarse resolution is adequate for pattern measurement, because the errors of estimation of fringe positions, and the residual non-linearities of the basic fringe patterns are of the same order. Improvement in resolution beyond a factor of 2 would not give any subsequent improvement in accuracy without corresponding pattern improvements (See B (iv)).

The measurement procedure employed for each pattern is to align the picture with respect to the engraved moving strip to make the measurement axis normal to the fringe direction before securing the picture to the base with adhesive tape. The strip is then scanned from top to bottom of the pattern four times, measuring respectively a_{1-6}, b_{1-6}, c_{1-6}, and d_{1-6}, each number corresponding to the fringe position appearing on the digital ohmmeter. The numbers are registered in an electro-mechanical calculating machine during the measurement and only the ratio is permanently recorded, with m, the number of wavelengths between the sampling points. The pattern is untaped, and aligned so that the engraved strip is parallel to the wave-fronts in the pattern centre. The digital distance is then found from the position of identical parts of the wave at opposite ends of the picture. The "digital wavelength" is calculated by division by the number of wavelengths included, and this is converted into a real wavelength by multiplication with a factor representing the digital calibration. If each digit is found (by comparison with an accurate ruler) to be equivalent to d cm., and the lens magnification of the surface plane is k, then the digital distance is converted into a real length by multiplication with the factor d/k. The natural logarithm of the measured ratio is found from four figure tables, and division by the product of m and the wavelength gives the damping coefficient.

The magnification calibration holds for a given volume of liquid in the tank if the optical components are fixed, so a single calibration is sufficient for each set of results.

(ix) Advantages of the moiré technique.

The principal differences between the wave measurement technique developed in this work and the other techniques described in Chapter 3 lie in the production of an instantaneous record of the wave slope over a large area of liquid surface. The single flash exposure forms a simultaneous record of wavelength and damping, which is useful in systems where the surface properties are changing quickly with time. In its present form, the apparatus may be used to make pictures at 15 second intervals, limited by the manual transport of recording paper. Mechanisation of this would be expected to reduce the interval to 1 second. None of the other techniques so far developed are capable of instant measurements on time-varying systems, and since many liquid surfaces show time varying behaviour, the moiré technique should be very useful.

As the picture shows a large area of the waves, the presence of waveform distortion, inhomogeneity of wavefront, and irregularities in the wave generating system may be rapidly recognised.

The principal disadvantage of the method follows from its ultimate reliance on the accurate measurement of moiré fringe position, the difficulties encountered in performing this measurement being described in section (iv). The quality of the lens is the most fundamental factor

in the achievement of accuracy since its improvement allows the use of finer gratings, giving better defined fringes. With the lens used in this investigation, the sensitivity achieved is high enough at wavelengths greater than 0.3 cm to permit accurate measurements in the linear region. At smaller wavelengths however, distortion appears at less steep wave slopes, and the fringe amplitude must be reduced to remain in the linear region. This difficulty will appear in all the techniques which measure wave slope, but will be much less important for wave curvature techniques such as the telescope focussing method and the wave crest focussing technique. Whereas wave slope is proportional to h_o/λ and the amplitude h_o can be reduced as the wavelength decreases while retaining the same slope and fringe displacement, the wave curvature is proportional to h_o/λ^2 and the amplitude reduction can be greater. This enables curvature methods to be used at smaller wavelengths than the wave slope methods. An advantage of the moiré fringe technique over all of the others is that distortion can be easily recognised in the pictures. Point measurement techniques such as the focussing methods are not as likely to detect distortion until it has an effect on the measurements.

The accuracy of measurement of smaller wavelength ripples could be improved by the use of finer gratings, and the field size reduction possible with small wavelengths would help a lens to produce the necessary pattern linearity.

CHAPTER 5

THE ADSORPTION OF POLYMERS AT THE WATER/AIR SURFACE.

(i) General.

The type of surface activity described in Chapter 2 was that in which individual active molecules are composed of two sections which possess contrasting behaviour in their interaction with the water phase. Thus a fatty acid molecule can become stably adsorbed with its hydrophilic -COOH group anchored in the aqueous substrate, and its hydrophobic hydrocarbon chain mainly in the gaseous phase. This mechanism was suggested by Langmuir (1917), and is often termed "classical" behaviour.

The interaction of large polymer molecules with a surface might be expected to be different from the surface activity already described, partly because of the large size of the molecules, and partly because of their construction as semi-flexible chains of small molecular segments. The bonds between the segments are chemical, and the relative orientation of two adjacent members of the chain is restricted by the steric hindrance of their bond, the energy barriers which prevent the joined atoms from assuming certain relative positions. The flexibility of the molecule/results from the large number of joined segments and the consequent wide range of bond angle combinations. It is statistically a very unlikely event for a polymer molecule in bulk solution to be extended to its greatest possible length, and it may be shown by the analysis

of the probabilities of possible molecular configurations that the most likely shape is a three-dimensional random coil in which the distance between the ends of the molecule is much smaller than the maximum extension.

Polymers are observed to be adsorbed at a wide variety of liquid/gas and liquid/solid interfaces (Moilliet et al. 1961). The effect is often much greater than would be expected from the surface attachment properties of a single active segment, and at the liquid/air surface, polymer molecules exhibit activity which differs markedly from the "classical" behaviour so far described. Adsorption is not as dependent on the availability of strong hydrophobic/hydrophilic tendencies, and it appears that the presence of large numbers of connected weakly active chain segments is sufficient to make the whole molecule strongly surface active.

These properties are probably connected with the fact that a molecule has a large number of degrees of internal freedom, and also that it possesses a large number of identical points at which it can be adsorbed on the surface. Moilliet et al. (1961) suggest that examination of the entropy of the surface interaction may provide an explanation of cases of unexpectedly high surface activity. If the gain in translational entropy of the displaced solvent molecules is greater than the loss of translational, rotational, and vibrational entropy of the polymer molecule as it is adsorbed (due to the high degree of internal ordering

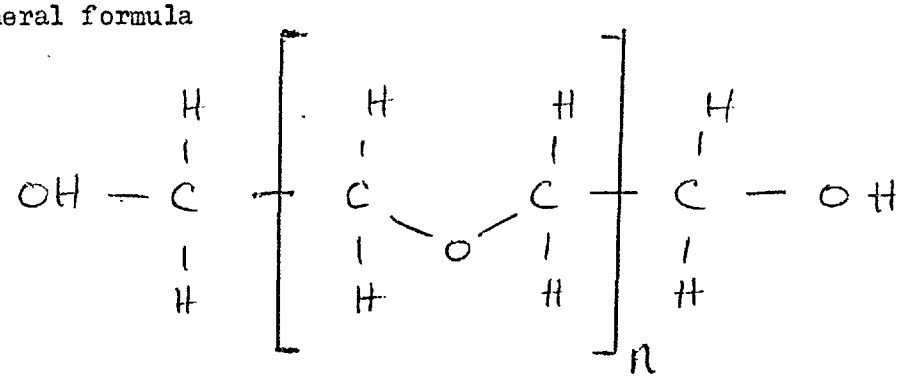
already present between the chain segments) then the adsorption will be enhanced in a way which is not directly dependent on the activity of an individual segment. It is reasonable to assume that if this sort of effect does occur, the Gibbs equation (Chapter 2, eqn. 2.6) may not describe the properties of polymers adsorbed at the liquid/air surface.

Although a considerable amount of work has been done on polymer adsorption at liquid/solid surfaces (Silberberg, 1962), and on the properties of water-insoluble polymer layers spread on water (Crisp, 1946, 1958), comparatively little has been done on the properties of water-soluble polymers at the solution/air and water/air surfaces. Crisp studied the soluble polymers polyvinyl alcohol, polyacrylic acid, and polymethacrylic acid, and he found that they could be spread on pure water as though they were insoluble. Polyvinyl alcohol will produce perfectly stable monolayers, although the other two need acidic substrates for stability. The case of polyvinyl alcohol appears to be the first in which a material fully soluble in water was shown to produce "insoluble" surface layers on pure water.

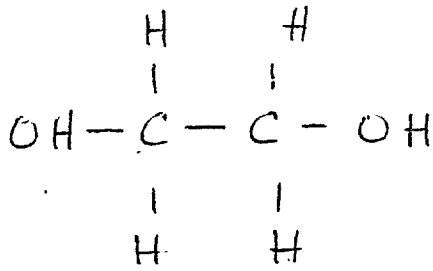
(ii) Poly(ethylene glycol).

Lovell and Hibbert (1940) examined the surface tension of poly(ethylene glycol) solutions using a capillary rise technique (see Chapter 2 section (ii) a). This linear polymer has the

general formula



where n represents the average number of ethylene oxide groups. The residual hydroxyl groups are a result of the polymerisation from ethylene glycol



The degree of polymerisation of the samples studied covered a wide range, the average number of segments in a chain (n + 1) varying between 3 and 186 (molecular weight averages between 150 and 8202). Assuming the validity of the Gibbs equation, the adsorption and the surface area occupied per molecule were calculated. Lovell and Hibbert found that up to the 18 segment molecule, the calculated areas agreed with those expected if the molecules were lying flat in the surface. The areas calculated for the higher members of the series did not continue this trend, the discrepancy becoming increasingly large. Lovell and Hibbert therefore concluded that

the long chains tend more and more to vertical orientation as the chain length is increased above 18 units (molecular weight 810).

Couper and Eley (1948) investigated solutions of fractions of the same polymer (Union Carbide, 1965) except restricted to the higher molecular weight members of the series between 1000 and 6000 (figure 5.1). Their results are in marked disagreement with those of Lovell and Hibbert, in that calculations of molecular area, (again assuming the Gibbs equation) indicated that the chains were lying flat in the surface over the whole range examined. The detailed results presented by Couper and Eley are so different from those in the earlier work that there must have been some fault in one of the two techniques used. The measurements by Couper and Eley were with a ring detachment technique (see Chapter 2, section (ii) c) in contrast to the capillary method of the earlier work, and up to 60 minutes was allowed for equilibrium to be reached. Another investigation reported in the same work found the ring technique unsuitable for a polyvinyl alcohol sample, because of the long equilibrium time required with solutions of this material. Short period ageing effects were also found with the highest molecular weight fraction of the poly(ethylene glycol). Although it must be assumed that every precaution was taken to ensure true equilibrium results, it is regrettable that neither of these two poly(ethylene glycol) investigations used a technique of surface tension measurement which was more suitable for time-varying

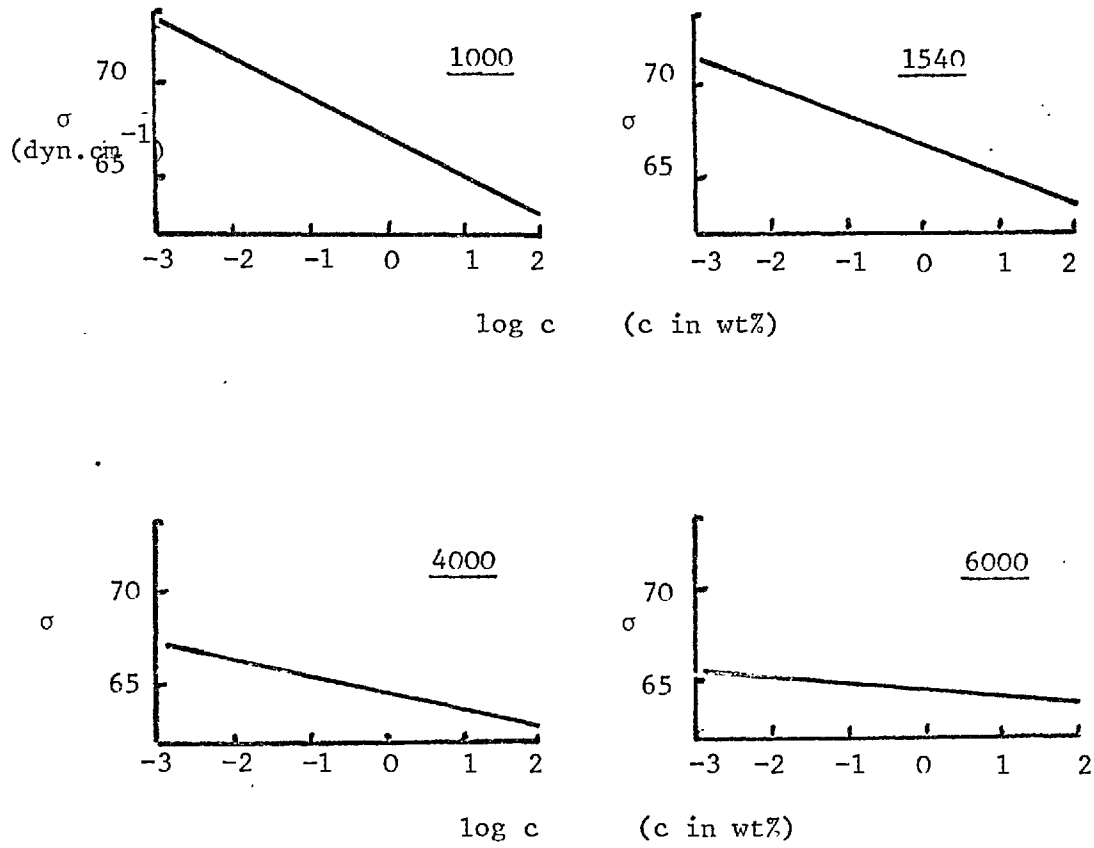
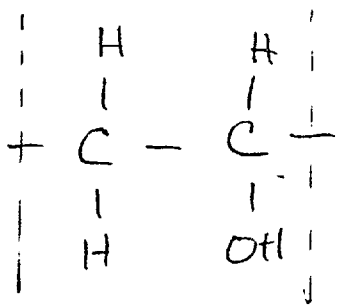


figure 1 The measurements of Couper and Eley (1948) on the "Carbowax" series of poly(ethylene glycol) fractions, identified by approximate molecular weight gradings.

surfaces. Since Couper and Eley used a much wider range of solution concentrations, and appear to have appreciated the effects of time variation, their results are possibly more acceptable than those of Lovell and Hibbert, although it must be concluded that there is not enough information available to vindicate either investigation.

(iii) Polyvinyl alcohol.

Frisch and Al-Madfai (1958) measured the surface tensions of aqueous solutions of polyvinyl alcohol, using the drop shape technique (Chapter 2, section (ii)f). This method appears to be satisfactory for investigation of surfaces whose properties change slowly with time, as there is no stretching of the surface at the time of measurement, and drops may be observed continuously over long periods of time. Polyvinyl alcohol is produced by the hydrolysis of polyvinyl acetate, and is ideally composed of segments



although hydrolysis of the acetate groups is never complete in the commercial process, and samples are usually copolymers of acetate and alcohol. A polyvinyl alcohol sample is therefore characterised by the fraction of the acetate segments which have been successfully converted, and this is often quoted as a

"percentage hydrolysis". Commercial samples are widely available in two main categories, 88% and 98% hydrolysed (DuPont, 1968, Hoechst, 1968). Frisch and Al-Madfai used an 88% sample, fractionated into two parts of different average molecular weight ($M = 7.7 \times 10^4$, 1.13×10^5), and measured the variation of surface tension of 1% solutions over a period of 3 hours. The sample of higher molecular weight showed a lower equilibrium surface tension, and the time variation of both samples appeared to be caused by the diffusion-controlled transport of molecules from the bulk to the surface.

Polyvinyl alcohol was also examined by Crisp (1946), who found that it could be spread on pure water as though it were insoluble. Figure 2 reproduces the published variation of surface pressure with the area available per segment of the spread polymer. (98% sample). The upper curve shows the measured values, while the lower was calculated by Crisp, making a correction for the residual acetate groups present in the surface. The monolayer is seen to be extremely compressible down to very small specific areas, and the region of compressibility was attributed mainly to the acetate contribution.

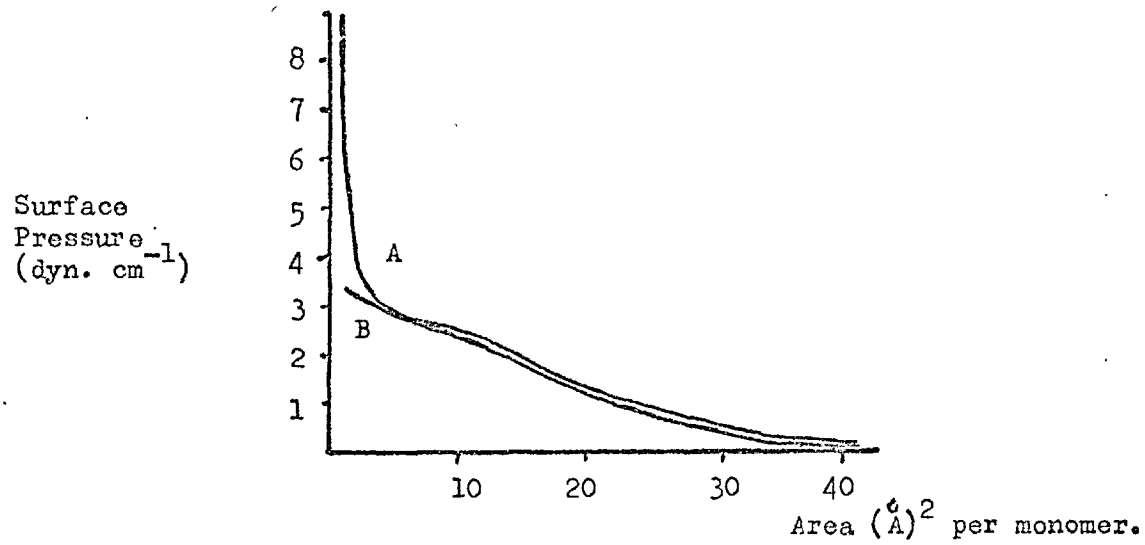
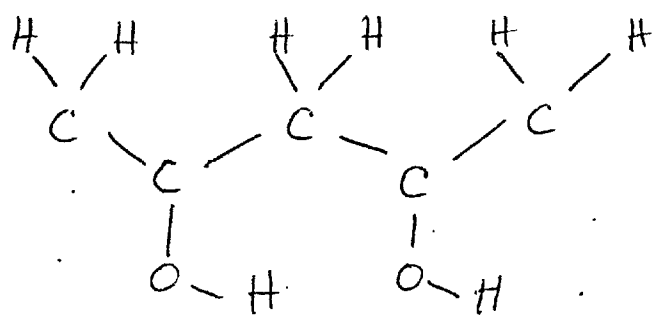


Figure 5.2. The properties of a spread monolayer of polyvinyl alcohol (98% hydrolysed). (Crisp, 1946).

Crisp deduced that the molecules were adsorbed with the hydroxyl groups (-OH) in the aqueous phase and the more hydrophobic hydrocarbon parts above i.e.



and with the help of measurements of surface moment (see Davies and Rideal, 1963), it was concluded that the hydrogen atoms in the hydroxyl groups were being shared along the chain.

The collapse of the polyvinyl alcohol monolayer is of great interest because the molecules are completely soluble in water. On this ground, the molecules should be desorbed and pass freely into solution as the film pressure is increased. This was not observed, the curve in figure 52 being reversible and not limited by the diffusion of desorbed molecules back to the surface. Crisp therefore interpreted the very low collapse pressure as indicating the formation of a surface microcrystalline state in which the internal energy is lowered by lattice forces.

Glass (1968a) examined solutions of polyvinyl alcohol, (89% and 99% hydrolysed) using a drop weight technique (Chapter 2 section (ii)e). In Chapter 2 it was emphasised that because at the moment of drop detachment the surface area of the drop is changing, this technique must be used with caution in cases where equilibrium does not occur rapidly. Solutions of polyvinyl alcohol have been shown to require a considerable time for equilibrium (Frisch and Al-Madfai, 1958) and Couper and Eley (1948) found that a similar "surface stretching" measurement, the ring detachment method was difficult to apply to such solutions. In anticipation of the slow equilibration, Glass assumed an exponential model for the approach of the surface tension to its ultimate value, and predicted equilibrium values from his measurements with drop lifetimes of 10 seconds, 30 seconds, and 60 seconds. In many cases, the equilibrium times associated with these extrapolated

values were calculated to be greater than 6 hours. Figure 5.3 shows the results of this investigation for both 89% and 99% samples, at a range of different temperatures. The 99% polymer was not investigated at 25°C because it was found to precipitate on standing at that temperature. These results are in general agreement with those of Crisp (1946) on spread monolayers, in that the acetate groups can be seen to provide the major contribution to the surface pressure. The results are also compatible with those of Frisch and Al-Madfai (1958).

The major advantage of the drop weight method used in this work appears to be the speed at which measurements may be made. It is felt, however, that the assumption made concerning the exponential variation of the surface pressure which was used to predict equilibrium results has not been adequately justified. The presence of diffusion-controlled adsorption, roughly verified by Frisch and Al-Madfai appears to be implied, in addition to some unknown adsorption isotherm. Glass himself mentioned the work of Fukawa et al. (1961), who suggested that diffusion was not the only ageing process at high solute concentrations, but he did not comment on the implications of this work on the exponential model.

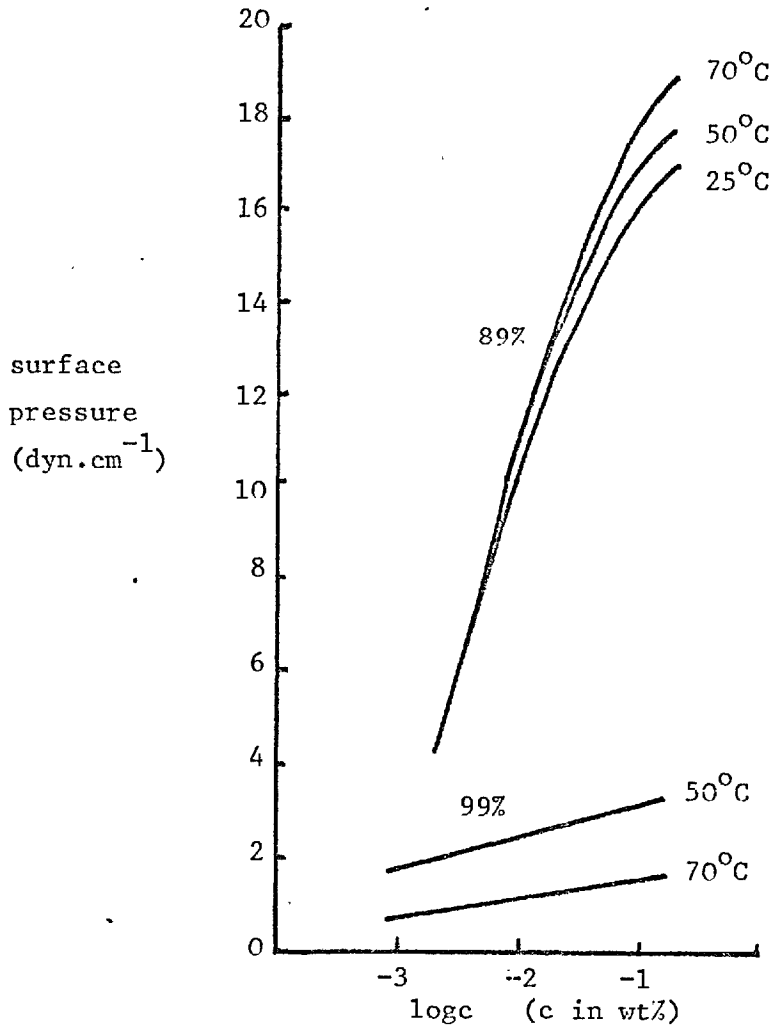
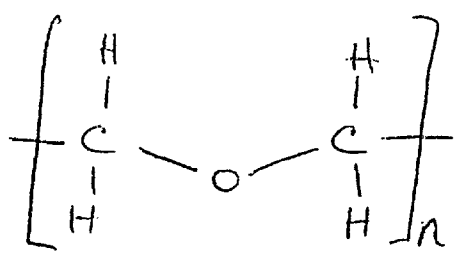


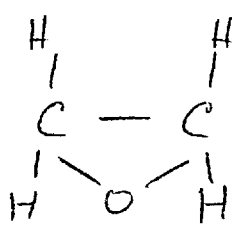
figure 53. The surface pressure of aqueous polyvinyl alcohol solutions by the drop weight method (Glass, 1968a)

(iv) Poly(ethylene oxide).

Glass (1968b) used the same drop weight method as above in an investigation of the surface properties of aqueous poly(ethylene oxide) solutions, intended to resolve the opposing conclusions of Lovell and Hibbert (1940) and Couper and Eley (1948) regarding the situation of the ethylene oxide segments in the interface. The same drop lifetimes were employed (10, 30, and 60 seconds) and the same exponential extrapolation made in estimation of equilibrium values. In this case, the particular material selected for examination had not previously been reported as a surface active agent, and therefore prior information about the time variation of its adsorbed surfaces was not available. Poly(ethylene oxide) is only marginally different from poly(ethylene glycol) however, since the repeated monomer segment is common to both:-



Whereas the glycol polymer is formed by polymerisation of ethylene glycol as mentioned earlier, poly(ethylene oxide) is produced by direct polymerisation of ethylene oxide



ethylene oxide molecule

and therefore does not possess hydroxyl groups as chain terminations. Glass appears to have assumed that these groups should not be significant in the properties of the molecule, and that equilibrium behaviour should be the same as for the glycol polymers. Indeed, there is no clearly evident reason why the presence or absence of terminal hydroxyl groups should affect adsorption of the extremely large numbers of intermediate ethylene oxide segments.

Two of Glass' samples were commercially produced poly(ethylene oxide) of molecular weight 2.4×10^6 and 4.3×10^5. It will be noted that these molecular weights are considerably higher than those of any of the materials examined by both Lovell and Hibbert(1940) and Couper and Eley (1948), who were limited to glycol polymers of mean maximum molecular weight about 8×10^3. The other materials investigated by Glass were laboratory prepared specimens, being a 10^4 molecular weight sample and a 1.3×10^4 molecular weight (methoxyl-initiated) sample.

The results obtained for the highest molecular weight material (M.W. = 2.4×10^6) at 25°C are shown in figure 4. The three lower curves are the experimentally determined surface pressures at 10, 30, and 60 seconds, and the top curve is the result of the extrapolation procedure described above (Glass, 1968a). The lack of information at concentrations lower than those presented is presumably explained as it was in the earlier paper, by

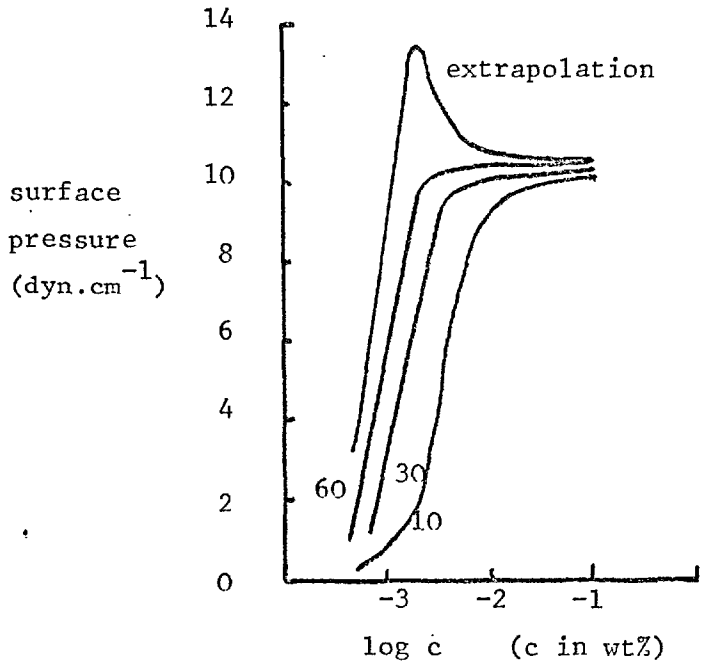


figure5.4. The measurements of Glass (1968b) on solutions of poly(ethylene oxide), molecular weight 2.4 x 10^6, at 25°C.

"experimental inaccuracies at low concentrations". The curious maximum in the surface pressure "equilibrium" curve, presumably because it is so unlikely, is taken by Glass to invalidate the use of the exponential model in this case, although no explanation is offered as to why the model should remain valid in the other cases investigated.

The calculations of equilibrium time, based on this exponential model are sometimes greater than 12 hours for the two high molecular weight poly(ethylene oxide) samples, and it is therefore not a little surprising to find comparisons of different polymers made on the basis of 60 second drop lifetime results figure5.5. Non-equilibrium comparisons of results produced in such specialised experimental conditions are expected to be of limited value.

Measurements were also made on lower molecular weight glycol products, the monomethyl-, monoethyl-, dimethyl-, and diethyl- derivatives of triethylene glycol, and in these cases, the 30 second data were taken to be equilibrium values.

Glass concluded from his measurements that the surface activity of the poly(ethylene oxide) series decreases with molecular weight below a value of 10^4. He also found that the ethylene oxide

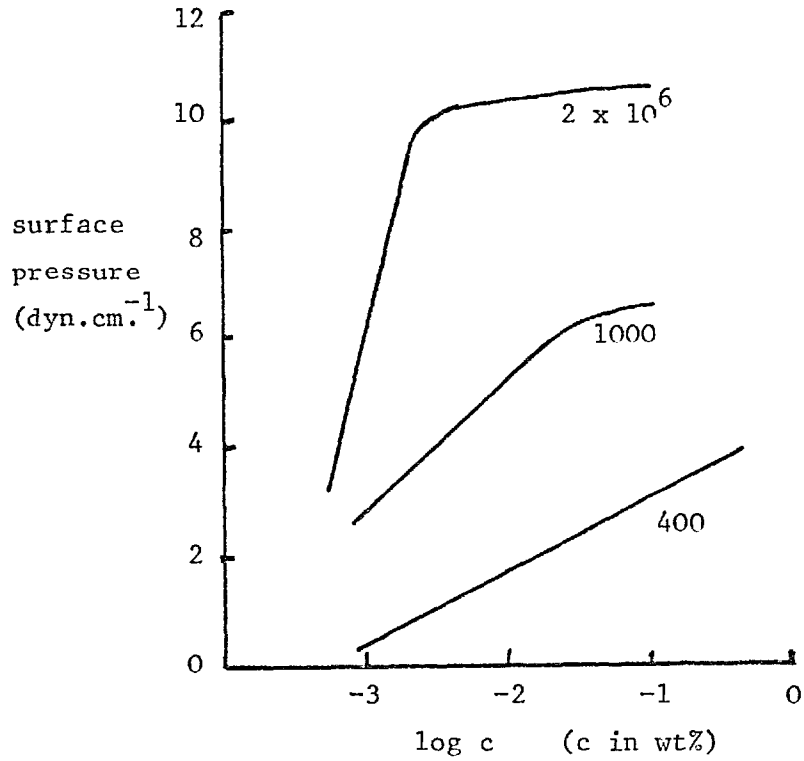


figure 55 Comparison of three ethylene oxide polymers of different molecular weight, on the basis of 60 second lifetime drop weight results (Glass, 1968b).

segments were not all adsorbed in the manner suggested by Couper and Eley, but that there were always portions of the chains oriented out of the surface region, as indicated by Lovell and Hibbert.

Recent work by Shuler and Zisman (1970) on a commercially obtainable sample of poly(ethylene oxide) (Union Carbide WSR N10) is strikingly similar to that carried out in the present investigation (Chapter 7). The principal measuring technique was that of ripple measurement, as in the present work, and the material examined (molecular weight 9×10^4) is also investigated here. The discovery of the spreading properties of the polymer was reported, and in this respect, the polymer is very similar to polyvinyl alcohol (section iii) and polymethacrylic acid (section v), being completely water soluble and also able to produce stable spread layers. Shuler and Zisman's work was solely concerned with these spread layers.

The ripple measurement technique used is described in Chapter 3 (section (ii)d) and has been called the wave crest focussing technique. In addition to the ripple measurement, the surface pressure was measured with a form of Langmuir film balance (Chapter 2, section (ii)d) and the surface potential was measured with a radioactive electrode technique (see Davies and Rideal, 1963). The polymer was spread on distilled water at pH3, although the implication of this acidic substrate was not discussed

in the report. Four different spreading solvents, chloroform, carbon tetrachloride, water, and benzene were found to give concordant results, and it was therefore concluded that the poly(ethylene oxide) was being spread without loss of material to form a stable monolayer. That the film properties should not be dependent on the spreading solvent is regarded by Gaines (1966) as a useful test of the completeness of spreading.

The variation of surface pressure with surface area per monomeric segment is shown in figure 6. These curves were obtained by compression of three different known amounts of polymer spread on a Langmuir trough. The working range of specific area for a single spread quantity of active material is limited by the trough design, which explains the division of the compression curve into three. The graphs also show curves obtained when the films were expanded following the maximum compression of each, and an interesting hysteresis is observed following compression to less than 20 $(\text{Å})^2$ per monomer. Subsequent recompression showed that the film properties had undergone a definite change since the initial compression, and this change was reported to be permanent and irreversible. A possible cause of the hysteresis is the loss of polymer from the layer by solution in the bulk liquid, and the experiment was repeated with a 35% ammonium sulphate solution as substrate, designed to reduce the solubility of the polymer. This technique is often used to produce spread monolayers of soluble

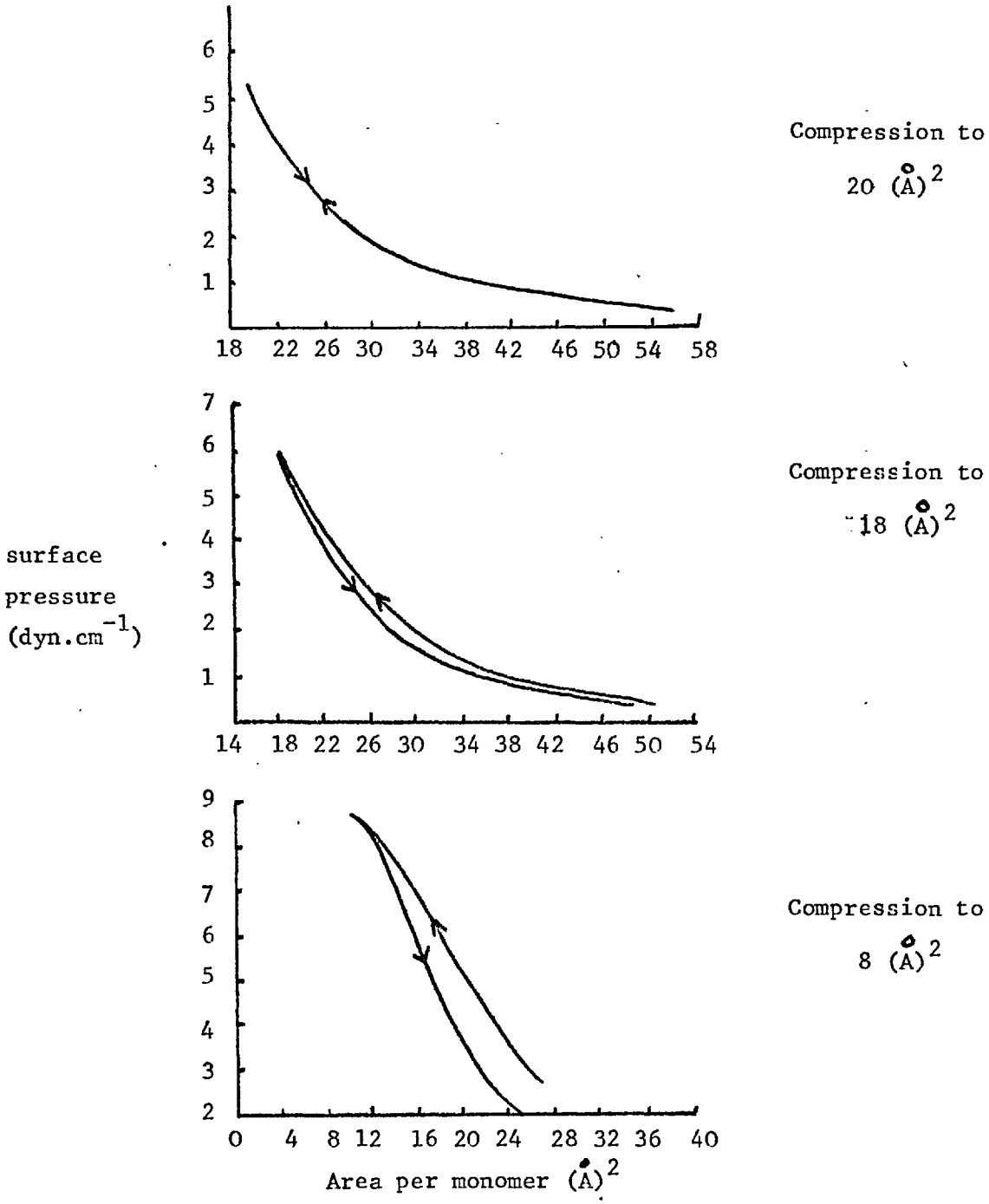


figure 56 Pressure/area curves for poly(ethylene oxide) WSR N10 spread monolayers (Shuler and Zisman, 1970), showing hysteresis effect.

active agents which will not normally spread on pure water (Meader and Criddle, 1953, Schick, 1962). In this case, the hysteresis was unaffected. The possibility that some of the lower molecular weight components of the sample were being forced out of the layer on compression was tested by extracting the polymer with acetone, which should have removed some of these components. The resulting sample, of narrower molecular weight distribution, had unchanged surface properties. It was therefore concluded that the observed hysteresis was not caused by transfer of material from monolayer to substrate.

The surface dilational elasticity, or surface compressional modulus (Chapter 2, section (iv)) of the monolayers was evaluated from the pressure/area curves shown in figure 56, and this is shown in figure 57. The effect of expansion after compression is also given. It is remarkable in this polymer system that the dilational elasticity reaches a distinct maximum, but is comparatively small at both large and small specific areas. This is a result of the tendency (shown in figures 56 and 59) of the surface pressure to approach a limiting value as the monolayer concentration increases, while the monolayer apparently retains its stability. For the great majority of surface active substances, the surface pressure increases continuously as the layer is compressed only as far as a certain limiting area, at which the monolayer is observed to collapse, forming uneven "thick" layers or dissolving (Gaines, 1966).

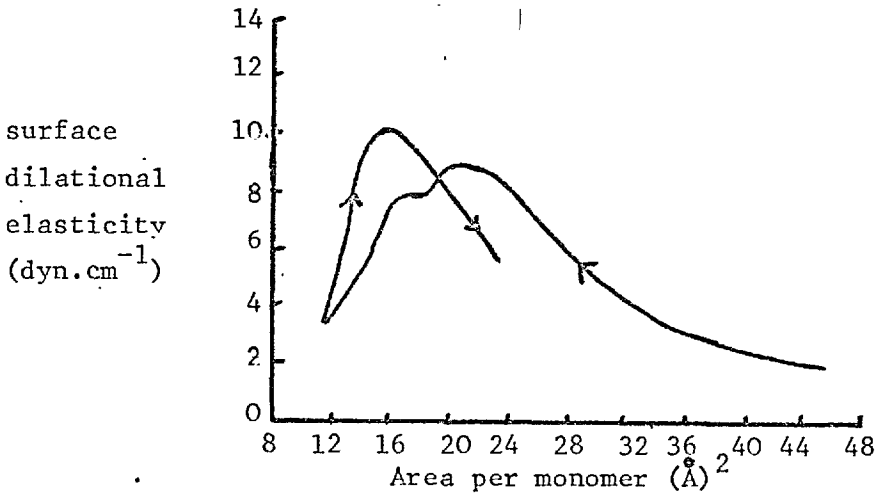


Figure 57. Elasticity of the poly(ethylene oxide) spread monolayer (Shuler and Zisman, 1970).

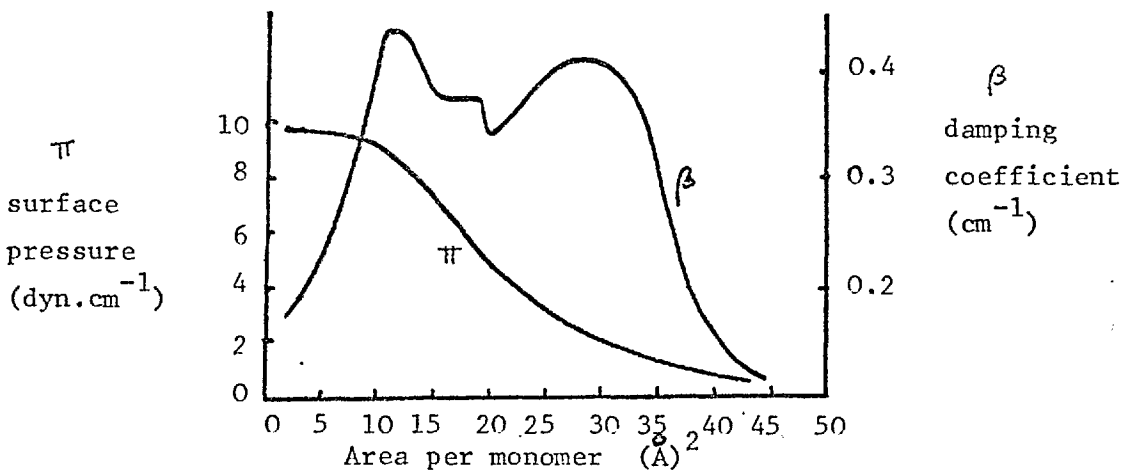


Figure 59. Single compression measurements of surface pressure and 50 Hz ripple damping for the poly(ethylene oxide) spread monolayer (Shuler and Zisman, 1970).

Spread polymer layers are also observed to be limited in this way (Crisp, 1946). Although it is possible that water-soluble polymers might exhibit singular behaviour, Crisp found that his polyvinyl alcohol monolayer was limited by gelation and solidification at high surface concentrations, (figure 5.2). Gelation was also found to limit monolayers of polyacrylic and polymethacrylic acids.

It is significant that the maximum in the elasticity curve (figure 5.7) occurs near $20(\text{Å})^2$, the area at which the film behaviour was found to show irreversibility. Shuler and Zisman assumed that in this state of compression the polymer segments, all fully adsorbed at the surface, are in a close packed arrangement, the specific area being related to the size of the monomer segment.

Wave damping measurements on the poly(ethylene oxide) monolayers, again carried out over separate sections of the range of interest, (figure 5.8) show that as the specific area is decreased, the damping rises to a peak, and then decreases slightly before reaching a second peak. The effects of re-expansion are also shown in the figure. In Chapter 3 it was described how measurements of ripple properties were related to the characteristics of the surface, and it was emphasized that knowledge of both wavelength and damping coefficient for a given frequency was required in order to describe the surface fully. Lucassen and Hansen (1966) showed how the dilational elastic modulus and the surface tension could often be

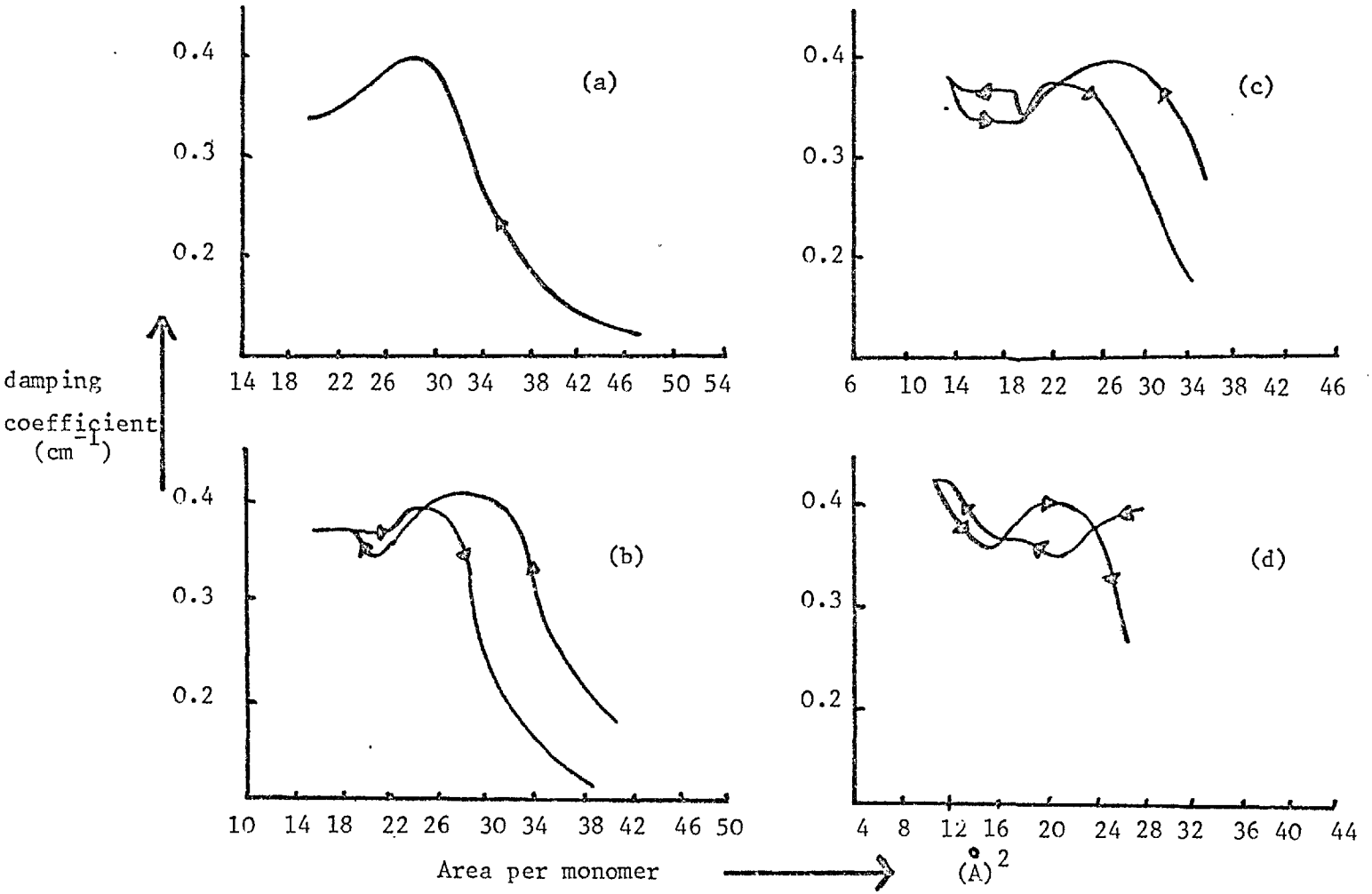


figure 5.8. Measurements of the damping of 50 Hz ripples on spread monolayers of poly(ethylene oxide) during compression and subsequent expansion (Shuler and Zisman, 1970).

derived from these measurements, but apparently unaware of this possibility, Shuler and Zisman presented only damping coefficient measurements. Conclusions drawn from these results were completely without reference to the established hydrodynamic theory which Lucassen and Hansen have found to be in excellent agreement with experiment for several surface active materials (see Chapter 3, sections (iv), (v), and (vi)).

The inconvenience of the sectioned nature of the results in figure 8 was overcome by a further experiment in which the surface concentration was steadily increased by small additions of dissolved polymer to the surface. The result of this procedure is given in figure 9. The two peak behaviour is quite clear, and there are two other features of the curve which are of interest in the interpretation of the results in terms of hydrodynamic theory. Examination of figure 9 shows that the two peaks, occurring at specific areas of approximately $28(\mathring{A})^2$ and $11(\mathring{A})^2$ are associated with surface pressures of about 2.3 and 8.8 dyn. cm^{-1}. Reference to figure 7 indicates that the corresponding dilational elasticities are about 6.0 and 3.0 dyn. cm^{-1}. These figures are in accord with the prediction of hydrodynamic theory that as the surface pressure increases, lower elasticities are able to produce a damping peak (Appendix 2). The second interesting fact is that the value of damping coefficient at the $11(\mathring{A})^2$ peak is greater than that at the $28(\mathring{A})^2$ peak. This agrees with the theoretical prediction that the peak

height increases as the surface pressure increases (Appendix 2).

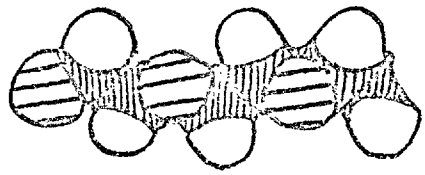
Shuler and Zisman's approach to the interpretation of wave damping results begins from the basic concept that since re-arrangement of adsorbed molecules on a liquid surface can alter the free energy of the system, the wave damping properties of the polymer monolayer should provide evidence of the molecular re-arrangement and structural changes within the layer. This approach is definitely valid, as long as the hydrodynamics of the complete wave system is fully appreciated, bearing in mind the modification of the surface elastic properties by the monolayer. Wave energy can be dissipated in two principal ways, 1) by viscous losses in the substrate shear flow accompanying the wave motion, and 2) by irreversible intermolecular energy transactions in the surface layer specifically due to the presence of adsorbed molecules (Chapter 3 section (ii)). The hydrodynamic theory is at present only suitable for the description of the first effect, although Hansen and Mann (1964) considered the existence of the second type of mechanism. Shuler and Zisman (1970), apparently agreeing with Garrett and Zisman (1970) in their abandonment of hydrodynamic theory as inadequate, confine their deductions of monolayer properties to explanations of the second type of energy loss.

Whereas damping peaks are considered in the hydrodynamic approach to denote mere coincidences of elastic modulus and surface tension (Chapter 3 section (iv)), a "molecular interaction" explanation must postulate specific behaviour of the molecules which causes high dissipation at the relevant surface concentrations. Shuler and Zisman therefore postulated that the 28 $(\text{Å})^2$ maximum denotes the area at which the monolayer changes from a gaseous "dilute" film to a more close-packed structure. A dilemma then arose because the monolayer had not been found to lose its reversibility until compressed to 20 $(\text{Å})^2$ per segment, and it was thus considered most likely that 20 $(\text{Å})^2$ denotes the closest approach of the horizontal adsorbed segments. What then causes the 28 $(\text{Å})^2$ "transition"? Shuler and Zisman suggested that at areas greater than 28 $(\text{Å})^2$, each monomer segment is associated with two water molecules, and that compression to smaller areas "squeezes out" these molecules. Measurements by Rösch (1956) of the viscosity of poly(ethylene oxide) solutions support this hypothesis. A further difficulty was that although the 20 $(\text{Å})^2$ transition was marked by a peak in the elasticity curve, there is no observable deviation from smoothness of the elasticity curve in the 28 $(\text{Å})^2$ position. It was necessary therefore to explain this absence in terms of an unusual compressibility of the hydrated segment at this specific area, which makes the irregularity of the elasticity curve so small that only the more sensitive damping measurement is capable of being affected.

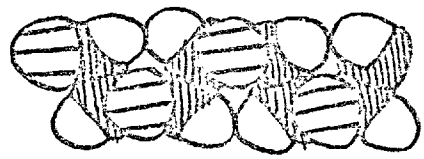
The damping minimum between the peaks occurs close to 20 $(\mathring{A})^2$, the "established" transition area. Hydrodynamic theory would interpret the region between two peaks as being associated with either a maximum or a minimum in the elasticity curve, and the observed maximum supports this interpretation. Shuler and Zisman interpret the minimum as being caused by the decreased "drag" of polymer molecules on the substrate consequent on the removal of the attached water molecules. The second peak at 11 $(\mathring{A})^2$ is interpreted as indicating film collapse, although again, the elasticity curve gives no support to this.

Enough indication has been offered here of the difficulties likely to be encountered if the dynamic properties of the surface are interpreted as though the monolayer were an entity divorced from its liquid substrate. The example is somewhat similar to the interpretative difficulties present in surface viscosity measurements discussed in Chapter 2 (section (iii)). Correct deductions are sometimes possible, but very often the mechanisms invoked are unnecessary and misleading.

In the absence of wavelength measurements complementary to the damping coefficient results, it is not possible to examine the measurements accurately from the point of view of the hydrodynamic theory. The indications are, however, that the values of surface dilational elasticity implied by the damping and surface pressure measurements would show a variation of the same type as found by



(a)



(b)

hydrogen

carbon

oxygen

figure 10. Possible configurations of the (ethylene oxide) polymer segment in a spread monolayer (Shuler and Zisman, 1970). (a) has a calculated area of 20.1 $(\mathring{A})^2$, and (b) has a calculated area of 16.1 $(\mathring{A})^2$.

static measurements (figure 57). This static curve is an important contribution to the study of adsorbed polymers. The peak at about 20 $(\mathring{A})^2$ and the inflexion point which can be seen at 16 $(\mathring{A})^2$ appear to denote important transitions in the monolayer structure. Shuler and Zisman's model experiments indicate two different segment configurations which are expected to occupy surface areas of 20.1 $(\mathring{A})^2$ and 16.1 $(\mathring{A})^2$, and it appears likely that these models represent the behaviour of the polymer segments. Figure 510 reproduces drawings of the two configurations as would be seen looking from substrate to the surface. (For each carbon atom pictured, there is a hydrogen atom above the surface which is not visible in this drawing). The region below 16 $(\mathring{A})^2$ is ascribed to film collapse, which, although plausible from the point of view of the extremely small specific areas involved, leaves the reason for the observed re-expansion of the layer from areas as low as 12 $(\mathring{A})^2$ still unclear.

(v) Polymethacrylic acid.

Katchalsky and Miller (1951) carried out an interesting investigation of the properties of polymethacrylic acid at the solution/air interface. Crisp (1946) had shown that this water-soluble polymer could be spread on the surface of pure water without being dissolved, although he found that the monolayer was only stable on compression if the substrate was acidic. Katchalsky and Miller examined a range of different molecular weight fractions of the

polymer, both in solution, using a drop weight method, and spread on the surface, in a Langmuir trough apparatus. Since this is the only published work on both the spread and dissolved states of a polymer, it is of considerable interest. The measurement technique using the drop weight technique allowed for ageing by adjusting the liquid flow so that the drop lifetime was long enough for the weight of the drop not to increase with more time. It was found that 5 minutes was adequate for the range of concentrations examined.

The striking point about the findings of this work is that the two states of adsorption appear to be independently stable, there being no transition possible between them. The layer adsorbed from solution was examined in a Langmuir trough, where compression by a moving barrier of the area on one side of the measuring barrier failed to increase the surface pressure in that area relative to the pressure in the uncompressed area. This indicates that when the solution adsorbed layer is compressed, molecules are desorbed in order to regain the same equilibrium surface pressure relevant to the particular solute concentration. The molecules are therefore in a state different from the spread monolayer, which may be compressed and expanded reversibly without polymer desorption. The difference in the state of adsorption in the two types of layer was emphasized by an experiment in which monolayers were spread from alcoholic solution on to an equilibrium adsorbed solution surface. There was no transition between the spread molecules and those already adsorbed.

The explanation suggested for this behaviour involves consideration of the difference in the energy states of the polymer molecules in the two types of adsorption. In the spread layer, segment area measurements indicate that the molecule is unfolded and lying flat, with each segment fully adsorbed. Desorption would involve simultaneous removal of all the segments, and this transition is highly improbable, which explains the stability of this and other spread layers of soluble polymers such as polyvinyl alcohol (section (iii)) and poly(ethylene oxide) (section (iv)). In solution, however, the molecules appear to be tightly coiled due to hydrogen bonding of the carboxyl groups, and adsorption would involve partial uncoiling of this structure. Adsorption of the whole molecule as found in spread layers requires the uncoiling of the whole molecule, and therefore is energetically unlikely.

Thus, although the complete adsorption state is probably more stable than the partly adsorbed, partly coiled state, the transition between them may require considerably more energy than the difference in their energy levels might indicate.

(vi) Summary of experimental work.

It may be seen from the above sections that information about polymer molecules adsorbed at the water/air surface is in general rather scanty and inconclusive. In the poly(ethylene glycol) system,

available evidence is in direct contradiction, and none of the published work is entirely free from criticism. Experiment on the related system of poly(ethylene oxide) has been concerned either with solution properties or spread monolayer properties but the relation between them has never been investigated. The poly(ethylene glycol) series has never been considered as a spreading polymer, and while spreading cannot be ruled out, there may be a significant difference here between the two series of ethylene oxide polymer. The question of the attitude of the adsorbed segments with respect to the surface is still unresolved, with the added complication that the effect of the terminal hydroxyl groups is not known.

It seems to be well established that when a polymer can be spread on the water surface, reproducibly and with stability, then it is adsorbed at each component segment. This follows from the independence of the monolayer properties on the molecular weight (Crisp, 1946). The stability of this adsorption in the case of water-soluble molecules appears to be due to the requirement that all segments should be desorbed simultaneously if the molecule is to diffuse into the bulk liquid phase.

The behaviour of polymer molecules adsorbed from solution is less well understood. At least in the polymethacrylic acid system, there appears to be a type of adsorption quite different from the spread situation. The two types are not interchangeable. Polyvinyl alcohol and poly(ethylene oxide) have been examined in solution by

Glass, but conclusions are made difficult by his employment of a non-equilibrium technique. Experimental inadequacies may also mar the available results on poly(ethylene glycol) solutions.

Use of the Gibbs equation has not been fully justified, and the whole question of the theoretical treatment of the system is made difficult by the general lack of information about the surface tension of polymer solutions.

The problem of the time variation of the surface properties of polymer solutions has also received little attention. Although Frisch and Al-Madfai found agreement in polyvinyl alcohol systems with the proposal that diffusion of the active molecules from the bulk is the primary contribution to time-dependence, Fukawa et al (1961) suggested that other considerations appeared at high concentrations of the same system. Assuming that the law of diffusion is the same for polymers as it is for other solutes, and that the diffusion constant is of the same order, then the equilibrium time for a given concentration should depend only on the final value of the adsorption. Since polymeric materials often appear to require a long time for equilibration, it is therefore indicated that equilibrium requires a higher proportion of solute to be adsorbed than is usual.

(vii) The theoretical treatment of polymer adsorption.

Polymer adsorption at the air/water surface is usually described in terms of a large number of chain-linked segments, each capable of reversible adsorption on to a lattice of adsorption "sites". Singer (1948) proposed a model for the adsorption in which all the polymer segments occupy lattice sites, the chain as a whole lying in the surface. This "two-dimensional" type of treatment provides a useful basis for the examination of spread polymer monolayers (Davies, 1954), but it is possible in the case of very flexible chains that not all the segments lie in the surface (Frisch and Simha, 1956). Frisch and Simha described a model which is more nearly like the bulk solution random coil, only a fraction of the segments being adsorbed, the others forming loops in the bulk liquid phase. The model proposed by Silberberg (1962), intended to be valid for both liquid/solid and liquid/gas interfaces, applied a different approach to essentially the same pictorial description of polymer adsorption. This model appears to be successful in explaining at least some of the interesting trends found in the systems described in the earlier sections of this Chapter. The linear relationship between surface tension and log (solution concentration), found by Couper and Eley (1948) with poly(ethylene glycol) (figure 51) is predicted by Silberberg, as well as the variation of line slope with molecular weight. It is also indicated that for low molecular

weight polymers, the surface pressure should tend to a limit at high degrees of surface coverage, but it is unlikely that this is related to the behaviour of high molecular weight poly(ethylene oxide).

CHAPTER 6

EXPERIMENTAL PROCEDURES

(i) Materials.

(a) Water Preparation.

The most important aspect of any experimental work involving liquid/air surfaces is the purity and cleanliness of all the materials concerned, solid, liquid, and gaseous. The most troublesome of these is usually the liquid which forms the basis of the examination (in the present case, water) and in investigations of the water/air surface, the solid and gas contamination is principally effective in its action on the water with which it is in contact. In order to assess the effect which added materials have on the properties of the aqueous surface, the water must ideally be initially perfectly pure. The pure, clean surface layers should be composed only of water molecules, with perhaps some insignificant foreign molecules dissolved from the adjacent gaseous phase. It is usually assumed that the unreactive components of air, such as oxygen and nitrogen, have a negligible effect on the surface behaviour of pure water, and that any other more reactive components are present in such small quantities that they may be ignored for observations of short duration. More predictable atmospheres, such as of pure nitrogen, are often used, but it is comparatively rare for the gaseous phase to be entirely of water vapour.

Water is exceptionally prone to contamination, and extreme care must be taken in its purification, handling, and storage if valid measurements are to be made. The surface concentrating property of surface active

materials has the effect of making a small amount of material very important in the determination of surface properties, although its actual concentration when dispersed in the water may be too small to detect by other means. Even atmospheric dust particles, without being specifically surface active, can physically reduce the surface area available to the adsorbed molecules under investigation.

Precautions must be taken during water purification to ensure the complete absence of likely surface active substances. Ordinary tap water, apart from its inorganic mineral content, is expected to contain a wide variety of dissolved and suspended organic materials, originating from the water source, the cleansing procedures, or the storage and supply system. Processing of tap water with ion-exchange resins, although removing the majority of the inorganic content, is unlikely to remove important organic material, and may even increase this form of contamination (Drost-Hansen,1965). Straightforward distillation of raw tap water may also prove inadequate, because of the volatility of certain important contaminants.

The actual procedure used in the preparation of pure water varies widely between laboratories, possibly due to variations in the quality of the original source. Some workers find that simple distillation of de-ionised water is adequate, whereas others employ multiple distillation techniques involving intermediate treatments designed to remove specific contaminants.

The criteria used for assessment of the final product are of necessity empirical to a greater or lesser degree, because of the absence of quantitative measurements of trace concentrations. Measurement of electrical conductivity, a much used test of water purity, is expected to be of little use if non-ionic surfactants are likely to occur. A much used criterion is whether the experimental results obtained for a given system are consistent and reproducible, although the contamination sensitivity of the various surface property measurement techniques varies considerably. A more satisfactory test of surface purity was suggested by Kitchener (1964) in his analysis of the foaming properties of liquids. The persistence of a foam in a pure liquid should be determined only by the draining of liquid from the gas bubbles under surface tension and gravitational forces. The presence of small quantities of surface active material gives the liquid films elastic properties which resist bubble rupture and retard the collapse process. Kitchener therefore considered that the persistence of a bubble on water for as long as one second indicates the presence of impurities, and it appears that this test may be the best means of assessing the surface purity of water. The test also has the advantage of extreme simplicity.

In the work to be reported in Chapter 7, the water used was distilled in an all-glass apparatus from alkaline potassium permanganate solution made with fresh tap water. Each quantity so prepared was accumulated in a glass bottle, and was discarded if bubbles were found to persist for longer than one second. It was found however that if the distillation apparatus was kept clean, and the permanganate solution was changed after every

distillation of about 5 Litres of water, then the resulting water usually passed the foaming test. Redistillation of this water from fresh permanganate solution was observed to leave the foaming properties unchanged.

The employment of potassium permanganate in the removal of contamination follows its use by Davies and Vose (1965) and Nakamura and Sasaki (1967) in water preparation for surface work. Simple distillation of both tap water and de-ionised water was found to be unsatisfactory, the products supporting bubbles for over 3 seconds. Another useful rapid assessment of surface cleanliness was found to result from simple observation of the persistence of ripples on the water surface. Although without quantitative measurement of the damping coefficient, this test is not as sensitive as the foaming test, it was found to be useful on occasions when the surface cannot be disturbed violently enough to produce bubbles. A sharp tap on the side of the containing vessel will promote waves which are observed to reverberate round the enclosed surface for several seconds. If sufficient contamination is present, the waves appear to be damped out much more quickly, even though the measured surface tension of the water might agree with the accepted value.

Water distilled in the manner described above was usually used for investigation within 24 hours, during which time it was kept in a 5 Litre glass bottle, covered to avoid dust contamination. All the glass surfaces likely to be encountered by the clean water were thoroughly cleaned in chromic acid (concentrated sulphuric acid saturated with potassium

dichromate) and rinsed with much tap water before a final rinse in clean distilled water. Tap water was not allowed to stand in contact with the glass for longer than one minute.

(b) The Ripple Tank.

The tank used for the investigation of ripple damping had internal dimensions 44cm. x 29cm. x 7cm. and was constructed from ½inch "Perspex" sheet. This material was used principally because the moiré fringe technique of observation requires the base of the tank to be transparent and of good optical quality. Glass might have been a better material from the point of view of cleaning, as more violent cleaning agents may be used, but there are construction problems with that material concerned with the joining of the sides to the base. The only sealing material which does not contaminate the water appears to be paraffin wax, and this does not give a construction with the permanence of a robust all-"Perspex" tank.

Construction from "Perspex" is exceptionally easy, joints being made by cementing with a concentrated solution of the material itself in an organic solvent such as chloroform. When the solvent has had time to diffuse through the solid away from the closed joint, the solid is continuously welded, no foreign material being present. A possible objection to the use of "Perspex" is that it may slowly allow adjacent water to dissolve away some of the lower molecular weight material from the surface, and that this could be surface active. It was found, however, that the ripple damping properties of water contained in the tank for periods of more than 24 hours were little changed. Another possible

objection to this material is that it cannot be cleaned by the procedures found necessary with glass. Chromic acid dissolves the surface layers of the polymeric material, producing a white opaque finish. It was found that scrubbing with hot tap water and commercial (washing-up) detergent appeared to be most efficient, the properties of contained water remaining unchanged after 24 hours. One advantage in the use of this hydrophobic material was that the speed of draining could be easily observed. Even, steady, and complete draining from the vertically-held base was a feature of the well-scrubbed and rinsed tank. As with the glass containers, the final rinse was with clean distilled water.

The tank was not designed as a traditional Langmuir trough because this was initially considered to be an unnecessary refinement, solutions being the principal subject of investigation. A major advantage of a Langmuir trough type of construction is that moving barriers may be used to "sweep" the surface, thus removing foreign adsorbed material. Although the water used may be prepared under the most scrupulous conditions, it is often reported to be advisable to sweep the surface several times before experiments begin. In abandoning the Langmuir trough design, this facility was sacrificed. The advantages of the Langmuir trough in the investigation of the properties of spread monolayers are described in (d).

Another way of surface cleaning is described by Davies and Vose (1965) and Gaines (1966), which involves dusting talc on the surface of the water, and sucking away the whole surface layer with a fine capillary. Insoluble foreign material is removed along with the talc. This method was tried in the present investigation, but it was found that the amount of liquid removed was rather unpredictable, and since the moiré fringe visualisation method is very sensitive to changes in liquid depth (see Section (iii)), water had to be added or removed following the talc operation to achieve the correct level. This involved further risk of contamination, and the talc suction method was not adopted as regular procedure.

A cover for the tank was made from 1/8 inch glass plate, being in three sections to facilitate adjustment and removal. The volume above the surface enclosed by the cover could be filled with pure nitrogen from a cylinder, via a pressure reducing valve. These measures were intended to reduce the risk of contamination from the atmosphere during experiments of long duration.

(c) Solution Preparation.

It was found during the present investigation that certain precautions were necessary in the preparation of homogeneous polymer solutions which may not be necessary in the preparation of solutions of simpler molecules. At high concentrations, up to 0.5%, the higher molecular weight materials may require an extremely long time for solution, and the result in some cases is a viscoelastic gel. At lower concentrations,

with which this work is principally concerned, it is the homogeneity of the solutions which is sometimes questioned. The problems of equilibrium of polymer solutions were mentioned in Chapter 5, in connection with the assumptions made by Glass (1968b) in his work on poly(ethylene oxide) (Chapter 5, section iv). Also, the possibility that equilibrium might depend on the initial state of the dissolved polymer was indicated by Katchalsky and Miller (1951) who showed that a spread monolayer of polymethacrylic acid behaved in a manner markedly different from a polymer layer adsorbed in equilibrium from solution (Chapter 5, section (v)).

Because the volume of liquid in the ripple tank was large, being usually between 4 and 6 Litres, it was found impractical to make up solutions initially in the concentrations required for surface property examination. The low concentrations usually examined allowed all the solid polymer to be dissolved in a small volume of water, between 100 and 300 cc., which was added to the bulk of the water shortly before observations began. Extremely small concentrations could be produced in this way, adding the concentrated solution with a range of pipettes. This technique can also allow the age of the surface to be estimated with reasonable accuracy. The measured addition of concentrate can be made below the surface, while stirring continuously, and the adsorption process should always begin with zero adsorbed material. There is a danger when making up the solutions directly by adding the solid polymer to the correct volume of water, that some material may spread from the solid, and create adsorption conditions quite different from the true solution equilibrium state. Also, in the

cases where the water must be heated for complete solution to take place, such as with polyvinyl alcohol, the conditions of changing temperature may affect the final adsorption equilibrium.

Solutions were always made up with fresh, clean distilled water which passed the foaming test, the polymer being weighed on a chemical balance before addition to the water in a thoroughly cleaned glass flask. In cases where solution was only complete at a temperature higher than the ambient temperature, the flask was heated by an electric mantle, the temperature being monitored with a clean thermometer. All solutions were allowed to attain room temperature before volumetric addition to the bulk liquid.

The standard procedure for investigation of a series of concentrations of a polymer solution began with the preparation of the concentrated solution as described. The additions of this solution to the bulk of the water were made by filling a pipette of the required volume and releasing the concentrate below the liquid surface, stirring rapidly. In order to prevent the spreading of polymer on to the water surface from the outside of the pipette, before allowing the pipette to enter the water it was thoroughly wiped with a clean paper tissue. There appears to be no way of avoiding this contact with material of unknown cleanliness in this method of solution preparation, but tests carried out with pure water additions, employing the same tissue cleaning step, did not indicate that contamination was being introduced.

The problem of equilibrium attainment in polymer solutions, mentioned in Chapter 5, has been investigated and will be reported in Chapter 7. Partly because the solutions examined exhibited widely varying behaviour, this was found to be a major problem in the examination of solutions at the low concentrations used for this work. It was found to be difficult to predict the time which should be allowed for a given polymer to arrive at a state which might be called equilibrium. A useful technique for the monitoring of time variation of the order of tens of minutes was developed in the investigations on poly(ethylene oxide) solutions (Chapter 7). In order to reduce the surface excess of the solute to zero at the beginning of a set of observations, the surface was lightly skimmed with a vertical, partly immersed "Perspex" sheet, 1/16 inch thick, and nearly as long as the tank width. This appeared to compress the adsorbed layer ahead of the plate, as well as producing turbulence in the solution which mixed the polymer back into the bulk. Although vigorous stirring with a rod was found to have little effect, the skimming technique appeared to reduce the surface excess almost to zero, as evidenced by the "pure water" values of ripple parameters which the new surface exhibited.

(d) Spreading Technique.

The spreading of polymeric materials on water was reported in detail by Crisp (1946, 1958), and it was shown that a water-soluble polymer, polyvinyl alcohol, could be spread from aqueous solution on to a pure water substrate. This behaviour was also found in the present work

with polyvinyl alcohol samples, as well as with poly(ethylene oxide). The variation of surface properties with mass of polymer per unit area provides a direct determination of the equation of state of the polymer, and the investigation of the spread layer is therefore a useful adjunct to measurements of solution properties.

The preparation of solutions for spreading was exactly the same as the preparation of the concentrate for subsequent dilution in the investigation of solutions (described in c). Spreading solution concentrations for all materials investigated were between 1×10^{-3} and 5×10^{-3} by weight (0.1% and 0.5%). Solutions of the higher molecular weight poly(ethylene oxide) samples (M.W. $\geq 10^6$) possess such high viscosity in the more concentrated part of this region that it was usual to employ concentrations of between 1×10^{-3} and 2×10^{-3} (by weight).

Spreading was performed using an "Agla" micrometer syringe. This instrument consists of an accurately ground all-glass syringe whose plunger is moved by a micrometer screw head. The smallest graduation of the micrometer produces a volume expulsion of 2×10^{-4} cc., and the total calibrated volume is 0.5cc. Continuous addition of solution therefore allowed an extremely wide range of surface concentrations to be produced. Two kinds of spreading needle were tried with this syringe. One was of stainless steel with a sharpened oblique tip, and the other kind was made of glass, with a blunt tip. The objection to the use of stainless steel in surface work is that it is difficult to clean, strong acids being corrosive. Whenever this type of needle was employed, it

was flushed out forcefully with a hot solution of commercial detergent, and rinsed thoroughly with tap water and distilled water. The glass needles were always left in chromic acid for long periods, and rinsed thoroughly before use.

Spreading was performed by slow expulsion of the necessary volume of solution on to the needle tip, using the micrometer adjustment, and then a gentle touch of the tip on the water surface. In order to prevent evaporation of solvent from the tip between additions, which could have the effect of reducing the expelled volume of the subsequent drop (perhaps to zero), concentrating the solution still in the needle, the tip was kept below the surface of a quantity of pure solvent contained in a small dish. Dilution of the spreading solution by diffusion of solute into the pure solvent is expected to be small in the short time between additions, because the needle bore is small. The loss of solvent from the tip by evaporation while the needle is out of the solvent is negligible, because relatively small changes in the actual spread volume do not change the mass of polymer being spread.

As already implied, the "continuous addition" method of monolayer production was exclusively used in the experiments to be described. With this method, the surface concentration was increased incrementally from zero by adding drops of regular volume from the syringe tip. The advantage which the continuous addition technique has over the more usual barrier compression technique is that a much wider range of surface concentration is possible. As Shuler and Zisman (1970) found, this wide range is extremely useful for examination of polymer monolayers, which

often exhibit a range of interest much more extensive than "classical" surfactants because of their complex collapse behaviour.

The more usual technique of investigating the properties of a spread monolayer by varying surface concentration is to spread a single known mass of material from the syringe tip between the surface barriers of a Langmuir trough, the surface concentration being changed by adjustments in spread area by one or two movable barriers. The advantages of this procedure are that not only can the surface concentration be decreased as well as increased, but also that the efficiency of spreading can be assessed from comparison of single spreading operations. If the same surface tension/surface concentration curve is produced by successive experiments in which different quantities of active material are spread, each in a single operation, then it may usually be assumed that the spreading is complete, and that the spreading technique is adequate. It was found that this certainty was not possible with the continuous addition type of investigation, since the production of a single tension/concentration curve involves a large number of successive additions.

The other main advantage of the barrier compression method, amply demonstrated by Shuler and Zisman (see Chapter 5, section (iv)) is that the monolayer may be examined during expansion as well as compression. It is therefore acknowledged that the barrier compression method is superior to the continuous addition method for the study of spread monolayers, and that exclusive use of the latter technique in the present

work may have restricted the scope of the spread monolayer experiments to be reported.

In the experiments which used spreading solvents other than water, such as carbon tetrachloride and benzene, the solvent was freshly distilled from "Analar" grade substance, using a clean, dry, all-glass still. The absence of active impurities in these solvents was verified by spreading 0.5 cc. of pure solvent on to the pure water surface (area 1300 cm^2), no change in surface properties being observed.

(ii) Surface Tension Measurement.

In addition to the ripple measurement experiments to be described in section (iii), which form the major part of this work, some surface tension measurements were made using a version of the Wilhelmy plate apparatus (Chapter 2, section (ii)b) in order to clarify the ripple results. Only spread monolayers were investigated with this technique, as the experimental difficulties sometimes encountered with solution observations (section (iii))were not as easily overcome as in the ripple measurement.

The apparatus used was similar to that described by Nakamura and Sasaki (1967), employing a torsion wire to oppose the surface tension forces, and an optical lever to magnify the plate movement. Figure 1 shows the arrangement used, the position of the counter-balancing weight being adjusted so that when the Wilhelmy plate rests on the liquid, just wetted by it, the beam is horizontal.

Initially, the dry plate, mass M, is hung from the arm, which is restrained in a horizontal position by a fixed stop above the arm, and the position of the light beam h_o is noted. A pure sample of the liquid under examination is slowly raised to meet the horizontal lower edge of the plate, care being taken to avoid ripples. The plate is pulled by the surface tension, but as previously arranged, does not leave the fixed stop. The position of the light beam h is then measured for a range of weights m added to the scale pan, the resulting m(h) curve being found to be almost linear for a small range of torsion angles. By extrapolation, the mass m_o is found which allows the arm to rest at the h_o position without reaction from the fixed stop, and without significant immersion below the liquid surface. The liquid is then removed, and the added mass m_a is determined which will return the dry plate to its balanced h_o position. The two measurements just described are necessary in order to allow for the effect of varying plate immersion as the surface tension changes.

The surface tension of a given liquid may be measured with an apparatus calibrated in the above manner by replacing the plate in the h_o position, the arm against the stop, and raising the liquid as before. A mass m_s is added to the scale pan, which makes the plate sink into the liquid. Observation of the resulting value of h ($h = h_s$) allows the surface tension σ to be found from knowledge of M, m_o, m_a, m_s, h_s, the m(h) curve and the perimeter p of the plate/liquid/gas interface, using the equation

$$\sigma = (m(h_s) - m_s + m_a - M - m_o)/ p$$

where g is the gravitational acceleration.

For a given torsion wire and plate, M, m_o, m_a, p, and m(h) are fixed, and σ can be found by recording m_s and the resulting h_s. The apparatus is therefore useful if the surface properties show time variation, which is observed as a variation of h_s for a given fixed m_s.

In the form used in the present investigation, the torsion wire was a piece of steel piano wire, 20 cm. long. The glass plate, 5.1 cm. x 7.6 cm. x 0.2 cm. and mass 13.0 gm. was ground with carborundum/water paste to improve its wetting properties. Liquids were contained in a circular Pyrex tray, of radius 7.9 cm. and depth 6.8 cm. which was cleaned with chromic acid. The liquid surface could be covered almost completely by two sheets of 1/8 inch "Perspex" placed on either side of the ground glass plate. The light source and scale comprising the optical lever were located at a distance of 1 m. from the mirror attached to the balance arm.

The apparatus was found to be convenient in use, and was easily set up and calibrated. Constant reference to the m(h) curve was in many cases unnecessary, because the range of surface tension investigated allowed the curve to be assumed linear, thus simplifying the calculation. Care was necessary in the observation of spread monolayers, as oscillation of the plate in and out of the surface is likely either to encourage solution of the material or to deposit a layer on the plate, affecting its surface properties. The monolayers were always examined by setting up initially with pure water, and then spreading the polymer as described in section (i) d. Observations of the position of the light beam, h_s, were

made without further adjustment to the apparatus.

The sensitivity of the measurement was such that a change of 1 mm. in h_s represented a change in σ of 0.67 dyn. cm^{-1}.

(iii) Measurement of Ripple Properties.

The principles of the moiré fringe surface wave measurement technique developed for this work are fully described in Chapter 4 of which section B (vi) describes and explains the optical alignment procedures necessary to produce moiré fringe patterns of the requisite standard. Alignment is best done before any of the cleaned parts, such as the "Perspex" tank, is incorporated into the apparatus, the avoid risk of contamination. The final adjustments to the optical components do require the tank to be in position, containing the same volume of water as is about to be examined, but tap water is quite adequate for this purpose. After alignment, the glass tank covers are removed, the tank is drained, removed, and cleaned as described in (i) b. All water is wiped from the underside of the tank before its replacement in the apparatus and its filling with water from the distillate storage bottle. It was found that the volume of water put into the tank could be made the same as that used for alignment merely by adding water until the quiescent fringe pattern showed fringes which were horizontal. More or less water produced a pattern which, though not perfectly focussed, was of good quality, and showed fringes at a slight inclination to the horizontal. It is estimated that volumes were reproducible in this way to within 40 cc. in a total volume of 4000 cc.

Once filled, the tank is covered and allowed to reach thermal equilibrium with the rest of the apparatus while solutions are prepared and the ancillary items of apparatus wuch as thermometer and syringe are cleaned. The wave generating plate, made of 1/8 inch "Perspex" sheet is carefully cleaned and is then set between the two Goodmans vibrators which excite the oscillation, the lower edge of the plate being adjusted to be horizontal, about 1 mm. above the liquid surface. Permanent contact with the water is obtained by an initial gentle depression of the moving coils of the vibrators.

The standard procedure for examining the properties of both spread and solution monolayers was initially identical in all the experiments performed. The clean pure water surface was always examined before addition of surface active material, as a check on both the apparatus adjustment and the water cleanliness. A picture of the "no wave" pattern of straight parallel horizontal fringes was made, followed by pictures of the decay characteristics at each of the frequencies to be examined subsequently. As a check on the water purity, the wave pattern was usually observed at a higher frequency than usual, such as 300 Hz, because although damping measurements are not very accurate at that frequency, the decay of the waves over the 10 cm. observed field was always sensitive to low concentrations of impurity.

Since the frequencies used were invariably low (20 Hz to 300 Hz) they were measured most accurately by sampling the periodic time of the oscillation with the timer/counter (Gresham Lion GFT 15). The oscillator was found to be stable at the set frequency to within 0.1%, drift after the

first hour of operation being negligible.

After the pure water observations, additions of polymer were begun, either by spreading on the surface, as described in section (i) (d) or by addition to the liquid bulk, continuously stirring, as described in section (i) (c). After spreading, the fringe pattern was observed visually for several minutes to see if the surface properties were changing, perhaps due to solution of the monolayer. It was found to be very useful to be able to observe the waves continuously during spreading additions, because damping changes were immediately noticeable. In cases where dissolving of the monolayer was suspected, fringe pictures were made at different times so that the effect could be examined more quantitatively.

Solution observations were much more difficult. Spreading of polymer from the fairly concentrated added solution had to be avoided during the addition, and this was done as already described, by wiping the outside of the pipette with a clean tissue and letting the polymer flow well below the surface. It was found in the case of poly(ethylene oxide) that unless the addition was performed slowly while stirring the bulk, it was possible for a local high concentration to be formed, which could spread polymer quickly over the whole surface. This could be observed in the immediate response of the moiré fringe wave pattern observed in stroboscopic light. Again, the continuous viewing facility proved extremely useful in this respect.

Difficulties also arose in the investigation of poly(ethylene oxide) from the extremely low bulk concentrations which would exhibit a surface effect. This had the effect of increasing the observation time in a very unpredictable manner, and it also led to certain interesting conclusions about the polymer which will be described in Chapter 7. The "skimming" procedure described in section (i) (c) was found to be very useful in ensuring that spreading effects were negligible, and in defining a time origin for the slowly changing surface.

Pure nitrogen atmospheres were available for the experiments which lasted long enough for air contamination to be expected as a hazard. None of the polymers examined was expected to react chemically with atmospheric oxygen, but poly(ethylene oxide) monolayers were observed under both air and nitrogen for comparison, since in the drag reduction effect (Chapter 1) polymer efficiency is impaired by oxidative degradation - breaking of the polymer chains into shorter lengths. Since the results described in Chapter 7 appear to be independent of the molecular weight of the sample used, in agreement with the work of Crisp (1946) and others, it was not expected that degradation would affect the adsorption behaviour of the polymer. The identity of the results under air and nitrogen confirms this view.

CHAPTER 7

RESULTS AND DISCUSSION

A. PRELIMINARY INVESTIGATIONS

(i) General Approach.

It was explained in Chapter 1 that the aim of the present work was to show how water-soluble polymers of the type found efficient in the phenomenon of turbulent flow drag reduction affect the regular circular particle motions associated with the propagation of transverse surface waves, or ripples. Poly(ethylene oxide), whose high molecular weight fractions have been found to be among the most efficient of drag-reducing additives, was found from preliminary investigations to have an extremely large effect on the ripple damping in the range of solution concentration found useful for drag reduction (10^{-6} to 10^{-4} by weight). These preliminary investigations were with simply made up solutions, using tap water, no attempt being made at surface cleanliness and with no consideration given initially to the form of equilibrium behaviour which such solutions might exhibit. Damping showed an immediate increase with the lowest concentrations examined (about 10^{-6}), and then increased further as concentrations of 10^{-3} were approached. The other polymers examined, principally polyacrylamides and sodium carboxymethyl cellulose, were found to lack this strong damping effect.

Repetition of the preliminary work under surface clean conditions emphasized the singularity of poly(ethylene oxide) among the drag reducing polymers. Effects due to polyacrylamide samples were found, but these were at concentrations much higher than those in poly(ethylene oxide) (about 10^{-4}), and they were therefore thought unlikely to have been caused by the same effect, whether produced by the bulk liquid or by the surface properties. Moreover, the effects tended to vary considerably between different samples of similarly prepared polymers. It was concluded from the high solution concentration needed that the damping effects were more likely to have been produced by contamination of the polymer by surface active agents intruding from the commercial production processes than from any intrinsic property of the polymer. Similar conclusions were reached following comparison of experiments on two samples of sodium carboxymethyl cellulose (I.C.I., Joseph Crosfield Ltd.).

Work was continued on the poly(ethylene oxide) samples, and it is this work which will be reported in this chapter. However, it is of relevance to consideration of the materials found to be inactive in production of ripple damping effects to mention that the effects of poly(ethylene oxide) on the water surface have been well explained by consideration of the elastic properties of surface containing adsorbed polymer. The lack of an effect in solutions of polyacrylamide and sodium carboxymethyl cellulose is associated with the absence of surface elasticity in these systems. This view is supported by the relative

reluctance of the solutions to support a foam, compared with the stability of poly(ethylene oxide) foams.

The absence of strong elastic effects on surfaces of polyacrylamide solutions indicates that this polymer is far more suited to the original intention of the ripple damping work than poly(ethylene oxide) was found to be (see Chapter 1). It is possible that in a pure condition, this polymer forms ideally homogeneous solutions whose wave damping properties reflect the response of the molecules to the ripple shear flow. As already indicated, the present investigation was not able to confirm this, probably due to the presence in the polymer samples examined of relatively small quantities of more surface active materials which become adsorbed and affect the ripple damping. The magnitude of the effect which small surface excesses have on the damping can be extremely large, as shown in Appendix 2, and it may be very difficult to produce samples of the polymer so free from this sort of contamination that truly homogeneous solutions could be produced.

(ii) The Ripple Damping Properties of Pure Clean Water.

It is an obvious and imperative test of the accuracy of any ripple measurement technique to check that its measurements are in agreement with accepted previous work. The only system which has been adequately investigated is the pure water surface, but the damping characteristics of this have been measured in such a way that there is little doubt about the accuracy of the measurements. Goodrich (1961) and Davies and Vose (1965) have independently shown with precision that the Stokes (1845)

formula accurately predicts wave damping on pure water surfaces. This formula can be written (see Chapter 3)

$$\beta_0 = \frac{4 \chi^3 \eta}{3 \rho \omega} \qquad 3.6$$

where β_0 = amplitude damping coefficient (cm^{-1})

χ = 2π /wavelength (cm^{-1})

η = bulk liquid shear viscosity ($g.cm^{-1}s^{-1}$)

ρ = pure liquid density ($g.\ cm^{-3}$)

ω = 2π x wave frequency (s^{-1})

The relation between wave number χ and angular frequency ω, for a pure liquid, has been shown to be accurately predicted by the Kelvin(1871) equation:

$$\sigma \chi^3 + \rho g \chi = \omega^2 \rho \qquad 3.5$$

where σ = pure liquid surface tension (dyn. cm^{-1})

and g = gravitational acceleration ($cm.s^{-2}$)

By combining these equations, the damping coefficient β_0 may be evaluated at any frequency. Figure7.1 shows a FORTRAN computer program which evaluates wavelength and damping over a range of wave frequencies for fixed values of surface tension. Also calculated are the maximum damping predicted by Lucassen and Hansen's hydrodynamic ripple theory (eqn. 3.8) and the value of surface dilational elasticity which is expected to cause this maximum (eqn. 3.9). Implicit in the calculations are the values

```
      PROGRAM SCOTT  (INPUT,OUTPUT,TAPE5=INPUT,TAPE6=OUTPUT)
C     OUTPUT DEPENDENT ON FREQUENCY NOT WAVELENGTH
      WRITE(6,6)
    6 FORMAT(39H1ITEMS  LAMDA  FREQ.  RZERO  BMAX  EMAX )
      SIGMA = 73.0          surface tension starting condition
   10 PFREQ = 15.0
   20 WAV = 2.000
   30 SI = 2.0 * 3.1416/WAV
      SI3 = SI*SI*SI
C     KELVIN FORMULA     PURE LIQUID WAVELENGTH
      W = SQRT(SIGMA*SI3 + 980.0*SI)
      FREQ=W/(2.0*3.1416)
      DFREQ = FREQ - PFREQ
      IF(DFREQ.LT.1.0) GO TO 40
C     STOKES FORMULA      PURE LIQUID DAMPING
      BZ=(4.0*SI3*0.01)/(3.0*W)
C     DAMPING PREDICTED AT THE MAXIMUM
      BETAMAX=SI*SI*SQRT(2.0*0.01/W)/3.0
C     ELASTICITY NEEDED FOR MAXIMUM DAMPING
      EMAX=SQRT(2.0*W*W*W*0.01)/(SI*SI)
      WRITE(6,39)SIGMA,WAV,FREQ,BZ,BETAMAX,EMAX
   39 FORMAT(1X,F4.1,2X,F5.3,1X,F7.2,2X,F6.4,1X,F6.4,1X,F6.4)
      IF(WAV-0.220) 66,66,50
   50 PFREQ = FREQ
   40 WAV = WAV - 0.001
      GO TO 30
   66 SIGMA = SIGMA - 1.0
      IF(SIGMA-69.0) 63,10,10
   63 CONTINUE
      END
```

Figure7.1 FORTRAN computer program for the calculation of wavelength and damping coefficient for water ripples.

$$\rho = 1.00 \text{ g.cm}^{-3}$$

$$\eta = 0.01 \text{ g.cm}^{-1}\text{. s}^{-1}\text{.}$$

Figure 7.2 depicts graphically the damping coefficient calculations produced by this program with the University of London CDC 1600 computer. It will be observed that the effect of changing surface tension on the damping properties of the pure surface is quite small. A decrease of 10.0 dyn. cm^{-1} from 73.0 dyn. cm^{-1} increases the damping of 100 Hz ripples from 0.110 cm^{-1} to 0.127 cm.^{-1}. This is very small compared with the effect of low values of surface elasticity (Appendix 2), which can increase the damping by a factor of 5, and it follows that the damping effect of trace surface active contamination is much more likely to be produced by its associated surface elasticity than as a direct consequence of any decrease of surface tension.

Measured values of ripple damping between 30 Hz and 300 Hz are shown in figure 7.3, together with the curve predicted by the Stokes formula computations for a surface tension of 72.0 dyn. cm^{-1}. The water temperature was 24.1°C. The comparatively large scatter in the results in the low frequency region is due to the rather low damping exhibited by the surface in this region. Since the maximum observed travel of the waves in the moiré fringe apparatus is limited to 10 cm., the difference in wave amplitude between the two most extreme points of measurement is small, and the near-unity ratio of the amplitudes is sensitive to small moiré fringe distortions and inhomogeneities of the wavefront. The technique is hardly less useful for the investigation of monolayer

figure 7.2 Ripple damping on pure water of different surface tension.

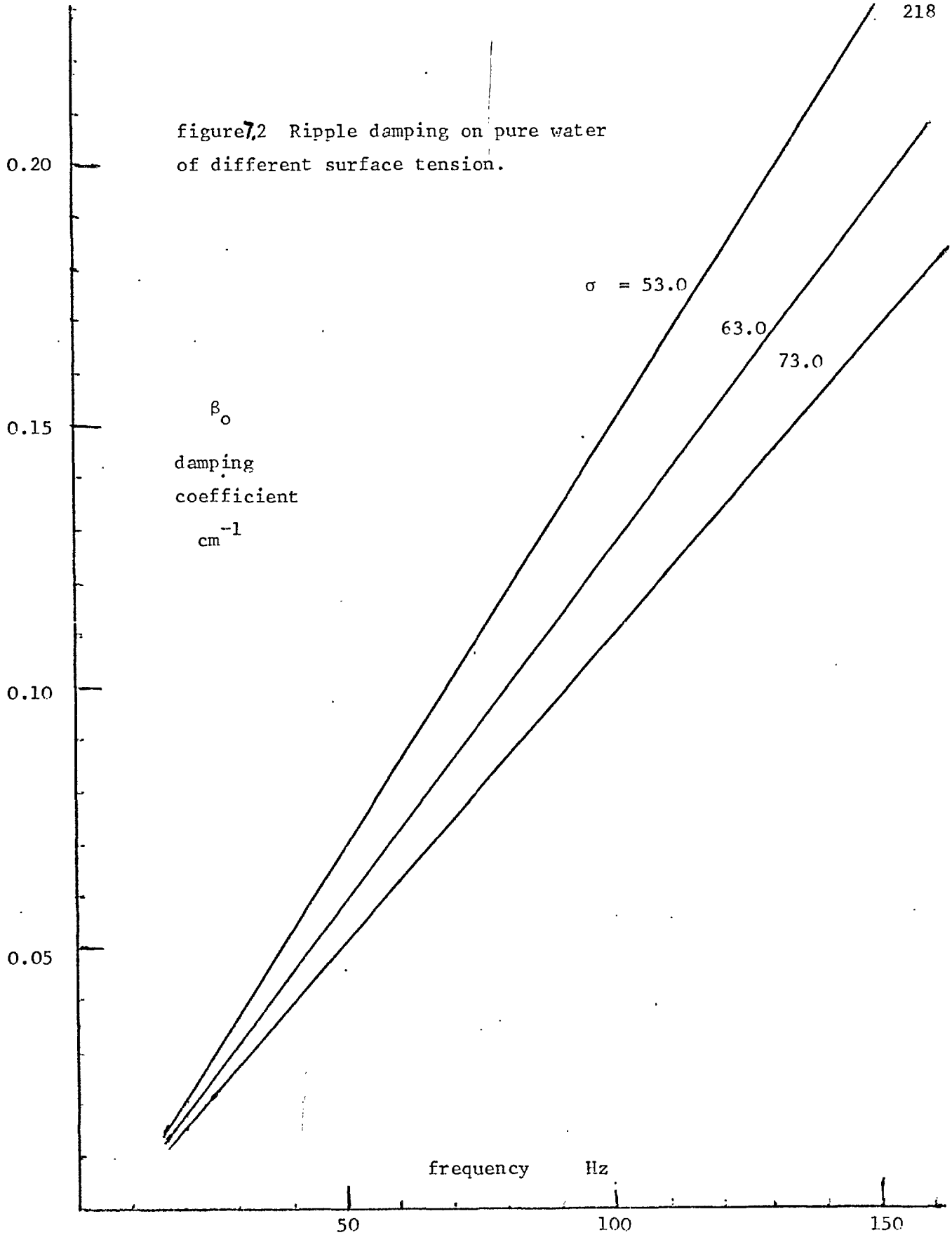
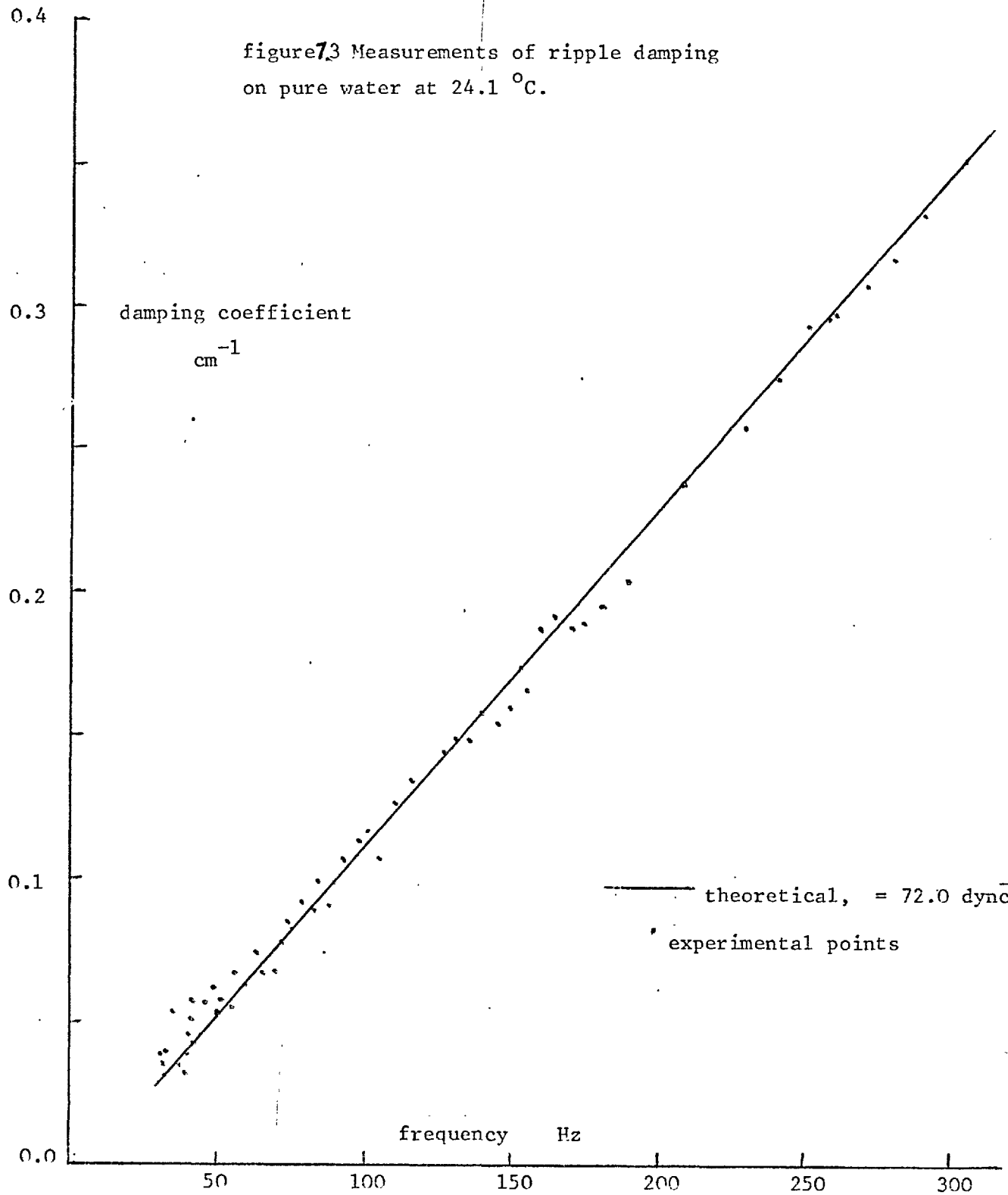


figure 7.3 Measurements of ripple damping on pure water at 24.1 °C.



damping at these frequencies because of this, as the most interesting region of elasticity is characterised by considerably higher damping coefficients.

The highest frequency at which these results were obtained was 300 Hz, principally because the particular pair of gratings employed in the fringe production (65 lines per inch) did not allow accurate measurement of significantly higher frequencies in the region of wave height for which the ripple system is linear. An improvement to the apparatus which should allow the frequency range to be extended would involve refinement of the imaging lens.

In the measurement of damping coefficients greater than the pure water values, additional difficulties sometimes arose. It was found that the efficiency of wave generation with the vertically oscillating "Perspex" plate tended to be reduced as the surface elasticity increased, and the wave amplitude therefore decreased for a fixed amplitude of plate movement. This effect has not been reported in other investigations of wave damping, and indeed in some it was specifically assumed that the initial wave amplitude should be independent of surface elasticity (Thiessen and Scheludko, 1967, see Chapter 3 (vii)c).

The cause of the efficiency reduction is not known, but it may follow from the particular method of wave generation used in this case. The effect of a vertical plate, initially just touching the meniscus distorted surface, and moving downwards, is twofold: the distortion of

the surface is changed, and this change will be propagated away from the plate at the group velocity of wave motion; there will also be a certain amount of bulk liquid displaced by the entry of the plate, which flow may affect the surface distortion. The presence of surface elasticity is expected to produce a further constraint on the movement of the surface, but it is not clear why the generating efficiency should be thus impaired. Effects due to the varying plate immersion will be absent if the plate is initially so far immersed as to reduce any effect of the induced liquid flow on the surface motion, and this may indicate why the Thiessen and Scheludko method should have different charactistics.

An attempt made to assess the improvement due to this use of a deeply immersed plate was not conclusive, because it was found to be impossible to achieve a uniform, homogeneous wavefront with an immersed "Perspex" plate. The moiré fringe technique relies on the identity of all the fringes composing the "wave pictures" in order to measure the average wave height at a certain distance from the plate. Small variations in wave height across the observed wavefront tend to upset the measurement, and sufficient variation was found in this instance to make the measurement inaccurate. The inhomogeneity appeared only when a polymer monolayer had been spread, and it is thought to have been caused by incomplete or uneven wetting of the "Perspex" in the presence of the monolayer.

The important effect of the reducing wave efficiency was that in the region where the damping was high, the wave amplitude became

much smaller, and measurements were less accurate at frequencies for which the pure water damping is already high. An improvement in measurement sensitivity is expected to extend the frequency range available in the high damping region.

B. POLY(ETHYLENE OXIDE)

(i) Introduction.

Previous work on ethylene oxide polymers was reviewed in Chapter 5, and the controversial nature of existing results was indicated. Two polymer series have the same segment of ethylene oxide as the polymeric repeat unit : poly(ethylene oxide) and poly(ethylene glycol). The only chemical difference between the two series appears to be that terminal hydroxyl groups are present on the ends of the glycol chains which do not occur on the oxide chains.

Investigation of the adsorption from solution of the glycol series, by Lovell and Hibbert (1940) and Couper and Eley (1948) produced a difference of opinion on whether the polymer molecules were being adsorbed with all of their segments lying horizontally in the surface or were attached at only a small proportion of their segments, the intermediate sections of molecule being looped into the bulk solution. Theories of polymer adsorption have indicated that the looped state should be produced when the molecules are adsorbed from solution (Silberberg, 1962), and the observed "horizontal" adsorption of water soluble material after spreading on the surface (Crisp, 1946;

Katchalsky and Miller, 1951) has no place in theories of this type. Other theories, starting by assuming the horizontally adsorbed state (Singer, 1948; Davies, 1954) are similarly incapable of explaining the observed cases of looped adsorption. Gaines (1966) has even questioned the use of the term "monolayer" for the looped state, preferring to restrict it to the spread state.

In his attempt to elucidate the adsorption properties of ethylene oxide segments, Glass (1968b) assumed that the two polymer series were identical in their equilibrium properties, and examined a mixed range of oxide and glycol polymer samples on this basis (Chapter 3 section iv). He concluded that all of the members of the series adopted looped configurations.

Other work which may have a bearing on the state of the adsorbed ethylene oxide segments has been done with so-called non-ionic surfactants, which are composed of a hydrophobic end group attached to a short ethylene oxide polymer chain. Meader and Criddle (1953), Schick (1962), and Lange (1962) showed that when these molecules were spread on to an aqueous surface, making them insoluble by salting the substrate, the hydrophobic portion was oriented out of the surface, with the ethylene oxide segments horizontally adsorbed. However, Schick showed that in adsorption from solution, the ethylene oxide section assumed the "looped" type of behaviour, forming coils in the substrate.

To summarize, the main issue concerning the adsorption characteristics of ethylene oxide polymers has been the determination of the orientation of the segments in the surface region. For spread material, especially following the recent wave damping experiments of Shuler and Zisman (1970), it has been established that poly(ethylene oxide) becomes adsorbed with all or nearly all of its segments firmly attached horizontally to the surface, probably with the ether oxygen in each segment providing the necessary attraction for the water phase. Poly(ethylene glycol) spreading has not been reported. For dissolved material of both polymer series the situation is not clear, and evidence from the glycol series is available which will support both horizontal and looped postulates. Couper and Eley (1948) supported the horizontal attitude, whereas Lovell and Hibbert (1940), Glass (1968b), and the non-ionic surfactant work of Schick (1962) supported the looped state.

In the light of this previous work, with the exception of the recent results of Shuler and Zisman, the investigation of the surface properties of aqueous solutions of poly(ethylene oxide) was begun. The samples of polymer were kindly supplied by Union Carbide Ltd., and were part of their "Polyox" series. The following table, given by Harding and Rose (1968) gives the approximate average molecular weight of this polymer series.

Polyox Grade	Approximate Molecular Weight ($x10^5$)
WSR N10	1
WSR N80	2
WSR N750	3
WSR N3000	6
WSR 35	2
WSR 205	6
WSR 301	40
Coagulant	50

Members of the WSR N series produce lower solution viscosities than the WSR series for the same concentration and average molecular weight. This appears to be due to a narrower molecular weight distribution. The grades investigated in this work were WSR N10, WSR 205, and WSR 301, and they were used as supplied, without attempt at purification. All of the samples were creamy white powders, some more granular than others, but all freely flowing. Solution in water was effected by sprinkling the powder slowly on to a quickly swirling water surface. If the powder was not dispersed in this way while it was being wetted, then it would readily form large floating aggregates covered in gel, which would not dissolve in less than 12 hours. During the solution process, the opaque grains of material gradually became transparent, forming swollen "tears" of visibly different refractive index, much larger than the original grains of solid. The solutions required occasional stirring to

avoid accumulation and gelation on the surface. Solution of 0.1% of any of the grades could usually be completed within one hour without having to heat the liquid. Other solution details were as already described in Chapter 6.

(ii) The First Solution Experiments.

The preliminary tests using tap water solutions and without special cleanliness procedures, which were described in Part A, indicated that important damping effects occurred in the concentration range between 10^{-7} and 10^{-6} for the WSR 301 sample. Accordingly, three bulk solutions of this sample were prepared, of concentrations 10^{-8}, 10^{-6}, and 10^{-4} (by weight), so that additions of these solutions by pipette to the 7 Litre bulk of water would produce an extensive range of concentration including the indicated region of interest. Following the conclusions of the previous published work on other polymers, it was assumed that equilibrium should be close after about 20 minutes, and the system was observed for this length of time after each addition of polymer. It was found that with polymer additions as high as 300 cc of concentration 10^{-6}, which should have given a bulk concentration of about 4×10^{-8}, no effect was observed on the ripple damping. However on the further addition of 10 cc of the 10^{-4} solution, the damping immediately increased, and appeared to stay constant for the 20 minutes before the pattern was recorded photographically. Assuming an efficient

dispersion throughout the bulk liquid the concentration was then 1.5 x 10^{-7}, and the measurements of damping at a range of frequency are shown in figure 7.4. Additions of 10^{-4} solution were continued, and the damping decreased, as shown by the other curve in figure 7.4, which represents a concentration of 3.0 x 10^{-6}. The theoretical pure water curve is also included in this figure.

After an addition, the damping appeared to settle to a steady value very quickly, and did not subsequently change significantly over 20 minutes. It was therefore assumed that equilibrium had been achieved.

Successive experiments attempted to make measurements at lower concentrations than 1.5 x 10^{-7}, without having to add polymer from the low concentration adding solutions such as the 10^{-6}, which had failed to produce any damping effect. In adding smaller and smaller quantities of 10^{-4} by pipette, the additions became increasingly gentle, and it was only when a micrometer syringe was found necessary for the addition process that it was realised that the polymer was being spread directly on to the surface, and not forming a true solution. It had been assumed that the vigorous stirring with a glass rod following an addition was producing a homogeneous solution, whereas it was really having a negligible dispersing effect.

The observed lack of strong surface active effects with the 10^{-8} and 10^{-6} solution additions is adequately explained by proposing that they produced truly homogeneous solutions, which had not had time to show a surface effect during the 20 minutes of observation. The 10^{-4} solution alone had an equilibrium surface tension low enough to

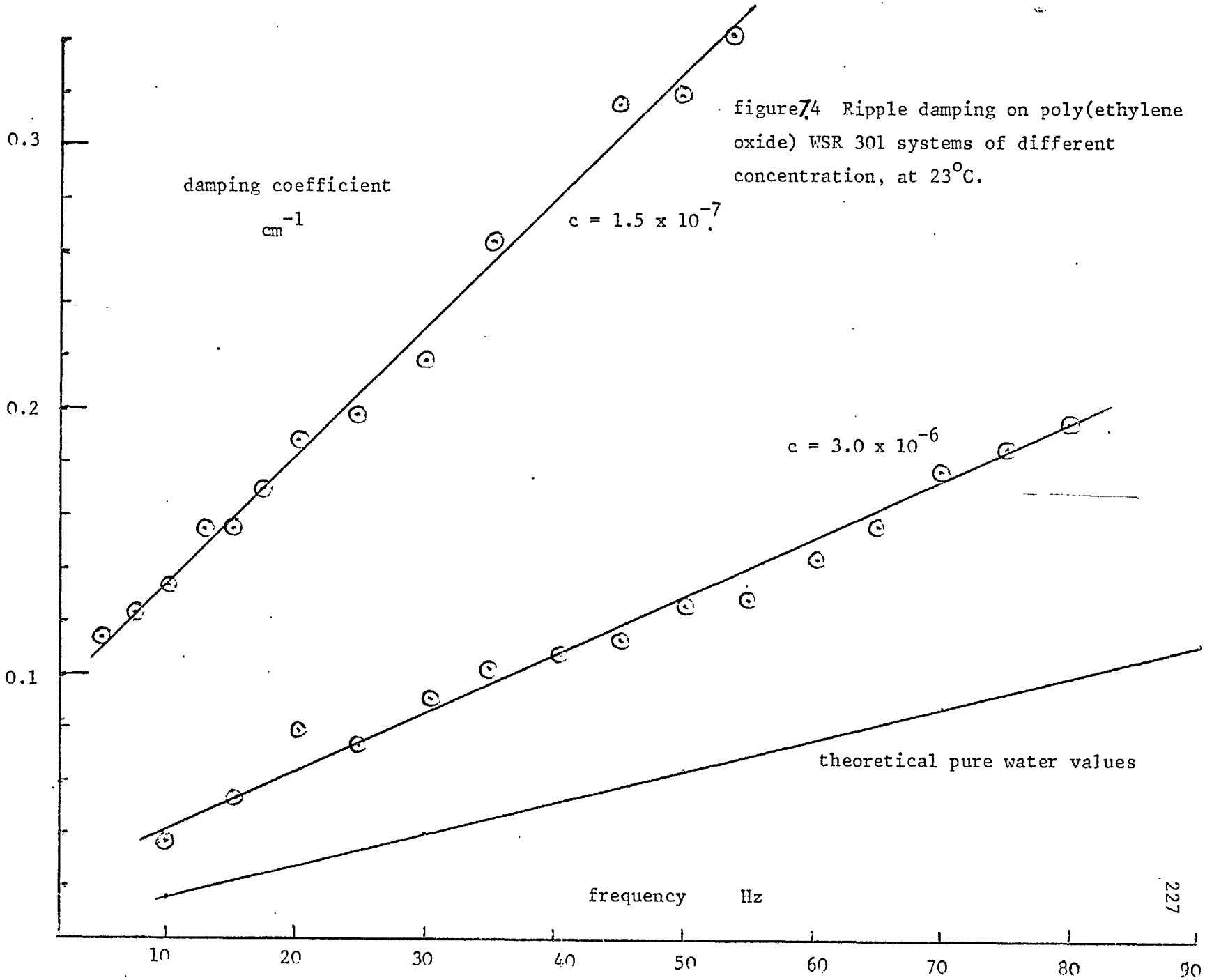


figure 74 Ripple damping on poly(ethylene oxide) WSR 301 systems of different concentration, at 23°C.

encourage spreading as soon as the added quantity touched the surface. The spreading properties, discovered in this way, have been specifically investigated, and will be described in the next section.

One extremely useful fact emerged from the experiments just described. As can be seen from figure 7.4, the damping properties of the surface were not found to be frequency dependent over the range studied (20 Hz to 200 Hz), which allows characteristic measurements to be made on the spread monolayer systems at a single frequency.

Once the spreading properties of poly(ethylene oxide) had been appreciated, it was possible to take precautions to isolate the two different types of polymer monolayer. The spread monolayers will be described first, because understanding of the measurements made on solutions is aided by prior knowledge of the spread monolayer properties.

(iii) Spread Monolayers.

(a) Results. The spreading technique employed in the present work has been described in Chapter 6 (i) d, and was a continuous addition method, monolayer density being increased by addition of concentrated solution rather than compression of a single spread quantity between moving surface barriers. Figure 7.5 depicts a typical set of measurements of wavelength and damping coefficient at a frequency of 30 Hz for a spread sample of WSR 301. The abscissa in this graph is in terms of the practical quantity of adsorbed polymer in the experiment, which is expressed in units of mass per unit area, rather than the

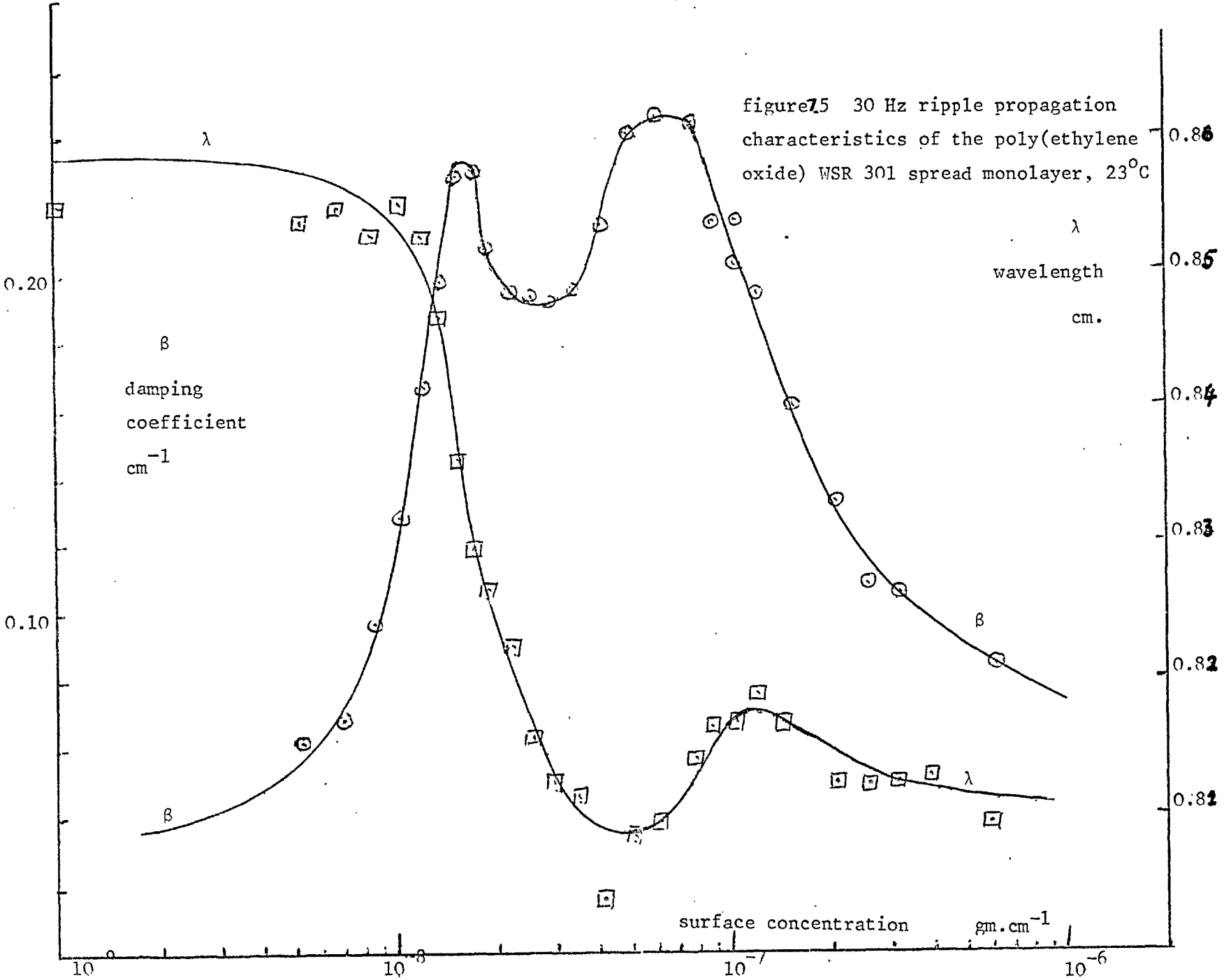


figure 7.5 30 Hz ripple propagation characteristics of the poly(ethylene oxide) WSR 301 spread monolayer, 23°C

quantity more usually used to describe perfectly spread polymer monolayers, which is the area available per monomer segment. As the polymer surface concentration is increased from zero, the damping coefficient is observed to increase rapidly and it shows two distinct peaks before decreasing quickly to a constant value much less than the peak values, but greater than the initial pure water damping coefficient. The wavelength decreases steadily during the first damping peak, reaching a minimum at about the position of the second damping peak, before attaining a steady value.

No monolayer collapse was evident even at the highest surface concentrations of the layer, although the area theoretically available to each polymer segment would at that stage have been much smaller than the area which the segment would be expected to occupy. Gaines (1966) mentioned this difficulty with polymer monolayer observation, and suggested that it is due to the small refractive index difference between polymer solution and pure solvent.

Although the stringent cleanliness precautions described in Chapter 6 were adhered to throughout these experiments, it was not found possible to achieve perfectly reproducible results in successive experiments. Of a total of thirteen independent experiments on the three samples, using identical spreading technique, although they all produced damping curves of the same distinctive two peak shape as figure 75, the concentration at which the damping variation began was not the same in each case. The variation between different experiments using the same polymer sample, and even the same spreading solution was hardly smaller than the variation between different samples. Taking for purposes of comparison the low concentration

damping peak, this was observed to occur at widely different surface concentrations, between 1.65 and 2.45 x 10^{-8} gm. cm.$^{-2}$. It can be seen that the example given in figure 7.5 has its peak at the low concentration end of this range. All of the three polymer samples examined produced first peaks within the range, when spread from aqueous solution. In that the molecular weight range covered by these three samples was very large, between 10^5 and 4 x 10^6, the similar region of surface activity of the polymer in each case indicates that, as established by Crisp (1946) for many other polymers, the surface activity is a function of the number of monomeric segments present rather than the number of molecules. However, the lack of reproducibility precludes the accurate establishment of an equation of state for the polymer.

(b) The Lack of Reproducibility.

It was attempted during the design and execution of the large number of experiments on this polymer series to find the cause of the wide variation observed between experiments. The possible causes of variation are:

1) the presence of adsorbed contamination on the water surface, which effectively reduces the area available to the spreading polymer, and may possibly encourage subsequent solution of the polymer molecules.

2) inefficient spreading, in which either some of the segments of a molecular chain are not properly adsorbed, and form "loops" in the bulk liquid.

3) experiments not performed at the same temperature.

4) the use of inhomogeneous or inaccurately prepared spreading solutions, the concentration of the solution actually reaching the surface being different from that expected.

5) differences in composition within the sample of solid polymer from which solutions were prepared.

1) The presence of contamination on the water substrate can never be completely eliminated. However, strenuous efforts were made to ensure that the water used was prepared under clean conditions, and before use the foaming test was employed to detect contamination. Water was discarded if the surface was found to support any bubbles for as long as one second. The "Perspex" tank used to contain the liquid during the experiment was always vigorously cleaned, and the liquid surface was protected from the atmosphere by a clean glass cover.

2) The possibility of inefficient spreading is greater with the technique used in this work than it would have been if a barrier compression technique had been used in place of the continuous addition technique. When the material is added in a succession of steps rather than a single operation, the chance of poor spreading is correspondingly increased.

In order to reduce the possibility of spreading differences the technique of spreading was standardised for all of the experiments. Each addition was made by expelling volumes of between 1×10^{-3} cc. and 4×10^{-3} cc. and slowly touching the needle tip on to the water surface.

Reasonable time was allowed between additions for the polymer to spread from the point of touching, this being judged by the effect of the addition on the visual appearance of the moiré fringe pattern. The smaller drops, representing polymer masses of approximately 10^{-6} gm. were used until the total polymer mass was greater than 10^{-5} gm., when the drop volume was progressively increased to 4×10^{-3} cc.

Spreading of surface active material depends on the reduction of free energy by the adsorption process. The force which causes molecules of active material to move from the spreading tip to the rest of the liquid surface depends on the surface tension of the surface with respect to that of the spreading liquid. In this respect, the mechanism of spreading is governed by surface elasticity. When water is used as the spreading medium, the difference in surface tension between the spreading solution and the substrate will necessarily reduce to zero as the surface concentration increases to saturation. Thus the efficiency of spreading from aqueous solution is expected to be highest in the low surface concentration region, becoming progressively poorer as the surface concentration increases.

Various concentrations of spreading solution were employed, to see if the spreading might be more predictable with certain concentrations. The available range was limited to between 1×10^{-3} and 2×10^{-3} by the more viscous nature of stronger solutions, and the possibility that more dilute solutions might have higher surface tensions, leading to a smaller spreading pressure. It was found that variations persisted at all of the spreading concentrations examined.

Further investigation of the spreading technique was carried out in experiments using carbon tetrachloride or benzene as the spreading solvent.

Neither of these solvents is recognised as a particularly effective spreading solvent, such as petroleum ether.However,both are excellent solvents for the polymer,and were therefore considered to be worthy of comparison with water as a spreading solvent.Six experiments using carbon tetrachloride solutions produced first peaks between 2.7 and 5.0 x 10^{-8}gm. cm^{-2}., all significantly higher than the water-spread results. This would indicate that spreading was poorer from this solvent than it was with water. A single experiment using benzene showed the first peak at 3.8 x 10^{-8}gm. cm^{-2}., again indicating a less efficient solvent.

The fact that all solvents tried produced widely varying results neither confirms nor denies that the variation is due to poor spreading. In that the water-spread monolayers appear without exception to be the most surface active, it could be inferred that spreading is better with this solvent. Had all the solvents produced variation in the same concentration range,then it would have been implied that the efficiency of spreading was independent of solvent,and in this case it would have been more likely that all were spreading perfectly, the variation arising from another cause.The experiments were not conclusive, but it appears that spreading difficulties may have affected the results.

3) The effect of temperature differences was reduced by maintaining a reasonably constant temperature of observation of 22 $\pm$ 1 ^{o}C.No special precautions were employed for this, as observations were made with freshly distilled water which had reached equilibrium with the laboratory temperature,and this appeared to remain quite stable during the observations.

4) If the concentration of the spreading solution as it left the spreading tip were different from that calculated, then the region of surface action would appear to be removed.The techniques used in the preparation of the spreading

solutions were all simple,and care was taken that the polymer was always completely dissolved.Evaporation of solvent was inhibited by the sealing of containing flasks during solution,and the spreading syringe was always flushed out with the solution before its final charge was introduced.

The effect of adsorption on to the solid surfaces of the containing flask and the syringe would be to reduce the amount of polymer actually expelled from the tip. The adsorbed quantity would probably increase with the time the solution was left in contact with the solid surfaces, and therefore it might be different in successive experiments.

An experiment to assess the likelihood of both of the above "inaccurate concentration" effects involved three spreading experiments executed in rapid succession, all using the same carbon tetrachloride solution. Two of the three were spread from the same syringe load, but the syringe was reloaded for the third experiment. The damping curves showed the usual two peak shape, but their positions, as before, showed considerable variation. The first two showed first peaks at 4.0 and 4.4×10^{-8} gm. cm^{-2}. and the third occurred at 2.7×10^{-8} gm. cm^{-2}.

It is concluded from the variation between these three separate runs that the variation cannot be solely due to inaccuracies in the solution preparation.

5) If the samples of polymer from which the solutions were made had been of grossly varying polymer content, then solutions of unknown concentration would have resulted, which would be expected to have different properties for successive solution preparations. The experiment described above which used three quantities of the same solution and

still found large variations would tend to show that varying sample composition was not the principal cause of the lack of reproducibility of the results.

The experiments described above failed to elucidate the cause of the lack of predictability in the measurements of ripple damping. It is felt that 4) and 5) have been reasonably discounted, at least as principal causes. 3) is expected to be small, and so 1) and 2) emerge as the most likely causes of the variation. Comparison of different solvents indicated that water was the most reliable spreading medium, but it could not be ascertained whether the polymer was being completely spread in this case.

Of the two main likely causes, spreading deficiencies can only cause errors resulting in the attribution of the surface effect to higher surface concentrations than obtain in practice. In this case, some of the added polymer, in the form of segment loops, or even whole molecules, would play no active part in the surface effect. The other possible cause of the lack of reproducibility, that of surface contamination, is likely to cause errors which make the surface effects appear at surface concentrations lower than expected, because the contamination effectively reduces the area available to the spreading polymer.

It therefore appears that the two most likely causes of variable results would tend to produce errors of surface concentration acting in opposing directions. A further feature in which the two causes differ is that the contamination effect is most likely to be noticed in the low concentration range, whereas spreading is expected to be most

efficient in this region, being most likely to cause difficulties in the high concentration region.

(c) Comparison with published work.

Recent work by Shuler and Zisman (1970), on the same polymer system using the WSR N10 sample, was described in Chapter 5. Comparison with their results would be useful at this stage. Figure 7.6 reproduces the 50 Hz wave damping curve presented by these workers, with the abscissae converted into the units gm. cm^{-2}. Since the monomer molecular weight is 44, the area available per segment in a surface concentration of d x 10^{-8} gm. cm^{-2}. is given by

$$A = \frac{44 \times 10^{16}}{A_o \times d} \quad \text{Å}^2$$

where A_o is Avogadro's number (= 6.02 x 10^{23} molecules/mole)

$$A = \frac{73.0}{d} \quad \text{Å}^2$$

The two peak behaviour is clearly confirmed, but in the present WSR 301 results (figure 7.5) the activity appears at much smaller surface concentrations than in Shuler and Zisman's work. The first peak of the Shuler and Zisman measurements occurs at a surface

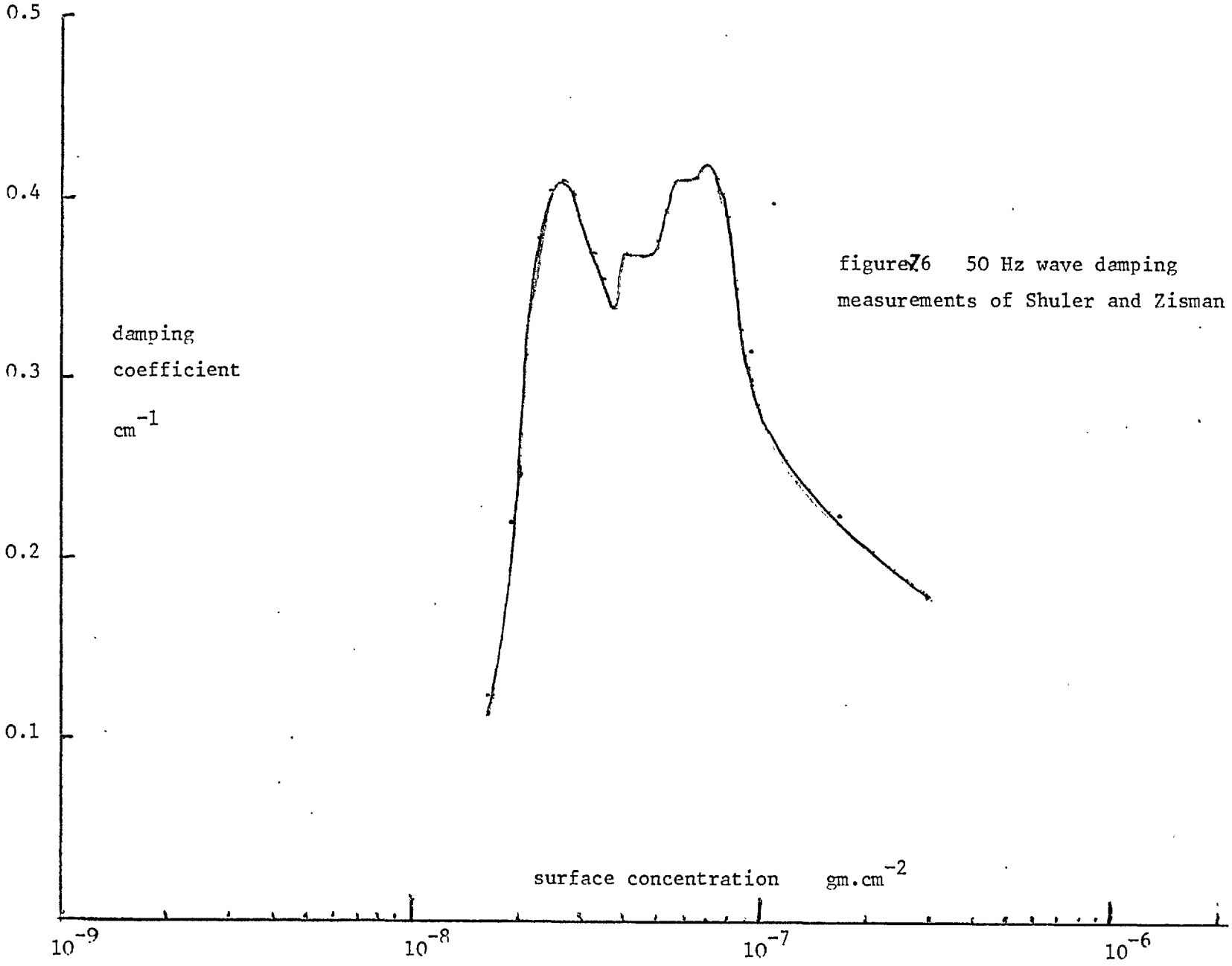


figure 76 50 Hz wave damping measurements of Shuler and Zisman (1970

concentration of 2.61×10^{-8} gm cm^{-2}, and it is worthy of note that Shuler and Zisman reported no problems with the reproducibility of their measurements, and achieved excellent agreement between experiments with four spreading solvents : water, carbon tetrachloride, benzene, and chloroform. Both continuous addition and barrier compression method of surface concentration variation were employed, both being apparently equally successful.

In comparison of the Shuler and Zisman first peak with the range of first peak positions found in the present work, it is found to occur close to the high concentration limit of the water spread results (1.65 to 2.46×10^{-8} gm. cm^{-2}.), and if it is assumed that in view of the apparent lack of experimental difficulties, the Shuler and Zisman result is more acceptable than the present work, then it would be strongly indicated that the present investigation is in error due to surface contamination, which reduces the surface area of water available for adsorption. As described above (section b), this would result in low apparent values of surface concentration.

It therefore appears that the measurements of ripple propagation characteristics of spread polymer monolayers during this work may have been in error due to the presence of impurities on the surface of the water samples used. Evidence for this view is principally that the surface concentration of polymer at which the observed surface activity was found often appeared to be considerably lower than the concentrations found in the independent work of Shuler and Zisman. That the latter

work was perfectly self-consistent, even when four different spreading solvents were used, favours its acceptance. A further point of confirmation of the presence of varying quantities of contamination is that the greatest concentrations at which the activity appeared in the present experiments using water-spread layers (first peak occurring at 2.46 x 10^{-8} gm. cm^{-2}.) is quite close to the Shuler and Zisman constant value. This nearest point of approach would represent the cleanest water sample used.

(d) Deductions from Hydrodynamic Ripple Theory.

It was shown in Chapter 3 that the propagation of ripples on monolayer-covered liquid surfaces could often be satisfactorily explained by modern hydrodynamic theory. The principal factors determining the propagation have been shown to be surface tension and surface dilational elasticity, and Lucassen and Hansen (1966) produced a formula derived by approximation of the solutions to the hydrodynamic equations which would allow these surface properties to be deduced from measurements of wavelength and damping. The properties of this formula for the 30 Hz system which forms the major part of this study are described in Appendix 2, where also is presented a FORTRAN computer program designed to execute the laborious calculations specified by the formula.

Since the hydrodynamic theory has to date been successful only in the prediction of the ripple properties of surface active materials which show a single peak in the damping curve, (Lucassen-Reynders and

Lucassen, 1969), it is of importance to determine whether two-peak curves such as found for poly(ethylene oxide) are equally capable of explanation. Garrett and Zisman (1970) rejected the theory as an explanation of the many-peak damping curves shown by certain polyorganosiloxanes, because the theory had previously been successful only with single peak curves. However, in common with Shuler and Zisman (1970) they did not give the theory an adequate trial. Moreover, the conceptual difficulties invited by the rejection of the theory, at least in the poly(ethylene oxide) system, described in Chapter 5, are considerable. It was indicated in Chapter 5 that Shuler and Zisman's results may be explained on the basis of the theory, but as wavelength information was not supplied with their damping measurements, it is not possible directly to test this view.

Because the wave damping measurements obtained in the present work appear to be similar to the Shuler and Zisman results, (bearing in mind the above-described indications that some contamination was often present during the experiments), the predictions of surface properties derived from processing the present measurements with the Lucassen and Hansen formula are expected to be also relevant to the Shuler and Zisman results.

It is described in Appendix 2 how interpretation of the "two root" nature of the equations for calculation of surface properties often requires knowledge of surface tension from an independent measurement. The more appropriate root may be found by comparison of the two surface

tension calculations with the independent measurements, the root providing the nearest surface tension correlation being selected to find the true surface elasticity.

A typical curve showing surface tension variation is given in figure 7.7. These measurements were with the WSR 205 sample, using the Wilhelmy plate apparatus described in Chapter 6 (ii). Spreading was done in the same way as for the ripple measurements, and it may be presumed that any failings in the standard of water purity indicated in the results of ripple measurement experiments are also likely to be present in these surface tension measurements. Indeed, the same sort of variation between results was found. The shape of the curves was always the same, the negative slope increasing to a maximum, and then decreasing again, apparently to zero, denoting a limiting surface pressure. As with the ripple experiments, there was no visible collapse of the monolayer even at the highest surface concentrations, although the molecular dimensions involved would suggest that some form of collapse is inevitable. It is highly probable with the highest surface concentration that solution of the molecules in the substrate would occur, especially with the water-spreading technique, where there is almost no difference between the surface tensions of spreading solution and the spread layer.

The steady surface tension decrease shown in figure 7.7 is of interest in the interpretation of the wavelength measurements shown in figure 7.5 Reference to that figure shows a minimum in the wavelength measurements in roughly the same place as the second damping peak, and the Kelvin

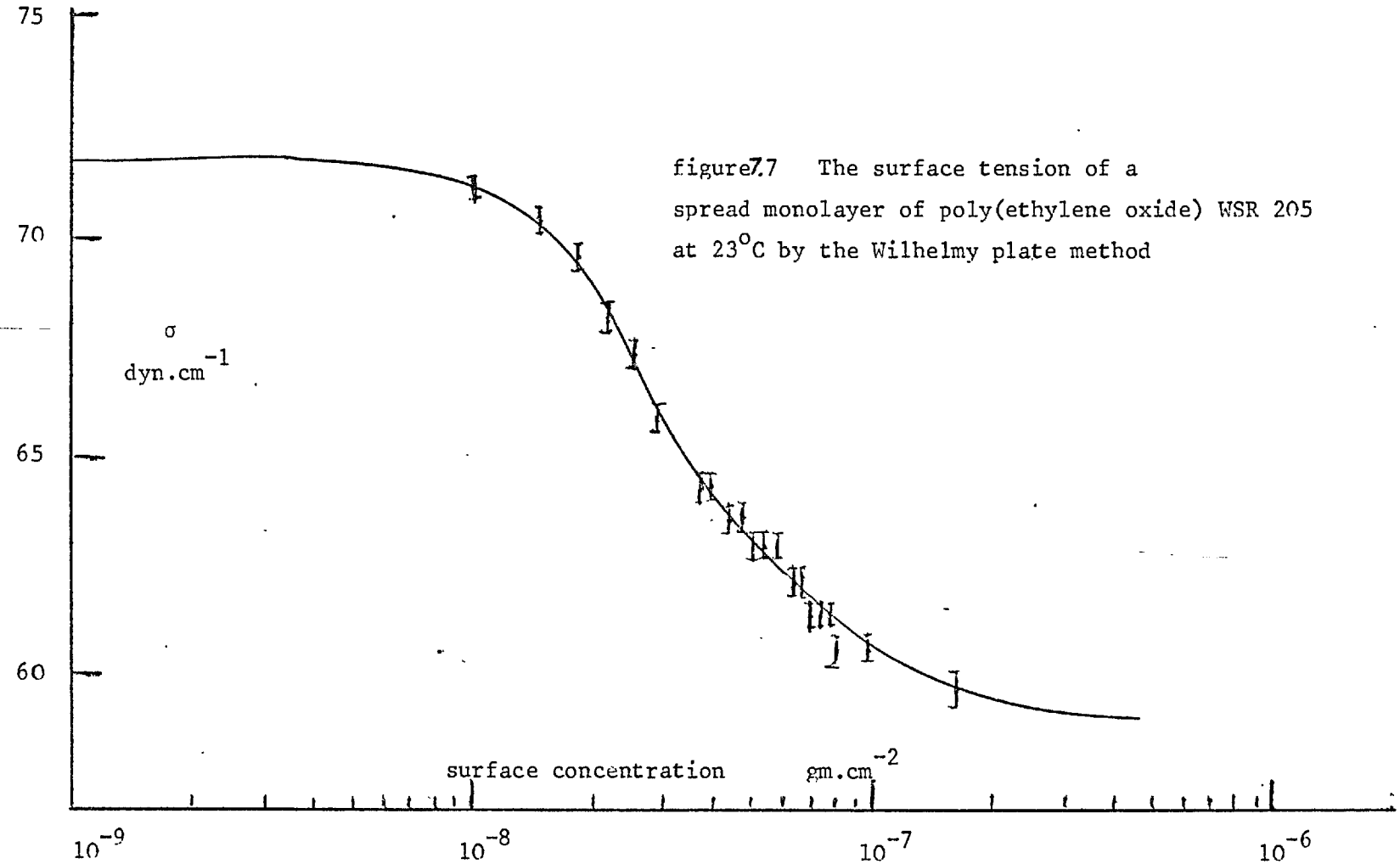


figure7.7 The surface tension of a spread monolayer of poly(ethylene oxide) WSR 205 at 23°C by the Wilhelmy plate method

equation would indicate from this that the surface tension should show a similar minimum in the same place. That the minimum does not appear in figure 7.7 shows the inadequacy of the Kelvin equation for the examination even of surface tension trends in monolayer investigations. It is a necessary requirement of hydrodynamic theory more rigorous than that of Kelvin that some explanation of the minimum should be suggested.

In order to test the Lucassen-Hansen hydrodynamic ripple theory in its interpretation of the two-peak damping behaviour found with poly(ethylene oxide), the results from WSR 301 shown in figure 7.5 were processed in the FORTRAN program (Appendix 2), with the University of London CDC 1600 computer. Each pair of ripple measurements, wavelength and damping coefficient, produces two sets of results, each set specifying a surface tension and a surface elasticity which together would produce the observed ripple propagation characteristics. The particular pair of results applicable in any case is shown to be dependent on the relative values of the wave speeds of the two modes of liquid surface wave propagation, transverse and longitudinal. At very low elasticities, the transverse waves have the higher phase velocity, and the negative square root value is appropriate (Appendix 2). At elasticities higher than a certain value, which is dependent on surface tension, the positive root is the relevant one. Transition between the two regions occurs at a critical point, at which the damping becomes exceedingly high, and is usually denoted by a peak in the variation of damping with surface concentration. The results shown in

figure 7.5 show two distinct peaks, and the actual values of damping at the peaks agree roughly with the interpretation that they are both critical points for the propagation of ripples (Appendix 2).

Figure 7.8 shows the surface tension results of the program, both roots being given. It can be seen that the shape of both curves is distinctly similar to the wavelength curve shown in figure 7.5. Application of the selection criteria outlined above proposes that the "negative root" curve is significant up to the first peak (point X on the graph) where the "positive root" curve assumes physical reality. The significance reverts to the "negative root" curve after the second peak (point Y on the graph). The result of this interpretation is shown in figure 7.9, in which only the "significant" points are presented. Bearing in mind the experimental inadequacies indicated by section (iii) c, regarding the cleanliness of the water used, this variation is in agreement with the independent surface tension determination shown in figure 7.7. The observed minimum in the wavelength variation has therefore been accounted for by the hydrodynamic theory, and appears to be an effect of the surface elasticity.

Using the same root selection criteria as for figure 7.9, the corresponding calculated values of ε_d are presented in figure 7.10. The two critical points are indicated as X, Y, as in figure 7.9 and it is seen that they occur in positions on the curve which appear to have little significance regarding the dilational elasticity of the monolayer.

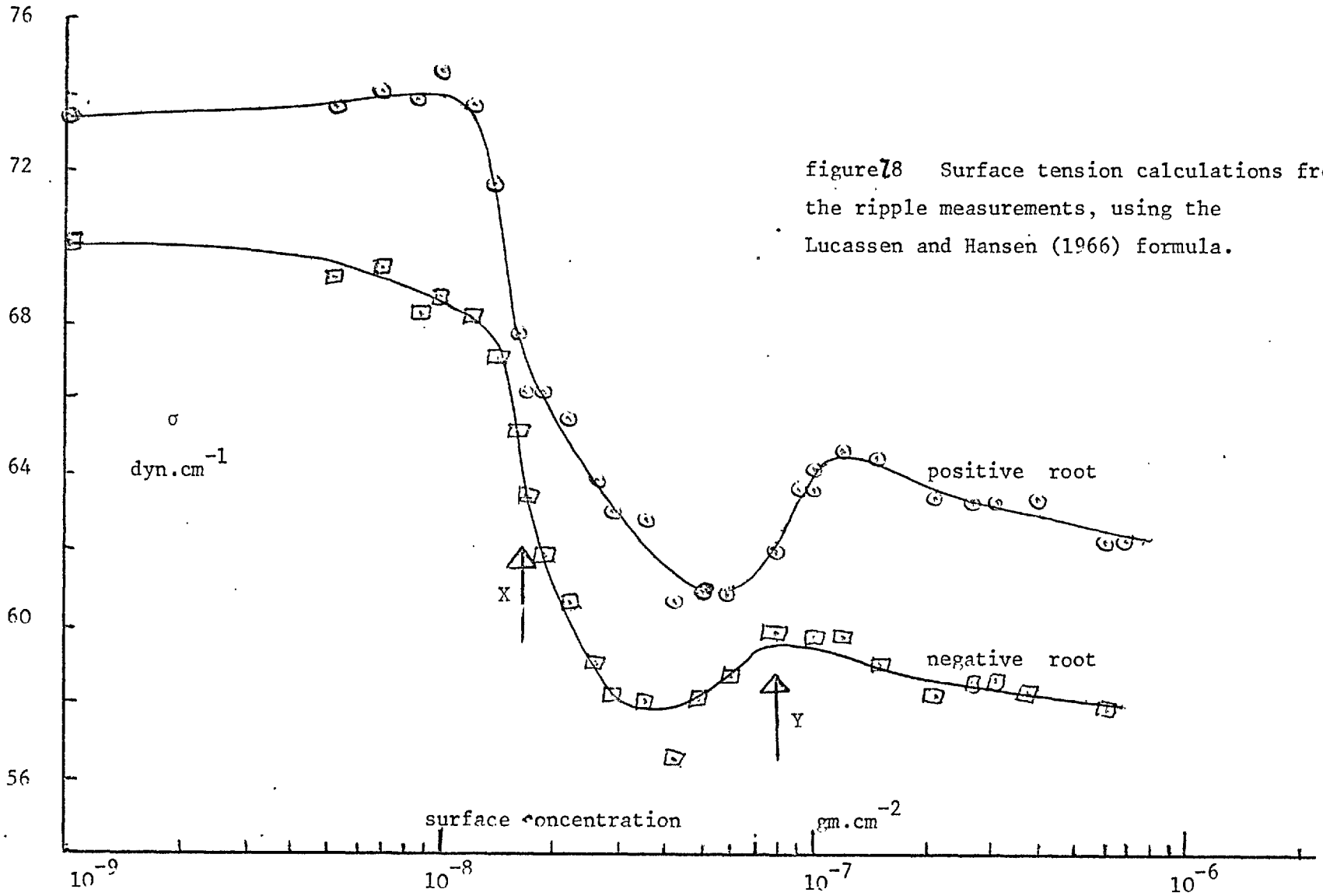


figure 8 Surface tension calculations fro the ripple measurements, using the Lucassen and Hansen (1966) formula.

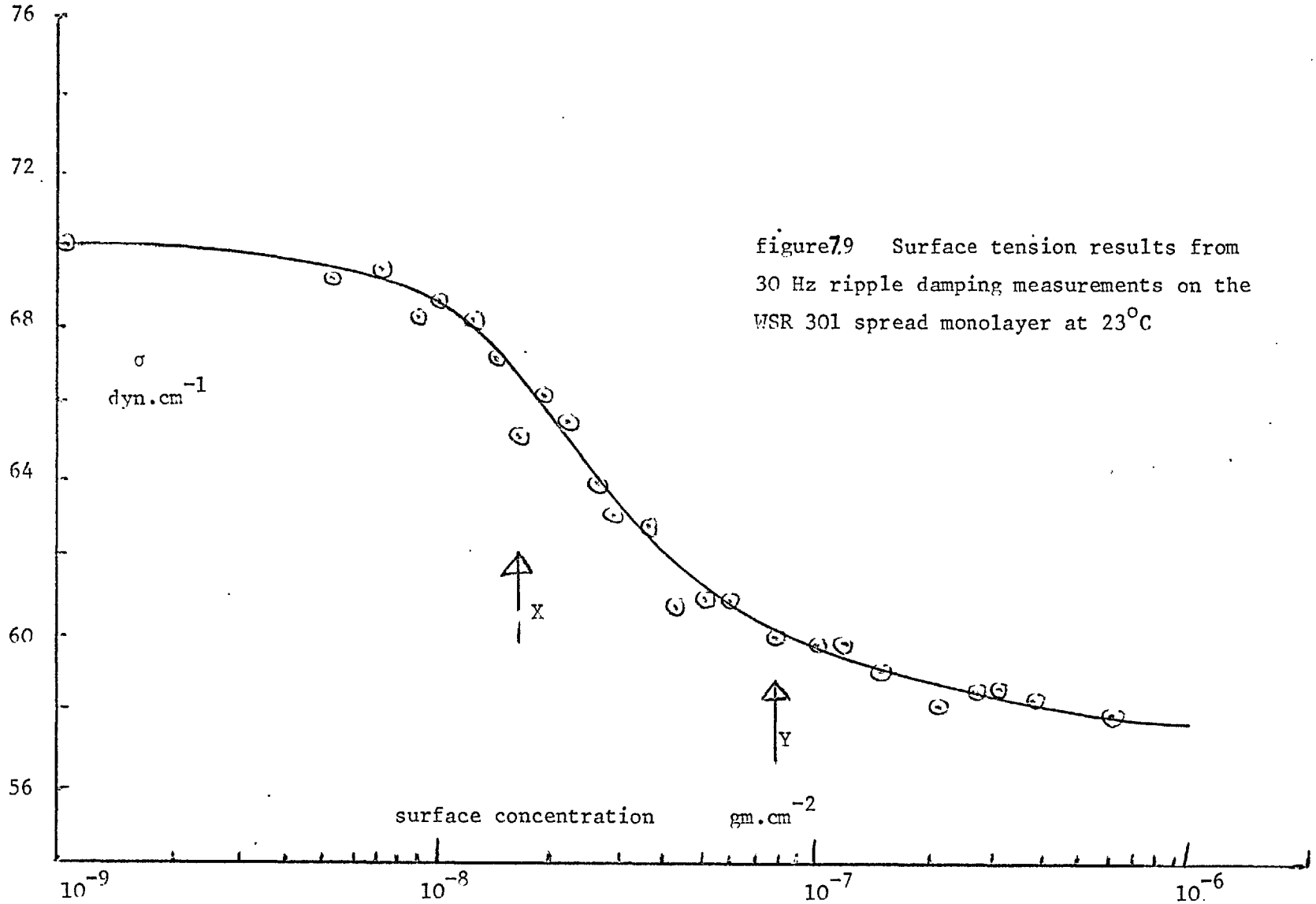
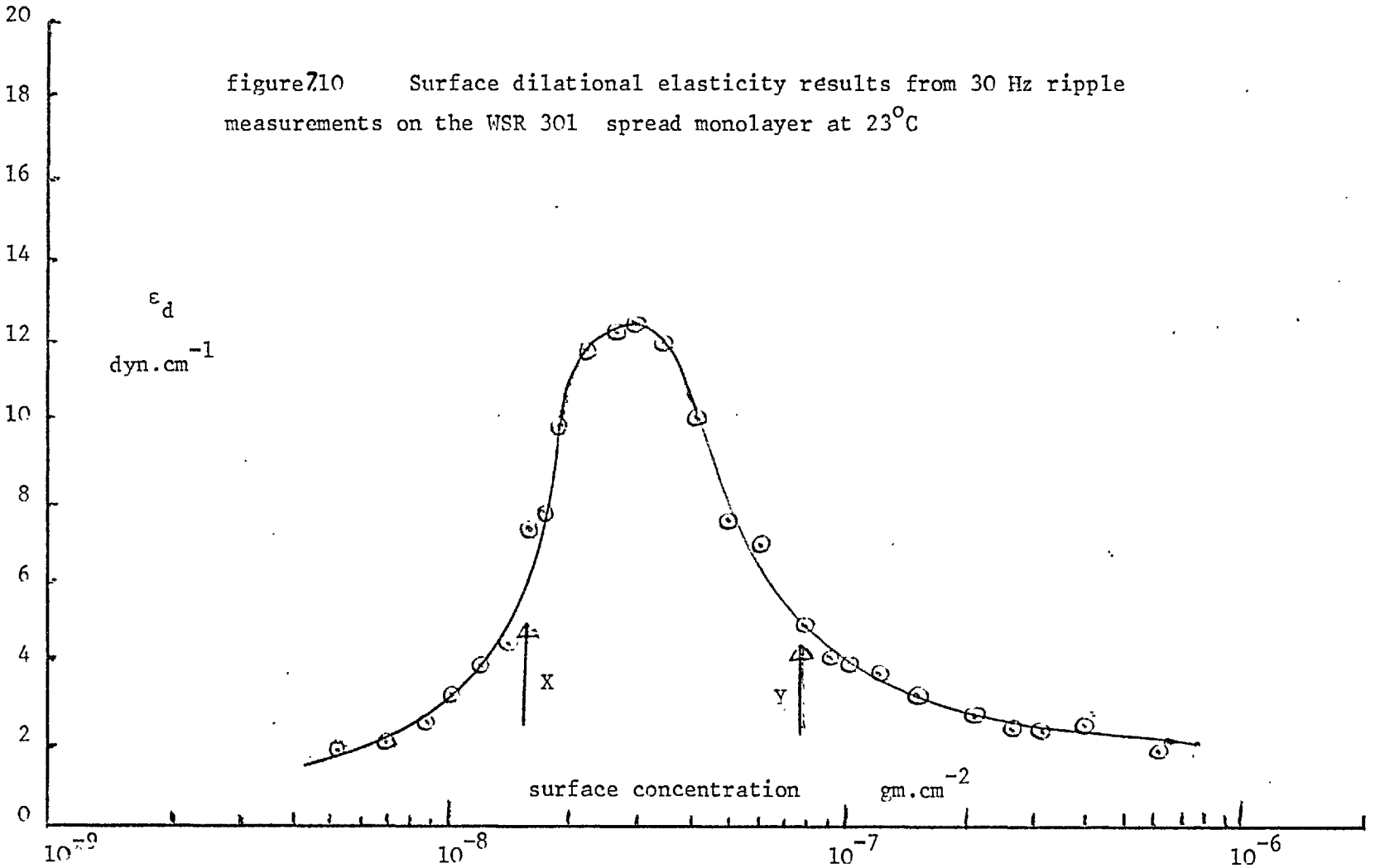


figure7.9 Surface tension results from 30 Hz ripple damping measurements on the WSR 301 spread monolayer at 23°C

figure 10 Surface dilational elasticity results from 30 Hz ripple measurements on the WSR 301 spread monolayer at 23°C



The peak of the elasticity curve is seen to occur in the position of the damping minimum between the two peaks, as was noted by Shuler and Zisman in their statically determined elasticity curve (figure 7.11). The lack of reproducibility of the results described in section (iii) b makes it impossible to check these elasticity calculations quantitatively with static measurements, but it does appear most probable that the ripple theory has accounted satisfactorily for the two peak damping behaviour of the polymer.

The fundamental prediction of hydrodynamic theory is that in a system where the dilational elasticity increases continuously with increase in surface concentration, only a single peak should be observed. If however, as in the case of poly(ethylene oxide), the equation of state is such that the elasticity rises to a peak value and then decreases again to very low values, two peaks may be observed both occurring at surface concentrations for which critical values obtain.

(iv) Solution Properties.

(a) Results. Glass (1968b) had deduced from his drop weight measurements on a range of poly(ethylene oxide) solutions that equilibrium times could be in excess of 12 hours, although none of his measurements was at a surface lifetime greater than 60 seconds. Initially, therefore, it was decided to examine the equilibrium attainment of certain solution concentrations, in order to decide how great an equilibrium time should be allowed for the majority of the observations.

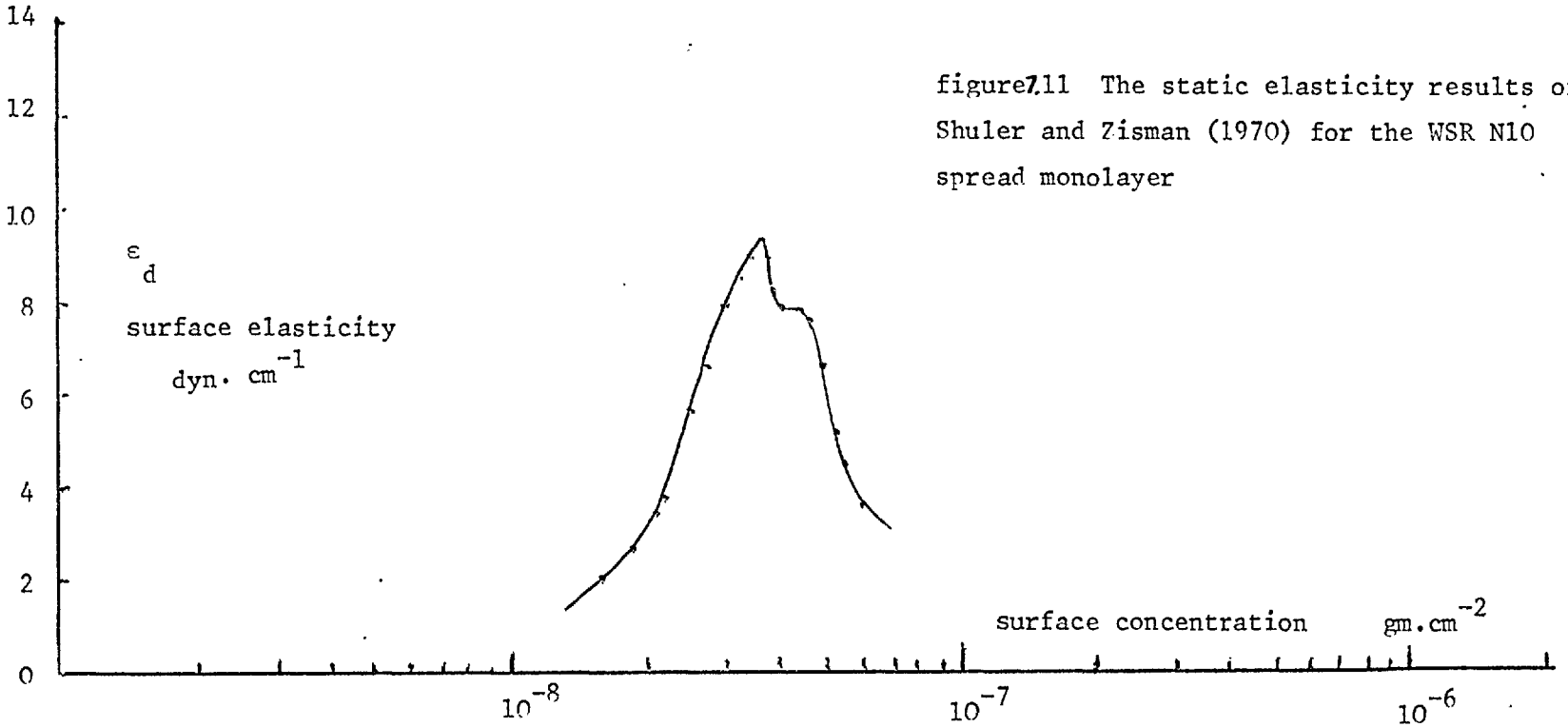


figure7.11 The static elasticity results of Shuler and Zisman (1970) for the WSR N10 spread monolayer

Solutions were prepared in the manner described in Chapter 6(i)c and the surface excess was reduced to zero by the "skimming technique" there described. The ripple frequency was set at 30 Hz, as for the majority of the spread monolayer experiments, and the ripples were observed continuously from the end of the skimming process, the surface lifetime being measured with a stop-watch. The first solution to be examined had a bulk concentration of 3.86×10^{-7} gm. cm^{-3}., the polymer being the lowest molecular weight fraction, WSR N10 (M.W. about 1×10^5). Moiré fringe pictures were begun as soon as the ripple damping appeared to change significantly, and observations were continued for a period of nearly 24 hours. The variation of damping coefficient with surface lifetime is shown in figure 7.12, and the shape of the curve is seen to be remarkably similar to the two peak damping curve shown in figure 7.5. It was seen in the preceding section that hydrodynamic theory interpreted the peaks in the spread monolayer curve as being simple coincidence of surface tension and surface elasticity. In a solution adsorbed monolayer slightly different conditions are present, and in Chapter 3 it was described how the elastic properties of the surface could be modified by "short-circuiting" of the surface tension

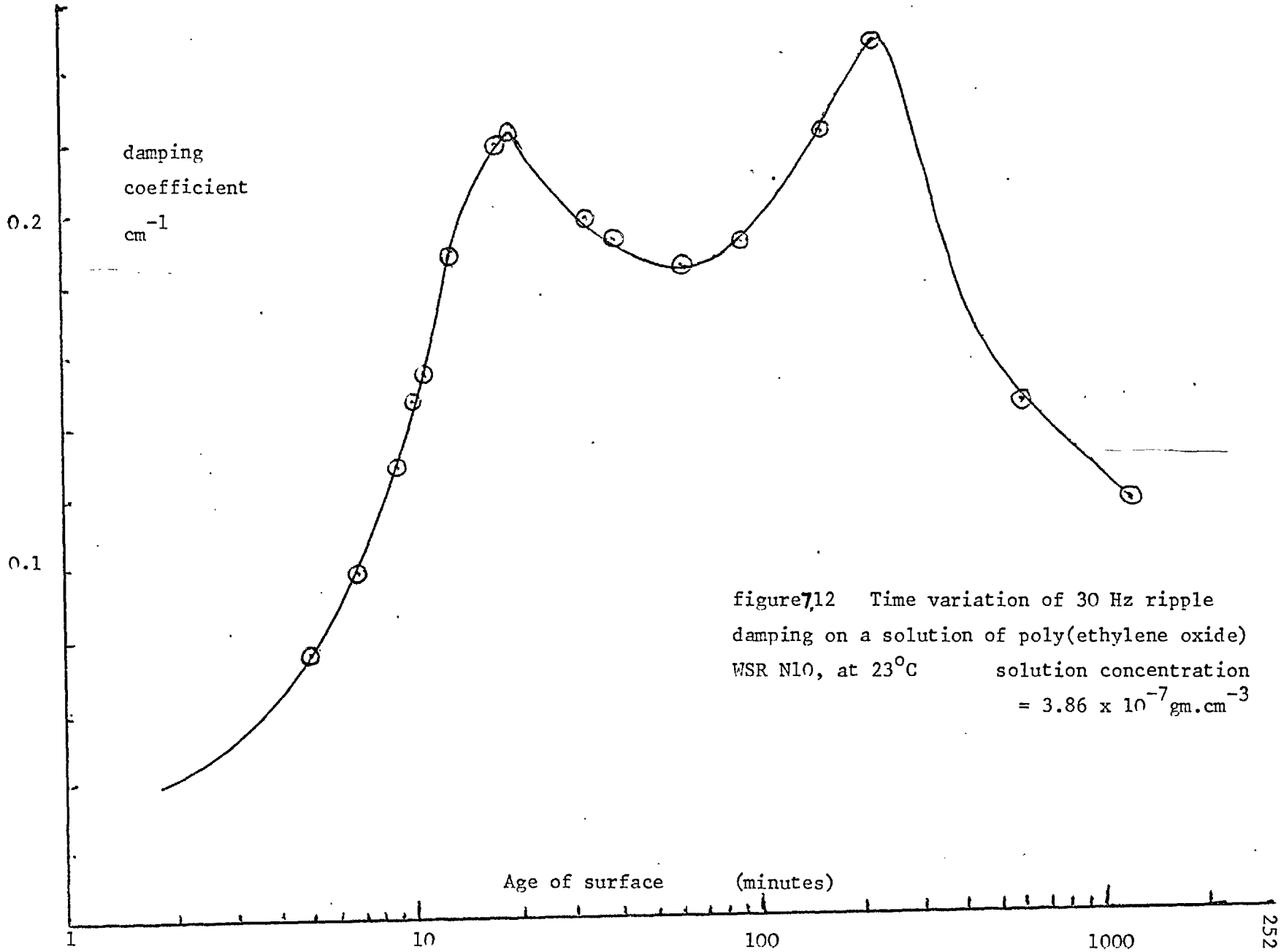


figure 7.12 Time variation of 30 Hz ripple damping on a solution of poly(ethylene oxide) WSR N10, at 23°C solution concentration = 3.86×10^{-7} gm.cm^{-3}

differences produced by the compression and dilation of the surface by the wave. It was seen that this effect could affect the wave damping in two ways:

1) in the reduction of the damping at a peak,

2) in the reduction of the generally high damping in the high solution concentration region.

The latter effect is not expected in the present system, since it was shown in the preceding section that the elasticity of the spread monolayer tended to low values at saturation surface concentration. "Short-circuiting" would produce only a negligibly small reduction in damping in this region. The former effect, of reduction in the peak damping, was not observed, as it may be seen clearly by comparison of figures 7.5 and 7.12 that the solution peaks are closely similar to the spread monolayer peaks. It therefore appears that diffusional interchange between surface layer and the bulk solution has no observable effect at the wave frequency and solution concentration used.

(b) Equilibrium. A second important point about the results shown in figure 7.12 is that the properties were still changing significantly after 12 hours, and possibly even after 24 hours. Consideration of the true meaning of this observation is complicated by the combination of two unknown factors: 1) the variation of surface excess Γ with time t, and 2) the variation of the surface properties with Γ. It may not immediately be assumed either that the equation of state is identical

for both spread and solution adsorbed material, or that the equilibrium mechanism assumed by Glass (1968b) is valid. Although Shuler and Zisman (1970) showed that spread polymer was adsorbed at each monomer segment, in a horizontal orientation, the majority of previous work on the properties of ethylene oxide polymer solutions led to conclusions that a different, less complete adsorption mechanism took place from solution.

In this particular instance, the principal features of the damping curve for a spread monolayer were interpreted by Shuler and Zisman as confirming the horizontal segment attitude, and the most important part of this interpretation, apart from that of the relatively unimportant peaks in the damping variation, has been supported by hydrodynamic theory. The shape of the solution time-variation curve is so similar to that of the spread monolayer curve, that in the absence of any strange variation of Γ with t, it seems very likely that the horizontal adsorption type of explanation is also valid in the solution case.

Let us therefore investigate the consequences of making the assumption that the orientation of the poly(ethylene oxide) segments adsorbed from solution at the air/water surface is identical to their orientation in the spread layer. It is not necessary at present to assume that whole molecules are simultaneously adsorbed in this way, since as long as non-adsorbed sections of chain have no effect on the surface tension, the surface properties should be independent of the

adsorbed state of whole molecules. In this case, therefore, for purposes of comparison with the spread layer, the surface excess Γ would be of actually adsorbed segments.

The first consequence of identical segment orientation is that the equations of state of the two types of adsorption should be identical, Γ being almost equal to the absolute value of surface concentration for the low solution concentrations which were observed in this experiment. It is therefore valid to imply a value of Γ for each point on the (β,t) curve (figure 7.12) corresponding to the same value of β in the spread monolayer damping curve. For this curve comparison procedure was taken one of the experimentally determined sets of WSR N10 monolayer results which agrees most closely with the Shuler and Zisman results (figure 7.13). The points of figure 7.12 were matched against corresponding points on the figure 7.13 curve, and the resulting values of time, t, and surface concentration, Γ, are given in figure 7.14. The relation between the two quantities appears to be acceptably linear, and the slope of the line $(\Gamma/t) = 0.51$, which suggests the relation

$$\Gamma = K_1 \cdot t^{\frac{1}{2}} + K_2 \qquad 7.1$$

where K_1 and K_2 are constants. Also marked on the graph is the value of Γ which represents liquid/air surface adsorption of the whole mass of the polymer present in the solution, i.e., this is the surface concentration which would have been produced if all of the available polymer had been spread on the surface: 1.31×10^{-6} gm.cm^{-2}.

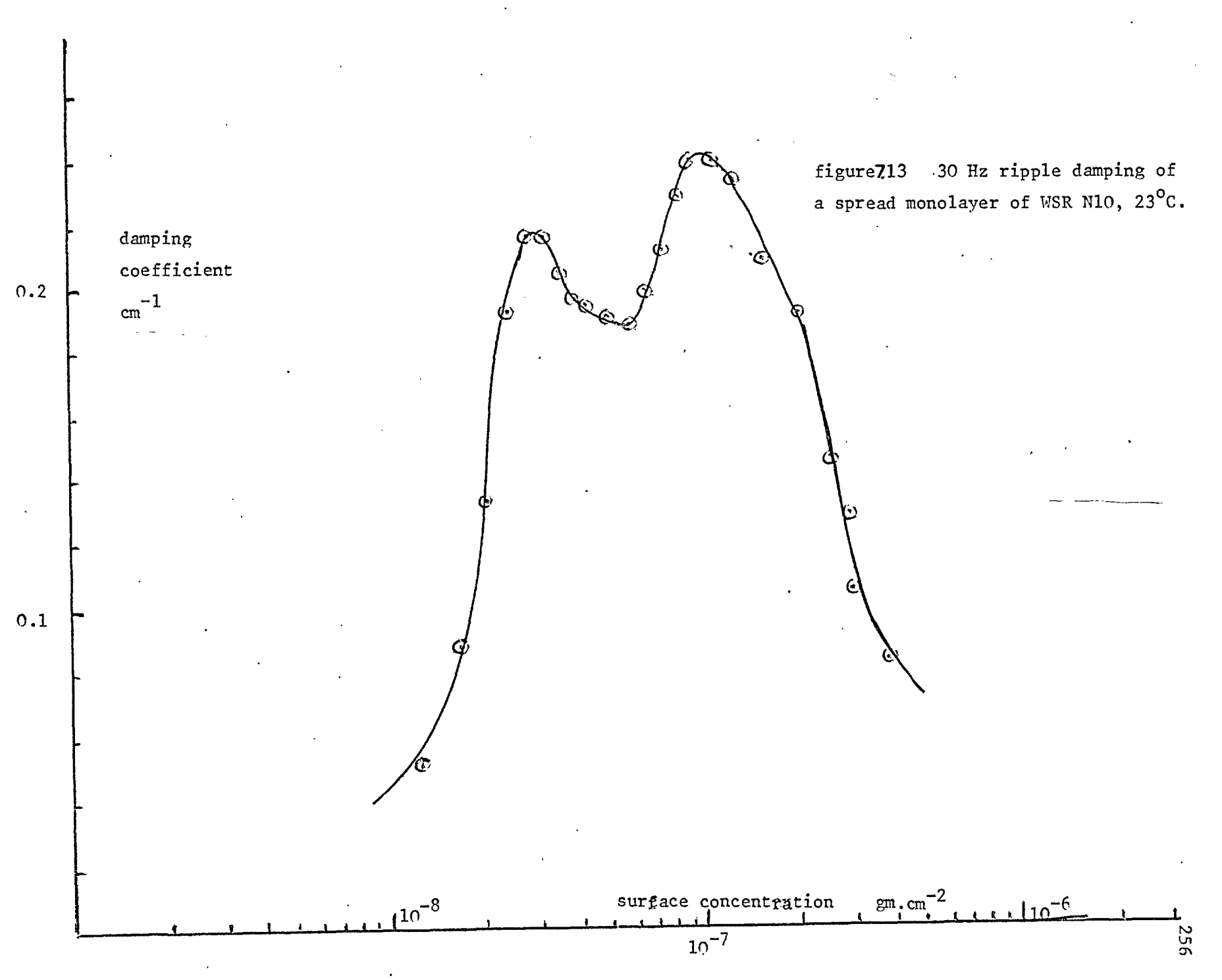


figure 13 30 Hz ripple damping of a spread monolayer of WSR N10, 23°C.

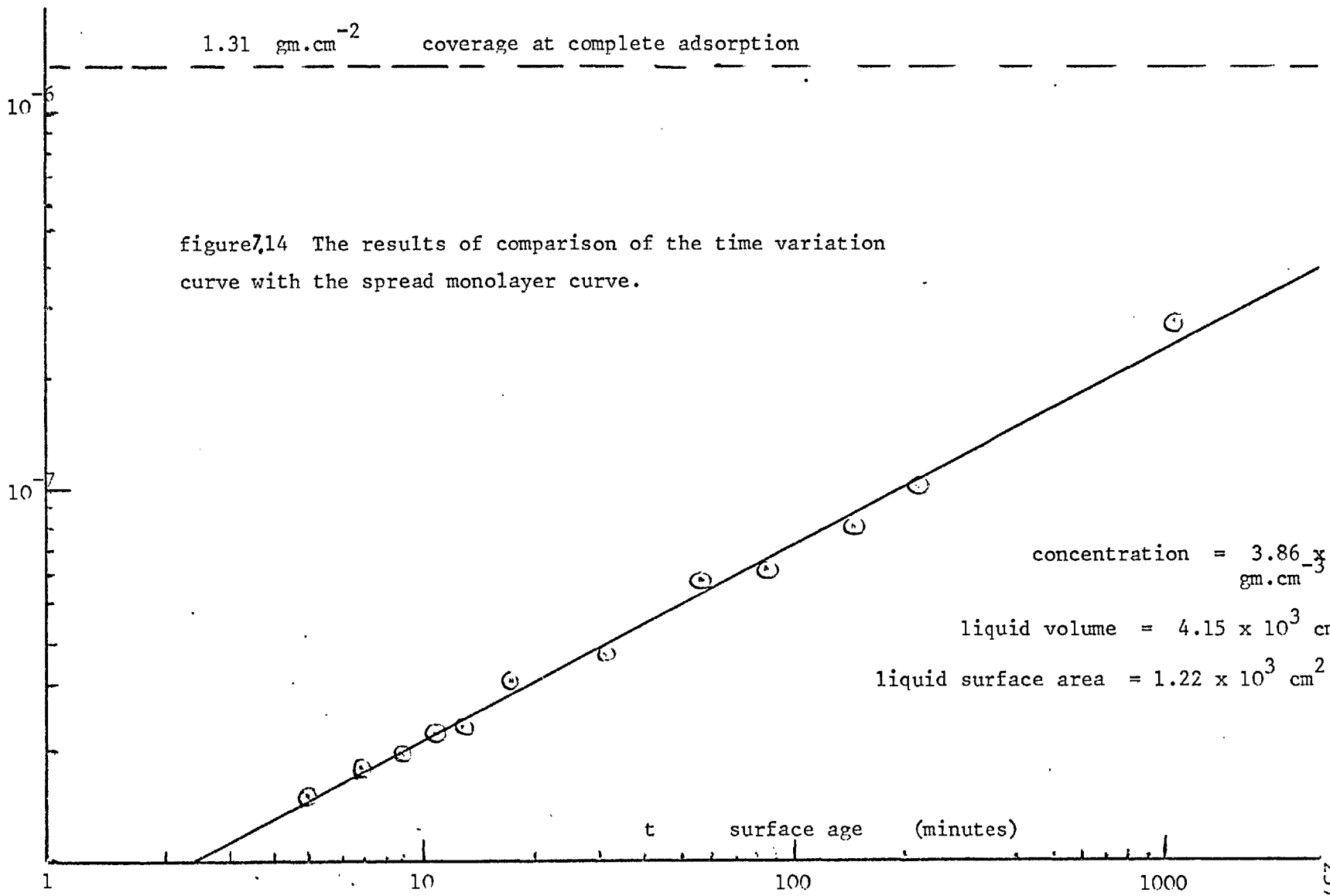


figure7.14 The results of comparison of the time variation curve with the spread monolayer curve.

Apart from the important observed dependence of the adsorption on the square root of the surface age, which will be considered later, this graph also indicates that after 24 hours of observation, the rate of adsorption is not slackening. At this point, the surface excess, or surface concentration, is shown to be approximately 2.6×10^{-7} gm. cm^{-2}., which represents 20% of the total mass of polymer initially present in the solution. This result is much greater than the surface excesses usually found with solutions of surface active agents, and it suggests a very high degree of surface activity. It appears that saturation adsorption is being approached with a solution of concentration 3.86×10^{-7} gm. cm^{-3}., which is about 4×10^{-9} mole/litre.

This is an extremely surprising result, and such behaviour has not been reported with any other polymer solutions. The possibility arises that the adsorption process being observed is irreversible.

(c) Irreversibility. Irreversibility would occur if on adsorption the segments so changed their physical or chemical state that they were incapable of returning dissolved to the bulk solution. Such a state would not necessarily be specified by the fact that this polymer will form stable spread monolayers. Although experiments showed that the surface properties of a spread layer of poly(ethylene oxide) would remain constant up to a surface age of 24 hours, it is possible that the system is not in true thermodynamic equilibrium, and that the only reason why the layer exhibits such stability is that the simultaneous desorption of all the segments of a polymer chain, necessary for passage

of the molecule into solution, is a very unlikely event. Measurements on the systems of polyvinyl alcohol and polymethacrylic acid (Chapter 5) have shown that an entirely different stable state of adsorption is attained when these polymers are adsorbed from solution, and this state is much more likely to be a true equilibrium state. In the case of these polymers, therefore, the adsorption process cannot be irreversible, although a metastable state can be induced by spreading.

The evidence presented above suggests that the solution equilibrium state of poly(ethylene oxide) is of a different character from that of the other two polymers. A much greater surface excess is produced, which seems to tend towards complete adsorption of the whole of the dissolved polymer. The solution equilibrium appears to be identical to the spread state, and it must be concluded that on reaching the surface, the polymer segments become adsorbed in a way that precludes their subsequent detachment, the usual form of dynamic equilibrium being rendered impossible.

If the process of adsorption from solution were to produce the same type of monolayer as is produced when polymer is deliberately spread on the water surface, then equilibrium of a solution of almost any concentration would be achieved only when the mass of polymer adsorbed was sufficient to saturate the surface. The equilibrium surface tension of all solutions would be identical, although the time taken for equilibration would increase steadily as the initial solution concentration was reduced, the time becoming infinite when the bulk

solution contained only enough molecules to saturate the available surface. Solutions of lower concentration than this would also reach equilibrium at infinite time, the eventual surface properties being the same as if all the polymer had been spread directly on to the surface.

The observed surface behaviour would certainly be explained by such a picture of irreversibility, but definite conclusive proof would require observation of solutions of much lower concentration than the one reported here, in order to see if the progress to equilibrium is as predicted. It is however not possible to perform an ideal experiment of this type in exactly the same way as the experiment described above, because it is not considered advisable to trust the continuity of water purity for periods greater than 24 hours. However, a series of experiments was made in which more dilute solutions were observed over a period of 24 hours, and the final values of wave damping achieved are shown in figure7.15. A certain amount of variation is to be expected in the results, since the "skimming" method of surface preparation may not always be perfect, and small quantities of spread polymer remaining at the beginning of the experiment will have a large effect on the final surface properties. Nevertheless, the points shown do suggest the usual two-peak curve, although insufficient measurements were made in the low concentration region.

Figure7.15 indicates that the surface excess after 24 hours is approximately proportional to the solution concentration, which is further evidence in favour of the irreversible behaviour explanation.

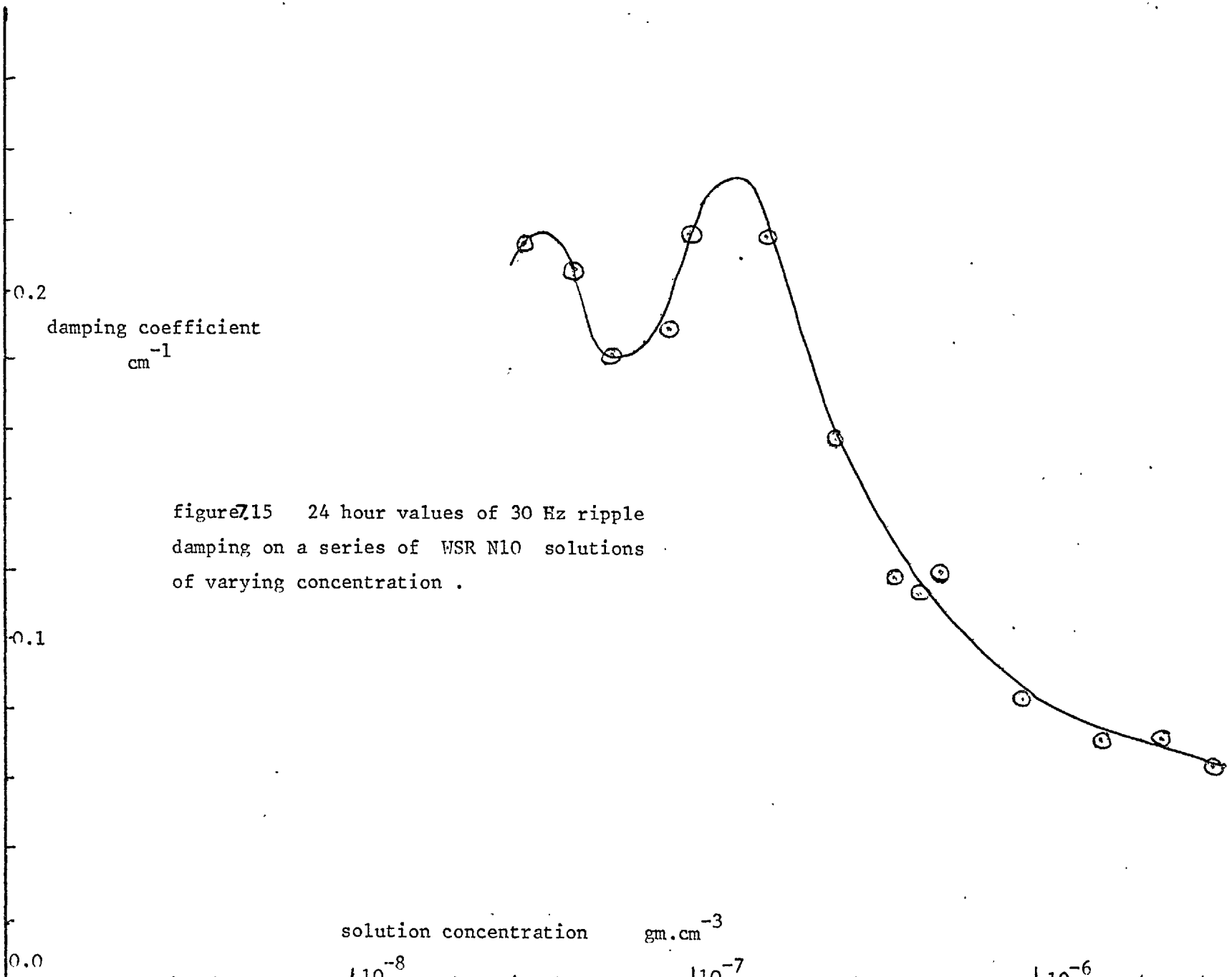


figure 7.15 24 hour values of 30 Hz ripple damping on a series of WSR N10 solutions of varying concentration .

These findings might explain the strange time variation observed by Glass (1968b) with his drop weight surface tension measurements technique. He found that the increments in surface pressure between drops of three different lifetimes (10, 30, and 60 seconds) suggested equilibrium surface pressures much greater than those actually observed, this effect being most important at low concentrations. It is possible that this effect is connected with the constant rate of adsorption which was here observed to obtain until the surface was saturated, the saturation surface excess being independent of the solution concentration. At the lower bulk concentrations, saturation would be further out of reach during all three drop lifetimes, and extrapolation would lead to excessive values. It is difficult to assess more exactly the effect of irreversibility on Glass' results owing to the complexity of the adsorption model employed in the extrapolation procedure. The hazards involved in predicting the equilibrium behaviour of an unknown material are amply illustrated by comparison of the present work with that of Glass, and the difficulties invited by the use of a non-equilibrium technique are emphasized.

If the adsorption mechanism is irreversible, then since polymer molecules diffuse in a random manner throughout the bulk of the solution, as they reach the surface, they become quickly adsorbed, and are then effectively removed from the solution, not being able to desorb and diffuse back into the bulk. Ward and Tordai (1946) analysed the diffusion kinetics of this type of system which is closely analogous

to the diffusion of heat from a body into a cooler heat sink. The net flow of molecules which are randomly diffusing through a homogeneous liquid is described by Fick's law:-

$$\frac{\partial n}{\partial t} = D \frac{\partial^2 n}{\partial x^2} \qquad 7.2$$

D is the diffusion coefficient, defined by this equation, and n is the concentration of solute at a distance x from a surface at time t. If the diffusion across a surface is specified as being restricted to one direction, as in irreversible adsorption, then the mass M of solute which diffuses through unit surface in time t is given as

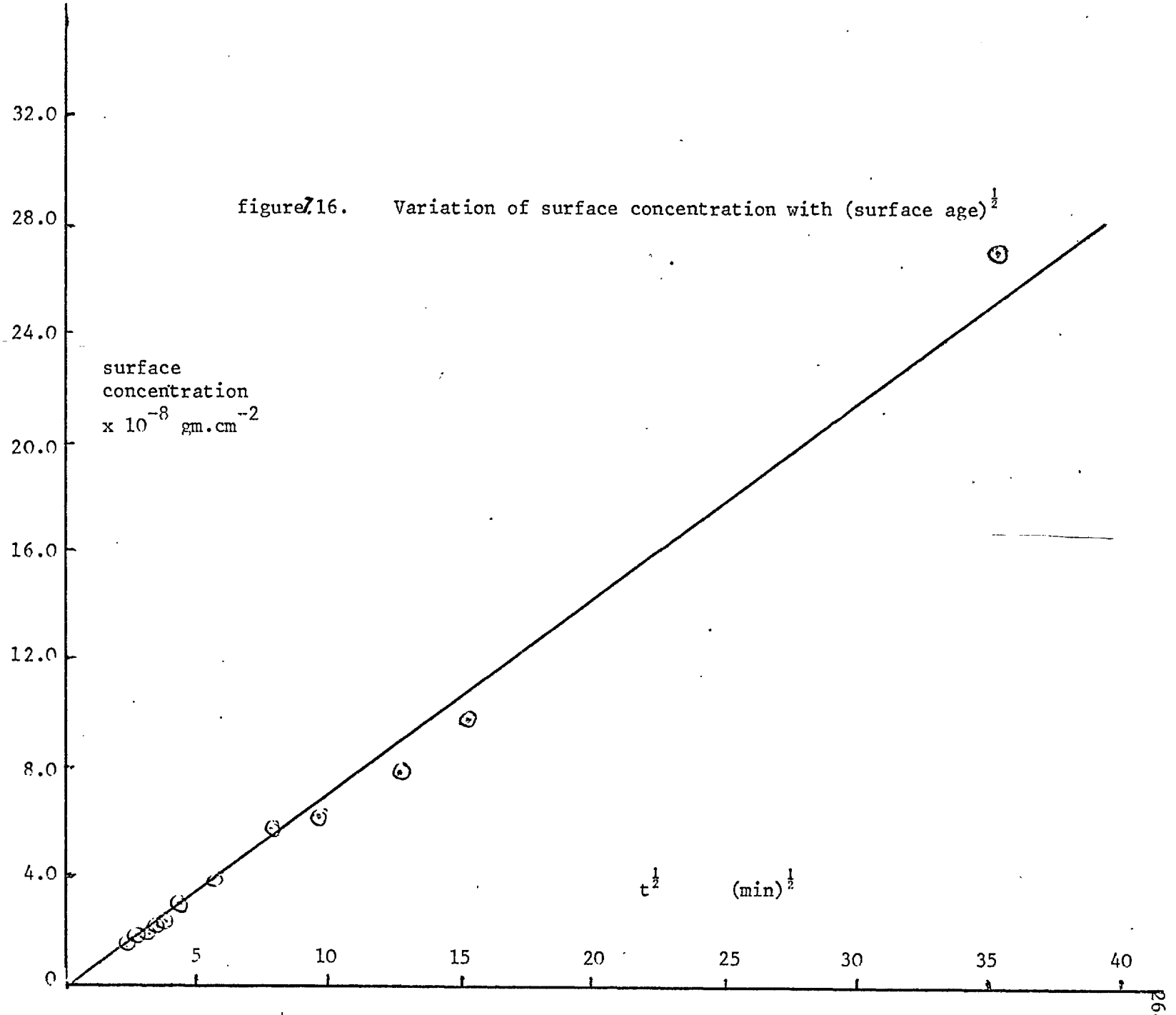
$$M = 2 n_o (D t/ \pi)^{\frac{1}{2}} \qquad 7.3$$

where n_o is the initial concentration of the homogeneous solution. This equation should be valid in cases where the total adsorbed mass is much less than the total dissolved mass, so that the solution concentration stays reasonably constant throughout the diffusion process. As mass is removed by adsorption, n_o effectively decreases and the rate of adsorption should correspondingly decrease.

The data of figure7.14 are replotted in figure7.16 as Γ against $t^{\frac{1}{2}}$, and from 7.3,

$$\Gamma = 2 n_o (D t/ \pi)^{\frac{1}{2}} \qquad 7.4$$

figure 16. Variation of surface concentration with (surface age)$^{\frac{1}{2}}$



the slope of the graph ($\Gamma/t^{\frac{1}{2}}$) being given by

$$(\Gamma/t^{\frac{1}{2}}) = 2\, n_o (D/\pi)^{\frac{1}{2}} \qquad 7.5$$

The diffusion coefficient D is given by

$$D = \frac{\pi\, (\Gamma/t^{\frac{1}{2}})^2}{4\, n_o^2} \qquad 7.6$$

From the graph,

$$(\Gamma / t^{\frac{1}{2}}) = \frac{1.44 \times 10^{-8}}{(2.4 \times 10^{4})^{\frac{1}{2}}} \quad gm.cm^{-2}sec^{-\frac{1}{2}}$$

and $n_o = 3.86 \times 10^{-7} gm.\ cm^{-3}$.

$$D = \frac{\pi \times 2.08 \times 10^{-14}}{4 \times 3.86^2 \times 10^{-14}}$$

$$\underline{D = 4.6 \times 10^{-6}\ cm^2 sec^{-1}}.$$

This value seems to be quite acceptable from comparison with the values of D for a wide range of organic alcohol/molecules quoted by Ward and Tordai, these values lying between 10^{-7} and 10^{-5}. Although in Chapter 1 it was stated that in shear flow conditions, polymer molecules are expected to become elongated by shear gradients, the fluid velocities associated with molecular diffusion are so small that the molecules are probably still tightly coiled.

It therefore appears that the time variation of the surface properties of the poly(ethylene oxide) solutions examined in this work can be explained satisfactorily simply be assuming that polymer molecules diffuse to the surface before adsorption. This supports the irreversibility hypothesis, since appreciable desorption of the polymer molecules would have resulted in the rate of increase of surface excess gradually reducing to zero as equilibrium is approached. Figure 7.16 would then have shown a curve of decreasing slope, tending to a constant value of Γ .

(v) Comparison with Poly(ethylene glycol).

In order to compare the above described results with the properties of the other series of ethylene oxide polymer, derived from ethylene glycol, some measurements were made on a sample of this polymer representing the "Carbowax" series (Union Carbide, 1965). So that the best comparison may be made with the poly(ethylene oxide) sample of molecular weight 1×10^5, the highest available molecular weight sample of the "Carbowax" series was chosen, designated Compound 20M, with average molecular weight in the range 1.5×10^4 to 2.0×10^4. The solid polymer is hard, white and waxy in appearance, very different from the white granular powders of the "Polyox" series.

(a) Spreading. Water solution spreading was investigated, which had proved so successful with the oxide polymers, and precisely the same procedure was followed in this case. 0.25% solution was spread gently from a glass syringe tip, while the effect of the addition on the wave damping was observed continuously. After each addition of polymer at low surface concentrations, the damping showed an immediate increase similar to that observed with poly(ethylene oxide) samples. The damping in this case subsequently decreased slightly, which indicated that the monolayer was not stable, perhaps dissolving in the bulk liquid. Regular additions of polymer were continued in spite of this, and although quantitative measurements are obviously not possible because of the uncertainty about layer stability, it was observed that the damping exhibited two distinct peaks in the same way as the oxide polymer samples.

The observed reluctance of the glycol polymer to produce monolayers with the stability found with oxide polymer spread layers must be due to some difference in the structure of the polymers, which are ostensibly composed of the same repeat unit, ethylene oxide. The two expected differences between the two polymers are that the glycol polymer examined was of much lower molecular weight than any of the oxide polymer series, and also that the glycol chains are terminated by hydroxyl groups, which are expected to be absent from the poly(ethylene oxide) chains. It seems unlikely that either of these differences should be the cause of such radically different surface active properties. All of the polymers examined had average molecular weights in excess of 10^4, and the presence

or absence of hydroxyl groups as terminations is not expected to be important. Similarly, although the discrepancy in molecular weight between the two samples observed (a factor of 7) is large, it would not be expected that the pattern of adsorption should change so markedly after a molecular weight of 10^4.

(b) Solutions. The difference between the polymer series persists in comparison of their solution adsorption properties. As found in all previous published work on the glycol series (Lovell and Hibbert,1940; Couper and Eley, 1948) the 20M polymer was observed to reach a real equilibrium surface state in less than 1 hour, none of the irreversible effects of poly(ethylene oxide) being noticed.

The two ethylene oxide polymer series appear to be significantly different in their adsorption behaviour, although there is no obvious reason why this should be so.

(vi) Discussion.

The properties of adsorbed poly(ethylene oxide) have been examined at the water/air surface, in both of its adsorbed states: spread and solution adsorbed. Observations of the behaviour of the spread polymer were in general agreement with the recent work of Shuler and Zisman (1970), although a certain lack of reproducibility in the measurements suggests the presence of contamination by foreign material of the water surfaces used. The possibility of imperfect spreading may also be indicated. The measurements of ripple damping and wavelength were shown to be in

support of the hydrodynamic ripple theory of Lucassen and Hansen(1966), although the variation of ripple damping with surface concentration exhibited a distinctive two peak appearance which may have at first appeared to fall outside the predictions of the theory.

The distinctive two peak damping variation occurred again in the time variation of the dissolved polymer, as observed using the facility of the moiré fringe observation system which allows a series of pictures to be made without intermediate adjustment of the apparatus. It has been suggested that the similarity of the damping variation implies that the surface orientation of the polymer segments when adsorbed from solution is "horizontal", in the same way as concluded by Shuler and Zisman for spread polymers, rather than the randomly attached coil configuration usually indicated by measurements on solution adsorbed samples of the glycol polymer series.

The observed variation of surface properties with time suggests that the mechanism of time variation is the slow steady diffusion of molecules to the surface from the bulk. The usual form of dynamic equilibrium was not observed, and it appeared that the polymer was being adsorbed in an irreversible state, a very large proportion of the available solute becoming eventually attached to the surface. This irreversible state of solution adsorption appears to be identical to the spread monolayer polymer state, in which the majority of the polymer segments are adsorbed horizontally at the surface.

The identity of the two adsorbed states of a soluble polymer has never been reported for any other material. Assuming that the stability of a spread polymer monolayer is due to the reduction in free energy of the system following the adsorption of a large number of inter-connected segments, then it would not be expected that this stability should be affected by the means of adsorption of the segments, whether from spreading or by diffusion from the bulk solution. Katchalsky and Miller (1951) postulate that the failure of poly(methacrylic acid) solutions to produce the same type of monolayer as was observed with spread layers was due to unusual stability of molecules in the dissolved state. No such consideration is expected with the ethylene oxide polymers, and there appears to be no reason why the molecules should not become adsorbed in their entirety. In this respect the liquid/air surface adsorption differs from that at the liquid/solid interface. Adsorption of the whole coil is not precluded by the adsorption of two widely separated segments on adjacent sites, because unlike a solid, the surface sites on a liquid are not rigidly fixed in relative positions.

One of the more surprising aspects of the identity of spread and solution adsorbed monolayers of poly(ethylene oxide) is that no such effect was indicated by the considerable quantity of work which has been done on systems of the glycol polymer series, although the two series are chemically almost identical. This basic difference between the polymers was confirmed by the brief experiments mentioned in section (v), in which

it was attempted to reproduce the poly(ethylene oxide) results with a high molecular weight poly(ethylene glycol) sample. It was suggested that the difference is associated with the molecular weight discrepancy between the two polymer series, although the two samples chosen were the closest commercially available. The other possibility indicated is that the difference is a result of the presence of hydroxyl groups on the glycol product.

It must be admitted that the evidence presented above confuses rather than clarifies the controversy (described in Chapter 5) concerning the orientation of adsorbed ethylene oxide polymer segments at the liquid/air surface. Further to the previous evidence, generally based on assumption of Gibbs-type adsorption in systems of the glycol polymers, it now appears that high molecular weight oxide polymers not only form very stable spread monolayers, but also produce the same type of adsorption from aqueous solution.

APPENDIX 1

Image distortion produced by an irregular refractive index discontinuity in a single lens, variable magnification imaging system.

Figure A1.1 shows the optical system used in the moiré fringe visualisation method for the production of a real image of object grating G_1 in the plane of the reference grating G_2. The presence of a bulk of water bearing a sinusoidal wave system has been represented in this figure merely as a discontinuity in refractive index, the rest of the water affecting only the physical distance u, instead of the optical distance.

For a ray leaving the object grid at x', the position x of incidence on the lens is, in the absence of any distortion,

$$x = x' - u\theta \qquad A1$$

and the position of arrival at the image, x" is

$$x'' = x - v(\theta+\phi). \qquad A2$$

Since the deviation ϕ produced by the lens is given by

$$\phi = x/f \quad , \qquad A3$$

$$x'' = x' - u\theta - v(\theta+(x' - u\theta)/f) \qquad A4$$

$$= x'(1 - v/f) - \theta(u + v - uv/f). \qquad A5$$

and since $u + v = uv/f$,

$$\underline{x'' = x'(1 - v/f)} \qquad A6$$

If a refractive index step is now introduced into a position an optical

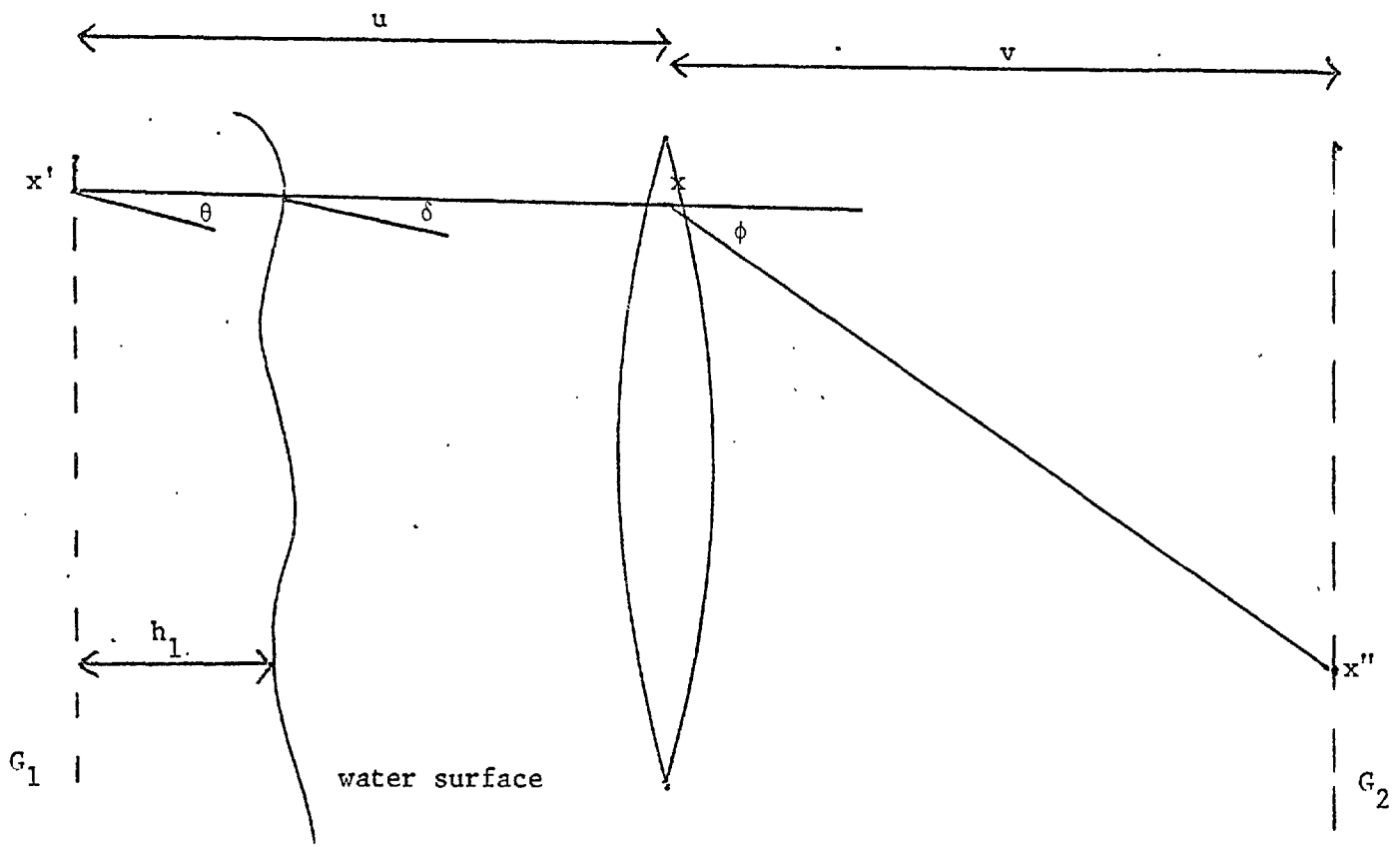


figure 11.1 The moiré fringe optical system.

distance h_1 from the object grid, deflecting the ray by an angle δ,

at the lens, $x_\delta = x' - u\theta - (u - h_1)\delta$, A7

and at the image,

$$x''_\delta = x_\delta - v(\theta + \phi_\delta + \delta)$$

$$= x' - u\theta - (u - h_1)\delta - v(\theta + (x' - u\theta - (u - h_1)\delta)/f + \delta)$$

$$= x'(1 - v/f) - \theta(u + v - uv/f) - (u - h_1)\delta + v(u - h_1)\delta)/f - v$$

$$= x'(1 - v/f) - \delta(h_1 v/f - h_1) \qquad A8$$

The shift in the image produced by the distortion,

$$\Delta x_i = x''_\delta - x''$$

$$= -h_1 \delta (v/f - 1) \quad , \qquad A9$$

and writing the magnification m of the system as :

$$m = 1 - v/f \quad , \qquad A10$$

$$\underline{\Delta x_i = - mh_1 \delta} \qquad A11$$

The negative sign signifies that the image shift is in the opposite sense to the original light deflection.

APPENDIX 2.

Use of the Lucassen and Hansen wave damping theory for the measurement of surface dilational elasticity.

It has been shown by Dorrestein (1951), Hansen and Mann (1964), van den Tempel and van de Riet (1965), and Lucassen and Hansen (1966), that the wavelength and rate of decay of small-amplitude ripples on liquids were determined critically by the surface tension and surface dilational elastic properties of the liquid/air surface. The other significant variables, liquid density and bulk liquid viscosity, appear to be more easily predictable in their effect on the propagation. The presence of surface dilational elasticity in a system has its greatest effect on the damping of ripples rather than their wavelength, and a maximum damping is observed in many surfactant/water systems which appears to be associated with the existence of longitudinal surface waves (Lucassen, 1968).

Lucassen and Hansen (1966) have published an equation which relates measured values of wavelength and damping coefficient to the surface tension and dilational elasticity of the surface, for the case in which the elasticity is independent of the rate of stretching of the surface, the dilational elasticity being then negligible.

The equation is in terms of the following dimensionless quantities -

$$\kappa \equiv \underline{\kappa}\sqrt{\frac{\eta}{\omega\rho}} \qquad \gamma \equiv \underline{\gamma}\sqrt{\frac{\rho}{\omega\eta^3}}$$

$$g \equiv \underline{g}\sqrt{\frac{\rho}{\eta\omega^3}}$$

$$\alpha \equiv \underline{\alpha}\sqrt{\frac{\eta}{\omega\rho}} \qquad \varepsilon \equiv \underline{\varepsilon}\sqrt{\frac{\rho}{\omega\eta^3}}$$

where

$\underline{\kappa}$	=	ripple wavenumber (cm^{-1})
$\underline{\alpha}$	=	damping coefficient (cm^{-1})
ω	=	angular frequency ($radians.sec.^{-1}$)
ρ	=	liquid density ($gm.cm.^{-3}$)
$\underline{g}$	=	gravitational acceleration ($cm.sec^{-2}$)
η	=	liquid viscosity ($gm.cm^{-1}.sec^{-1}$)
$\underline{\gamma}$	=	surface tension of solution ($g.sec^{-2}$)

From these,

$$t = \tfrac{1}{2}\sqrt{2}\sqrt{\kappa^2-\alpha^2+\sqrt{(\kappa^2-\alpha^2)^2+(2\kappa\alpha-1)^2}}$$

$$u = \tfrac{1}{2}\sqrt{2}\sqrt{-\kappa^2+\alpha^2+\sqrt{(\kappa^2-\alpha^2)^2+(2\kappa\alpha-1)^2}}$$

and using the variables

$$A_1 = u\alpha^2-2t\kappa\alpha-u\kappa^2+g\{4\kappa\alpha^3-4\kappa^3\alpha-3u\kappa\alpha^2+3t\kappa^2\alpha-t\alpha^3+u\kappa^3\}$$

$$A_2 = -t\alpha^2-2u\kappa\alpha+t\kappa^2+g\{\kappa^4+\alpha^4-t\kappa^3-u\alpha^3-6\kappa^2\alpha^2+3t\kappa\alpha^2+3u\kappa^2\alpha\}$$

$$B_1 = 3\kappa^2\alpha-\alpha^3$$

$$B_2 = 3\kappa\alpha^2-\kappa^3$$

$$C_1 = -6\kappa^5\alpha+20\kappa^3\alpha^3-6\kappa\alpha^5+t\{5\kappa^4\alpha-10\kappa^2\alpha^3+\alpha^5\}+u\{\kappa^5-10\kappa^3\alpha^2+5\kappa\alpha^4\}$$

$$C_2 = \kappa^6-15\kappa^4\alpha^2+15\kappa^2\alpha^4-\alpha^6+t\{-\kappa^5+10\kappa^3\alpha^2-5\kappa\alpha^4\}+u\{5\kappa^4\alpha-10\kappa^2\alpha^3+\alpha^5\}$$

$$D_1 = g\alpha+16\kappa^3\alpha-16\kappa\alpha^3-4\kappa^2+4\alpha^2+4t\{-3\kappa^2\alpha+\alpha^3\}+4u\{-\kappa^3+3\kappa\alpha^2\}$$

$$D_2 = -g\kappa-4\kappa^4+24\kappa^2\alpha^2-4\alpha^4-8\kappa\alpha+1+4t\{\kappa^3-3\kappa\alpha^2\}$$

The final equations may then be written:

for the surface tension roots :-

$$\gamma = \frac{-(D_2C_1-D_1C_2+A_1B_2-A_2B_1)}{2(C_1B_2-C_2B_1)} \pm \frac{(D_2C_1-D_1C_2+A_1B_2-A_2B_1)^2-4(C_1B_2-C_2B_1).(A_1D_2-A_2D_1)}{2(C_1B_2-C_2B_1)}$$

for the surface elasticity roots :-

$$\varepsilon = \frac{-(D_1C_2-D_2C_1+A_1B_2-A_2B_1)}{2(A_1C_2-A_2C_1)} \pm \frac{(D_1C_2-D_2C_1+A_1B_2-A_2B_1)^2-4(A_1C_2-A_2C_1).(B_2D_1-B_1D_2)}{2(A_1C_2-A_2C_1)}$$

A FORTRAN computer program to evaluate these equations is shown in figure A2.1 Liquid density, viscosity and the gravitational acceleration are already fixed in the program, for the common case of an aqueous substrate, as

ρ = 1.00 $gm.cm^{-3}$

η = 0.01 poise

$\underline{g}$ = 980.0 $cm.sec^{-2}$

The program will process sets of wavelength/damping coefficient information for any desired frequency. It was used in the analysis of many experimental results, some of which are reported in Chapter 7. A feature of the above equations is that each pair of wavelength and damping measurements produces two possible values for both surface tension and surface elasticity. It appears that it is valid to assume that either the positive root or the negative root should apply simultaneously to both surface tension and surface elasticity, and this allows the correct root to be selected if

```
      PROGRAM SURF  (INPUT,OUTPUT,TAPE5=INPUT,TAPE6=OUTPUT)
C     LUCASSEN AND HANSEN  SURFACE PROPERTY PROGRAM
C           (ORIGINAL)
C      REFERENCE - J.COLL.INT.SCI. 22, 32, (1966)
      REAL K,K2,K3,K4,K5,K6,J,M
      WRITE(6,6)
    6 FORMAT(49H1POLYCONC  FREQ WAVE    DAMPING  SURFACE  SURFACE  )
      WRITE(6,7)
    7 FORMAT(49H                  LENGTH  COEFF    TENSION  COMPRES /)
   99 READ(5,2)FREQ          (frequency input)
    2 FORMAT(F4.0)
      W=2.0*3.1416*FREQ
    8 READ(5,9)WAV,ALF       (wavelength, damping coefficient)
    9 FORMAT(F6.5,F6.4)
      IF (WAV.EQ.0.9999) GO TO 99
      IF(WAV.EQ.0.0)GOTO60
    4 CONTINUE
      WAVN=2.0*3.1416/WAV
      K=WAVN*0.1/SQRT(W)
      G=980.0*10.0/SQRT(W*W*W)
      A=ALF*0.1/SQRT(W)
      A2=A*A
      A3=A2*A                                    figure A2.1
      A4=A3*A
      A5=A4*A
      K2=K*K
      K3=K2*K
      K4=K3*K
      K5=K4*K
      K6=K5*K
      H=K2-A2
      J=(2.0*K*A-1.0)*(2.0*K*A-1.0)
      M=H*H+J
      RTM=SQRT(M)
      T=0.5*SQRT(2.0*(H+RTM))
      U=-0.5*SQRT(2.0*(-H+RTM))
      XX=4.0*K*A3-4.0*K3*A-3.0*U*K*A2+3.0*T*K2*A-T*A3+U*K3
      E1=U*A2-2.0*T*K*A-U*K2+G*XX
      XX=K4+A4-T*K3-U*A3-6.0*K2*A2+3.0*T*K*A2+3.0*U*K2*A
      E2=-T*A2-2.0*U*K*A+T*K2+G*XX
      B1=3.0*K2*A-A3
      B2=3.0*K*A2-K3
      XX=5.0*K4*A-10.0*K2*A3+A5
      YY=K5-10.0*K3*A2+5.0*K*A4
      C1=-6.0*K5*A+20.0*K3*A3-6.0*K*A5+T*XX+U*YY
      XX=-K5+10.0*K3*A2-5.0*K*A4
      YY=5.0*K4*A-10.0*K2*A3+A5
      C2=K6-15.0*K4*A2+15.0*K2*A4-A6+T*XX+U*YY
      XX=-3.0*K2*A+A3
      YY=-K3+3.0*K*A2
      D1=6*A+16.0*K3*A-16.0*K*A3-4.0*K2+4.0*A2+4.0*T*XX+4.0*U*YY
      XX=K3-3.0*K*A2
      YY=-3.0*K2*A+A3
      D2=-6*K-4.0*K4+24.0*K2*A2-4.0*A4-8.0*K*A+1.0+4.0*T*XX+4.0*U*YY
      X=D2*C1-D1*C2+E1*B2-E2*B1
      Y=C1*B2-C2*B1
      R=E1*D2-E2*D1
```

```
      GENORM=SQRT(W*0.000001)
      ARG=X*X-4.0*Y*R
      IF(ARG)20,25,25
   20 WRITE(6,13)
   13 FORMAT(40H                                        NEGROOT )
      ARG=-1.0*ARG
   25 GPOS=(-X+SQRT(ARG))/(2.0*Y)
      GPOS=GPOS*GENORM
      GNEG=(-X-SQRT(ARG))/(2.0*Y)
      GNEG=GNEG*GENORM
   45 Z=D1*C2-D2*C1+E1*B2-E2*B1
      Q=E1*C2-E2*C1
      S=B2*D1-B1*D2
      ARG=Z*Z-4.0*Q*S
      IF(ARG)21,26,26
   21 WRITE(6,14)
   14 FORMAT(47H                                              NEGROOT )
      ARG=-1.0*ARG
   26 EPOS=(-Z+SQRT(ARG))/(2.0*Q)
      EPOS=EPOS*GENORM
      ENEG=(-Z-SQRT(ARG))/(2.0*Q)
      ENEG=ENEG*GENORM
      WRITE(6,50)CONC,FREQ,WAV,ALF,GPOS,EPOS
   50 FORMAT(1X,E8.2,1X,F5.0,1X,F6.4,2X,F7.4,2X,F7.2,2X,F7.2)
      WRITE(6,51)GNEG,ENEG
   51 FORMAT(33X,F7.2,2X,F7.2)
   59 GOTO8
   60 CONTINUE
      END
```

GPOS GNEG	ARE THE TWO SURFACE TENSION ROOTS.
EPOS ENEG	ARE THE TWO SURFACE ELASTICITY ROOTS.

FIGURE A2.1 Computer program for the calculation of surface tension and surface elasticity from ripple measurements.

the surface tension is measured independently at the same time as the wavelength and damping coefficient.

It was found useful during the present investigation, the majority of which used the single frequency of 30 Hz, to examine the properties of the formula over a wide range of possible wavelength/damping values at this frequency. Figures A22 and A23 show the results obtained by allowing the computer to vary the damping coefficient for a series of fixed wavelengths λ. Figure A22, the elasticity variation, clearly shows the damping peak at relatively low ε, and this is seen to increase considerably as the wavelength decreases. As can be seen from figure A23, this decrease in λ represents a reduction in surface tension. For very low damping only one root appears in the ε variation, the other being in general large and negative, and apparently not corresponding to the usually observed ripple damping system.

If measurements are presented to the computer which will not fit on to these curves, having a value of damping either too large or too small for the wavelength measured, then the square roots in the final equations will be complex, and the results of little value. The curves therefore serve as a guide to the validity of the measurements, as well as a rough indication of the likely results of the computer processing.

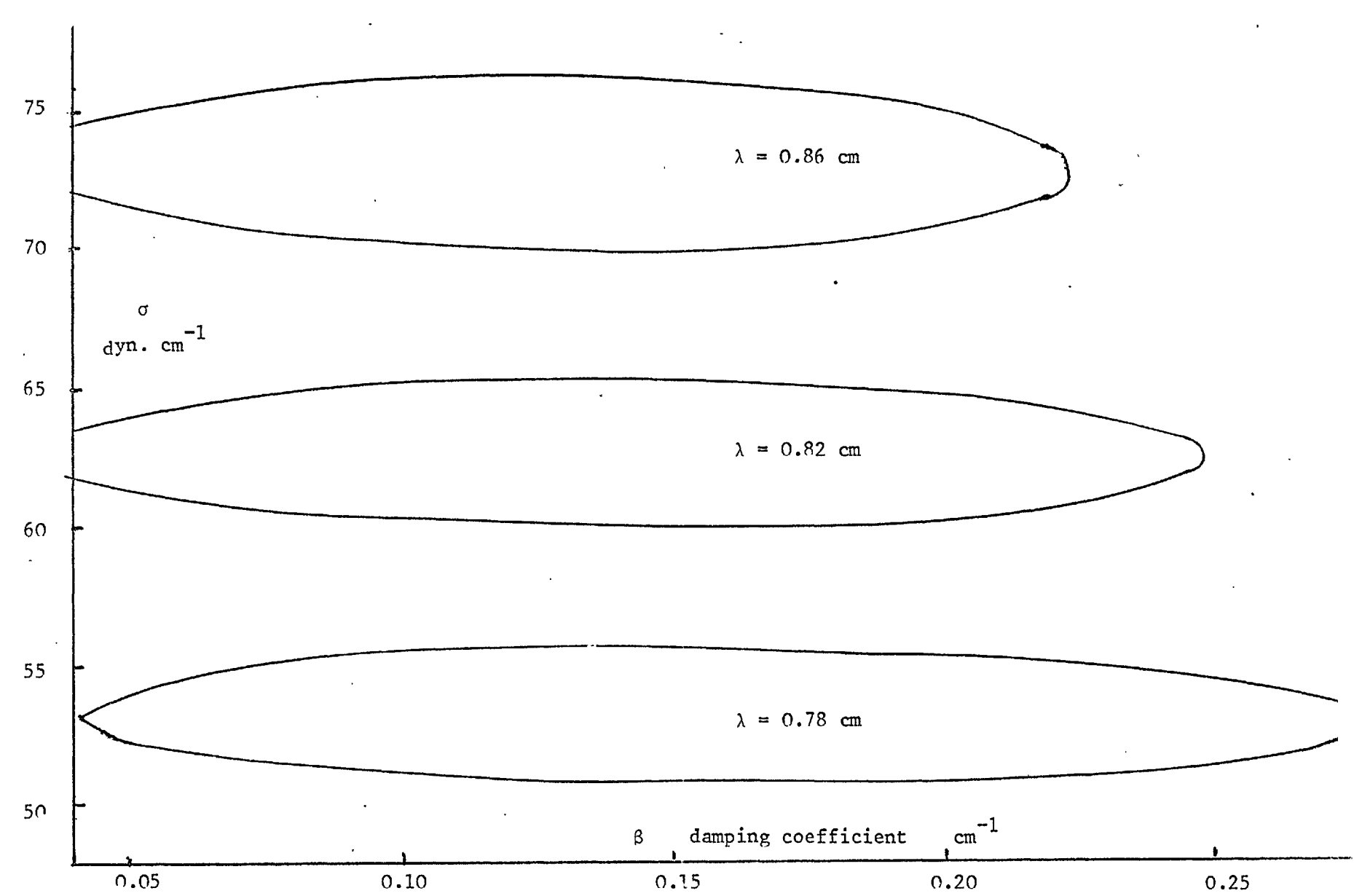


figure A2.2 Surface tension predictions for given wavelength/damping combinations

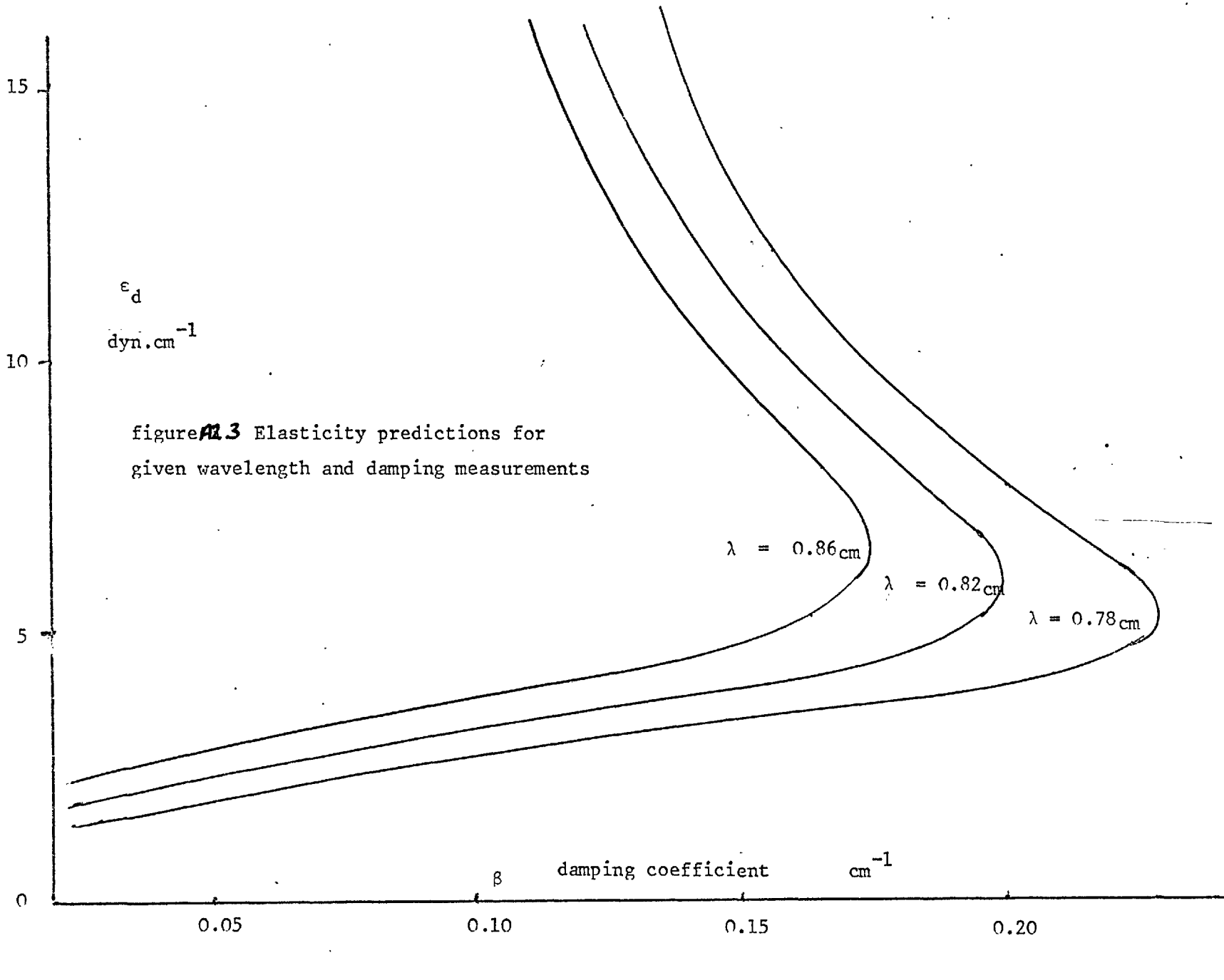


figure A2.3 Elasticity predictions for given wavelength and damping measurements

GUIDE TO SYMBOLS USED IN THE TEXT

á	constant representing the concentration of surfactant in a solution at which the adsorption is half the saturation value (mole. cm^{-3}, gm. cm^{-3})
A	specific surface area ($(\mathring{A})^2$ per molecule)
A_e	area of a surface element
a_i, b_i, c_i, d_i	digital fringe position numbers
c	concentration of solute (mole. cm^{-3}., gm. cm^{-3}.)
D	diffusion coefficient (cm^2. sec^{-1})
f	ripple frequency (Hz)
f_i	activity coefficient of component i
h	water depth (cm)
h_o	ripple amplitude (cm)
h_1	optical distance between G_1 and liquid surface
H^s	non-ideality parameter in surfactant adsorption
g	gravitational acceleration
k	lens magnification of the liquid surface
m	magnification of grating G_1 in the plane of G_2
N_i	mole fraction of component i
p_1, p_2	grating pitches of G_1 and G_2
R	gas constant
T	absolute temperature
x, x_1, x_s	directions across the optical axis in the moiré fringe apparatus
V_g	group velocity of ripple system

ΔY	fringe distortion
ΔY_o	fringe spacing of undistorted pattern
α	time damping coefficient (sec^{-1})
β	distance damping coefficient (cm^{-1})
β_0	damping coefficient for zero surface elasticity
β_∞	damping coefficient for infinite elasticity
β_{max}	damping coefficient for peak damping condition
Γ, Γ_i	surface excess (of component i) (mole. cm^{-2})
Γ_∞	saturation adsorption (mole. cm^{-2})
δ	angle of refraction of light by water surface
ε	complex dilational elastic modulus
ε_d	dilational elasticity
ε_s	shear elasticity
η_d	dilational viscosity
η_s	shear viscosity
η	liquid viscosity (poise)
λ	ripple wavelength (cm)
μ	refractive index (glass, water)
μ_i	chemical potential of component i
ρ, ρ_1	liquid density (gm. cm^{-3})
σ	surface tension (dyn. cm^{-1})
σ_o	surface tension of pure liquid
τ	dimensionless parameter defined by eqn. 2.18
θ	angle between rulings of G_1 and G_2
χ	wave number $= 2\pi / \lambda$
ω	angular frequency $= 2\pi \times$ frequency (sec^{-1})

Bibliography.

AIKEN, J. Proc. Roy. Soc. Edin. 12, 56,(1883)

AVETISYAN, R.A., and TRAPEZNIKOV, A.A. Russ.J. Phys. Chem. 38, 1660,(1964)

BARNETT, S.J. Phys. Rev. 6, 257,(1898)

BATTEZZATI, M. J. Coll. Int. Sci. 33, 24, (1970).

BENDURE, R.L. and HANSEN, R.S. J. Phys.Chem. 71, 2889, (1967).

BLANK, M., LUCASSEN, J., and van den TEMPEL, M. J.Coll. Int. Sci.33, 94,(1970).

BOHR, N. Phil.Trans. A209, 281,(1909).

BOHR, N. Proc.Roy.Soc. A84, 395,(1910).

BOUASSE, M. Ann.de Phys. 7, 599,(1937).

BOUCHER, E.A., GRINCHUK, T.M., and ZETTLEMOYER, A.C. J.Coll. Int.Sci. 23, 600, (1967).

BOYD, G.E., and VASLOW, F. J.Coll.Sci. 13, 275, (1958).

BRENNEN, C., and GADD, G.E. Nature, 215, 1368,(1967).

BROWN, R.C. Proc.Phys.Soc. 48, 312, 323, (1936).

BRUNAUER,S., EMMETT,P.H., and TELLER, E. J.Am.Chem.Soc. 60, 309,(1938).

BULAS, R., and KUMINS, C.A., J.Coll.Sci. 13, 429,(1958)

CHAMPION, F.C., and DAVY, N. "Properties of Matter", 3rd Edn., Blackie, London,(1959)

COUPER, A., and ELEY, D.D. J.Poly.Sci. 3, 345,(1948).

COUPER, A., and STEPTO, R.F.T., Trans.Farad.Soc. 65, 2486, (1969).

CRAPPER, G.D. J.Fl.Mech. 2, 532, (1957).

CRISP, D.J. J.Coll.Sci., 1, 49, 161,(1946).

CRISP, D.J. "Surface Phenomena in Chemistry and Biology", Ed. Danielli,F.J., Pankhurst, K.G.A., Riddiford, A.C., Pergamon,(1958).

DARLINGTON, M.W. Ph.D. Thesis, Southampton, (1967).

DAVIES, G.A. and PONTER, A.B. Nature, 212, 66, (1966.)

DAVIES, J.T. J.Coll.Sci. Suppl. 1, 9, (1954).

DAVIES, J.T., and MAYERS, G.R.A. Trans. Farad.Soc. 56, 690, (1960).

DAVIES, J.T., and RIDEAL,E.K. "Interfacial Phenomena", 2nd Edn. Academic Press, New York, (1963).

DAVIES, J.T., and VOSE, R.W. Proc.Roy.Soc., 286, 218, (1965).

DAVIS, A.H. Phys.Soc.Proc., 38, 234, (1926).

DAVIS, A.H. Phys.Soc.Proc., 40, 87, (1928.)

DECHAENE, R., DE COCK,J., and DE CALUWE, M. Strain, 4, 14, (1968).

DEFAY, R. and HOMMELEN, J.R., J.Coll.Sci., 13, 553, (1958).

DORRESTEIN, R. Proc.K.Ned.Akad.Wet. Ser.B 54, 260, 350, (1951).

DORSEY, N.E. Phys.Rev. 5, 170, 213, (1897).

DROST-HANSEN, W. Ind. and Eng.Chem. 57, 38, (1965).

DU PONT Booklet: "Elvanol : Polyvinyl Alcohol", Du Pont Co.(UK) Ltd.(1968).

ELPYERIN, I.T. and SMOLSKI, B.M. Vesti.Akad.Navuk Belarusk SSR. Ser.Fiz.Tekhn.Navuk, 2, 39, (1965)

FABULA, A.G. Proc. 4th Int.Cong.Rheol. (1963) Part 3, 455, Wiley Interscience, (1965).

FARADAY, M. Phil.Trans.Roy.Soc.Lond. 299, (1831).

FERGUSON,A. Phil.Mag. 25, 509, (1913).

FERGUSON, A. and KENNEDY,S.J. Proc.Phys.Soc. 44, 511, (1932).

FOX, H.W., TAYLOR, P., and ZISMAN, W.A. Ind.Eng.Chem. 39, 1401, (1947).

FRANKLIN, B. Phil.Trans. 64, 445, (1774).

FRISCH, H.L. and AL-MADFAI, S. J.Am.Chem.Soc., 80, 3561, (1958)

FRISCH,H.L., and SIMHA,R. J.Chem.Phys., 24, 652, (1956).

FRUMKIN, A. Z.Physik.Chem.(Leipzig) 116, 466, (1925).

FRYER,P.A. Optics Technology. 2 (1), 36, (1970).

GADD,G.E. Nature, 206, 463, (1965)

GADD,G.E. Nature, 212, 874, (1966).

GAINES, G.L. "Insoluble Monolayers at Liquid-Gas Interfaces", Wiley-Interscience, (1966.)

GARRETT, W.D. and BULTMAN, J.D. J.Coll.Int.Sci. 18, 798, (1963).

GARRETT,R.L. and ZISMAN, W.A. J.Phys.Chem. 74, 1797, (1970).

GHOSH, P.N., BANERJI,D., and DATTA,S.K. Phil.Mag. 1, 1252, (1926).

GIBBS, J.W. "Collected Works" Vol. 1, Longmans, New York, (1928).

GLASS, J.E. J.Phys.Chem. 72, 4450, (1968a).

GLASS,J.E. J.Phys.Chem. 72, 4459, (1968b).

GOODRICH,F.C. Proc.Roy.Soc. A260, 481,490,503, (1961).

GOODRICH,F.C. Proc.Roy.Soc. A310, 359, (1969).

GRÜNMACH,L. Ann.der Physik 9, 1261, (1902).

GUILD, J. "The Interference Systems of Crossed Diffraction Gratings", O.U.P. (1956).

GUILD,J. "Diffraction Gratings as Measuring Scales", O.U.P.(1960)

HANSEN,R.S., LUCASSEN,J., BENDURE, R.L., and BIERWAGEN,G.P., J.Coll.Int.Sci., 26, 198, (1968).

HANSEN,R.S. and MANN, J.A. J.Appl.Phys., 35, 152, (1964).

HANSEN,R.S., PURCHASE,M.E., WALLACE,T.C., and WOODY,R.W., J.Phys.Chem. 62, 210, (1958).

HARDING, R.H. and ROSE,J.K., "Water Soluble Resins", ed. Davidson, R.L. and Sittig,G.M., Rheinhold, New York, (1968).

HARKINS,W.D., and BROWN,F.E., J.Am.Chem.Soc. 41, 499, (1919).

HEISE,U. Exp.Mech. 7, 47, (1967).

HILYARD,N.C., and JERRARD,H.G. Nature, 194, 173, (1962).

HOECHST. Leaflet: Moviol. Farbwerke Hoechst AG, (1968).

HOLLAND, L. "The Properties of Glass Surfaces", Chapman and Hall, London, (1964).

HOYT,J.W., and FABULA,A.G. 5thSymp.Naval Hydrodynamics, Bergen, ONR Report ACR112, (1964).

JOLY,M. Kolloid-Z, 89, 26, (1939).

JOLY,M. "Recent Progress in Surface Science", Vol. 1, p1, ed. Danielli,J.F., Pankhurst, K.G.A., and Riddiford, A.C., Academic Press, (1964).

KALÄHNE,A. Ann.Physik. 7, 440, (1902).

KATCHALSKY,A. and MILLER, I.R. J.Phys.Coll.Chem. 55, 1182, (1951).

KELVIN, Lord. Phil.Mag. 42, 368, (1871).

KITCHENER,J.A. "Recent Progress in Surface Science", Vol.1,P51, ed.Danielli, J.F., Pankhurst,K.G.A., and Riddiford,A.C., Academic Press, (1964).

LAMB,H. "Hydrodynamics", C.U.P. (1895).

LANGE,H. Kolloid-Z, 182, 123, (1962).

LANGMUIR,I. J.Am.Chem.Soc. 39, 1848, (1917).

LEVICH,V.G. Acta Physicochimica URSS, 14, 307, 321, (1941).

LEVICH,V.G. "Physicochemical Hydrodynamics", Prentice Hall,(1962).

LIGTENBERG,F.K. Proc.S.E.S.A. 12, 83, (1955).

LITTLE,R.C. Naval Research Lab. Report 6542, (1967).

LITTLE,R.C. Ind.Eng.Chem.Fund., 8, 520, (1969b).

LITTLE,R.C. Ind.Eng.Chem.Fund. 8, 557, (1969a)

LLOWARCH,W. "Ripple Tank Studies of Wave Motion", O.U.P. (1961).

LOVELL,E.L. and HIBBERT,H.J. J.Am.Chem.Soc. 62, 2144, (1940).

LUCASSEN,J. Trans.Farad.Soc. 64, 2221, 2230, (1968).

LUCASSEN,J. and HANSEN,R.S. J.Coll.Int.Sci., 22, 32, (1966).

LUCASSEN,J. and HANSEN, R.S. J.Coll.Int.Sci. 23, 319, (1967).

LUCASSEN,J. and LUCASSEN-REYNDERS,E.H. J.Coll.Int.Sci., 25, 496, (1967).

LUCASSEN-REYNDERS,E.H. J.Phys.Chem. 70, 1777, (1966).

LUCASSEN-REYNDERS,E.H. and LUCASSEN,J. Adv.Coll.Int.Sci., 2, 374, (1969).

LUCASSEN-REYNDERS,E.H., and van den TEMPEL, M. Proc.4th Int. Cong.Surf. Active Subst. Burssels, Vol. 2, p779, (1964).

LUXMOORE,A.R., and HOUSE,C. "Engineering uses of Holography" ed.Harvey,J.M., and Robertson,E.R., C.U.P. (1970).

MANN,J.A. and AHMAD,J. J.Coll.Int.Sci. 29, 158, (1969).

MANN,J.A. and HANSEN, R.S. J.Coll.Sci. 18, 757, (1963a).

MANN,J.A. and HANSEN, R.S. J.Coll.Sci. 18, 805, (1963b).

MANNHEIMER,R.J. and SCHECHTER,R.S. J.Coll.Int.Sci. 32, 225, (1970).

MARANGONI, C.G.M. Ann.Phys.(Poggendorf), 143, 337, (1871).

MEADER, A.L. and CRIDDLE,D.W. J.Coll.Sci. 8, 170, (1953).

MOILLIET,J.L. COLLIE,B., and BLACK, W. "Surface Activity", Spon, London, (1961).

NAKAMURA,M. and SASAKI, T., J.Sci.Inst. 44, 835, (1967).

NISHIJIMA,Y. and OSTER,G. J.Op.Soc.Am. 54, 1, (1964).

ÖHRN, O.E. J.Poly.Sci. 17, 137, (1955).

ÖHRN,O.E. Arkiv Kemi. 12, 397, (1958).

van OSS,C.J. J.Sci.Inst. 41, 227, (1964).

OSTER,G., WASSERMANN,M., and ZWERLING,C. J.Op.Soc.Am. 54, 169, (1964).

PADDAY,J.F., andRUSSELL,D.R. J.Coll.Sci. 15, 503 (1960).

PALMER,F. Phys.Rev. 33, 528, (1911).

PEN'KOV,S.N. Opt.Spect. 10, 343, (1961).

PETERLIN,A. J.Poly.Sci. 12, 45, (1954).

PETERLIN,A. J.Poly.Sci. A2, 5, 179, (1967a).

PETERLIN,A. Polymer, 8, 21, (1967b).

POWELL,R.L. and STETSON,K.A. J.Op.Soc.Am. 55, 1593, (1965).

RAYLEIGH, Lord.Phil.Mag. 47, 193, (1874).

RAYLEIGH, Lord.Phil. Mag. 30, 386, (1890).

REYNOLDS, O. Brit.Ass.Report, (1880).

RIDEAL,E.K., and SUTHERLAND,K.L. Trans.Farad.Soc. 48, 1109, (1952).

RIGHI,A. Nuovo Cimento, 21, 203, (1887); 22, 10, (1888).

RONCHI,V. "La Prova del Sistemi Ottici", Attualite Scientifiche No.37 (Nicola Zanichelli, Bologna) Chap 9 (1925).

RÖSCH, M. Kolloid-Z. 147, 79, (1956).

ROUSE,P.R. J.Chem.Phys. 21, 1272, (1953).

RUDD,M.J. Nature, 224, 587, (1969).

SAVINS,J.G. "Viscous Drag Reduction", ed. C. Sinclair Wells, Plenum, New York, (1969).

SCHICK, M.J. J.Coll.Sci. 17, 801, (1962).

SCHOOLEY,A.H. NRL Report 3559, (1949).

SCHULTZE,H. Zeits F.Instr. 27, 354, (1907).

SCIAMMARELLA,C.A., and ROSS,B.E. Exp.Mech. 4, 283, (1964).

SCRIVEN,L.E., and STERNLING,C.V. Nature, 187, 186, (1960).

SHULER,R.L., and ZISMAN,W.A. J.Phys.Chem. 74, 1523, (1970).

SILBERBERG,A. J.Phys.Chem. 66, 1884, (1962).

SINGER,S.J. J.Chem.Phys. 16, 872, (1948).

SMITH,C.M. Proc.Roy.Soc.Edin., 17, 115, (1889).

STEPHENS,R.W.B., and BATE,A.E. "Acoustics and Vibrational Physics", Arnold, London, (1966).

STOCKER,H. Z.Phys.Chem. 94, 149, (1920).

STOKES,G.G. Cambridge Trans. 8, 287, (1845).

SUBRAMANYAM,S.G. Phys.Rev. 27, 632, (1926).

SUTHERLAND,K.L. Ph.D.Thesis, London, (1950).

von SZYSZKOWSKI,B. Z.Phys.Chem. (Leipzig), 64, 385, (1908).

TAKASAKI,H. App.Opt. 9, 1467, (1970).

van den TEMPEL,M., LUCASSEN,J., and LUCASSEN-REYNDERS,E.H., J.Phys.Chem. 69, 1798, (1965).

van den TEMPEL,M., and van de RIET, R.P. J.Chem.Phys. 42, 2769, (1965).

THEOCARIS,P.S. J.Sci.Inst. 41, 133, (1964).

THEOCARIS, P.S. Exp. Mech. 7, 289, (1967).

THEOCARIS,P.S., and KOUTSABESSIS,A. J.Sci.Inst. 42, 607, (1965).

THEOCARIS,P.S., and KOUTSABESSIS,A. B.J.App.Phys. 18, 513, (1967).

THEOCARIS,P.S. and KOUTSABESSIS,A. Exp.Mech. 8, 82, (1968).

THIESSEN,D., and SCHELUDKO,A. Kolloid-Z. 218, 139, (1967).

THIESSEN,D., and SCHWARTZ,P. Z.Physik Chem. 236, 363, (1967).

THURSTON,G.B., and SCHRAG,J.L. J.App.Phys. 35, 144, (1964).

TOMS,B.A., Proc.1st Int.Cong.Rheol.Vol.2. p135. North-Holland, (1948).

TRELOAR,L.R.G. "Polymer Systems", ed. Whetton,R.E. and Whorlow,R.W. p.33, Macmillan, (1968).

TSCHOEGL, N.W. J.Coll.Sci. 13, 500, (1958).

TYLER,E. Phil.Mag. 31, 209, (1941).

UNION CARBIDE "Carbowax Polyethylene Glycols", (1965).

VINCENT,J.H. Phil.Mag. 44, 411, (1897), 45, 191, (1898).

VINES,R.G. Australian J.Phys. 13, 43, (1960).

van VOORST VADER,F., ERKENS, Th.F., and van den TEMPEL,M. Trans.Farad.Soc. 60, 1170, (1964).

WALBRIDGE,N.L. Rev.Sci. Inst. 39, 672, (1968).

WALTON,A.J. Contemp.Phys. 10, 489, (1969).

WARD,A.F.H., and TORDAI,L. J.Chem.Phys. 14, 453, (1946).

WATSON,F.R. Phys.Rev. 12, 257, (1901).

WATSON,F.R. Phys.Rev. 15, 20, (1902).

WELLS, C.S. and SPANGLER,J.G. Phys. of Fluids 10, 1890, (1967).

WILTON,J.R. Phil.Mag. 29, 688, (1915).

ZANDMAN,F. Exp.Mech. 7, 19A, (1967).

ZIMM,B.H. J.Chem.Phys. 24, 269, (1956).

ACKNOWLEDGEMENTS

The author is grateful to the Ministry of Technology for financial support, and he wishes to thank the following for their invaluable assistance with the progress of the work :

The Acoustics Group of Imperial College, who promoted many stimulating and helpful discussions, especially Mr. John Bradley, who advised about computer programming.

Mr.E.Archbold, of the National Physical Laboratory, for the loan of high quality moiré grids.

Mr.G.C.Scott, of Hartlepool, for the provision of much useful optical and photographic equipment.

Miss Sandra Atkins, of Imperial College, for help with surface tension measurements.

Dr.R.W.B.Stephens, for his valuable supervision of this work, and his critical assistance in the preparation of this thesis.

The author also wishes to record his appreciation of the largely uncritical sympathy shown by his wife and daughter.

GLOSSARY

Birefringence. If the molecules or smallest particles of a material are asymmetrical in their electrical polarizabilities at optical frequencies, then these basic units will have a differing effect on incident light depending on the attitude of the optical axes of the unit with respect to the plane of polarization of the light. In the bulk material, if there is some ordering of the basic units as to their attitude, then the optical anisotropy will appear as a dependence of the velocity of light on its polarization with respect to the optical axes formed in the material. This difference in the effective refractive index is called the birefringence. Flow birefringence occurs in a liquid, where the lack of long range ordering forces prevents even strongly anisotropic particles from producing a total birefringence, but where the setting up of shear flow in the liquid can orientate the particles with respect to the flow shear gradient.

Dilational Viscosity η_d represents the time dependent part of the surface dilational elastic modulus in the rheological description of liquid interfaces. This elastic modulus describes the forces which oppose expansion and compression of an interfacial area, and the time dependence is composed of two parts: one due to the reduction of surface tension differences in the interface by diffusion of surface active molecules to and from the surface, and the other due to time-dependent interactions between these molecules in the surface. It has the dimensions dyn.cm^{-1}sec.

Drag Reduction is the phenomenon in which the energy required to maintain turbulent flow in a liquid may be reduced by the addition of small quantities of certain soluble materials. Of the polymeric materials found to be effective, the higher the mean molecular weight, the greater is the effect.

Fibre Optics. By coating thin flexible glass fibres with a thin layer of material whose refractive index is a certain specific value, less than that of glass, light can be made to travel along the fibres without leakage. Bundles of these fibres, often called light guides, can be made to transmit light efficiently through non-straight paths, and are useful for the supply of light to inaccessible places.

Holography. If the interference pattern due to two coherent beams of monochromatic light is recorded photographically, the the processed photographic plate, a hologram, contains information about the phase and amplitude differences between the beams. Thus when one of the beams is directed on to this plate in the same way as during the exposure, the plate produces a "reconstruction" of the other beam, by imposing the difference between the beams on the first beam. If one of the beams came from an object, then as much light will be produced representing that object as was there initially, and the object appears to be recon-structed in three dimensions.

Holographic Interferometry utilises the fact that many holograms may be recorded on a single plate. If two of these are of the same object, the only

difference being a small displacement relative to the plate, then the two mutually coherent reconstructions will interfere,and give interference fringes representing the displacement difference.

Moiré Fringes. are dark and light areas arising from the geometrical obstruction of one regular line grid by another. The fringe positions are very sensitive to small movements of the component grids, and this gives rise to the use of the fringes in moiré interference techniques.

Spatial Frequency is a space analogue (in terms of repeat patterns per unit length) of the more usual temporal frequency in terms of cycles or events per unit time.

Spatial Filtering is a means of removing unwanted spatial frequencies, by bringing light from the spatial pattern to a focus. For example, an optical diffraction grating will produce regularly spaced points of light, the diffraction orders, each representing a harmonic of the basic spatial frequency of the grating. By blocking some of these harmonics in the focussing plane, they are filtered from the light coming from the grating.

Hydrophilic-Hydrophobic. Certain sections of organic molecules, such as the hydroxyl (-OH) group, are energetically acceptable to the structure of liquid water, while others, such as paraffin chain sections, display a relative dislike for this structure. The former are termed hydrophilic, "water-loving", and the latter hydrophobic, "water-hating".

Normal Stress. When a viscoelastic liquid is subjected to a shear force, the resulting flow is associated with the storage of elastic energy in the liquid, and a force is observed to act perpendicular to the shear plane.

Surface Pressure. The reduction of surface tension by the positive adsorption of organic molecules is analogous to the production by the adsorbed molecules of a two-dimensional "pressure", with units $dyn.cm^{-1}$, which acts in opposition to the pure liquid surface tension force.